IHSM
La Mayora

Instituto de Hortofruticultura Subtropical y Mediterránea
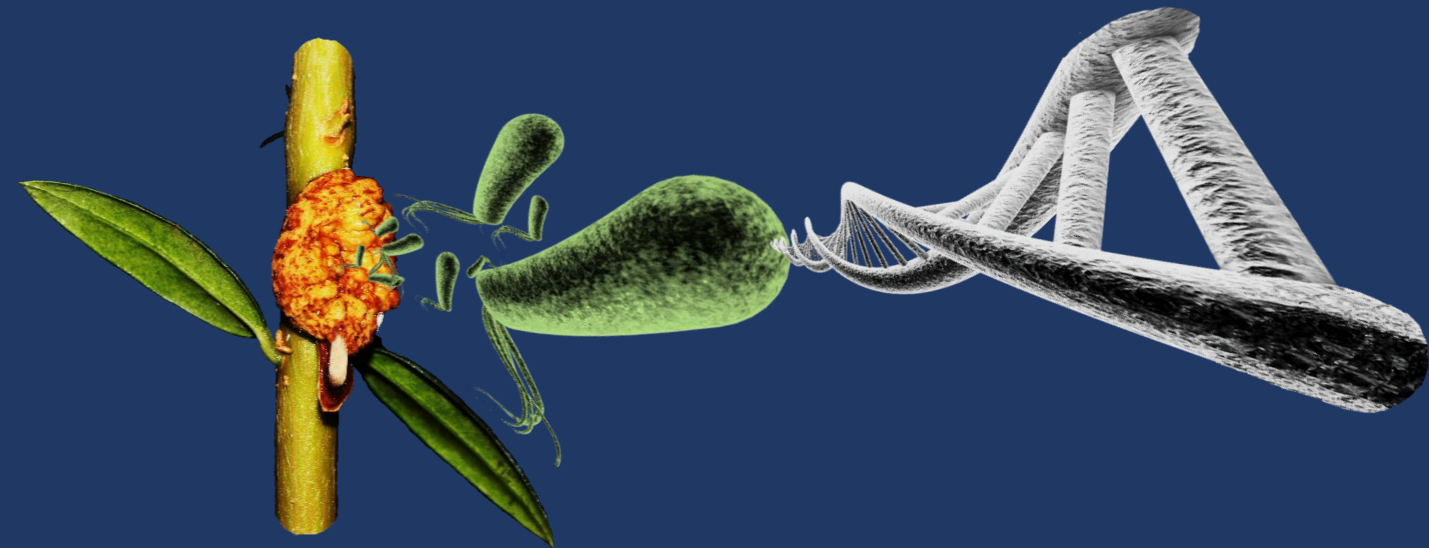
u ma
UNIVERSIDAD
DE MÁLAGA

Eloy Caballo Ponce

TESIS DOCTORAL

2017

Host specificity and virulence of the phytopathogenic bacteria *Pseudomonas savastanoi*

TESIS DOCTORAL

Eloy Caballo Ponce

Director: Cayo Ramos Rodríguez
Programa de Doctorado: Biotecnología Avanzada

Año 2017

Memoria presentada por:

Eloy Caballo Ponce

para optar al grado de Doctor por la Universidad de Málaga

Host specificity and virulence of the phytopathogenic bacteria *Pseudomonas savastanoi*

Director: Cayo J. Ramos Rodríguez

Catedrático. Área de Genética.

Departamento de Biología Celular, Genética y Fisiología.

Instituto de Hortofruticultura Subtropical y Mediterránea (IHSM)

Universidad de Málaga – Consejo Superior de Investigaciones Científicas

Málaga, 2016

UNIVERSIDAD
DE MÁLAGA

AUTOR: Eloy Caballo Ponce

http://orcid.org/0000-0003-0501-3321

COMITÉ EVALUADOR

Presidente

Dr. Jesús Murillo Martínez

Departamento de Producción Agraria

Universidad Pública de Navarra

Secretario

Dr. Francisco Manuel Cazorla López

Departamento de Microbiología

Universidad de Málaga

Vocal

Dra. Chiaraluce Moretti

Departamento de Ciencias Agrarias, Alimentarias y Medioambientales

Universidad de Perugia

Suplentes

Dr. Pablo Rodríguez Palenzuela

Departamento de Biotecnología – Biología Vegetal

Universidad Politécnica de Madrid

Dr. Diego Romero Hinojosa

Departamento de Microbiología

Universidad de Málaga

Dr. Roberto Buonaurio

Departamento de Ciencias Agrarias, Alimentarias y Medioambientales

Universidad de Perugia

Área de Genética.

Departamento de Biología Celular, Genética y Fisiología.

Instituto de Hortofruticultura Subtropical y Mediterránea (IHSM)

Universidad de Málaga – Consejo Superior de Investigaciones Científicas

Dr. **CAYO J. RAMOS RODRÍGUEZ**, Catedrático del Área de Genética del Departamento de Biología Celular, Genética y Fisiología.

INFORMA:

Que **ELOY CABALLO PONCE** ha realizado en este Departamento y bajo mi dirección el trabajo titulado "Host specificity and virulence of the phytopathogen bacteria *Pseudomonas savastanoi*", que constituye su memoria de Tesis Doctoral para aspirar al grado de Doctor con Mención Europea en Biotecnología Avanzada. Y para que así conste, y tenga los efectos que correspondan, en cumplimiento con la legislación vigente, extiendo el presente informe.

En Málaga, a 14 de octubre de 2016.

Fdo: Cayo J. Ramos Rodríguez

A mi familia

A Blanca

A los que sois o habéis sido componentes del laboratorio de Carmen. A Javi Ruiz por echarme más de un cable burocrático. A Carmen por aclararme cuando me liaba con los pAMEs y echarme un capotazo en algún congreso. A Jose por su ayuda con cualquier pregunta de plásmidos, efectores y sistemas de defensa, ¡mucha suerte en tu etapa asiática! Al Picha, un máquina de las qRT siempre disponible para resolver dudas relacionadas. A Niebla y Javi por vuestra energía y entusiasmo. A "los padres" de la generación actual: Adela, Ainhoicilla, Charo y Juanjo. A Luiso, el único que entiende las palabras "chaleco" y "botines", el experto en montajes y vídeos absurdos. A Eduardo por aconsejarme cómo mantener las plantas y sus continuas bromas. A los genéticos de la Torre: Pepe, Maikel, Álvaro, Bego (en el fondo sigues siendo genética), Manolo, Ana Luna, Edgar, Tábata y Nati. A los demás profesores del Área de Genética por dedicarme su tiempo cuando se lo he pedido. A los técnicos Mayte, Silvia, Jessi, Rocío y, especialmente, a Pablo por que no nos faltase de ná. A todos los alumnos internos con los que he coincidido en el Área de Genética. A Eli, Pulido, Javi y Lucía por la producción y cuidado de las plantas. A Manoli por el procesamiento de tumores *in vitro*. Muchísimas gracias a todos.

A todos los jefes del grupo de Biología y Control de Enfermedades de Plantas del IHSM: Antonio, Francis, Alejandro, Diego, Juan Antonio y Lola. A todos los que se fueron y a los que llegado durante mi Tesis: Guti, Víctor, David, Claudia, Nuria, Laura, Houda, Eva, María, Davinia, Jesús Martínez, Carmen, Jesús Cámara, Conchita, Joaquín, Jesús Hierrezuelo, Irene, Marisa, Zahira, Saray, France, Sandra, Alvarito y al gran magister Nacho. Muchas gracias por los consejos en los seminarios; la ciencia y el ocio en los congresos; y, sobretodo, vuestra disponibilidad siempre que lo he necesitado.

A Pieter y Regina por acogerme en la EEZ, dedicar mucho de vuestro tiempo a enseñarme el manejo del HPLC y ver la historia desde otro punto de vista. A Chusmari y Silvia por facilitarme la vida en el laboratorio. A Nené, Javi, Elena, Laura, Ali, Bertrand, María…Y por su puesto a Carlos, timasso en Málaga!! Gracias, gracias y mil veces gracias. To Vittorio for his time, motivation and making me feel part of the group from the very beginning (I would never had imagined drinking beers with my boss on my bench). To the Bacteriology lab: Giulia, Iris, my dear Gordi, Luca, Fede, Gowri and specially to Meng, hope to see you again anywhere. To everyone who shared so many moments with me in Trieste: Ramit, Riccardo, Nadja, Costo, Ketaki, Tea...Thanks!!!!

A todos mis amigos de fuera del laboratorio. No os nombro porque, afortunadamente, sois muchísimos. No puedo dejar de agradeceros la cantidad de buenos momentos que hemos

vivido y el contar con vosotros en los no tan buenos. Me habéis escuchado y dado buenos consejos para seguir adelante estos años.

A la familia Sabarit Peñalosa, gracias por acogerme entre vosotros y por la comodidad que siento en vuestra casa siempre.

A toda mi familia. Habéis tenido la mala suerte de criaros en una posguerra y, aun así, conseguisteis sacar a vuestras familias adelante en tiempos difíciles, pero siempre con la humildad e integridad que os caracteriza. Gracias por vuestro esfuerzo abuelos, por vosotros somos hoy lo que somos. Sois mi ejemplo. A mis tíos y primos por iluminar mi cara cada vez que nos juntamos. A mis hermanos Irene y Fernando (ayyy mi Cinín) por comprender lo que he necesitado en cada momento, gracias por preocuparos siempre por mí. Y, sobre todo, a mis ejemplares padres (José y Encarnación) por transmitirnos los valores que os inculcaron y de los cuales me siento más que orgulloso. Por darnos siempre lo mejor en nuestra crianza, pero sin excesos para así aprender a valorar el esfuerzo y el sacrificio. Por sentirme seguro con vuestro respaldo y por vuestros sabios consejos con el viento a favor y, especialmente, en contra. Si algún día soy padre querría ser como vosotros. Muchísimas gracias, presumo de tener esta familia.

Puse mis ojos en ti nada más llegar y hemos recorrido en el mismo vagón este camino. Sabes mejor que nadie lo que me ha costado llegar a la última estación, tienes mucha culpa de que logre alcanzarla. Has tenido que soportar mis malos humos, mis resoplidos y mis agobios sin tener culpa. Aun así, te han quedado fuerzas para intentar buscarle un sentido a lo que yo no se lo encontraba, todo para hacerme feliz. Por todo ello, por compartir tu vida conmigo y por mil cosas más, muchas gracias Blanca. Me bajo de este tren, buen viaje para lo que te queda.

La verdadera ciencia enseña, sobre todo, a dudar y a ser ignorante

Miguel de Unamuno

Index

UNIVERSIDAD
DE MÁLAGA

Abbreviations

AHL: acyl-homoserine lactone

ANOVA: Analysis of variance

Ap: Ampicillin

ASAP: A systematic annotation package

bv: biovar

Blast: Basic local alignment search tool

bp: Base pair(s)

cCNA: Complementary DNA

CECT: Colección española de cultivos tipo

cfu: Colony forming units

CI: Competitive index

CK: Cytokinin

Cm: Cloramphenicol

CV: Crystal violet

DNA: Deoxyribonucleic acid

dpi: Days post-inoculation

DW: Dry weight

E. coli: Escherichia coli

EPS: Exopolysaccharides

GFP: Green fluorescent protein

Gm: Gentamycin

h: Hours

HSL: homoserine lactone

HPLC: High performance liquid chromatography

HPLC-MS: High performance liquid chromatography-mass spectrometry

HR: Hypersensitive response

IAA: indole 3-acetic acid

ICMP: International Collection of Microorganisms from Plants

Kb: Kilobase

KB: King B medium

Km: Kanamycin

LB: Luria Bertani medium

M: Molar

MEGA5: Molecular evolutionary genetic analysis

mg: Milligrams

min: Minutes

ml: Millilitres

mM: Millimolar

mV: Millivolts

M9A: M9 minimal medium with anthranilate

NCPPB: National collection of plant pathogenic bacteria

nm: nanometre

OD: Optical density

ORF: Open reading frame

PCR: Polymerase chain reaction

ppb: parts per billion

PG: Phylogroup

Psd: *Pseudomonas savastanoi* isolated from dipladenia

Psf: *Pseudomonas savastanoi* pv. fraxini

Psn: *Pseudomonas savastanoi* pv. nerii

Psr: *Pseudomonas savastanoi* pv. retacarpa

Pst: *Pseudomonas syringae* pv. tabaci

Psv: *Pseudomonas savastanoi* pv. savastanoi

Psy: *Pseudomonas syringae* pv. syringae

RACE: Rapid amplification of cDNA ends

RNA: Ribonucleic acid

Rt: Retention time

RT-PCR: Reverse transcription polymerase chain reaction

RT-qPCR: Reverse transcription quantitative polymerase chain reaction

SOB: Super optimal broth medium

STM: Signature-tagged mutagenesis

T3SS: Type three secretion system

UV: Ultraviolet

WHOP: Woody host and *Pseudomonas*

µg: Micrograms

Resumen

El complejo *Pseudomonas syringae* se constituye principalmente de bacterias Gram (-) patógenas de plantas con importancia desde el punto de vista económico y agrícola. El resurgir de antiguas enfermedades de plantas (como la mancha bacteriana del tomate causada por *P. syringae* pv. tomato) y la aparición de nuevas infecciones en todo el mundo (por ejemplo, el chancro del castaño de indias provocado por *P. syringae* pv. aesculi) colocan a *P. syringae* a la cabeza de un ranking de bacterias fitopatógenas de plantas en función de su importancia científica y económica (Mansfield *et al.*, 2012). En base a su rango de huésped, las bacterias de este complejo se clasifican en más de 60 patovares y 10 especies diferentes. Las bacterias del complejo *P. syringae* también se pueden clasificar mediante criterios moleculares: basados en hibridaciones DNA-DNA se distinguen 9 genomospecies (Gardan *et al.*, 1999) y por tipificación multilocus de secuencias se diferencian 13 filogrupos (Berge *et al.*, 2014). A grandes rasgos, la clasificación en filogrupos se correlaciona con las genomospecies.

Pseudomonas savastanoi es una de las especies englobadas dentro del complejo *P. syringae*. Los síntomas generados por *P. savastanoi* incluyen crecimientos hiperplásicos (tumores) o excrecencias en el tallo y las ramas de la planta y, rara vez, en los frutos y las hojas. Esta especie se divide en 4 patovares: savastanoi (aislados de olivo), nerii (aislados de adelfa), fraxini (aislados de fresno) y retacarpa (aislados de retama). Aparte de los mencionados, *P. savastanoi* puede infectar otros huéspedes como el jazmín, mirto, granado o dipladenia (plantas del género *Mandevilla*). La infección producida en este último huésped está adquiriendo una importancia significativa debido a su creciente expansión (se han descrito casos en Estados Unidos y varios países de Europa) y las consecuencias que conlleva, con hasta el 70% de plantas no comercializables (Pirc *et al.*, 2014). Sin embargo, la tuberculosis del olivo es la enfermedad más conocida provocada por *P. savastanoi*. A pesar de que la tuberculosis del olivo es probablemente la primera enfermedad de plantas descrita y que la identificación de su agente causal se remonta a finales del siglo XIX (Savastano, 1886), el estudio de la interacción entre *P. savastanoi* y sus huéspedes ha captado poca atención. La secuenciación del genoma de *P. savastanoi* pv. savastanoi NCPPB (Psv) 3335 (Rodriguez-Palenzuela *et al.*, 2010) junto con el establecimiento de un material vegetal adecuado y la puesta a punto de ensayos de virulencia (Rodriguez-Moreno *et al.*, 2008) ha establecido a Psv como la bacteria modelo para el estudio de las interacciones bacteria-planta leñosa (Ramos *et al.*, 2012). En este sentido, en los últimos años se han descubierto una serie de factores necesarios para la adaptación y la virulencia de Psv en el olivo. El ácido 3-indolacético (IAA) y las citoquininas (CKs), fitohormonas producidas por Psv, juegan un papel crucial en el desarrollo del tumor (Magie & Wilson, 1962; Smidt & Kosuge, 1978; Surico *et al.*, 1985; Iacobellis *et al.*, 1994). La biosíntesis de IAA se produce a través

de la ruta de la 3-indolacetamida, en la que, en primer lugar, el triptófano se convierte en 3-indolacetamida por la enzima triptófano 2-monooxigenasa (codificada por *iaaM*). La 3-indolcetamida se transforma posteriormente en IAA por la enzima 3-indolacetamida hidroxilasa (codificada por *iaaH*) (Magie *et al.*, 1963; Kosuge *et al.*, 1966). Cepas mutantes de estos genes ven mermada su virulencia y producción de IAA, aunque ésta no se bloquea por completo (Aragon *et al.*, 2014). Por otro lado, se ha demostrado que cepas del patovar nerii son capaces de conjugar el IAA a lisina mediante la acción de la proteína codificada por el gen *iaaL*, disminuyendo la actividad de la fitohormona (Hutzinger & Kosuge, 1968). Además, esta enzima también es relevante para la formación del tumor aunque cepas del patovar nerii mutantes del gen *iaaL* son avirulentas (Glass & Kosuge, 1988) o hipervirulentas (Cerboneschi *et al.*, 2016) en adelfa. Por el contrario, la ruta biosintética de citoquininas no se han estudiado a fondo, aunque la producción de esta fitohormona se distribuye entre las bacterias fitopatógenas que generan tumores (Morris, 1986). Inicialmente, la enzima isopentenil transferasa convierte el adenosín monofosfato en isopentenil adenina e isopentenil adenosina. Ambas moléculas se hidroxilan para generar trans-zeatina y trans-ribosilzeatina. Sólo el gen *ptz* se ha descrito en *P. savastanoi* (Powell y Morris, 1986), que se encuentra tanto en plásmidos como cromosomas de los aislados de oliva y de adelfa (Powell & Morris, 1986; Iacobellis *et al.*, 1994; Perez-Martinez *et al.*, 2008). El sistema de secreción tipo III (T3SS por sus siglas en inglés) es una jeringa molecular que permite la translocación de proteínas, denominadas efectores, desde el citoplasma bacteriano a la célula vegetal, donde interfiere con los procesos celulares y conducen (o no) al establecimiento de la enfermedad (Büttner & He, 2009). La formación de tumores depende fundamentalmente de la funcionalidad del T3SS (Sisto *et al.*, 2004; Perez-Martinez *et al.*, 2010; Matas *et al.*, 2012), dado que la mutación de diferentes elementos de este sistema conlleva una drástica reducción de la virulencia. Aunque la función concreta de la mayoría de los efectores del T3SS en la interferencia con los sistemas de defensa de las planta aún se desconoce, el conjunto de éstos podría ser uno de los factores más importantes en la determinación del espectro de huésped en las bacterias fitopatógenas (Baltrus *et al.*, 2011). El genoma de Psv NCPPB 3335 contiene 33 posibles efectores del T3SS. La mayoría de ellos están ubicados en el cromosoma y sólo dos (hopAF1-1 y hopAO1) se localizan en plásmidos (Bardaji *et al.*, 2011; Matas *et al.*, 2014). Recientemente se ha demostrado la translocación de nueve de estos efectores a través del T3SS y su interferencia con las respuestas de defensa de la planta (Matas *et al.*, 2014; Castaneda-Ojeda *et al.*, 2016). El metabolismo del segundo mensajero di-GMP cíclico (c-di-GMP) también contribuye a la virulencia de Psv. El c-di-GMP se sintetiza por la acción de diguanilato ciclasas y enzimas fosfodiesterasas son las encargadas de su degradación. Recientemente se ha demostrado que tanto una fosfodiesterasa como una diguanilato ciclasa

de Psv NCPPB 3335 están implicadas en la virulencia de Psv NCPPB 3335 en plantas de olivo (Matas *et al.*, 2012; Aragon *et al.*, 2015a; Aragon *et al.*, 2015b). Otro de los factores de virulencia de Psv descritos hasta la fecha es el sistema de regulación por *quorum sensing*, constituido por una proteína de la familia LuxI que sintetiza una molécula señal y una proteína, de la familia LuxR, que se una a la molécula señal y modifica la transcripción de una serie de genes. Mutantes de las proteínas homólogas a LuxI y LuxR de una cepa de Psv aislada en Italia, denominada DAPP-PG 722, no generan tumores en olivo (Hosni *et al.*, 2011). Dentro del complejo *P. syringae*, sólo se han determinado los genes regulados por *quorum sensing* en patógenos de plantas no leñosas (Yu *et al.*, 2014; Taguchi *et al.*, 2015), quedando por dilucidar los genes controlados por este sistema en *P. savastanoi*. Mediante una mutagénesis aleatoria por inserción de transposones se han identificado otros factores relacionados con la adaptación y la virulencia de Psv. Entre otros, se identificaron genes implicados en el metabolismo bacteriano, la tolerancia a estrés o estructuras de la superficie celular (Matas *et al.*, 2012). Además de todos los elementos mencionados anteriormente, existen otros que podrían ser necesarios para la adaptación y la virulencia de Psv. Uno de ellos consiste en una región cromosómica de Psv NCPPB 3335 de unas 15 kilobases, inicialmente denominada VR8 y referida durante esta Tesis Doctoral como región WHOP, que codifica genes cuya función está posiblemente relacionada con el metabolismo de compuestos aromáticos. La región WHOP está ausente en los genomas de bacterias patógenas de plantas herbáceas, pero presente con otros patógenos de plantas leñosas (Ramos *et al.*, 2012). Por tanto, la región WHOP podría estar implicada en la adaptación de bacterias a huéspedes leñosos, aunque aún no se ha demostrado

Esta Tesis Doctoral se ha dirigido al estudio de factores relacionados con la especificidad de huésped y la virulencia de *P. savastanoi*: el capítulo I se concentra en el estudio de la región WHOP, el capítulo II analiza el sistema de regulación por *quorum sensing* en Psv NCPPB 3335 y el capítulo III ahonda en la biología de cepas de *P. savastanoi* aisladas de dipladenia.

El papel de la región WHOP en la adaptación a huéspedes leñosos y en el catabolismo de compuestos aromáticos derivados de las plantas se ha propuesto por diversos autores (Green *et al.*, 2010; Rodriguez-Palenzuela *et al.*, 2010; O'Brien *et al.*, 2011; Ramos *et al.*, 2012). La codificación de una serie de genes incluidos en la región WHOP se ha relacionado con la capacidad de varias cepas del complejo *P. syringae* de crecer de manera endofítica en plantas de kiwi, un comportamiento que no muestran otras cepas del complejo *P. syringae* carentes de estos genes. Este resultado sugiere que la WHOP juega un papel importante en la colonización de huéspedes leñosos (Bartoli *et al.*, 2015a). Para la mayoría de los patovares del complejo *P. syringae* los genomas de, al menos, una cepa se encuentran disponibles en las bases de datos,

lo cual nos permitió analizar la distribución de la región WHOP dentro del complejo *P. syringae*. La región WHOP se conserva completamente en 16 patovares de *P. syringae*, en los 4 patovares de *P. savastanoi* y en las especies *Pseudomonas amygdali* y *Pseudomonas meliae*. La gran mayoría de ellas son patogénicas en órganos leñosos y pertenecen a los filogrupos 1 y 3, lo cual concuerda con observaciones previas (Bartoli *et al.*, 2015a; Nowell *et al.*, 2016). Por el contrario, la región WHOP está ausente en prácticamente la totalidad de las bacterias patógenas de plantas herbáceas y que infectan hojas de plantas leñosas. Esta región está parcialmente conservada en algunas cepas del filogrupo 2, cuyos genomas contienen homólogos a los genes del operón *catBCA*. No obstante, el origen filogenético del operón *catBCA* de estas bacterias es diferente al de las bacterias que contienen la región WHOP.

En la región WHOP se localizan catorce genes, algunos de los cuales son homólogos a otros previamente caracterizados. Los genes PSA3335_3199 a PSA3335_3201 y PSA3335_3202 a PSA3335_3204 son homólogos, respectivamente, a los operones *catBCA* y *antABC*, que se encuentran en otras bacterias del género *Pseudomonas* (Houghton *et al.*, 1995; Nojiri *et al.*, 2002; Maeda *et al.*, 2003; Urata *et al.*, 2004; Li *et al.*, 2010). El operón *antABC* participa en la conversión de antranilato en catecol, que se transforma posteriormente en 3-oxoadipato enol-lactona por la las enzimas del operón *catBCA*. Los genes PSA3335_3205 (*antR*) y PSA3335_3213 (*benR*), orientados en el sentido opuesto a los demás, codifican los reguladores transcripcionales de los operones *antABC* y *benABCD*, respectivamente. El operón *benABCD* está implicado en la degradación de benzoato a catecol en *Pseudomonas putida* (Jeffrey *et al.*, 1992); sin embargo, este operón no está presente en el genoma de Psv NCPPB 3335. Aunque los genes PSA3335_3207 a PSA3335_3211 no son homólogos a ningún otro descrito con anterioridad, es posible que intervengan en el metabolismo de compuestos aromáticos (Rodriguez-Palenzuela *et al.*, 2010). Inicialmente, se determinó la organización de todos estos genes mediante retrotranscriptasa-PCR (RT-PCR) utilizando cebadores diseñados para amplificar las regiones intergénicas. Los resultados obtenidos demostraron que la región WHOP se organiza en cuatro operones diferentes (*catBCA*, *antABC*, *ipoABC* y *dhoAB*) y tres genes que se transcriben de manera independiente (*antR*, PSA3335_3206 y *benR*). Con el objetivo de determinar la función y el papel en la virulencia y la adaptación de Psv a plantas de olivo de cada uno de estos clusters se construyeron cepas mutantes por intercambio alélico de los operones *catBCA*, *antABC*, *ipoABC* y *dhoAB* y del gen PSA3335_3206; junto con cepas complementantes que expresaban el cluster correspondiente desde un plásmido. Para analizar la implicación del operón *antABC* en el metabolismo del antranilato la cepa Psv NCPPB 3335, un mutante en el gen *antA* y la cepa complementante se expusieron a un medio mínimo suplementado con antranilato y se analizó

la concentración de este compuesto pasadas 24 horas mediante cromatografía líquida de alta eficacia (HPLC). En el sobrenadante correspondiente a la cepa silvestre Psv NCPPB 3335 no se detectó antranilato, confirmando la capacidad de esta bacteria de degradarlo. Por el contrario, una cantidad de antranilato prácticamente igual a la del inicio del experimento se detectó en el medio correspondiente al mutante del gen *antA*. En la cepa mutante *antA* complementada con el operón *antABC* completo se detectó una pequeña cantidad de antranilato (aproximadamente el 10% de la cantidad inicial) y la acumulación de catecol en el medio, posiblemente debido a la generación de un cuello de botella en la asimilación de catecol en esta cepa. Para confirmar el papel del operón *catBCA* en el metabolismo de catecol se empleó una metodología análoga a la descrita anteriormente, con la excepción de suplementar el medio mínimo con catecol en lugar de antranilato. En el medio correspondiente a Psv NCPPB 3335 no se detectó catecol, indicando que esta cepa consumió completamente el catecol presente en el medio. Por el contrario, en el sobrenadante de una cepa mutante del gen *catB* se detectaron varios compuestos que no se pudieron identificar, pero que posiblemente estaban relacionados con el catetol al presentar un tempo de retención y un espectro de absorción en el ultravioleta (UV) muy similar al de este compuesto. Esta hipótesis se ve reforzada por el hecho de que la cepa mutante del gen *catB* complementada con el operón *catBCA* no acumuló en el sobrenadante estos compuestos posiblemente relacionados con el catecol. Relacionado con el operón *catBCA*, se ha descrito que la actividad dienolactona hidrolasa (posiblemente codificada por el gen *dhoA*) está involucrada en el metabolismo de catecoles halogenados en la cepa *Pseudomonas* B13 (Schlomann *et al.*, 1990), en la que también participan las enzimas CatA y CatB. Para analizar la posible participación de los operones *dhoAB* y *catBCA* en el catabolismo del 4-clorocatechol en Psv NCPPB 3335, la cepa silvestre y sus mutantes Δ*catB* y Δ*dhoAB* se expusieron a un medio mínimo suplementado con 4-clorocatecol durante 24 horas y el sobrenadante fue analizado por HPLC. No se detectó 4-clorocatecol en el sobrenadante de Psv NCPPB 3335 y el mutante del operón *dhoAB*, mientras que en el mutante *catBCA* la concentración del compuesto era cuatro veces inferior a la inicial. Por tanto, Psv NCPPB 3335 puede degradar 4-clorocatecol por la acción, en parte, de las enzimas del operón *catBCA*, pero de forma independiente del operón *dhoAB*. Finalmente, se determinó que el operón *ipoABC* presenta actividad oxigenasa sobre compuestos aromáticos. A esta conclusión se llegó gracias al hecho de que determinadas oxigenasas son capaces de oxidar la molécula de indol y, tras una serie de pasos que ocurren espontáneamente, conducir a la formación del compuesto azul índigo. En este sentido, el cultivo en un medio mínimo suplementado con indol de una cepa de Psv que expresa el operón *ipoABC* desde un plásmido multicopia resultó en la producción de indigo.

Debido a que la región WHOP se encuentra principalmente en patógenos órganos leñosos dentro del complejo *P. syringae*, resultó particularmente interesante analizar su papel en la interacción de Psv NCPPB 3335 con plantas de olivo. Para este fin se utilizaron dos modelos diferentes, plantas de olivo micropropagadas (no leñosas) y plantas de un año de edad (leñosas). Las plantas se inocularon con Psv NCPPB 3335 y cada una de sus cepas mutantes en los clusters de la región WHOP. Transcurridos 30 días desde la inoculación, no se observaron diferencias visuales en el tamaño de los tumores desarrollados en plantas micropropagadas entre la cepa silvestre y sus mutantes. De hecho, la cuantificación del volumen tumoral usando un escáner 3D confirmó que el volumen de los tumores generados por los mutantes no era significativamente diferente al de Psv NCPPB 3335. Sin embargo, sí se observaron diferencias en el tamaño del tumor generado en plantas leñosas 90 días después de la inoculación. La mayor reducción en el volumen de los tumores se obtuvo para el mutante Δ*antA*, 3.1 veces más pequeñas en comparación con la cepa silvestre. Además, las plantas inoculadas con los mutantes Δ*catB* y Δ*ipoABC* desarrollaron tumores que eran, respectivamente, 2.37 y 1.57 veces más pequeños que los producidos por Psv NCPPB 3335. Por tanto, los operones *antABC*, *catBCA* e *ipoABC* juegan un papel en la virulencia de Psv NCPPB 3335 en las plantas de olivo leñosas, pero no en plantas no leñosas. Se ha propuesto que durante la degradación de IAA pueden generarse catecol y antranilato (Leveau & Gerards, 2008). El antranilato es un precursor en la síntesis del triptófano, sustrato inicial en la ruta de la 3-indolacetamida para la biosíntesis de IAA. Teniendo en cuenta que la cepa mutante del operón *antABC* acumula antranilato, podría producirse un desequilibrio en la cantidad de triptófano y, por tanto, en la biosíntesis de IAA causando una disminución en la virulencia de la bacteria.

También se llevaron a cabo infecciones mixtas de la Psv NCPPB 3335 con cada uno de los mutantes afectados en la región WHOP tanto en olivos leñosos como no leñosos. En plantas de olivo no leñosas, los valores del índice competitividad (CI por sus siglas en inglés) no fueron estadísticamente diferentes a uno, a excepción de la del mutante Δ*ipoABC* (CI= 0.39±0.16). Sin embargo, cuando las inoculaciones mixtas se llevaron a cabo en olivos leñosos, los valores de CI obtenidos fueron estadísticamente menor que uno, excepto para el mutante Δ*antA*. De manera similar a los resultados descritos anteriormente para la virulencia de las cepas mutantes, los mutantes Δ*catB*, ΔPSA3335_3206 y Δ*dhoAB* están afectados en su crecimiento competitivo exclusivamente en plantas de olivo leñosas. Aunque la estructura química de la madera no se puede definir con precisión para una especie determinada, se compone principalmente de los polisacáridos celulosa y hemicelulosa (65-75%) y lignina (18-35%) (Pettersen, 1984). La lignina es un polímero complejo sintetizado a partir de tres alcoholes hidroxicinamil (alcoholes p-

cumaril, coniferil y sinapil) (Boerjan *et al.*, 2003; Ralph *et al.*, 2004). Se sabe que la degradación de moléculas relacionadas con la lignina se canaliza vía protocatecuato y catecol. Mientras que la maquinaria de degradación catecol se limita a varios patovares dentro del complejo *P. syringae*, la degradación de protocatecuato en intermediarios del ciclo de Krebs es una característica ampliamente distribuida en las bacterias del complejo *P. syringae*. Por lo tanto, la presencia de la región WHOP podría permitir la degradación vía catecol de compuestos relacionados con la lignina y facilitar la colonización de órganos leñosos.

El capítulo II de esta Tesis Doctoral se centró en el estudio del sistema de regulación en respuesta a la densidad celular, denominado *quorum sensing*, en Psv NCPPB 3335. Como se mencionó anteriormente, este sistema se compone principalmente de proteínas pertenecientes a las familias LuxI y LuxR y una molécula señal denominada acil-homoserinalactona (AHL) en bacterias Gram (-).; El análisis de 265 genomas bacterianos mostró que el número de proteínas LuxI y LuxR no siempre es coincide: además del par *luxI/luxR* canónico, muchos genomas también contienen genes *luxR* adicionales que no están asociados a un *luxI* (Case *et al.*, 2008). Las proteínas codificadas por estos *luxR*, llamados *luxR* solos (Subramoni & Venturi, 2009), responden a las AHL producidas por la propia bacteria (Chugani *et al.*, 2001) u otras bacterias que se encuentren en el mismo cercanas (Ahmer *et al.*, 1998). Además, se ha descrito una sub-familia de *luxR* solos exclusivos de bacterias asociadas de plantas y que, posiblemente, responden señales producidas por la planta (Patel *et al.*, 2013). El sistema de *quorum sensing* de *P. syringae* está bien caracterizado en *P. syringae* B728a (Quinones *et al.*, 2004; Quinones *et al.*, 2005), habiéndose identificado los genes regulados por *luxR* en esta cepa (Yu *et al.*, 2014). Además, un reciente estudio transcriptómico identificó los genes regulados por *quorum sensing* en *P. syringae* pv. tabaci 6605 (Taguchi *et al.*, 2015). Ambos estudios se han llevado a cabo en cepas patógenas de plantas herbáceas; sin embargo, se sabe muy poco de este sistema de regulación en bacterias del complejo *P. syringae* patógenas de huéspedes leñosos. *P. syringae* pv. actinidiae, patógeno de kiwi, no produce AHLs, pero sí responde a ellas gracias a la presencia de varios *luxR* solos en su genoma (Patel *et al.*, 2014). Por otro lado, los genes *pssI* y *pssR* de Psv DAPP-PG 722, homólogos a *luxI* y *luxR* respectivamente, juegan un papel importante en la virulencia de esta bacteria (Hosni *et al.*, 2011). Dado que *P. syringae* pv. actinidiae y *P. savastanoi* pv. savastanoi difieren en el la presencia/ausencia de *luxI*, se llevó a cabo la búsqueda de homólogos a los genes *luxI* y *luxR* en los genomas de 27 cepas pertenecientes a los filogrupos 1 a 4. Mientras todas las cepas del filogrupo 3 analizadas contienen un homólogo a *luxI*, la presencia de éste en las cepas analizadas de los filogrupos 2 y 3 es variable, incluso entre aislados diferentes del mismo patovar. Por otro lado, el número y tipo de homólogos a *luxR* también es

variable entre las cepas analizadas. Mientras que todas las cepas del filogrupo 3 analizadas contienen tres homólogos a *luxR* (dos de ellos *luxR* solos), salvo *P. syringae* pv. aesculi NCPPB 3681 que contiene un tercer *luxR* solo, el número y tipo de homólogo a *luxR* es diverso entre las bacterias del filogrupo 2 y varía ligeramente entre las cepas del filogrupo 1. El genoma de Psv NCPPB 3335 contiene el par *luxI*/*luxR* canónico junto con dos *luxR* solos, una organización que está conservada en otras cepas pertenecientes a los cuatro patovares de *P. savastanoi* cuyos genomas se han secuenciado recientemente (Moretti *et al.*, 2014; Bartoli *et al.*, 2015b; Thakur *et al.*, 2016). Sin embargo, y aunque la secuencia de ambos *pssI* es 100% idéntica, Psv NCPPB 3335 y Psv DAPP-PG 722 producen diferentes tipos de AHL. Dado que en Psv DAPP-PG 722 el sistema de regulación por *quorum sensing* juega un papel fundamental en la virulencia de la bacteria, decidimos determinar los genes cuya expresión depende de la síntesis de AHLs en Psv NCPPB 3335, la cepa que usamos rutinariamente en nuestro laboratorio. Para ello, construimos un mutante por intercambio alélico en el gen *pssI* de Psv NCPPB 3335 e hicimos un análisis comparativo del transcriptoma de esta cepa con la silvestre, a partir del cual se concluyó que pocos genes muestran una expresión diferencial. Se seleccionaron los genes sobreexpresados/reprimidos 1.87 o más veces en el mutante con respecto a la cepa silvestre para su validación mediante RT-PCR cuantitativa (RT-qPCR). Se validó la expresión diferencial de tres de estos genes (*pssR*, *pdhT* y *pdhQ*), todos ellos sobreexpresados en el mutante Δ*pssI*. Por tanto, en las condiciones ensayadas, el regulón *pssI* está compuesto por tres genes, un resultado contrasta con el gran número de genes cuya expresión depende del respectivo homólogo a *luxI* en el patógeno de tabaco *P. syringae* pv. tabaci 6605 (Taguchi *et al.*, 2015). Para comparar los sistemas de regulación de las dos cepas, se seleccionaron los seis genes más sobreexpresados/reprimidos en el mutante del homólogo a *luxI* en *P. syringae* pv. tabaci 6605 y se analizó su expresión mediante RT-qPCR en Psv NCPPB 3335. Ninguno de los genes examinados mostró la misma regulación dependiente de *luxI* observada *P. syringae* pv. tabaci 6605, dado que la transcripción de la mayoría estos genes es independiente de *pssI* en Psv NCPPB 3335. Estos resultados indican que, aunque ambas cepas producen el mismo tipo de molécula señal, la regulación por *quorum sensing* es diferente en Psv NCPPB 3335 y *P. syringae* pv. tabaci 6605.

En *P. syringae* pv. syringae B728a LuxR promueve la transcripción de *luxI* al llegar a un umbral de concentración de AHLs (Quinones *et al.*, 2004), un fenómeno común en otros sistemas de *quorum sensing*. Puesto que la regulación por *quorum sensing* en Psv NCPPB 3335 parece ser diferente a otras cepas del complejo *P. syringae* decidimos analizar si PssR promueve la expresión de *pssI*. Para ello, el promotor de *pssI* se fusionó al gen *lacZ* y se midió la actividad

β-galactosidasa a lo largo de una curva de crecimiento en Psv NCPPB 3335 y sus cepas mutantes de los genes *pssI* y *pssR*. En la cepa silvestre se observó un aumento de la actividad enzimática al aproximarse a la fase estacionaria de cultivo que también ocurre en las cepas mutantes de los genes *pssI* y *pssR*. Estos resultados sugieren, por tanto, que el aumento de la transcripción de *pssI* es independiente de la síntesis de AHLs y de PssR, lo cual coincide con lo observado por otros autores en Psv DAPP-PG 722 (Hosni *et al.*, 2011). Además, otra diferencia importante entre los sistemas de *quorum sensing* entre Psv NCPPB 3335 y *P. syringae* pv. syringae B728a aparece al analizar la actividad β-galactosidasa asociada al promotor de *pssI* en *P. syringae* pv. syringae B728a. La actividad enzimática medida en B728a fue, por lo general, 60 veces más alta que en NCPPB 3335 bajo las mismas condiciones experimentales, lo cual refuerza la hipótesis de una regulación por *quorum sensing* diferente en bacterias muy relacionadas filogenéticamente. Curiosamente, se ha descrito que cepas de *Pseudomonas aeruginosa* aisladas de nichos diversos difieren en los genes regulados por *quorum sensing* (Chugani et al., 2012). Además de las diferencias observadas entre Psv NCPPB 3335 y otras cepas del complejo *P. syringae*, resultados generados en esta Tesis Doctoral también muestran diferencias entre aislados de Psv. Además de no producir el mismo tipo de AHL, la virulencia y la producción de exopolisacáridos están controlados por *quorum sensing* en Psv DAPP-PG 722, pero no en Psv NCPPB 3335.

Finalmente, el capítulo III se ha centrado en la caracterización de varias cepas de *P. savastanoi* patógenas de dipladenia, las cuales producen manchas necróticas en las hojas y tallos además de tumores en éstos. El primer aislamiento de estas cepas se produjo en Estados Unidos en 2010 (Putnam *et al.*, 2010) y se han descrito casos en Francia (Eltlbany *et al.*, 2012), Alemania (Eltlbany *et al.*, 2012) y Eslovenia (Pirc *et al.*, 2014). Durante el desarrollo de esta Tesis Doctoral se detectaron plantas con los síntomas típicos de la necrosis bacteriana de la dipladenia al sur de España, procediéndose al aislamiento e identificación del agente causal (Caballo-Ponce & Ramos, 2016). En este capítulo se trabajó con una colección de aislados procedente de cada uno de los países donde se ha descrito la enfermedad. Anteriormente se ha sugerido que los aislados de *P. savastanoi* patógenos de dipladenia (denominados aquí Psd) podrían haberse originado a partir de plantaciones infectadas de adelfa en el sur de Francia (Eltlbany *et al.*, 2012). En esta Tesis Doctoral se construyó un árbol filogenético basado en las secuencias parciales de cuatro genes *housekeeping* que confirmó la identificación de los Psd como *P. savastanoi*. Además, la agrupación de los Psd con cepas de *P. savastanoi* pv. nerii en una sub-rama dentro de la rama correspondiente a la especie *P. savastanoi* apoya la relación entre ambos. Para caracterizar el rango de huésped de los Psd se llevaron a cabo inoculaciones en olivo, adelfa, fresno, dipladenia y retama. Los resultados mostraron que todos los aislados de dipladenia son patógenos, además

de en dipladenia, en olivo y fresno, aunque la sintomatología generada en éste es variable. Ninguna de las cepas de los patovares savastanoi, fraxini y retacarpa inoculadas en dipladenia desarrollaron síntomas. Por el contrario, la sintomatología generada por las cepas del patovar nerii en dipladenia variaba desde la formación de un tumor a la ausencia de síntomas. Estos resultados indican que las cepas de *P. savastanoi* aisladas de dipladenia constituyen un nuevo patovar dentro de la especie *P. savastanoi* y apoyan la relación entre las cepas Psd y *P. savastanoi* pv. nerii. Se procedió a una caracterización a nivel molecular de los Psd en base al genotipo del gen *iaaL* y el perfil de plásmidos nativos. Para estudiar el genotipo del gen *iaaL* se empleó una técnica diseñada para distinguir entre diferentes alelos del gen empleando PCR-RFLP (Matas *et al.*, 2009). El patrón de bandas obtenido en todos los PSDs fue idéntico, lo que contrasta con la variabilidad observada entre cepas diferentes de *P. savastanoi* pv. savastanoi (Matas *et al.*, 2009). De manera similar, el número y tamaño de los plásmidos nativos era muy parecido entre diferentes *P. savastanoi* aisladas de dipladenia, mientras que el perfil plasmídico en cepas de *P. savastanoi* pv. savastanoi varía de un aislado a otro (Perez-Martinez *et al.*, 2008). Teniendo en cuenta que en el año 2010 se describió por primera vez la enfermedad y que los Psd son muy parecidos en las características moleculares analizadas en esta Tesis Doctoral se podría especular con que la generación de estas cepas ocurrió recientemente y no ha transcurrido el tiempo suficiente para originar variabilidad entre ellas. Dado que el contenido de plásmidos nativo es similar entre los diferentes PSDs y que el aislado *P. savastanoi* Ph3 contiene una copia plasmídica del gen *iaaM* (Eltlbany *et al.*, 2012), decidimos generar una cepa curada de este plásmido siguiendo un método descrito previamente (Comai & Kosuge, 1980). Conseguimos curar la copia plasmídica del gen *iaaM*, pero no el plásmido que contiene dicha copia (llamado aquí pIAAM). Los resultados sugieren que se produjo una reorganización de los plásmidos que condujo a la curación de otro plásmido (denominado pPh3A) y no del pIAAM. En cualquier caso, la cepa obtenida, a la que llamamos CRpiaaM, mostró una atenuación severa de la virulencia y la supervivencia en plantas de dipladenia, además de la producción de IAA. Sin embargo, CRpiaaM produce cantidades pequeñas de IAA que aumentan cuando el medio se suplementa con triptófano. Este resultado refuerza la hipótesis propuesta por nuestro grupo de investigación de la existencia de una ruta de biosíntesis de IAA alternativa a la de la 3-indolacetamida en cepas de *P. savastanoi* (Aragon *et al.*, 2014)

General introduction

1. The *Pseudomonas syringae* complex

The *Pseudomonas syringae* complex includes a great number of Gram (-) phytopathogenic bacteria with a special significance from an economic, agricultural and scientific point of view. The resurgence of ancient plant diseases (as the bacterial speck of tomato caused by *P. syringae* pv. tomato) and the continuous outbreak of new infections worldwide (for instance, the bleeding canker of horse chestnut caused by *P. syringae* pv. aesculi) placed the *P. syringae* complex on the top of the ranking of plant-pathogenic bacteria (Mansfield *et al.*, 2012). Strains from the *P. syringae* complex show high variability in their epiphytic survival and host range, including many economically important crops, woody plants and weeds, such as the model plant *Arabidopsis thaliana*. Moreover, *P. syringae* infections cause high diversity of symptoms, including spotting and necrosis on leaves, fruit rooting and knots and cankers on stems (Fatmi *et al.*, 2008). Besides plant–associated bacteria, the *P. syringae* complex includes strains isolated from other diverse habitats such as snowmelt waters, irrigation canals or epilithic biofilms (Morris *et al.*, 2007; Morris *et al.*, 2010; Berge *et al.*, 2014).

Based on the host range, the *P. syringae* complex currently encompasses over 60 different pathovars and 10 species (Young, 2010; Parkinson *et al.*, 2011), which have been classified following two diverse methodologies. On one hand, bacterial strains were sorted in nine genomospecies by DNA-DNA hybridizations, although some incongruence in the nomenclature appeared (Gardan *et al.*, 1999). For instance, genomospecie 2 includes *Pseudomonas savastanoi, Pseudomonas ficuserectae*, *Pseudomonas meliae* and *Pseudomonas amygdali* type strains and, therefore, should be considered synonyms and the correct name should be *P. amygdali*, as it was the earliest recorded (Gardan *et al.*, 1999). However, the scientific community refers to these strains as separate species. On the other hand, Multi Locus Sequence Typing (MLST) classified the strains of the *P. syringae* complex in phylogroups (PGs). Initially four different groups were identified (Sarkar & Guttman, 2004) that have been sequentially widened to 13 different phylogroups, which in turn split in several clades (Berge *et al.*, 2014). The classification in phylogroups correlates to genomospecies (Fig. 1), although small differences are found (Parkinson *et al.*, 2011; Berge *et al.*, 2014).

N2355 *P. syringae* pv. *ciccaronei*
N3278 *P. savastanoi* pv. *nerii*
N639 *P. savastanoi* T AB039514
N4050 *P. savastanoi* pv. *retacarpa*
ICMP7711 *P. savastanoi* pv. *fraxini*
N3617 *P. syringae* pv. *daphniphylli*
ICMP11894 *P. syringae* pv. *cunninghamiae* PTS
N3618 *P. syringae* pv. *raphiolepidis*
N2607 *P. amygdali* T AB039509
N3143 *P. syringae* pv. *myricae*
N3465 *P. tremae* T
N3033 *P. meliae* T
N3682 *P. syringae* pv. *hibisci*
N2411 *P. savastanoi* pv. *glycinea*
JCM2400 *P. ficuserectae* T AB039501
ICMP17524 *P. syringae* pv. *cerasicola*
N2356 *P. syringae* pv. *mellea*
N1427 *P. syringae* pv. *tabaci*
N1016 *P. syringae* pv. *sesami*
N3681 *P. syringae* pv. *aesculi*
N2331 *P. syringae* pv. *eriobotryae*
N3464 *P. syringae* pv. *dendropanacis*
ICMP9419 *P. syringae* pv. *castaneae*
N3688 *P. syringae* pv. *photiniae*
N632 *P. syringae* pv. *ulmi*
ICP13650 *P. syringae* pv. *broussoneti*
N52 *P. savastanoi* pv. *phaseolicola*
N1034 *P. syringae* pv. *mori*

PG 3; G.sp 2

N187342 *P. caricapapayae* T AB039507
N2640 *P. syringae* pv. *helianthi*
N2488 *P. syringae* pv. *tagetis*

PG 6; G.sp 7

N958 *P. syringae* pv. *aceris*
ICMP16925 *P. syringae* pv. *solidagae*
N225 *P. syringae* pv. *dysoxyli*
N2848 *P. syringae* pv. *papulans*
N3093 *P. syringae* pv. *japonica*
PDDCC3023 *P. syringae* T AB039516
N2096 *P. syringae* pv. *lapsa*
N2585 *P. syringae* pv. *pisi*
N871 *P. syringae* pv. *aptata*
N2612 *P. syringae* pv. *atrofaciens*

PG 2; G.sp 1

N2397 *P. syringae* pv. *atropurpurea*
N588 *P. syringae* pv. *garcae*
N3690 *P. syringae* pv. *zizaniae*
N1898 *P. syringae* pv. *striafaciens*
N3364 *P. syringae* pv. *porri*
N600 *P. syringae* pv. *coronafaciens*
N3683 *P. syringae* pv. *oryzae*

PG 4; G.sp 4

N1921 *P. syringae* pv. *viburni*
N3487 *P. avellanae* T
N2995 *P. syringae* pv. *morsprunorum*
N3739 *P. syringae* pv. *actinidiae*
N2598 *P. syringae* pv. *theae*

G.sp 8

N2724 *P. syringae* pv. *berberidis*
N1106 *P. syringae* pv. *tomato*
N1817 *P. syringae* pv. *antirrhini*
N1626 *P. syringae* pv. *apii*
N1879 *P. syringae* pv. *delphinii*
CFBP5524 *P. syringae* pv. *spinaceae*
N4290 *P. syringae* pv. *avii*
N2761 *P. syringae* pv. *persicae*
N537 *P. syringae* pv. *lachrymans* PTS
N2039 *P. syringae* pv. *maculicola*

PG 1; G.sp 3

N133 *P. syringae* pv. *primulae*
PDDCC2848 *P. viridiflava* T AB039520
N963 *P. syringae* pv. *ribicola* PTS

PG 7; G.sp 6

N3257 *P. syringae* pv. *philadelphi* PTS
ICMP15200 *P. syringae* pv. *alisalensis* PTS
N1437 *P. cannabina* T
N3781 *P. syringae* pv. *coriandricola* PTS

PG 5; G.sp 9

N943 *P. cichorii* T AB039526

P. cichorii

0·02

Figure 1. Phylogenetic analysis of the *Pseudomonas syringae* complex**.** The tree was constructed using the *rpoD* partial sequences of species type strains (STS) and pathovar type strains (PTS). Asterisks indicate phylogroups defined by Parkinson *et al.* (2011). PG; phylogroup; G.sp; genomospecie. Picture adapted from Parkinson *et al.* (2011).

2.   *Pseudomonas savastanoi*

DNA-DNA hybridizations defined *P. savastanoi* as a different specie from *P. syringae* including three different pathovars: savastanoi, glycinea and phaseolicola (Gardan *et al.*, 1992a) and placed these strains in the genomospecie 2 of the *P. syringae* complex (Gardan *et al.*, 1999). A recent phylogeny of the core genome of *P. syringae* grouped *P. savastanoi* pv. savastanoi NCPPB 3335 with *P. syringae* pv. aesculi strains 2250 and NCPPB 3861 together with other strains of the PG3. However, the integration of pathovars glycinea and phaseolicola within *P. syringae* instead of *P. savastanoi* is widely accepted; *P. syringae* pv. phaseolicola 1448A and *P. syringae* pv. glycinea strains race 4 and B076 actually grouped in a different sub-branch within the main branch of PG3 in a phylogeny of the *P. syringae* core genome (Nowell *et al.*, 2014). In this PhD thesis, we will consider phaseolicola and glycinea as *P. syringae* instead of *P. savastanoi* pathovars.

Symptoms generated by *P. savastanoi* include hyperplasic growths (tumorous galls or knots) or excrescences on stem and branches of the plant and, rarely, on fruits and leaves (Fig. 2). Currently, *P. savastanoi* strains are classified into four pathovars: pv. savastanoi (Psv), pv. nerii (Psn), pv. fraxini (Psf) and pv. retacarpa (Psr), which correspond to strains isolated from the woody hosts olive, oleander, ash and Spanish broom, respectively. In addition, *P. savastanoi* isolates infect many other woody hosts, including jasmine (Gardan *et al.*, 1992b), privet (Gardan *et al.*, 1992b), mock privet (Gardan *et al.*, 1992b)*,* forsythia (Bradbury, 1986), buckthorn (Temsah *et al.*, 2007a), pomegranate (Bozkurt *et al.*, 2014), myrtle (Goumas *et al.*, 2000; Temsah *et al.*, 2007b; Cinelli *et al.*, 2014) and dipladenia (Putnam *et al.*, 2010; Eltlbany *et al.*, 2012; Pirc *et al.*, 2014; Caballo-Ponce & Ramos, 2016). The hosts infected by *P. savastanoi* belong to diverse plant families: *Apocynaceae*, *Oleaceae*, *Fabaceae*, *Lythraceae, Myrtaceae* and *Rhamnaceae* (Table 1), although the most common and studied hosts correspond to *Oleaceae* and *Apocynaceae* families.
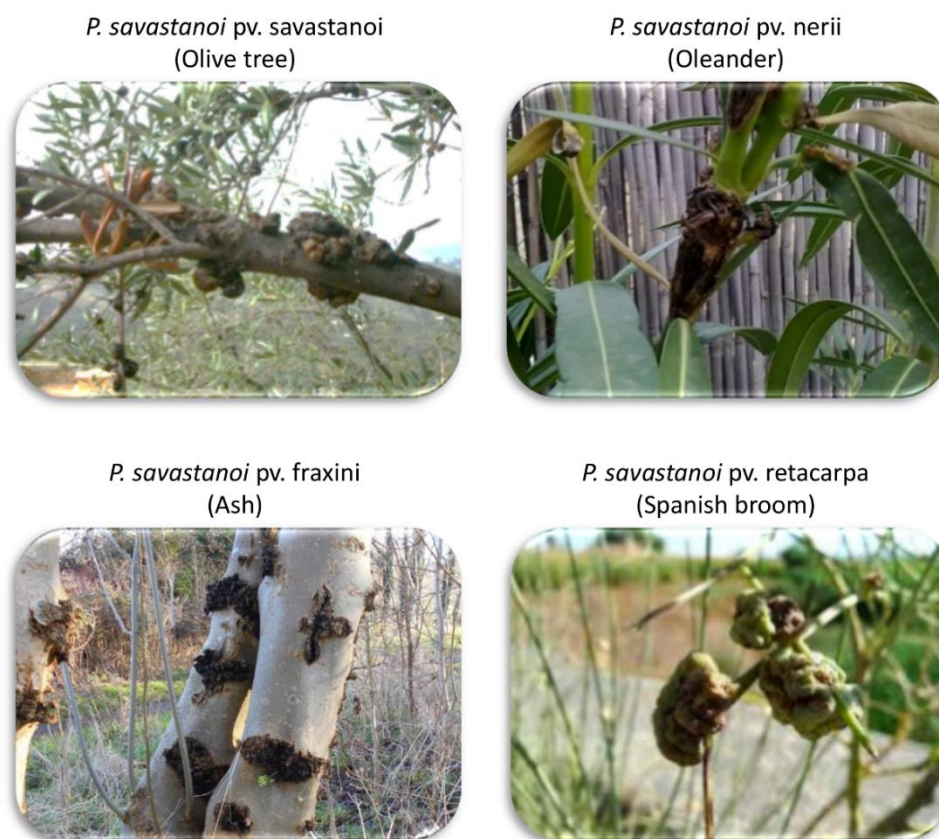
Figure 2. Typical symptoms induced by *P. savastanoi* strains on olive, oleander, ash and Spanish broom

Table 1. Susceptible hosts to *P. savastanoi* infections

Family	Specie	Common name	Pathovar[a]	Reference
Apocynaceae	*Mandevilla* spp.	Dipladenia	NA	(Eltlbany *et al.*, 2012)
	Nerium oleander	Oleander	nerii	(Janse, 1982)
Fabaceae	*Retama sphaerocarpa*	Spanish broom	retacarpa	(Alvarez *et al.*, 1998)
Lythraceae	*Punica granatum*	Pomegranate	savastanoi[b]	(Bozkurt *et al.*, 2014)
Myrtaceae	*Myrtus communis*	Myrtle	NA	(Goumas *et al.*, 2000)
Oleaceae	*Fontanesia phillyreoides*	Fontanesia	savastanoi[b]	(Mirik *et al.*, 2011)
	Forsythia spp.	Forsythia	NA	(Bradbury, 1986)
	Fraxinus excelsior	Ash	fraxini	(Janse, 1982)
	Jasminum spp.	Jasmine	NA	(Gardan *et al.*, 1992b)
	Ligustrum spp.	Privet	NA	(Gardan *et al.*, 1992b)
	Olea europaea	Olive	savastanoi	(Janse, 1982)
	Phillyrea spp.	Mock privet	NA	(Gardan *et al.*, 1992b)
Rhamnaceae	*Rhamnus alaternus*	Buckthorn	NA	(Temsah *et al.*, 2007a)

[a]NA, not assigned

[b]Assignation of *P. savastanoi* strains isolated from pomegranate to pathovar savastanoi was made in the bases of their ability to induce knot formation in olive plants; however, pathogenicity tests in other hosts were not performed. For fontanesia isolates, the identification as *P. savastanoi* pv. savastanoi based on non pathovar-specific PCR amplifications.

Cross-pathogenicity test revealed the host range of *P. savastanoi* pathovars (Janse, 1982; Alvarez *et al.*, 1998; Iacobellis *et al.*, 1998; Ramos *et al.*, 2012) (Table 2). In this sense, some isolates infect more than one host, as Psn strains, which induce knot formation on olive and oleander, whereas Psv only incite knot development on olive (Janse, 1982). Although cross-pathogenicity tests have been carried out for dipladenia (Eltlbany *et al.*, 2012), myrtle (Cinelli *et al.*, 2014) and jasmine (Taghavi & Hasan, 2012) isolates, they have not been ascribed to any of the established *P. savastanoi* pathovars. In addition, the pathogenicity of buckthorn, mock privet, forsythia and privet isolates on other hosts remains unknown.

Table 2. Cross-pathogenicity of *P. savastanoi* pathovars

P. savastanoi pv.	Host[a]			
	Ash	Oleander	Olive	Spanish broom
Fraxini	C	-	C	-
Nerii	K	K	K	-
Savastanoi	K	-	K	-
Retacarpa	-	-	-	K

[a]Ash, *Fraxinus* spp.; Oleander, *Nerium oleander*; Olive, *Olea europaea*; Spanish broom, *Retama sphaerocarpa*. C, cankers accompanied by wart-like excrescences; K, knots; -, no visible symptoms. Adapted from Ramos *et al.* 2012.

2.1 The olive knot disease

The olive knot has probably been the first plant disease clearly described. Theofrastus, considered the "father of botany" for his work on plants, reported knots and warts developed on olive trees for the first time in the IV century before Christ (Scortichini *et al.*, 2004). Luigi Savastano isolated and described 2200 years later the causative agent of the olive knot disease, originally named *Bacillus oleae tuberculosis* (Savastano, 1886) and currently known as *P. savastanoi* pv. savastanoi. Other non-pathogenic bacterial species have been found together with Psv within the olive knot, which has converted this disease as a model to study interspecies communities in a plant disease (Buonaurio *et al.*, 2015). For instance, *Pantoea agglomerans* (Cimmino *et al.*, 2006; Marchi *et al.*, 2006), *Erwinia toletana* (Rojas *et al.*, 2004) and *Erwinia oleae* (Moretti *et al.*, 2011) have been isolated from olive knots. These previous reports are only the top of the iceberg, given that a metagenomic analysis based on the sequencing of partial 16s rRNA from nine olive knots collected from different Italian geographical locations and olive cultivars revealed the existence of a more complex microbiome within the olive knot (Passos da Silva *et al.*, 2014).

The olive knot is considered one of the most relevant diseases affecting the olive crop, although its economic losses has not been estimated accurately (Young, 2004). Psv produces

knots or galls mainly on olive branches, although occasionally the pathogen has been isolated from the tree leaves, fruits and roots (Young, 2004). The major damage results on young trees, causing weaknesses in the branches that will form the future structure of mature trees. The vigour and growth of olive trees together with total yield and fruit fill might be moderate to severely affected by the olive knot disease (Schroth *et al.*, 1973). Olive trees cv. Arbequina inoculated with Psv showed a reduction in the vigour of the plant compared to non-inoculated trees. In this study, plant vigour was estimated as the fructifying surface, the fructifying volume and the area of trunk-cross sections (Quesada *et al.*, 2009). Psv is widely distributed to almost every region where olive tree is cultivated around the world, but its incidence depends on the geographical location and the cultivar. In this regard, olive knot appears to be most severe on autumn and spring, probably because of high temperatures and rainfalls (Surico, 1977). A recent study of Mediterranean populations of Psv adumbrated that the current Psv population is the result of a clonal expansion of a single strain. Nonetheless, rep-PCR identified two main Psv clusters, which in turn split in two sub-clusters that were associated with the geographical origin of the strains (Moretti *et al.*, 2016).

2.1.1 Disease cycle

Psv lives epiphytically on the surfaces of leaves and stems reaching the highest cell densities in warm and rainy months, whereas a decrease is observed in hot and dry months (Ercolani, 1978; Quesada *et al.*, 2007). Epiphytic bacteria can disseminate over short distances in olive orchards and, in addition, a connection between the epiphytic bacterial population and the number of knots developed on infected trees has been found (Quesada *et al.*, 2009). Psv can penetrate into plant tissues, taking advantage of wounds generated by climate conditions or agricultural practices, and changes from an epiphytic to a pathogenic lifestyle. As a pathogen, Psv multiply in the plant tissues and reach different population densities depending on the susceptibility of the cultivar (Varvaro & Surico, 1978; Penyalver *et al.*, 2006). The increase of bacterial populations leads to a proliferation of the cambium and the development of a knot, where elements of the xylem and phloem are more or less organized (Surico, 1977; Rodriguez-Moreno *et al.*, 2009). Psv cells aggregate inside the knot creating microcolonies and multilayer biofilms over the plant cell surfaces and the interior of plasmolysed cells facing the air-tissue interface of internal opened fissures. Additionally, Psv surrounds the stem vascular system and fills the lumen of newly generated xylem vessels (Rodriguez-Moreno *et al.*, 2009). The pathogen also colonizes the tissues around the infection point and disrupts the integrity of host cells trough pectolytic and hemicellulolytic enzymes, producing cavities filled with bacteria. These

cavities reach the knot surface trough fissures and favours bacterial dissemination to the environment (Surico, 1977; Rodriguez-Moreno *et al.*, 2009).

2.1.2 Disease control

The raise of olive plantations and the change in production methods bring the necessity of utilizing a sanitary guaranteed plant material. In this regard, Spain has implemented a certification for nurseries where periodic official inspections are carried out to ensure the quality of the plant material. There are no olive cultivars resistant to the knot disease, although plants can be divided into three categories according to their sensitivity to Psv infections (Penyalver *et al.*, 2006). Agricultural practices focusing on the reduction of the inoculum should be done to eradicate Psv from olive plantations, as to prune diseased branches and decrease the injuries produced during harvesting (Wilson, 1935; Trapero & Blanco, 1998). Pruning of diseased branches has been shown to be more efficient that tumour removal since fewer injuries are produced on the plant and epiphytic populations of Psv are reduced (Wilson, 1935; Teviotdale & Krueger, 2004; Quesada *et al.*, 2010). Chemical treatments with cupric compounds have also demonstrated their efficiency in the control of epiphytic populations of Psv on olive trees. The application of Bourdeaux mixture, cooper hydroxide, cooper oxyclorure and cooper-mancozeb has been demonstrated to efficiently control the olive knot disease (Wilson, 1935; Teviotdale & Krueger, 2004; Quesada *et al.*, 2010). Little information is available about the biological control of the olive knot disease. Strains of *P. syringae* pv. ciccaronei (Lavermicocca *et al.*, 2002), *Pseudomonas fluorescens* (Maldonado-González *et al.*, 2013) and *Bacillus subtilis* (Krid *et al.*, 2012) have been reported as antagonistic against Psv, although their ability to control the disease remains to be proved in the field. An integrated control strategy that includes all the methods mentioned before should be performed to control the olive knot disease efficiently

2.2 Leaf and stem spot and galls on dipladenia

Although the olive knot is the best-known plant disease caused by *P. savastanoi*, other infections caused by this pathogen are gaining relevance over the last years. Dipladenia, name referred to plants of the *Mandevilla* genus very appreciated in the ornamental market, has been reported as a susceptible host for *P. savastanoi* infections. This pathogen constitute today a major constraint for dipladenia nurseries, where symptomatic and unmarketable plants have reached up to 70% (Pirc *et al.*, 2014). Symptoms generated on dipladenia, reported for the first time in USA (Putnam *et al.*, 2010), consist on necrotic spots surrounded by a chlorotic halo on leaves (Fig. 3A) and the development of necrotic galls on stems (Fig. 3B). Later investigations

focused on a deeper identification and molecular characterization of the causal agent of this emergent disease, which initially was related phylogenetically to Psv and Psn. Besides, these authors identified the presence of typical *P. savastanoi* virulence factors in the plasmids sequences of bacterial strains isolated from dipladenia in Germany and France (Eltlbany *et al.*, 2012). Another study has enlarged the distribution of the bacterial necrosis of dipladenia to Slovenia (Pirc *et al.*, 2014). Understanding the biology of the causative agent of this disease will help to face its control and limit its consequences.
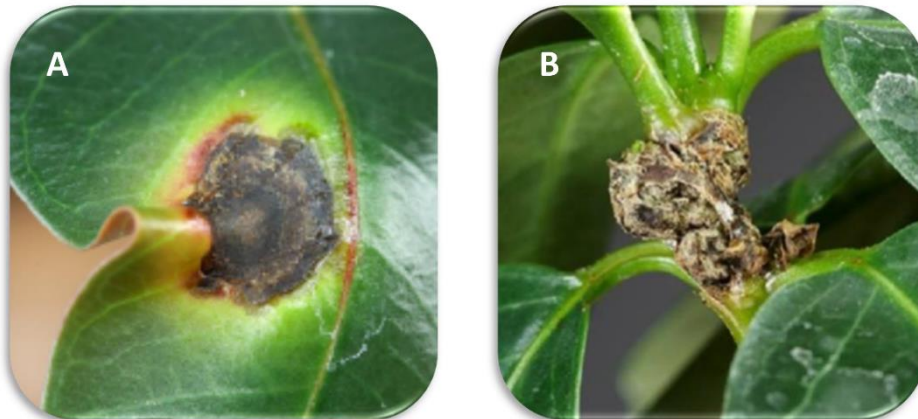
Figure 3. Symptoms induced by *P. savastanoi* strains on dipladenia (A) leaves and (B) stems. Pictures taken from Eltlbany *et. al.* (2012)

3. *P. savastanoi* virulence and adaptation factors

Sequencing of the first Psv genome (strain NCPPB 3335) revealed a vast repertoire of genes potentially involved in the virulence of the pathogen (Rodriguez-Palenzuela *et al.*, 2010; Bardaji *et al.*, 2011) and, together with the establishment of suitable plant material (Rodriguez-Moreno *et al.*, 2008) (Fig. 4), established Psv NCPPB 3335 (Perez-Martinez *et al.*, 2007) as a model bacterial pathogen to study its interaction with a woody host (Matas *et al.*, 2012; Ramos *et al.*, 2012). The genomic sequence of Psv strains DAPP-PG 722 (Moretti *et al.*, 2014), PseNe107 (Bartoli *et al.*, 2015b) and ICMP 4352 and those of the type strains of Psn ICMP 16943, Psf ICMP ICMP 7711 and Psr ICMP 16945 (Thakur *et al.*, 2016) have been recently published. Bioinformatics analysis of all these genomes should shed light into the host specificity determinants of this bacterial complex. Importantly, co-resident bacteria can also promote the virulence of Psv in olive plants, contributing to knot formation (Hosni *et al.*, 2011; Buonaurio *et al.*, 2015).

Figure 4. Typical symptoms of olive knot disease. White arrows in (A) mark knots induced on naturally infected plants. Symptoms induced by artificial inoculation of *P. savastanoi* pv. savastanoi NCPPB 3335 on (B) woody and (C) micropropagated (non-woody) olive plants.

3.1 Production of phytohormones

The development of knots on olive and oleander plants by *P. savastanoi* strains depends on bacterial production of the phytohormones indole 3-acetic acid (IAA) and cytokinins (CKs) (Magie & Wilson, 1962; Smidt & Kosuge, 1978; Surico *et al.*, 1985; Iacobellis *et al.*, 1994; Aragon *et al.*, 2014). The biosynthesis of IAA in *P. savastanoi* occurs via the indole 3-acetamide pathway (Fig. 5), where tryptophan is initially converted into indole 3-acetamide by a tryptophan 2-monooxygenase (encoded by the *iaaM* gene). Indole 3-acetamide is further transformed into IAA by the enzyme indole 3-acetamide hydroxylase (encoded by the *iaaH* gene) (Magie *et al.*, 1963; Kosuge *et al.*, 1966). Both *iaaM* and *iaaH* are co-transcribed in an operon, generally located on plasmids in Psn strains or in the chromosome in Psv (Comai & Kosuge, 1980; Caponero *et al.*, 1995; Perez-Martinez *et al.*, 2008). Two chromosomal copies of the *iaaMH* operon (named *iaaMH*-1 and *iaaMH*-2) were found in the genome of Psv NCPPB 3335 (Rodriguez-Palenzuela *et al.*, 2010); however, only *iaaMH*-1 contributes to the synthesis of IAA (Aragon *et al.*, 2014). A mutation in the *iaaMH*-2 operon did not affect the virulence of Psv NCPPB 3335 on olive trees, whereas a mutant strain in *iaaMH*-1 and a double mutant affected in both *iaaMH* operons (named *iaaMH*-1.2) induced identical attenuation of knot size in comparison to the wild type strain (Aragon *et al.*, 2014). Interestingly, small amounts of IAA are produced by the *iaaMH*-1 and the *iaaMH*-1.2 mutants of Psv NCPPB 3335 (Aragon *et al.*, 2014), suggesting that an alternative pathway for the biosynthesis of this phytohormone should be present in *P. savastanoi*. Additionally, *P. savastanoi* strains carry the *iaaL* gene, which in Psn has been shown to encode a protein that conjugates the IAA to lysine, leading to a less active IAA derivative (Hutzinger & Kosuge, 1968). This gene has been demonstrated to be involved in the virulence of Psn; however, *iaaL* mutants of Psn strains have been reported either not to cause

gall symptoms on oleander (Glass & Kosuge, 1988) or to be hypervirulent (Cerboneschi *et al.*, 2016). On the other hand, an *iaaL* mutant of *P. syringae* pv. tomato DC3000 has been reported to be hypovirulent in tomato plants (Castillo-Lizardo *et al.*, 2015). IAA not only favours the formation of the knot, but also acts as a signal molecule. It was recently demonstrated that the addition of IAA to a culture of Psv NCPPB 3335 resulted in reduction of the expression of two type three secretion system (T3SS) genes, as well as in an increased transcription of a type VI secretion system gene (Aragon *et al.*, 2014).
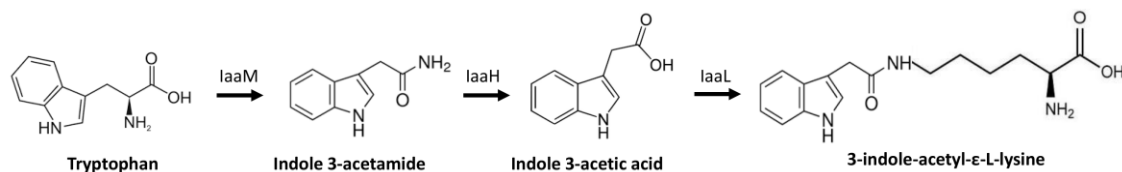
Figure 5. Metabolism of the auxin indole 3-acetic acid in *P. savastanoi* strains. IaaM, tryptophan 2-monooxigenase; IaaH, indole 3-acetamide hyrolase; IaaL, 3-indole-acetyl-ε-L-lysine synthase.

Production of cytokinins is distributed among knot-forming phytopathogenic bacteria (Morris, 1986). Initially, an isopentenyl transferase enzyme converts adenosine monophosphate into isopentenyl adenine and isopentenyl adenosine. Later, both molecules are hydroxylated to generate trans-zeatin and trans-zybosilzeatin. Only the *ptz* gene (*Pseudomonas* trans-zeatin) has been described in *P. savastanoi* (Powell & Morris, 1986), which is located in both plasmids and chromosome of olive and oleander isolates (Powell & Morris, 1986; Iacobellis *et al.*, 1994; Perez-Martinez *et al.*, 2008). Psv NCPPB 3335 carries a copy of the *ptz* gene in one of its three native plasmids (pPsv48A). Curing of pPsv48A led to an attenuation of the virulence in Psv NCPPB 3335, but did not affect the growth of the strain within the plant tissues (Bardaji *et al.*, 2011).

3.2 Type III secretion system

The T3SS is a molecular syringe that allows the translocation of proteins, named effectors, from the bacterial cytoplasm to the plant cell, where interference with cellular processes might help the pathogen to establish a disease (Büttner & He, 2009). Knot formation critically depends on the functionality of the T3SS (Sisto *et al.*, 2004; Perez-Martinez *et al.*, 2010; Matas *et al.*, 2012). A Psv ITM 317 miniTn5-insertion mutant in the *hrcC* gene (coding for a structural element of the T3SS) was impaired in knot development. Similarly, a knockout mutant of the *hrpA* gene (coding for the component of the T3SS pilus) showed a drastic attenuation of the virulence on woody olive trees compared to the parental strain Psv NCPPB 3335 (Perez-Martinez *et al.*, 2010). Not only structural elements of the T3SS play a role in the virulence of *P.* savastanoi: a miniTn5-

insertion mutant in the *hrpR* gene, coding for a positive regulator of the T3SS in *P. syringae* (Hutcheson *et al.*, 2001), was considered non-virulent compared to the wild type Psv NCPPB 3335 (Matas *et al.*, 2012). In addition, a Psv NCPPB 3335 derivative affected in the positive regulatory gene *hrpL* was described not to induce knot formation in olive (Matas *et al.*, 2014). Neither the *hrpA* nor the *hrpR* GFP-tagged mutant strains of Psv NCPPB 3335 colonize the plant hypertrophied tissue generated during the infection nor create the internal cavities observed in the knots developed by Psv NCPPB 3335. (Perez-Martinez *et al.*, 2010; Matas *et al.*, 2012).

T3SS effectors are important during different stages of pathogen-host interactions as they (i) promote the penetration and persistence of the pathogen in the host tissue; (ii) suppress the plant defence responses; and (iii) contribute to the access to nutrients, proliferation and growth of the pathogen (Gohre & Robatzek, 2008). Although the concrete function of the majority of T3SS effectors in the interference with plant defences remains unknown, the T3SS effector repertoire of phytopathogenic bacteria is one of the most relevant factors in determining the host range (Baltrus *et al.*, 2011). The genome of Psv NCPPB 3335 contains 33 putative effectors of the T3SS; most of which are encoded in the chromosome and only two (*hopAF1-1* and *hopAO1*) are plasmid-encoded (Bardaji *et al.*, 2011; Matas *et al.*, 2014). Recent studies from our laboratory have demonstrated the translocation of nine of these effectors through the T3SS and their interference with responses associated with plant immunity (Matas *et al.*, 2014; Castaneda-Ojeda *et al.*, 2016).

3.3 Metabolism of c-di-GMP

The modified nucleotide cyclic-di-guanylate (c-di-GMP) is a relevant secondary messenger in bacteria that mainly regulates the transition between sessile and planktonic lifestyles. In particular, c-di-GMP controls swimming and swarming motilities, synthesis of the extracellular matrix components and exopolysaccharide production (Zogaj *et al.*, 2001; Solano *et al.*, 2002; Christen *et al.*, 2006; Recouvreux *et al.*, 2008; Pérez-Mendoza *et al.*, 2011). This second messenger is synthesized from two molecules of guanosine triphosphate (GTP) by diguanylate cyclases and is degraded by phosphodiesterases. A characteristic GGDEF catalytic domain is found in diguanylate cyclases (Paul *et al.*, 2004), whereas EAL (Christen *et al.*, 2005; Tischler & Camilli, 2005) or HD-GYP (Ryan *et al.*, 2007) are the typical domains of phosphodiesterases. The genome of Psv NCPPB 3335 contains 34 proteins with a GGDEF domain, of which 14 also encode for an EAL domain (Rodriguez-Palenzuela *et al.*, 2010). Results from our laboratory demonstrated that a mini-Tn5 insertion mutant in a phosphodiesterase (BifA) exhibited a reduced virulence in comparison to Psv NCPPB 3335 (Matas *et al.*, 2012). Recently, a deeper

analysis of the BifA protein confirmed its involvement in the virulence and fitness of Psv in olive plants, as well as in controlling swimming motility (Aragon *et al.*, 2015a). The diguanylate cyclase DgcP is Pseudomonads-specific and has been shown to control biofilm formation, swimming motility and virulence not only in Psv NCPPB 3335, but also in *Pseudomonas aeruginosa* PAK (Aragon *et al.*, 2015b). In addition, the DgcP-mediated modulation of c-di-GMP is related with the regulation of the type VI secretion system-related genes in both Psv NCPPB 3335 and *P. aeruginosa* PAK (Aragon *et al.*, 2015b).

3.4 The quorum sensing system

Bacteria modulate their behaviour in a cell density-dependent manner through a mechanism named quorum sensing. Gram (-) bacteria synthesize a signal molecule, commonly *N*-acyl-homoserine lactones (AHLs), by the action of a LuxI-family protein. AHLs diffuse through the plasma membrane and accumulates in the bacterial environment. Upon reaching a threshold concentration of AHLs (the quorum), a LuxR-family protein binds to its cognate AHL and modulate the expression of target genes (Fuqua *et al.*, 2001; Whitehead *et al.*, 2001) (Fig. 6). Several transcriptomic analysis have concluded that the presence of AHLs regulates the expression of a vast number of genes in plant-associated bacteria (Coutinho *et al.*, 2013; Kim *et al.*, 2013; Kim *et al.*, 2014). Interestingly, a mutant in the *luxI* homolog of the tobacco pathogen *P. syringae* pv. tabaci, closely related to *P. savastanoi*, showed over 200 genes which expression differed compared to the wild type strain (Taguchi *et al.*, 2015). The quorum sensing system controls traits related with the virulence and epiphytic fitness of phytopathogenic bacteria (Von Bodman *et al.*, 2003). In this regard, this regulatory network is crucial for the virulence of Psv DAPP-PG 722 , as mutant strains in the *luxI* and *luxR* homologs induced the generation of knots significantly smaller than those generated in plants infected with the wild type strain (Hosni *et al.*, 2011). However, genes which expression is under the control of the quorum sensing system in Psv remain to be elucidated.
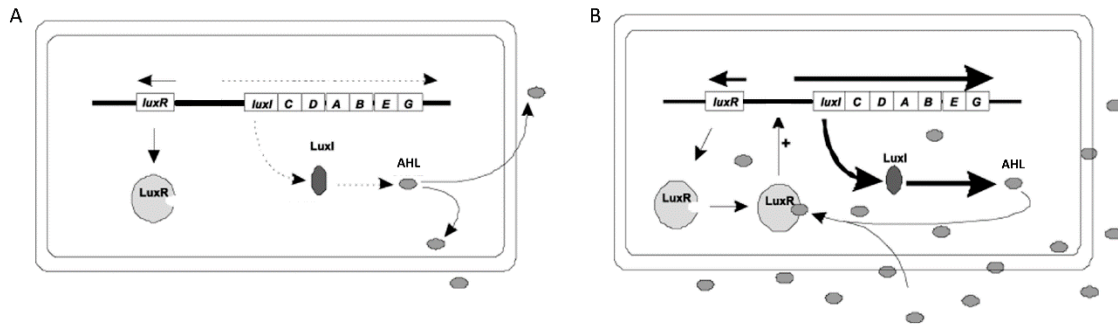
Figure 6. The quorum sensing regulation at (A) low cell densities and (B) high cell densities. LuxI synthesizes the signal molecule (AHL) that binds to LuxR at high cell densities and modulate the expression of target genes. Picture adapted from Witehead *et al.* (2001).

3.5 Other virulence and adaptation factors

Previous work in our laboratory following a signature-tagged mutagenesis (STM) strategy identified 58 genes necessary for the full virulence and growth of Psv on olive trees (Matas *et al.*, 2012) (Fig. 7). Genes required for the synthesis of nine amino acids and three vitamins were identified, as well as genes coding for transporters of compounds present in the plant apoplast, such as citrate, sulphate and glutamate. Aside from the *hrpR* gene mentioned above (see section "Type III secretion system"), other factors identified include genes of the types II and IV secretion systems, as well as proteins taking part in stress tolerance or the synthesis of the cell wall, the phytohormone IAA and the second messenger c-di-GMP.
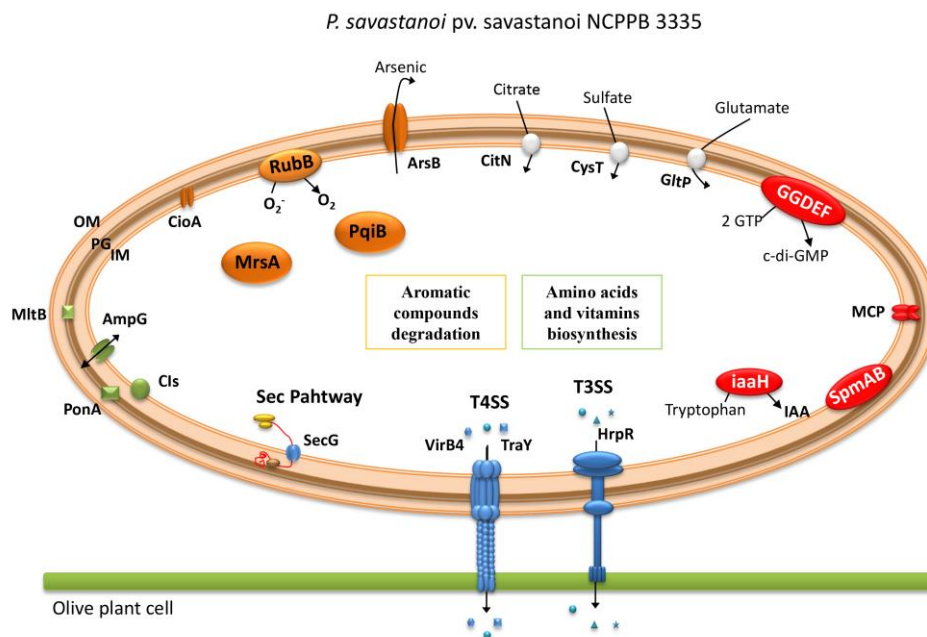
Figure 7. Schematic representation of virulence-associated mechanisms in *Pseudomonas savastanoi* pv. savastanoi identified by signature-tagged mutagenesis. Functional categories are represented in different

colors: blue, secretion systems; green, cell-surface structures; orange, stress tolerance; gray, transporters; and red, others. OM, outer membrane; PG, peptidoglycan; IM, inner membrane; T3SS, type III secretion system; T4SS, type IV secretion system; MCP, methyl-accepting chemotaxis protein; GGDEF, GGDEF/EAL domain protein-coding gene; IAA, indole 3-acetic acid. Picture from Matas *et al.* (2012).

The degradation of aromatic compounds is also crucial for the virulence and fitness of Psv NCPPB 3335 on olive knots. A Psv NCPPB 3335 *catJ* mutant, impaired in the final steps of the β-ketoadipate pathway of aromatic compounds degradation (Fig. 8), induced the generation of smaller knots compared with the wild type strain and was severely impaired in its competitive growth (Matas *et al.*, 2012).
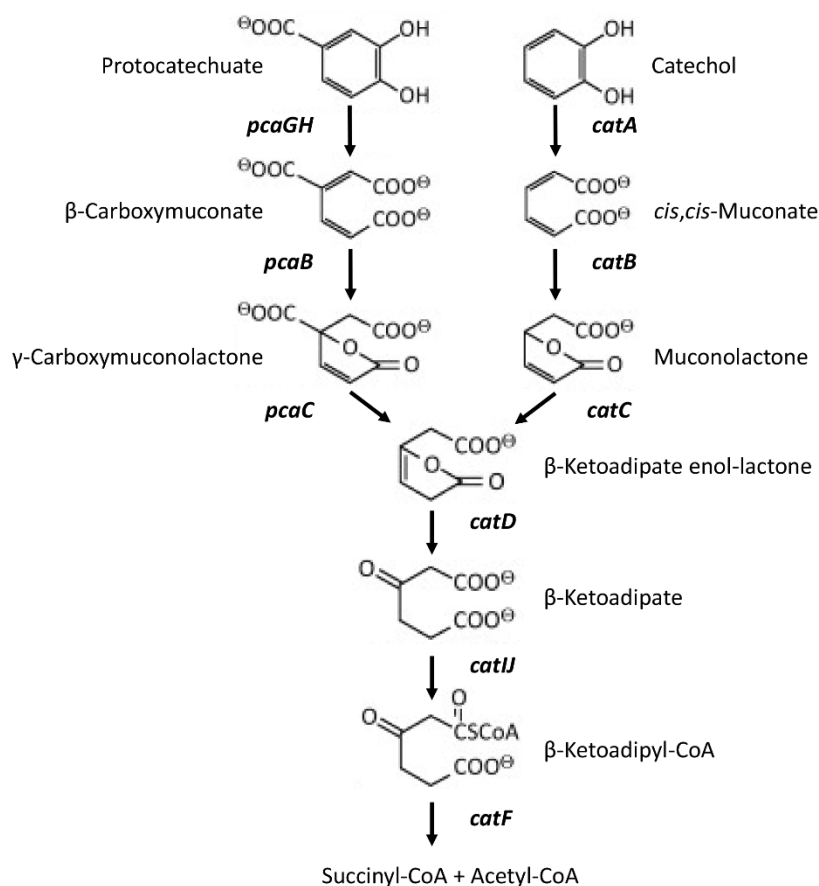
Figure 8. Schematic representation of the β-Ketoadipate pathway for the bacterial degradation of aromatic compounds into intermediaries of the Krebs cycle. Genes coding for the enzymes of this pathway are shown next to the arrows. Picture adapted from Harwood & Parales (1996).

The comparison of the genome of Psv NCPPB 3335 with other *P. syringae* strains infecting herbaceous host unveiled a region of about 15 kb unique to Psv that encodes for genes likely related with the metabolism of aromatic compounds (Rodriguez-Palenzuela *et al.*, 2010). This region, originally named VR8 and referred as the WHOP (from woody host and *Pseudomonas*) region in this PhD Thesis, is shared with other strains of the *P. syringae* complex isolated from woody hosts, and is absent in *P. syringae* strains pathogenic on non-woody hosts (Ramos *et al.*, 2012) (Fig. 9). Among others, the *catBCA* operon, which is implicated in the degradation of catechol through the β-Ketoadipate pathway (Fig. 8), is located within the WHOP region (Fig. 9). Moreover, this region has been associated with the ability of *P. syringae* strains to colonize kiwifruit trees (Bartoli *et al.*, 2015a). However, the role of this region in the virulence and adaptation of Psv to olive plants has not been addressed up to date.
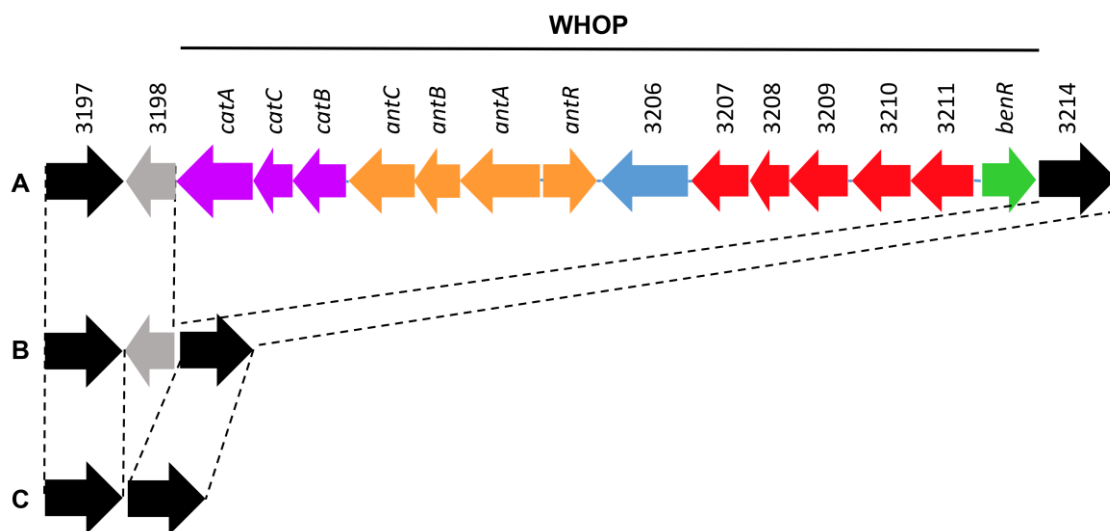
Figure 9. Schematic map of the WHOP region in the genomes of *P. savastanoi* pv. *savastanoi* NCPPB 3335 and other *P. syringae* strains which genome have been sequenced. (A) *P. savastanoi* pv. savastanoi NCPPB 3335, *P. syringae* pathovars aesculi strains 2250 and NCPPB 3681, morsprunorum MAFF 302280 and actinidiae MAFF 302091. (B) *P. syringae* pathovars tabaci ATCC 11528, mori 301020, phaseolicola 1448A, glycinea race 4, lachrymans MAFF 302278 and japonica MAFF 301072. (C) *P. syringae* pathovars syringae B728a, tomato DC3000 and oryzae 1_6. Picture adapted from Ramos *et al.* (2012).

Objectives

Understanding the virulence mechanisms of phytopathogenic bacteria and the factors contributing to its adaptation to their plant hosts are pivotal for the design of strategies to control plant diseases. The main goal of this Thesis was to analyse elements possibly involvedin the virulence and adaptation of *Pseudomonas savastanoi* to its woody hosts following different approaches. Firstly, the genome of the olive pathogen *P. savastanoi* pv. savastanoi NCPPB 3335 harbours a region of about 15 kb that is shared with other strains of the *Pseudomonas syringae* complex infecting woody plants, which role in the adaptation to woody hosts has been suggested (Ramos *et al.*, 2012). Secondly, the virulence of *P. savastanoi* pv. savastanoi DAPP-PG 722 has been shown to depend on cell to cell communication via the quorum sensing system (Hosni *et al.*, 2011), although genes controlled by this system in *P. savastanoi* pv. savastanoi remain to be elucidated. Finally, an emerging disease caused by *P. savastanoi* on dipladenia is becoming widespread worldwide and understanding the biology of these isolates is crucial to control the disease. Considering all this information, the following objectives were proposed:

1. To determine the role of the WHOP region in the adaptation and the virulence of *P. savastanoi* pv. savastanoi NCPPB 3335 to olive plants.

2. To identify the genes regulated by the quorum sensing system in *P. savastanoi* pv. savastanoi NCPPB 3335.

3. To identify the causal agent of dipladenia leaf and stem spot in Spain.

4. To characterize phenotypically a collection of *P. savastanoi* strains isolated from symptomatic dipladenia plants in several countries.

Chapter I

WHOP, a genomic region associated to woody hosts in the *Pseudomonas syringae* complex, contributes to the virulence and fitness of *Pseudomonas savastanoi* pv. savastanoi in olive plants

INTRODUCTION

Bacteria belonging to the *Pseudomonas syringae* complex cause diseases in a wide variety of both herbaceous and woody plant species. In fact, *P. syringae* is one of the most important models for the molecular analysis of plant-pathogen interactions (Mansfield *et al.*, 2012). Most research on the molecular interactions established by *P. syringae* has focused on herbaceous plant pathogens, since herbaceous plants are easier to handle than woody hosts. Moreover, the tomato plant pathogen *P. syringae* pv. tomato DC3000, whose genome sequence was published more than 10 years ago, infects the well-known model plant *Arabidopsis thaliana* (Buell *et al.*, 2003). However, diseases caused by *P. syringae* on woody hosts, and especially on fruit trees, are of extreme relevance. For example, the economic losses due to the bacterial canker of kiwifruit caused by *P. syringae* pv. actinidiae in New Zealand were estimated to cost over US$ 885 million over a 15-year period (Lamichhane *et al.*, 2014).

During the last decade, considerable efforts have been made to establish suitable models to study the interaction of bacteria from the *P. syringae* complex with woody plants. In this sense, three model systems have predominantly been used: *P. savastanoi* pv. savastanoi/olive (Rodriguez-Palenzuela *et al.*, 2010; Matas *et al.*, 2012; Ramos *et al.*, 2012), *P. syringae* pv. aesculi/horse chestnut (Green *et al.*, 2010) and *P. syringae* pv. actinidiae/kiwi (McCann *et al.*, 2013; Petriccione *et al.*, 2014; Bartoli *et al.*, 2015a; Gao *et al.*, 2016). Comparison of the draft genome sequence of *P. savastanoi* pv. savastanoi (Psv) NCPPB 3335 with those of other *P. syringae* strains that infect herbaceous hosts (i.e., *P. syringae* pv. tomato DC3000, *P. syringae* pv. phaseolicola 1448A and *P. syringae* pv. syringae B728a) revealed the presence of 12 regions longer than 10 kb unique to Psv NCPPB 3335. One of the most striking features found in one of these variable regions was a cluster of genes possibly related to the metabolism of phenolic compounds (Rodriguez-Palenzuela *et al.*, 2010; Ramos *et al.*, 2012). Similar genome comparisons carried out among four *P. syringae* pv. aesculi strains isolated from horse chestnut, i.e., the type-strain NCPPB 3681 isolated from leaf spots on Indian horse chestnut and three strains isolated from bleeding stem cankers on European horse chestnut in Britain, revealed the presence of a similar variable genomic region in all strains but not in the sequenced genomes of other *P. syringae* pathovars (Green *et al.*, 2010). Subsequent genome sequencing of *P. syringae* strains isolated from woody hosts revealed that this variable region, herein referred to as WHOP (from woody host and *Pseudomonas*), was also present in *P. syringae* pv. morsprunorum MAFF 302280 and *P. syringae* pv. actinidiae MAFF 302091, which are pathogenic to apricot and kiwi trees, respectively (Ramos *et al.*, 2012). Among other genes encoded in the WHOP region, the *antABC* and the *catBCA* operons were found, which are responsible for the transformation of

anthranilate into catechol and the degradation of catechol into β-ketodipate enol-lactone via the *ortho* (β-ketoadipate) pathway, respectively, in other *Pseudomonas* spp. (Taniuchi *et al.*, 1964; Ornston, 1966; Houghton *et al.*, 1995; Nojiri *et al.*, 2002; Urata *et al.*, 2004; Li *et al.*, 2010). In addition to the *antABC* and *catBCA* operons, other genes potentially related to the metabolism of phenolic compounds were found in the Psv NCPPB 3335 WHOP region (Rodriguez-Palenzuela *et al.*, 2010) and in the genomes of *P. syringae* pv. aesculi strains (Green *et al.*, 2010).

One role of the WHOP region in bacterial adaptation to woody hosts and the catabolism of plant-derived aromatic compounds has been proposed by several authors (Green *et al.*, 2010; Rodriguez-Palenzuela *et al.*, 2010; O'Brien *et al.*, 2011; Ramos *et al.*, 2012), and a recent comparative genomic analysis revealed that this region in *P. syringa*e phylogroups (PGs) 1 and 3 is significantly associated with woody hosts (Nowell *et al.*, 2016). However, functional studies of the genes encoded in the WHOP region are still scarce. A recent study reported a correlation between the presence of a cluster of genes located in the WHOP region and the ability of several *P. syringae* and Psv strains, all belonging to phylogroups PG1 and PG3, to grow endophytically in kiwifruit, i.e., *P. syringae* pv. actinidiae strains of bv. 1, bv. 3 and bv. 4; *P. syringae* pv. morsprunorum MAFF 302280; *P. syringae* pv. aesculi 0893_23; *P. syringae* pv. theae NCPPB 2598; and Psv strains NCPPB 3335 and PseNe107. In contrast, other *P. syringae* strains isolated from water or herbaceous hosts lacking this cluster did not colonize kiwifruit plants, suggesting a role for these genes in the colonization of the plant vascular system where lignin is an important compound (Bartoli *et al.*, 2015a). A role in knot development on olive plants has been reported for the Psv NCPPB 3335 *catJ* gene (Matas *et al.*, 2012). This gene, which is not encoded in the WHOP region but is present in the genomes of *P. syringae* strains isolated from non-woody hosts, encodes the subunit B of a putative β-ketoadipate CoA-transferase, an enzyme of the β-ketoadipate pathway involved in the conversion of β-ketoadipate enol-lactone into succinyl Co-A (Matas *et al.*, 2012). Conversely, epidemic strains of *P. syringae* pv. actinidiae have been reported to possess a plasmid encoding two gene clusters also related to the metabolism of aromatic compounds that are shared with the xylem pathogen *Xylella fastidiosa*. Interestingly, one of these clusters is reportedly related to the biosynthesis of anthranilate. In addition, a putative phenylacetate CoA ligase encoded in the second cluster has also been proposed to use anthranilate as a substrate (McCann *et al.*, 2013).

In this work, we analyse the organization, distribution, function and role of the WHOP region in the virulence and fitness *in planta* using the well-established model pathogen of woody hosts, Psv. The genetic organization of the WHOP region has been determined, as well as the

function of several genes located within this chromosomal region. Our results broaden the distribution of the WHOP region to other PG1 and PG3 members infecting woody hosts and show its partial conservation in only three PG2 pathovars. Furthermore, we demonstrate that several of the genes located within this region contribute to the fitness and virulence of this bacterium in woody olive plants but not in non-woody olive plants.

MATERIALS AND METHODS

Bacterial strains, media and growth conditions

Bacterial strains used in this study are listed in Table 1. Psv and *Escherichia coli* were grown at 28 °C or 37 °C, respectively, in Luria-Bertani (LB) media (Miller, 1972), Super Optimal Broth (SOB) (Hanahan, 1983) or M9 minimal salts medium with an additional carbon source (Sambrook, 2001). Solid and liquid media were amended with the appropriate antibiotic when required. Antibiotic concentration used were: kanamycin (Km) 10 µg ml^{-1} for Psv and 50 µg ml^{-1} for *E. coli*; gentamycin (Gm) 10 µg ml^{-1}; ampicillin (Ap) 400 µg ml^{-1} for Psv and 100 µg ml^{-1} for *E. coli*; and tetracycline 10 µg ml^{-1}.

Table 1. Strains used in this study

Strain	Relevant characteristics[a]	Source
***P. savastanoi* pv. savastanoi**		
NCPPB 3335	Wild type strain	(Perez-Martinez *et al.*, 2007)
Δ*catB*	*catB* (PSA3335_3199) deletion mutant (Km^R)	This work
Δ*antA*	*antA* (PSA3335_3204) deletion mutant (Km^R)	This work
Δ*06*	PSA3335_3206 deletion mutant (Km^R)	This work
Δ*ipoABC*	*ipoABC* operon deletion mutant (Km^R)	This work
Δ*dhoAB*	*dhoAB* operon deletion mutant (Km^R)	This work
Escrherichia coli		
DH5α	*F-, ɸ80dlacZ M15, (lacZYA-argF) U169, deoR, recA1, endA, hsdR17 (rk – mk-), phoA, supE44, thi-1, gyrA96, relA1*	(Hanahan, 1983)
GM2929	*F-, ara-14, leuB6, thi-1, tonA31, lacY1, tsx-78, galK2, galT22, glnV44, hisG4, rpsL136, xyl-5, mtl-1, dam13::Tn9, dcm-6, mcrB1, hsdR2, mcrA, recF143* (Sp^R Cm^R)	(Palmer & Marinus, 1994)
XL1-Blue	*hsdR17, supE44, recA1, endA1, gyrA46, thi, relA1, lac/* F´ [*proAB$^+$ lacZ^q M15*::Tn10 (Tc^R)]	(Bullock *et al.*, 1987)

[a]Km, kanamycin; Cm, chloramphenicol; Sp, spectinomycin; Tc, tetracycline

Construction of bacterial strains and plasmids

Plasmids and oligonucleotides used in this study are listed in Tables 2 and 3. For the generation of Psv NCPPB 3335 mutants, DNA fragments of approximately 1 kb, corresponding to the upstream and downstream flanking regions of the gene/operon to be deleted, were amplified in independent three rounds of polymerase chain reaction (PCR) using genomic DNA from NCPPB 3335 as a template and Expand High Fidelity polymerase (Roche Applied Science, Mannheim, Germany). Restriction sites for *EcoR*I (for the plasmid pECP1), *BamH*I (for the plasmid pIMC) or *Hind*III (for the plasmids pECP2, pECP3 and pECP4) were included in the primers as described previously (Matas *et al.*, 2014). The resulting products, consisting of

upstream and downstream flanking regions separated by the one of the mentioned restriction sites, were cloned into pGEMT and sequenced to discard mutations. Next, the kanamycin resistance gene *nptII* was extracted by enzyme restriction from pGEM-T-KmFRT- *EcoR*I, pGEM-T-KmFRT- *Hind*III or pGEM-T-KmFRT- *BamH*I (Table 2) and cloned in the vectors described above to yield pECP1-Km, pIMC-Km, pECP2-Km, pECP3-Km and pECP4-Km, respectively. Then the kanamycin resistance cassette was cloned in an inverted position with respect to the transcription orientation of each cluster. All the plasmids generated for the construction of Psv NCPPB 3335 mutants were suicide vectors in Psv. Plasmids were transferred to NCPPB 3335 by electroporation (Perez-Martinez *et al.*, 2007) and transformants were selected in LB-Km plates. Plasmids pECP1-Km, pIMC-Km, pECP2-Km, pECP3-Km, and pECP4-Km were used for the construction of Δ*catB*, Δ*antA*, Δ*06*, Δ*ipoABC* and Δ*dhoAB,* respectively. To select the allelic interchange (double recombination event) and discard plasmid integration (single recombination event), individual colonies were replicated onto LB-Ap plates and Ap^R colonies were discarded. Finally, Southern blot analyses were carried out to confirm integration in the correct position in the genome.

Plasmids for the complementation of the mutants were generated as follows. The complete open reading frames of *catBCA*, *antABC*, *ipoABC* and *dhoAB* operons, and the PSA3335_3206 gene together with their corresponding promoter and transcriptional terminator regions were amplified by PCR using NCPPB 3335 genomic DNA as a template and Phusion DNA Polymerase (Thermo Scientific, MA, USA). Then, the fragments were cloned into pBluescript SK II (+) or pENTR/SD/D-TOPO (only for the *antABC* operon). After sequencing to discard mutations, the fragments were subcloned into pBBR1MCS-5, and the correct orientation was selected by PCR using primers hybridizing with the plasmid and the cloned fragment. Plasmids pBBR:*catBCA*, pBBR:*antABC*, pBBR:PSA3335_3206, pBBR:*ipoABC* and pBBR:*dhoAB* were used for the complementation of Δ*catB*, Δ*antA*, Δ*06*, Δ*ipoABC* and Δ*dhoAB*, respectively

For the generation of promoter fusions to *lacZ*, a fragment of 274 bp upstream from the *antA* gene was amplified by PCR using NCPPB 3335 genomic DNA as a template and with primers which included the *Kpn*I and *Bgl*II restrictions sites. The fragment was A/T cloned into pGEMT, the sequence verified, and then subcloned into pMP220 (Spaink *et al.*, 1987).

Table 2. Plasmids used in this study

Name	Description[a]	Source
pGEM-T *easy*	Cloning vector containing ori f1 and *lacZ* (Ap[R])	(Promega, Madison, WI, USA)
pBluescript II SK (+)	Cloning vector containing ori f1 and *lacZ* (Ap[R])	(Agilent Technologies, Santa Clara, CA, USA)
pENTR/SD/D-TOPO	Cloning vector containing pUC ori (Km[R]).	(Invitrogen Corp, CA, USA)
pBBR1MCS-5	Broad host-range cloning vector (Gm[R])	(Kovach *et al.*, 1995)
pGEM-T-KmFRT-*EcoR*I	Contains Km[R] from pKD4 and *EcoR*I sites (Ap[R] Km[R])	(Zumaquero *et al.*, 2010)
pGEM-T-KmFRT-*Hind*III	Contains Km[R] from pKD4 and *Hind*III sites (Ap[R] Km[R])	(Aragon *et al.*, 2014)
pGEM-T-KmFRT-*BamH*I	Contains Km[R] from pKD4 and *BamH*I sites (Ap[R] Km[R])	(Ortiz-Martin *et al.*, 2010)
pIMC	pGEMT-derivative containing 1kb on each side of the *antA* (PSA3335_3204) gene from NCPPB 3335 (Ap[R]).	This work
pIMC-Km	pGEMT-derivative containing 1kb on each side of the *antA* (PSA3335_3204) gene from NCPPB 3335 interrupted by the kanamycin resistance gene *nptII* (Ap[R], Km[R]).	This work
pECP1	pGEMT-derivative containing 1kb on each side of the *catB* (PSA3335_3199) gene from NCPPB 3335 (Ap[R]).	This work
pECP1-Km	pGEMT-derivative containing 1kb on each side of the *catB* (PSA3335_3199) gene from NCPPB 3335 interrupted by the kanamycin resistance gene *nptII* (Ap[R], Km[R]).	This work
pECP2	pGEMT-derivative containing 1kb on each side of the PSA3335_3206 gene from NCPPB 3335 (Ap[R]).	This work
pECP2-Km	pGEMT-derivative containing 1kb on each side of the PSA3335_3206 gene from NCPPB 3335 interrupted by the kanamycin resistance gene *nptII* (Ap[R], Km[R]).	This work
pECP3	pGEMT-derivative containing 1kb on each side of the PSA3335_3207 to PSA3335_3209 operon from NCPPB 3335 (Ap[R]).	This work
pECP3-Km	pGEMT-derivative containing 1kb on each side of the PSA3335_3207 to PSA3335_3209 operon from NCPPB 3335 interrupted by the kanamycin resistance gene *nptII* (Ap[R], Km[R]).	This work
pECP4	pGEMT-derivative containing 1kb on each side of the PSA3335_3210 to PSA3335_3211 operon from NCPPB 3335 (Ap[R]).	This work
pECP4-Km	pGEMT-derivative containing 1kb on each side of the PSA3335_3210 to PSA3335_3211 operon from NCPPB 3335 interrupted by the kanamycin resistance gene *nptII* (Ap[R], Km[R]).	This work
pBBR:*catBCA*	pBBR1MCS-5-derivative containing the Psv NCPPB 3335 *catBCA* and *catBCA* promoter region (263 bp) flanked by *EcoR*I restriction sites (Gm[R])	This work

Table 2. Plasmids used in this study (continuation)

Name	Description[a]	Source
pBBR:*antABC*	pBBR1MCS-5-derivative containing the Psv NCPPB 3335 *antABC* operon and its promoter region (241 bp) flanked by *EcoR*I restriction sites (Gm[R])	This work
pBBR: PSA3335_3206	pBBR1MCS-5-derivative containing the Psv NCPPB 3335 PSA3335_3206 gene and its promoter region (168 bp) flanked by *Hind*III restriction sites (Gm[R])	This work
pBBR:*ipoABC*	pBBR1MCS-5-derivative containing the Psv NCPPB 3335 PSA3335_3207 to PSA3335_3209 operon (*ipoABC*) and its promoter region flanked by *Hind*III restriction sites (187 bp) (Gm[R])	This work
pBBR:*dhoAB*	pBBR1MCS-5-derivative containing the Psv NCPPPB 3335 PSA3335_3210 to PSA3335_3211 operon (*dhoAB*) and its promoter region (381 bp) flanked by *Hind*III restriction sites (Gm[R])	This work
pMP220	Broad-host-range, low-copy-number promoter probe vector, IncP replicon, *lacZ* (Tc[R])	(Spaink *et al.*, 1987)
pMP220-P*antABC*	Contains a fragment of 274 bp corresponding with the *antABC* promoter from Psv NCPPB 3335 directionally cloned with *Kpn*I and *Bgl*II restriction sites (Tc[R]).	This work

[a]Ap, ampicillin; Tc, tetracycline; Gm, gentamycin; Km, kanamycin

Table 3. Oligonucleotides used in this study

Name	Sequence (5'→3')
RT-PCR	
catA_R46	ACTGTTGCACATCGTCGG
catB_F1012	CGAAGACATTCTGGTCGAGC
catB_R221	GACAAGAAGCGGAGCGAAC
antC_F874	CGGTTACATCGTCGATCACC
antC_R224	TGGCAGCTCAGCACCTTG
antB_F282	CACGCTGCACCTGATCAGC
antB_R23	GGTACAGGAACTGCTCGATGC
antA_F904	GCCTGGTGGAGGAATACG
00_R120	ATCGCGAGCGTAACCATG
01_F771	CTTCGCGACTGAGTATGCG
01_R352	GTTCGACAGGTAGCTGAGCTG
02_F378	CTGCTCGATGACGTGGTC
02_R251	GCACCGAGCACGTTGATC
03_F1059	GGAGCAGACCTTCGAGCAG
03_R185	CTGCAGCGAGGTGTTGAAC
04_R645	GGCTTCGTATCACCTGCTG
04_R118	CGTCAATGTCGAACAGCG
05_F1104	CAGCGAGATCGACTGGATG
Construction of the mutants strains	
TA-antA-R-13-mut	CCCTATAGTGAGTCGGATCCGTCATCAGCCTTGAACTG
TA-antR-R879	ATGTTGTAGCCACTGTGC
TD-antB-F6-mut	GGATCCGACTCACTATAGGGTGAGGTCTGAACATGAGC

Table 3. Oligonucleotides used in this study (continuation)

Oligonucleotide	Sequence (5'→3')
TD-antC-R673	CGATCTGATCGAGCATGC
TA-catB_R17	GAATTCGACTCACTATAGGGATCGTGATGGCACTCATGG
antC_F92	GCTGGATGCTGCGTTACG
TA-catB_R17	GAATTCGACTCACTATAGGGATCGTGATGGCACTCATGG
antC_F92	GCTGGATGCTGCGTTACG
TD-catB_F1144	CCCTATAGTGAGTCGAATTCGCCGGAGCACAAGACTAGC
catA_R659	ACGTTGACCATGACGACCC
TD-00_F1573	CCCTATAGTGAGTCAAGCTTGATCGTTAGCGGTTACGGC
antR_R853	TGGAATTCGAACATTCGGC
TA-00_R51	AAGCTTGACTCACTATAGGGGACCTTTGAGGTTGGTCCG
01_F28	GCAACTGATGTGTGTTTGCG
TD-01_R753	CCCTATAGTGAGTCAAGCTTACTGGCTCAAGCAGATCACC
00_R773	GTCCGATCAGTTCATGCAGC
TA-03_R416	AAGCTTGACTCACTATAGGGCAGCAGCACCAGATCATGG
04_R281	ACCTGCTGATCAACCTGGC
TD-04_F673	CCCTATAGTGAGTCAAGCTTGCCAACGTCGTGACTTTCC
03_R855	CATACCCAACACCTGACGTCC
TA-05_R208	AAGCTTGACTCACTATAGGGCTGTAACCCAGCTCGACGC
benR_R507	TAGCTCGCGTTAGGATGGG

Complementation of the mutant strains

antC_R1360	ACTCATGGGAATTCTGGTCAGCGAAGAGCAGG
catA_R1305	ACTCATGGGAATTCTGATCGTTCCTCACGCTCC
antR_R13	CACCGAATTCCAAGTCGTTGGGCAAAACAG
catB_R190	GAATTCGTTCACCTTGATGCTTTCCG
antR_F349	CACCGGATCCGATCAGTTCCATCTCCAGATCG
antR_R-1196	GGATCCCAGGTGGAGGGTTTGAGGAG
antR_F900	ACTCATGGGGTACCACAGTGGCTACAACATCGCG
01_F871	ACTCATGGGGTACCGTTCGTCAACGCGTACTTCG
04_F720	ACTCATGGGGTACCAGCAGCCAGCTTTGTCACC
00_R126	ACTCATGGGGTACCCTCATCGCGAGCGTAACC
benR_R60	ACTCATGGGGTACCGTTCTGCGCTGTAAACAGCG
03_R1029	ACTCATGGGGTACCGCCGATACCCTCGACAGC

5' RACE

antA_R68	CCGGGCAATGCGGTACACACCTTC
catB_R-20	GGCACTCATGGGGGTTCCGTCTG
antR_R34	GGTGCGCGGCATGAAGGCCATG

RT-qPCR

gyrA-R	TTCCAGTCGTTACCCAGCTCG
gyrA-F	GACGAGCTGAAGCAGTCCTACC
catB_F146	TGACGGCATTATCGGTATCG
catB_R248	CGTTGAGGTTGGTGGCG

Cloning of the *antABC* and *antR* promoters

*Bgl*II-antR_R12	AGATCTAGTCGTTGGGCAAAACAGC
*Kpn*I-antA_R17	GGTACCTGCTGCCATTGGCTTACG
*Bgl*II-antA_R17	AGATCTTGCTGCCATTGGCTTACG
*Kpn*I-antR_R12	GGTACCAGTCGTTGGGCAAAACAGC

Distribution of the WHOP region across the *Pseudomonas syringae* complex

Genome sequences of 96 strains belonging to the *P. syringae* complex, 49 (51%) of which correspond to strains isolated from woody hosts, were downloaded from GenBank and the presence of the WHOP region was analysed by blastn using Geneious software v7.1.13 (http://www.geneious.com) and the nucleotide sequence of the Psv NCPPB 3335 WHOP regions as template. Positive hits were determined using the "Grade" value, a percentage calculated by Geneious combining the query coverage, e-value and identity values for each hit with weights 0.5, 0.25 and 0.25, respectively. Genomes yielding a Grade value ≥ 90% were considered to encode a complete WHOP region. Genomes yielding pairwise alignments with > 70% identity to specific clusters, were considered to encode a partial WHOP region.

RNA extraction and RT-PCR

Psv NCPPB 3335 cells were grown in LB broth to OD_{600} 2, pelleted and stored at -80 °C. Total RNA was then extracted using the TriPure Isolation Reagent (Roche Applied Science, Mannheim, Germany) according to the manufacturer's instructions, except that the TriPure was preheated at 65 °C, the lysis step was performed at 65 °C, and 1-bromo-3-chloropropane (Molecular Research Center, Cincinnati, OH, U.S.A.) was used instead of chloroform as previously described (Matas *et al.*, 2014). The RNA concentration was determined spectrophotometrically and its integrity was assessed by agarose gel electrophoresis. Total RNA was treated with a TURBO DNA-free™-Kit (Applied Biosystems; CA, USA) as detailed by the manufacturer's instructions. Later the samples were tested for genomic contamination by PCR. DNA-free RNA was reverse transcribed using random hexamers included in the iScript™ cDNA synthesis kit (BioRad; CA, USA). 50 ng of cDNA were used as a template to amplify intergenic regions by PCR using GoTaq Polymerase (Promega; Madison, USA). PCR products were analysed by 1% agarose gel electrophoresis. Primers used for RT-PCR are listed in Table 3.

Promoter activity and identification

To measure *antABC* promoter activity two different β-galactosidase assays were performed. In a first experiment Psv carrying pMP220-P*antABC* were grown to OD_{600} 0.5 in LB broth, cultures were then split into two different flasks and 1 mg/ml (7.3 mM) of anthranilate was added to one of them. β-galactosidase activity was measured 2, 4 and 19 hours post-addition as previously described (Miller, 1972). In a second experiment, bacteria were grown in

LB or LB amended with 7.3 mM of anthranilate or 6-chloroantranilate and β-galactosidase activity was measured after 24 h.

To map the transcription start point of *antA*, *antR*, *catB* and *catA* Psv NCPPB 3335 cells were grown on LB to OD_{600} 0.5 and anthranilate was then added to a final concentration of 7.3 mM. After 4 hours bacteria were pelleted and stored at -80 °C for further RNA extraction. SMARTer RACE kit (Clontech, Mountain View, CA, USA) was used according to the manufacturer's instructions.

RT-qPCR assays

Psv and the Δ*antA* mutant were grown in LB to OD_{600} 0.5 and anthranilate was then added to a final concentration of 7.3 mM. After 4h bacteria were pelleted, frozen in liquid nitrogen and RNA was subsequently extracted. RNA extraction and cDNA synthesis were carried out as described above. Bacteria grown in unamended LB were used as a control. The primer efficiency tests, reverse transcription quantitative PCR (RT-qPCR) and confirmation of the specificity of the amplification reactions were performed as described previously (Vargas *et al.*, 2011). The relative transcript abundance was calculated using the ΔΔ cycle-threshold (Ct) method (Livak & Schmittgen, 2001). Transcriptional data were normalized to the housekeeping gene *gyrA* and are presented as the fold change of the expression in LB amended with anthranilate relative to the expression in unamended LB. The relative expression ratio was calculated as the difference in qPCR threshold cycles (ΔCt = Ctgene of interest – Ct*gyrA*). One PCR cycle represents a twofold difference in template abundance; therefore, fold-change values were calculated as $2^{-\Delta\Delta Ct}$ as previously described (Pfaffl, 2001; Rotenberg *et al.*, 2006).

Identification and quantification of aromatic compounds by high performance liquid chromatography

Separation and identification of aromatic compounds of interest and related compounds were performed by high performance liquid chromatography (HPLC) using a HP series 1050 chromatograph (Hewlett-Packard, Waldbronn, Germany) equipped with a diode array UV-Vis detector and a 5-μm C18RP column (Novapak C18, 150×3.9 mm, Waters S.A., Barcelona). Compounds were identified by comparison of their respective UV absorption spectra and retention times with commercial pure standards (Sigma Aldrich, San Luis, MO, USA).

To detect anthranilate, 6-chloroanthranilate and catechol, samples were run for 20 minutes at a flow rate of 1 ml/minute with the detector set at 210 and 230 nm. Eluents used were 0.1% *ortho*-phosphoric acid in deionized water and methanol in a gradient of concentrations: 5% to 25% methanol for 15 minutes, 25% to 5% methanol for 1 minute and a final step for column re-equilibration at 5% methanol for 5 minutes. Under these conditions, the retention times (Rt) for anthranilate, catechol and 6-chloroanthranilate were 9.72, 7.61 and 12.9 minutes, respectively. For the functional analysis of the *antABC* operon, bacteria were grown overnight in LB broth, washed twice in M9 medium and resuspended in M9 minimal medium amended with 5 mM succinate and 500 µM anthranilate to an approximate final concentration of 10^9 cfu/ml. After 24h of incubation at 28 °C cells were removed by centrifugation, the supernatant was then filtered (pore diameter 0.22 µm) and analysed by HPLC. An identical procedure was carried out for the analysis of 6-chloroanthranilate transformation, except that 500 µM of this compound was added to the M9 minimal media instead of anthranilate. For the functional analysis of the *catBCA* operon, the same procedure was followed, with the exception that 7.3 mM of anthranilate was added to the overnight culture of LB broth and 300 µM of catechol to the M9 minimal media instead of anthranilate. As a control, cell-free media were subjected to the same procedure. For the quantification of anthranilate and catechol in the media, calibration curves with pure standards were performed in which the concentration was compared to the area of each peak.

For 4-chlorocatechol detection, an isocratic protocol consisting of 30% methanol and 70% deionized water with 0.1% *ortho*-phosphoric acid was used. The flow rate was 1 ml/minute during 15 minutes and the detector was set at 210 and 230 nm. The retention time of 4-chlorocatechol was 5.05 minutes. Samples were prepared as described above for the analysis of the *catBCA* function with the exception that 300 µM 4-chlorocatechol was added to the M9 minimal media instead of catechol.

For indigo detection, the HPLC protocol consisted of an isocratic method with a mixture of 90% acetonitrile and 10% deionized water and a flow rate of 1 ml/min. The running time was 5 minutes and the detector was set to 290 nm. Cells were grown overnight in LB broth, washed twice, resuspended in M9 minimal media amended with 5mM succinate and 500 µM indole and incubated at 28 °C until the culture became blue. When formed, the blue compound was partially purified by centrifugation of 2 ml of the culture. A blue precipitate formed along the inner side of the tube and was then grazed with a scraper, solubilized in acetonitrile and transferred to a new tube without disrupting the cell in the pellet. The partially purified blue

precipitate was filtered and analysed by HPLC where it was compared to pure standard of indigo (Sigma, San Luis, MO, USA).

Plant infection and isolation of bacteria from knots

Olive plants were micropropagated, rooted and maintained as previously described (Rodriguez-Moreno *et al.*, 2008). Micropropagated (non-woody) plants were infected in a stem wound with a bacterial suspension (≈5.10^3 cfu) and incubated in a growth chamber for 30 days as described previously (Rodriguez-Moreno *et al.*, 2008). The morphology of the knots developed was observed with a stereoscopic microscope (Leica MZ FLIII; Leica Microsystems, Wetzlar, Germany). Bacteria were recovered from the knots using a mortar and pestle containing sterile 10 mM $MgCl_2$. Serial dilutions were plated on LB plates or LB supplemented with the corresponding antibiotic and population sizes were determined from three different knots. A minimum of three representative knots were 3D scanned and the knot size determined using the Neftabb Basic 5.2 software. Statistical analyses were performed by analysis of variance (ANOVA) test (α=0.05).

The pathogenicity of Psv was also analysed on 1-year old (woody) olive explants as previously described (Penyalver *et al.*, 2006; Perez-Martinez *et al.*, 2007; Matas *et al.*, 2012). Morphological changes scored at 90 dpi were captured with a high-resolution camera Canon D6200 (Canon Corporation, Tokyo, Japan). The knot volume was calculated from a minimum of three representative knots as described previously (Moretti *et al.*, 2008; Hosni *et al.*, 2011). Statistical analyses were performed by analysis of variance (ANOVA) using the software SigmaPlot 12.0.

Competitive assays between the wild type and mutant strains were carried out in both woody and non-woody plants as described previously (Rodriguez-Moreno *et al.*, 2008; Matas *et al.*, 2012). Bacteria were mixed in a 1:1 ratio and 5.10^3 cells were place on each inoculation point.

RESULTS

Distribution of the WHOP region in the *Pseudomonas syringae* complex.

Due to the development of next generation sequencing technologies, the genome sequences of almost every single pathovar (type and pathotype strains) of *P. syringae* and related species are currently available (Moretti *et al.*, 2014; Bartoli *et al.*, 2015b; Nowell *et al.*, 2016; Thakur *et al.*, 2016). To broaden the analysis of the distribution of the WHOP region to all phylogroups of the *P. syringae* complex including at least one sequenced strain, the genomes of 81 *P. syringae* strains (59 pathovars), seven *P. savastanoi* strains (four pathovars) and one strain of the remaining eight species of this complex were downloaded from GenBank and the presence of the WHOP region was analysed. Out of the 96 genomes examined, 49 (51%) corresponded to strains isolated from woody hosts. As shown in Table 4, a complete WHOP region is conserved in four PG1 pathovars (actinidiae, morsprunorum, actinidifoliorum, theae) out of the 14 analysed and several PG3 strains: 12 *P. syringae* pathovars (aesculi, castaneae, cerasicola, ciccaronei, cunninghamiae, daphniphylli, dendropanacis, eriobotryae, myricae, photinieae, rhaphiolepidis, and ulmi), all 4 *P. savastanoi* pathovars (fraxini, nerii, savastanoi and retacarpa), as well as *Pseudomonas amygdali* CFBP 3205 and *Pseudomonas meliae* CFBP 3225. All of these strains were isolated from woody hosts, causing most of the symptoms on the woody organs of their respective plant hosts. In contrast, the WHOP region is absent in the genomes of all sequenced *P. syringae* pathovars infecting herbaceous hosts or causing symptoms on the non-woody organs of woody plants, with the exception of *P. syringae* pathovars actinidifoliorum and ciccaronei, which cause leaf spot lesions on kiwifruit trees (Chapman *et al.*, 2012; Cunty *et al.*, 2015) and carob (Ercolani & Caldarola, 1972), respectively. These results, which are in agreement with those previously reported for a smaller number of PG1 and PG3 strains (Bartoli *et al.*, 2015a; Nowell *et al.*, 2016), broaden the distribution of the WHOP region to *P. syringae* pv. actinidifoliorum (PG1) and six additional members of PG3: *P. syringae* pathovars ciccaronei, cunninghamiae and photiniae, *P. savastanoi* pv. retacarpa, *P. amygdali* and *P. meliae*.
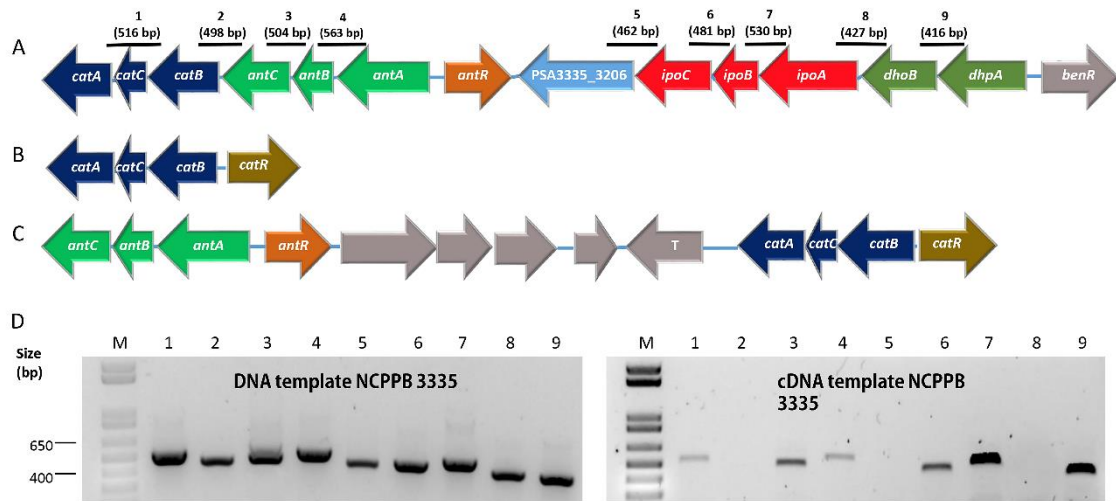
Figure 1. Schematic map of the WHOP region and related genes in the genomes of *P. savastanoi* pv. savastanoi NCPPB 3335 and other *P. syringae* strains. (A) *P. syringae* pathovars aesculi, actinidiae (ICMP 9617, MAFF 302091 and NCPPB 3871), morsprunorum MAFF 302280, actinidifoliorum (CFBP 8161, CFBP 8180 and CFBP 8043), castaneae ICMP 9419, cerasicola ICMP 17524, ciccaronei ICMP 5710, cunninghamiae ICMP 1894, daphniphylli CFBP 4219, dendropanacis CFBP 3226, eriobotryae ICMP 4455, myricae ICMP 7118, photinieae ICMP 7840, rhaphiolepidis ICMP 9756, theae ICMP 3923 and ulmi ICMP 3962; *P. savastanoi* pathovars savastanoi (NCPPB 3335, DAPP-PG 722, PseNe107 and ICMP 4352), fraxini ICMP 7711, nerii ICMP 16943 and retacarpa ICMP 16945; *P. amygdali* CFBP 3205 and *P. meliae* CFBP 3225. (B) *P. syringae* pv. coryli ICMP 17001 and *P. syringae* pv. spinaceae ICMP 16929. (C) *P. syringae* pv. japonica MAFF 301072; T, IS222 transposase protein *orfB*. (D) Gel electrophoresis (1% agarose) of RT-PCR amplicons obtained from Psv NCPPB 3335 (A). Black bars indicated the hybridization regions of the primers used (A) (Table 3). Genes in the same colour are transcribed as an operon. M, 1kb plus DNA ladder (Life technologies).

Partial conservation of the WHOP region was observed in three out the 12 PG2 *P. syringae* pathovars analysed, i.e., *P. syringae* pv. spinaceae ICMP 16929 and *P. syringae* pv. coryli ICMP 17001, which harbour only the *catABC* operon, and *P. syringae* pv. japonica MAFF 301072, which carries both the *catBCA* and *antABC* operons (Table 4). However, in these three strains, the *catBCA* operon was found in close proximity to the *catBCA* transcriptional activator gene *catR*, whereas *catR* was not present in the genomes of strains encoding a complete WHOP region (Fig. 1A-C). Furthermore, a gene encoding a transposase was found immediately upstream of the *catA* gene in the *P. syringae* pv. japonica MAFF 301072 genome (Fig. 1C), which encodes four additional open reading frames (ORFs) unrelated to the WHOP region between *antR* and *catA*. Conversely, the *catBCA* and *antABC* operons are located in close proximity in all strains carrying a complete WHOP region (Fig. 1A). These results suggest that horizontal transfer might have occurred in the evolution of the *catBCA* operon.

Table 4. Distribution of the WHOP region within the *Pseudomonas syringae* complex

Strain[a]	Accession	PG[b]	Host[c]	Symptoms[d]	WHOP[e]
P. syr. spinaceae ICMP 16929	LJRI00000000	2	Spinach		C
P. syr. coryli ICMP 17001	LJQC00000000	2	**European hazelnut**	Twig and branch dieback	C
P. syr. japonica MAFF 301072	AEAH00000000	2	Barley		AC
P. syr. actinidiae		1	**Kiwi tree**	Cankers on stems	+
ICMP 9617	AFTH01000000				
MAFF 302091	AEAL00000000				
NCPPB 3871	AFTF00000000				
P. syr. actinidifoliorum		1	**Kiwi tree**	Leaf spots	+
CFBP 8161	LJFL00000000				
CFBP 8180	LJFN00000000				
CFBP 8043	LJFM00000000				
P. syr. aesculi		3	**Horse chestnut**	Cankers on stems	+
NCPPB 3681	ACXS00000000				
2250	ACXT00000000				
P. syr. castaneae ICMP 9419	LJQD00000000	3	**Japanese chestnut**	Galls and cankers on twigs	+
P. syr. cerasicola ICMP 17524	LJQA00000000	3	**Cherry**	Galls on trunks and twigs	+
P. syr. ciccaronei ICMP 5710	LJPY00000000	3	**Carob**	Leaf spots	+
P. syr. cunninghamiae ICMP 1894	LJQE00000000	3	**Chinese fir**	Needle blight	+
P. syr. daphniphylli CFBP 4219	LJQF00000000	3	**Himeyuzuriha**	Galls on stems and twigs	+
P. syr. dendropanacis CFBP 3226	JYHG00000000	3	**Kakuremino**	Galls on trunks and twigs	+
P. syr. eriobotryae ICMP 4455	LJQI00000000	3	**Loquat**	Cankers on stems	+
P. sav. fraxini ICMP 7711	LLJL00000000	3	**European ash**	Cankers and blisters on stems	+
P. syr. myricae ICMP 7118	LJQV00000000	3	**Chinese bayberry**	Galls on trunks and twigs	+
P. syr. morsprunorum MAFF 302280	AEAE00000000	1	**Apricot**	Leaf spots, cankers on branches and trunks	+
P. sav. nerii ICMP 16943	LJQW00000000	3	**Oleander**	Knots on trunks, twigs and leaves	+
P. syr. photiniae ICMP 7840	LJQO00000000	3	**Japanese photinia**	Leaf spots, shoot blight	+
P. sav. retacarpa ICMP 16945	LJRD00000000	3	**Broom bush**	Knots on stems	+
P. syr. rhaphiolepidis ICMP 9756	LJRE00000000	3	**Sharinbai**	Galls on trunks and twigs	+
P. sav. savastanoi		3	**Olive tree**	Knots on stems	+
NCPPB 3335	ADMI02000000				
DAPP-PG 722	JOJV00000000				
ICMP 4352	LJRJ00000000				
PseNe107	JYHF00000000				
P. syr. theae ICMP 3923	LJRU00000000	1	**Tea**	Shoot blight	+
P. syr. ulmi ICMP 3962	LJRQ00000000	3	**Elm**	Bacterial spots, shoot blight	+

Table 4. Distribution of the WHOP region within the *Pseudomonas syringae* complex (continuation)

Strain[a]	Accession	PG[b]	Host[c]	Symptoms[d]	WHOP[e]
P. amygdali CFBP 3205	JYHB00000000	3	**Almond**	Cankers on stems and branches	+
P. meliae CFBP 3225	JYHE00000000	3	**Chinaberry**	Galls on twigs and shoots	+
P. syr. aceris		2	**Maple**	Leaf spots	-
ICMP 2802	LJPM00000000				
MAFF 302273	AEAO00000000				
P. syr. alisalensis ICMP 15200	LJPP00000000	5	Broccoli		-
P. syr. antirrihini ICMP 4303	LJPT00000000	1	Snapdragon		-
P. syr. apii ICMP 2814	LJPR00000000	1	Celery		-
P. syr. aptata		2	Sugar beet		-
ICMP 459	LJRP00000000				
DMS 50252	AEAN00000000				
P. syr. atrofaciens ICMP 4394	LJPO00000000	2	Wheat		-
P. syr. atropurpurea ICMP 4457	LJPS00000000	4	Italian ryegrass		-
P. syr. avellanae		1	**Hazelnut**	Twig dieback and cankers	-
ICMP 9746	ATDK00000000				
PaVt10	JYHC00000000				
P. syr. avii CFBP 3846	LIIJ00000000	1	**Cherry**	Cankers	-
P. syr. berberidis ICMP 4116	LJPU00000000	1	**Barberry**	Leaf spots	-
P. syr. broussonetiae ICMP 13650	LJPV00000000	3	**Paper mulberry**	Leaf spots	-
P. syr. coriandricola ICMP 12471	LJPZ00000000	5	Cilantro		-
P. syr. coronafaciens ICMP 3113	JSED01000000		Oat		-
P. syr. delphinii ICMP 529	LJQH00000000	1	Delphinium		-
P. syr. garcae ICMP 4323	LJQK00000000	4	**Coffee**	Leaf spots	-
P. syr. glycinea		3	Soybean		-
B706	AEGG00000000				
race 4	AEGH00000000				
ICMP 2189	LJQL00000000				
P. syr. helianthi ICMP 4531	LJQM00000000	6	Sunflower		-
P. syr. hibisci ICMP 9623	LJQN00000000	3	**Chinese hibiscus**	Leaf spots	-
P. syr. lachrymans		3	Cucumber		-
ICMP 3507	LJQP00000000				
MAFF 302278	AEAM00000000				
P. syr. lapsa ICMP 3947	LJQQ00000000	3	Corn hybrid		-
P. syr. maculicola		1	Cauliflower		-
CFBP 1657	JYHH00000000				
ES4326	AEAK00000000				
P. syr. mellea ICMP 5711	LJQS00000000	3	Tobacco		-
P. syr. mori		3	**White mulberry**	Leaf spots	-
ICMP 4331	LJQU00000000				
MAFF 301020	AEAG00000000				

Table 4. Distribution of the WHOP region within the *Pseudomonas syringae* complex (continuation)

Strain[a]	Accession	PG[b]	Host[c]	Symptoms[d]	WHOP[e]
P. syr. oryzae		4	Rice		-
ICMP 9088	LJQX00000000				
1_6	ABZR00000000				
P. syr. panici LMG 2387	ALAC00000000	ND[g]	Millet		-
P. syr. papulans CFBP 1754	JYHI00000000	2	**Apple**	Leaf and fruit spots	-
P. syr. phaseolicola		3	Bean		-
ICMP 2740	LJQZ00000000				
1448A	CP000058				
P. syr. philadelphi ICMP 8903	LJQY00000000	1	**Mock orange**	Leaf spots	-
P. syr. pisi 1704B	AEAI00000000	2	Pea		-
P. syr. porri ICMP 8961	LJRA00000000	4	Leek		-
P. syr. primulae ICMP 3956	LJRC00000000	7	Polyanthus		-
P. syr. ribicola ICMP 3882	LJRF00000000	7	**Golden currant**	Leaf spots	-
P. syr. sesame ICMP 763	LJRG00000000	3	Sesame		-
P. syr. solidagae ICMP 16925	LJRH00000000	1	Tall golden rod		-
P. syr. syringae		2	Bean, lilac, mango		-
B728a	CP000075				
ICMP 3023	LJRK00000000				
UMAF0158	CP005970				
P. syr. tabaci		3	Tobacco		-
ICMP 2835	LJRL00000000				
ATCC 11528	AEAP00000000				
P. syr. tagetis ICMP 4091	LJRM00000000	6	African marigold		-
P. syr. tomato		1	Tomato		-
DC3000	AE016853				
ICMP 2844	LJRN00000000				
NCPPB 1108	ADGA00000000				
Max13	ADFZ00000000				
T1	ABSM00000000				
K40	ADFY00000000				
P. tremae ICMP 9151	LJRO00000000	3	**Urajiroenoki**	Galls on trunks and twigs	-
P. syr. viburni ICMP 3963	LJRR00000000	1	**Viburnum**	Leaf spots	-
P. syr. zizaniae ICMP 8921	LJRT00000000	4	Rice		-
P. cannabina ICMP 2823	LJPX00000000	5	Indian hemp		-
P. caricapapayae ICMP 2855	LJPW00000000	6	**Papaya**	Leaf spots	-
P. congelans ICMP 19117 [f]	LJQB00000000	2	Grass phyllosphere		-
P. ficuserectae ICMP 7848	LJQJ00000000	3	**Inubiwa**	Leaf spots	-
P. viridiflava ICMP 2848	LJRS00000000	7	Bean		-

[a]*P., Pseudomonas; P. syr., Pseudomonas syringae; P. sav., Pseudomonas savastanoi.*

[b]PG, phylogroup

[c]Woody hosts are shown in bold

[d]Only for woody hosts pathogens

[e]+, presence of the WHOP region; -, absence of the WHOP region; AC, presence of the *antABC* and *catBCA* operons; C, presence of the *catBCA* operon

[f]*P. congelans* is not a confirmed plant pathogen

A phylogenetic tree based on the *catBCA* operon was constructed using maximum likelihood and showed that PG1 and PG3 strains clustered monophyletically to the exclusion of PG2. In addition *P. syringae* pv. japonica clustered separately from the other two PG2 strains encoding a partial WHOP region (Fig. 2). These results are discordant with the phylogeny of the *P. syringae* complex based on housekeeping genes (Berge *et al.*, 2014), reinforcing the hypothesis of horizontal transfer in the evolutionary history of this operon across the *P. syringae* complex.
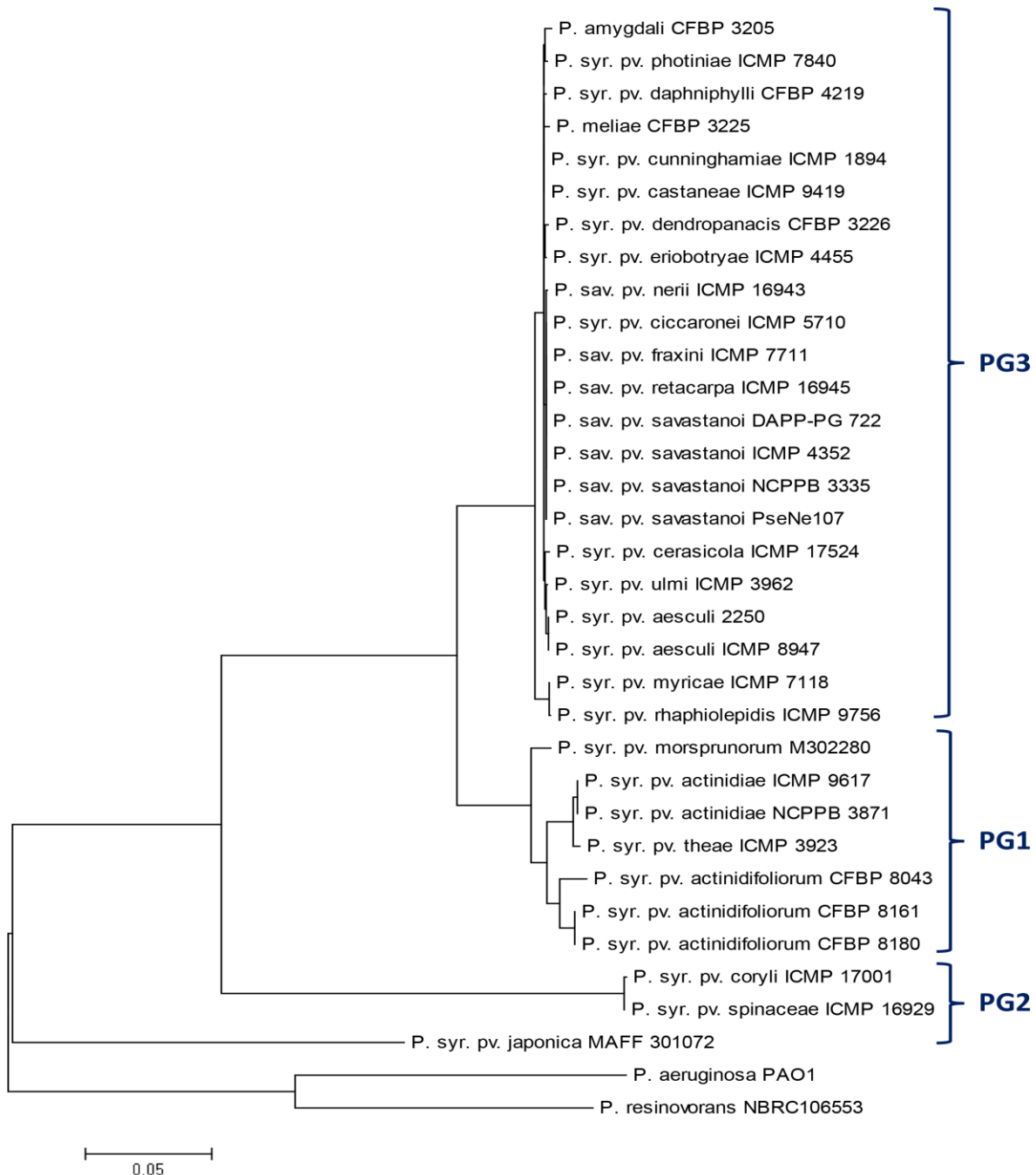
Figure 2. Phylogenetic analysis of the *catBCA* operon in the *P. syringae* complex. The tree was constructed using MEGA5 (Tamura *et al.*, 2011) with the maximum-likelihood method (Jones *et al.,* 1992) .The length of the sequence used for phylogenetic analysis was 2412 bp. *P. aeruginosa* PAO1 and *P. resinovorans* NBRC 106553 are included as outsiders. PG, phylogroup

The WHOP region is organized in four operons and two independently transcribed genes

Fourteen ORFs are encoded in the WHOP region (Fig. 1A, Table 5). PSA3335_3199 to PSA3335_3201 and PSA3335_3202 to PSA3335_3204 encode, respectively, homologs of the *catBCA* and *antABC* operons found in other pseudomonads (Houghton *et al.*, 1995; Nojiri *et al.*, 2002; Maeda *et al.*, 2003; Urata *et al.*, 2004; Li *et al.*, 2010). The *antABC* operon participates in the conversion of anthranilate into catechol, which is further transformed into β-ketoadipate enol-lactone by the *catBCA*-encoded activity. PSA3335_3205 (*antR*) and PSA3335_3213 (*benR*), which are the only genes oriented in the opposite direction to all others (Fig. 1A), encoded the positive transcriptional regulators of the *antABC* and *benABCD* operons, respectively. The *benABCD* operon is involved in the degradation of benzoate to catechol in *Pseudomonas putida* (Jeffrey *et al.*, 1992), however, this operon is not present in the genome of Psv NCPPB 3335.

Annotation of the PSA3335_3207 to PSA3335_3211 genes yielded functions likely to be involved also in the metabolism of phenolic compounds (Rodriguez-Palenzuela *et al.*, 2010). A search for protein domains using MyHits web tool (http://myhits.isb-sib.ch/) revealed that PSA3335_3206 (annotated as an aerotaxis receptor) might play a role in chemotaxis, since it encodes a protein containing a methyl-accepting domain and a bacterial chemotaxis sensory transducer domain. No specific domain was obtained for PSA3335_3207. The product encoded by this ORF annotates as a protein involved in the *meta*-pathway of phenol degradation but without a described function. The products of PSA3335_3208 and PSA3335_3209 contain two structural motifs characteristic of iron-sulphur proteins (2Fe-2S and 4Fe-4S centres) and an NADP-dependent oxidoreductase domain, respectively. The product of PSA3335_3211 (named *dhoA*) carries a dienelactone hydrolase family domain. This family of enzymes has been involved in the metabolism of halogenated catechols in *Pseudomonas knackmusii,* previously known as *Pseudomonas* sp. strain B13 (Schlomann *et al.*, 1990). PSA3335_3210, the product of which is annotated as a short chain alcohol dehydrogenase gene (hereafter named *dhoB*), encodes for a protein showing a KR domain, characteristic of bacterial polyketide synthases and involved in the reductive modification of the ß-carbonyl centres in the growing polyketide chain.

Table 5. Genes located within the WHOP region

Accession number[a]	Demonstrated function	Gene [b]	Annotated gene product
	Catechol metabolism		
PSA3335_3199		*catA*	Catechol 1,2-dioxygenase
PSA3335_3200		*catC*	Muconolactone isomerase
PSA3335_3201		*catB*	Muconate cycloisomerase
	Anthranilate metabolism		
PSA3335_3202		*antC*	Anthranilate dioxygenase reductase component
PSA3335_3203		*antB*	Anthranilate dioxygenase beta subunit
PSA3335_3204		*antA*	Anthranilate dioxygenase alpha subunit
PSA3335_3205		*antR*	*antABC* regulatory protein
	Indigo-producing oxygenase		
PSA3335_3207		*ipoC*	Involved in *meta* pathway of phenol degradation
PSA3335_3208		*ipoB*	Nitrilotriacetate monooxygenase component B
PSA3335_3209		*ipoA*	Putative oxygenase subunit
	Not determined		
PSA3335_3206		UN	Aerotaxis receptor
PSA3335_3210		*dhoB*	Short chain alcohol dehydrogenase
PSA3335_3211		*dhoA*	Dienelactone hydrolase
PSA3335_3213		*benR*	Positive regulator of the *benABCD* operon

[a]Accession number corresponding to the genome of *P. savastanoi* pv. savastanoi NCPPB 3335.
[b]UN - Unnamed

The organization of all genes encoded in the WHOP region into different operons was analysed by retrotranscriptase-polymerase chain reaction (RT-PCR) in Psv NCPPB 3335. Primers targeting sequential ORFs were used to amplify intergenic regions, except for those of the *catBCA* operon where a region spanning from PSA3335_3199 (*catA*) to PSA3335_3201 (*catB*) was amplified (Fig. 1A). Positive controls using genomic DNA as a template were used for all PCRs. As shown in Fig. 1D, a DNA fragment of identical size to those of the corresponding intergenic regions was observed for *antC-antB* and *antB-antC*, confirming their organisation as an operon of *antA, antB* and *antC*. A similar result was obtained for the region spanning from *catB* to *catA*, demonstrating the organisation of *catB, catC* and *catA* in operon. No amplification product was obtained for the intergenic region located between the *catBCA* and the *antABC* operons, showing that the transcription of *antABC* and *catBCA* are independent. Regarding the intergenic regions of PSA3335_3207-PSA3335_3208 and PSA3335_3208-PSA3335_3209, amplification products of the expected sizes were observed in both cases, while no amplification was observed for PSA3335_3206-PSA3335_3207 and PSA3335_3209-PSA3335_3210. These

results indicate that the transcription of the PSA3335_3206 gene is independent. However, PSA3335_3207 to PSA3335_3209 co-transcribe in an operon, here named the *ipoABC* operon (indigo producing operon), in relation to the ability of these genes to transform indole into the blue pigment indigo (see below). The intergenic region between PSA3335_3211 (*dhoA*) and PSA3335_3210 (*dhoB*) was also amplified, suggesting their organisation into an operon (hereafter called the *dhoAB* operon). No amplification products corresponding to the intergenic regions located immediately upstream or downstream from this operon were obtained. In summary, the results show that the genes encoded in the WHOP regions are organised into four operons (*catBCA*, *antABC*, *ipoABC* and *dhoAB*) and three independently transcribed genes (*antR*, PSA3335_3206 and *benR*).

Transcriptional analysis of the *antABC* and the *catBCA* operons

The transcriptional start site of the *catBCA* and *antABC* operons and that of the *antR* gene were determined by 5'-RACE and localized, respectively, 16, 31 and 56 nucleotides upstream from their corresponding start codons (Fig. 3). Alignment of the Psv NCPPB 3335 -10 and -35 boxes of the *catBCA* and *antABC* promoters revealed partial similarity with the same sequences of other pseudomonads.
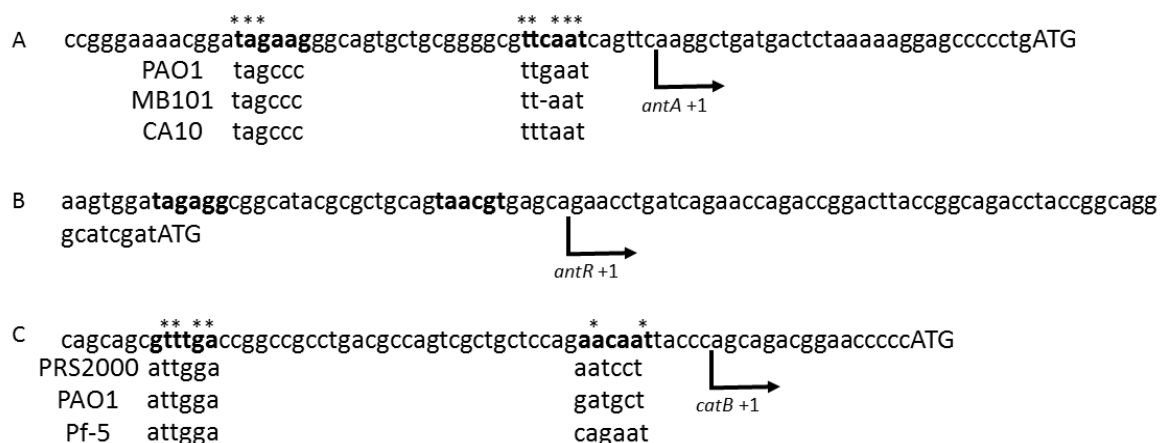
Figure 3. Determination of the transcription start points of (A) *antA*, (B) *antR* and (C) *catB* genes by 5'-RACE. Translational start codons are represented in capital letters. The proposed -10 and -35 boxes are shown in bold and the proposed -10 and -35 boxes in other pseudomonads are represented below. PAO1; *P. aeuruginosa* PAO1; MB101; *Pseudomonas fluorescens* MB101; CA10; *P. resinovorans* CA10; PRS2000, *P. putida* PRS2000; Pf-5, *P. fluorescens* Pf-5. Asterisks indicate conserved nucleotides. Dash indicate a gap to obtain maximal homology.

In other pseudomonads, the *antABC* and *catBCA* operons are involved in the degradation of anthranilate through the β-ketoadipate pathway (Fig. 4A). Anthranilate is known to be an inducer of the *antABC* operon in *P. resinovorans* (Urata *et al.*, 2004), *P. aeruginosa* (Kim *et al.*, 2012) and *P. fluorescens*. To analyse whether anthranilate also promotes the expression of *antABC* in Psv NCPPB 3335, a region expanding 274 bp upstream the *antA* gene was amplified and cloned into pMP220. The resulting plasmid (pMP220-P$_{antABC}$) was transformed into wild type Psv NCPPB 3335. Psv cells were grown in LB medium to mid-log phase (OD$_{600nm}$=0.5), the culture was then divided into two and anthranilate was added to one. As a control, Psv cells harbouring the 'empty' vector (pMP220) were used. After different periods of time, expression of the *antABC* promoter (P$_{antABC}$) was determined by β-galactosidase activity. Four hours after the addition, corresponding to late log phase cells (OD$_{600nm}$=0.9), the activity of P$_{antABC}$ was eightfold higher in anthranilate-amended medium (Fig. 4B). However, at 19 hours post-addition, corresponding to stationary-grown cells (OD$_{600nm}$= 2.3), a 27.6 fold increase of P$_{antABC}$ expression in the amended medium was observed, confirming anthranilate as an inducer of the transcription of *antABC* also in Psv NCPPB 3335. On the other hand, the higher activity of P$_{antABC}$ observed in Psv cells grown to stationary phase in comparison with exponentially-grown cells suggest that the *antABC* operon might be involved in secondary metabolic pathway(s), which activate during the stationary phase.

Other inducers of the expression of *antABC* have been reported in pseudomonads. In *P. fluorescens* MB101, 6-chloroanthranilate is a gratuitous inducer, promoting the expression of the operon without being degraded (Retallack *et al.*, 2006). Activation of P$_{antABC}$ by 6-chloroanthranilate was also analysed in Psv NCPPB 3335 cells harbouring pMP220:P$_{antABC}$. Bacterial cells were grown on LB medium or LB supplemented with anthranilate or 6-chloroanthranilate at the same concentration (7.3 mM), and β-galactosidase was measured 24 hours after the addition. As shown in Fig. 4C, both anthranilate and 6-chloroanthranilate induced the activity of P$_{antABC}$ to the same extent in comparison with the unamended medium, suggesting that transcription of the *antABC* operon might also be induced by other anthranilate-derived compounds.

Expression of the *catBCA* operon was analysed in both the wild type Psv NCPPB 3335 and its Δ*antA* mutant. For this purpose, Psv cells were grown in LB medium and LB amended with 7.3 mM anthranilate, and the expression of the *catB* gene was measured by RT-qPCR. Expression of *catB* in Psv NCPPB 3335 was 232 fold higher in the amended medium compared to LB (Fig. 4D). However, expression of the *catB* gene in the Δ*antA* mutant was similar in both media, suggesting that in this strain the *antABC* operon is essential for the activation of the *catBCA*

operon by anthranilate. Thus, and although the protein activator of the *catBCA* operon (CatR) is not encoded in the genome of Psv NCPPB 3335, catechol (the product of *antABC* activity), and perhaps other catechol-related compounds, might act as activators for *catBCA* expression.
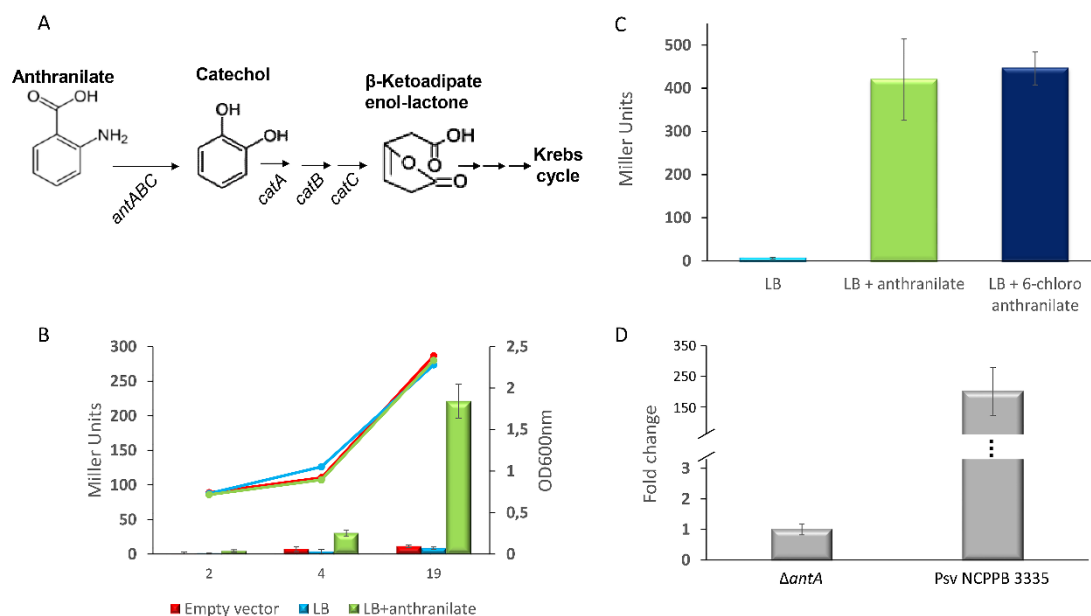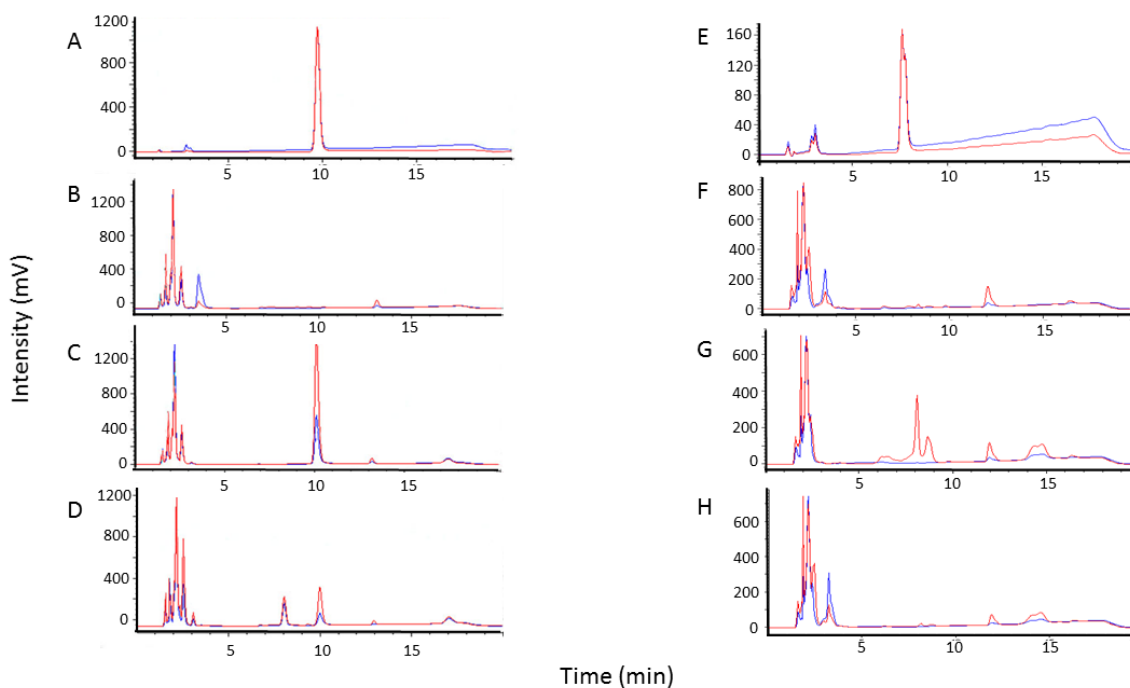

Figure 4. Transcriptional analysis of the *antABC* and *catBCA* operons. (A) Degradation pathways of anthranilate and catechol by proteins encoded in the *antABC* and the *catBCA* operons. (B) β-galactosidase activity of P$_{antABC}$ in Psv NCPPB 3335 cells grown in LB amended or not with anthranilate. Lines represent the OD$_{600nm}$ of the cultures. (C) β-galactosidase activity of P$_{antABC}$ in Psv NCPPB 3335 cells grown for 24 hours in LB and LB amended with anthranilate or 6-chloroanthranilate. Bars in Figures 4B and 4C correspond to the average Miller Units ± the standard deviation from the average of three different assays. (D) Quantification of the transcription of the *catB* gene by RT-qPCR in Psv NCPPB 3335 and its derivative Δ*antA* mutant. The fold change was calculated after normalization using the *gyrA* gene as an internal control. Fold change refers to the expression in LB amended with anthranilate relative to the expression in non-amended LB 4 hours after the addition of anthranilate. Bars represent the means of three replicates ± the standard deviation.

Involvement of the *antABC* operon in the degradation of anthranilate

The *antABC* and *catBCA* operons act sequentially in the degradation of anthranilate to β-ketoadipate enol-lactone (Fig. 4A), which is further degraded into the Krebs cycle (Harwood & Parales, 1996). To confirm the activity of the *antABC* operon in Psv NCPPB 3335, a Δ*antA* mutant and its complemented strain harbouring pBRR:*antABC* (Table 2) were constructed. Psv cells grown overnight on LB medium were transferred to M9 medium containing 500 µM of

anthranilate (M9A). After 24 hours, the filtered supernatants were analysed by HPLC. A single peak corresponding to anthranilate (Rt = 9.72 min) was observed in the chromatogram corresponding to uninoculated M9 plus anthranilate (Fig. 5A), whereas this peak was not present in the supernatant of M9A inoculated with the wild type strain Psv NCPPB 3335 (Fig. 5B), suggesting the total disappearance of the compound under the conditions tested. On the contrary, anthranilate hardly disappeared in the supernatant of M9A inoculated with the Δ*antA* mutant as an anthranilate peak corresponding to a concentration of 472 µM remained (Fig. 5C) which is only slightly lower than the initial concentration of 500 µM in M9A. When M9A was inoculated with the Δ*antA* mutant complemented with the *antABC* operon in a plasmid (pBBR:*antABC*), two peaks with Rt 7.8 min and 9.9 min were detected corresponding to catechol at a concentration of 229 µM and anthranilate at 66 µM, respectively. Thus, total degradation of the compound did not take place in the culture of the complemented strain. All these results confirm the implication of the Psv NCPPB 3335 *antABC* operon in the degradation of anthranilate to catechol. Since 6-chloroanthranilate also promotes the transcription of the *antABC* operon (Fig. 4C), we analysed the ability of Psv NCPPB 3335 to degrade this compound. However, no degradation of the compound was observed in the M9 medium amended with 6-chloroanthranilate inoculated with Psv NCPPB 3335 (data not shown). However, no degradation of the compound was observed in the M9 medium amended with 6-chloroanthranilate inoculated with Psv NCPPB 3335 (data not shown).
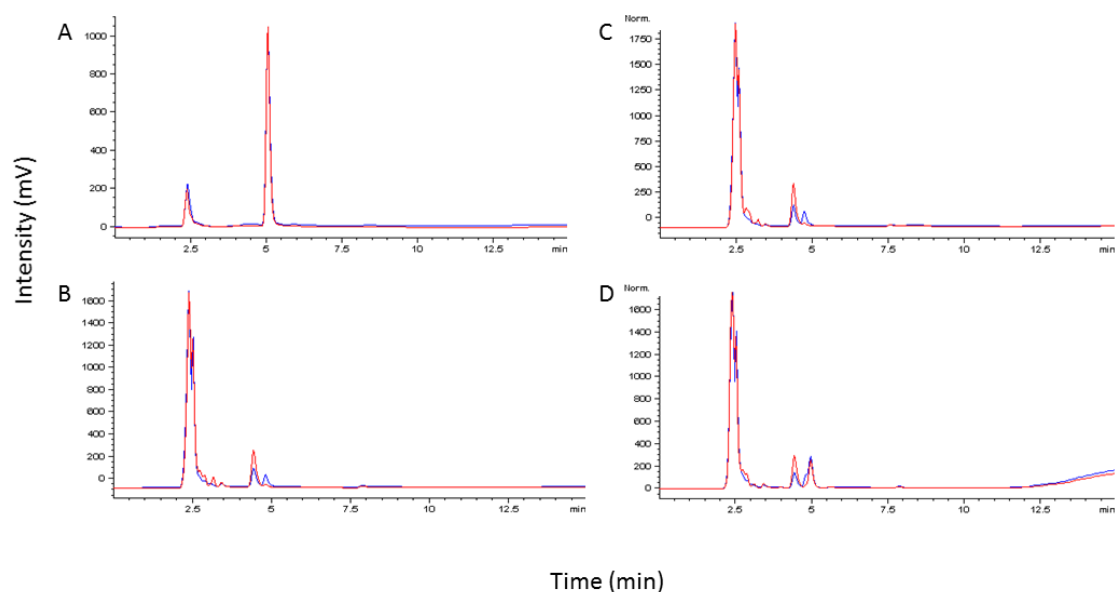
Figure 5. Functional analysis of the *antABC* and *catBCA* operons. HPLC chromatograms of filtered supernatants after 24h exposure to M9 minimal media supplemented with (A-D) 500 µM anthranilate or (E-H) 300 µM catechol. Simultaneous detection at 210 nm (blue lines) and 230 nm (red lines) was performed. (A) Control cell-free medium supplemented with anthranilate; (B) anthranilate-amended medium (M9A) inoculated with Psv NCPPB 3335; (C) M9A with the Δ*antA* mutant; (D) M9A with the Δ*antA* mutant complemented with pBBR:*antABC*; (E) Control cell-free medium supplemented with catechol; (F) catechol-amended medium with Psv NCPPB 3335; (G) catechol-amended medium with the Δ*catB* mutant; (H) catechol-amended medium with the Δ*catB* mutant complemented with pBBR:*catBCA*. The concentrations of the compounds were determined using a standard curve of anthranilate or catechol (5-500 µM). The intensity of the signal is measured as millivolts (mV).

Involvement of the *catBCA* operon in the degradation of catechol and halogenated catechols

To confirm the involvement of the Psv NCPPB 3335 *catBCA* operon in the metabolism of catechol, a Δ*catB* mutant was constructed. This mutation should have a polar effect over the transcription of the *catC* and *catA* genes located downstream from *catB*. A complemented Δ*catB* strain carrying the complete *catBCA* operon from Psv NCPPB 3335 in a plasmid, strain Δ*catB*-pBBR:*catBCA*, was also constructed. Psv cells were grown overnight in LB broth amended with anthranilate 7.3 mM to induce the expression of the *catBCA* operon, collected by centrifugation and transferred to M9 media containing 300 µM catechol. After 24 hours, the filtered supernatant was analysed by HPLC. As shown in Figure 5E, the chromatogram corresponding to

the cell-free medium showed a peak at Rt= 7.61 min, corresponding to non-modified catechol. On the contrary, the chromatogram of the wild type Psv NCPPB 3335 (Fig. 5F) showed no peak at this Rt, indicating that catechol was completely removed from the medium. However, several other peaks corresponding with the accumulation of unidentified compounds were observed in this chromatogram, some of which showed retention times between 1 and 4 minutes and a single additional peak at Rt = 12 min. Two large peaks at Rt= 8.01 and 8.66 min appeared in the chromatogram of the Δ*catB* strain (Fig. 5G). The UV absorption spectra of these peaks resembled that of catechol, suggesting that several catechol-related compounds accumulated in the culture supernatant of this strain. This hypothesis is reinforced by the fact that the chromatogram of the complemented Δ*catB* strain (Δ*catB*-pBBR:*catBCA*) did not display these peaks (Fig. 5H). Since the *catBCA* operon is unique in the genome of Psv NCPPB 3335, it can be speculated that other enzyme(s) of this strain can unspecifically transform catechol under the conditions tested.

Dienelactone hydrolases have been reported to be involved in the metabolism of halogenated catechols in *Pseudomonas* sp. strain B13 (Schlomann *et al.*, 1990). In this pathway, halogenated catechols are initially attacked by catechol 1,2-dioxygenase (CatA), followed by muconate cycloisomerase (CatB) activities. To address the possible involvement of the *dhoAB* and *catBCA* operons in the catabolism of 4-chlorocatechol in Psv NCPPB 3335, the wild type strain and the Δ*catB* and Δ*dhoAB* mutants were cultured in M9 media supplemented with 4-chlorocatechol. A peak corresponding to 4-chlorocatechol (Rt= 5.05 min) was observed in the cell-free culture (Fig. 6A). However, 4-chlorocatechol was not detected in the chromatogram corresponding to the supernatant of the wild type strain or its Δ*dhoAB* mutant (Fig. 6B, 6C), indicating the ability of the strain to degrade 4-chlorocatechol through a pathway independent of *dhoAB*. In addition, other peaks corresponding to unidentified compounds at Rt (4.45 and 4.85 min) close to that of 4-chlorocatechol were observed in these chromatograms, suggesting the accumulation of 4-chlorocatechol-related compounds in the culture medium of these two strains. In contrast, and although the 4-chlorocatechol was detected in the supernatant of the Δ*catB* mutant (Fig. 6D), the calculated area under the peak for this compound was approximately four fold lower than that of the cell-free medium (Fig. 6A), suggesting that partial degradation of this compound is dependent on the *catBCA* operon.

Figure 6. 4-Chlorocatechol transformation by the *P. savastanoi* pv. savastanoi NCPPB 3335 *catBCA* operon. HPLC chromatograms of filtered supernatants after 24h exposure to M9 minimal medium supplemented with 300 µM 4-chlorocatechol. Simultaneous detection at 210 nm (blue lines) and 230 nm (red lines) was performed. (A) Control cell-free medium; (B) Psv NCPPB 3335; (C) Δ*dhoAB* mutant; (D) Δ*catB* mutant.

Involvement of the *ipoABC* operon in the oxidation of indole into indigo

To analyse the function of the *ipoABC* operon, which genes were annotated as putative components of an oxygenase involved in the metabolism of aromatic compounds (Table 5), we constructed a plasmid harbouring the whole operon under the control of its own promoter region (plasmid pBBR:*ipoABC*, Table 2). Several authors have reported that heterologous expression of certain oxygenases in *E. coli* leads to the production of the blue pigment indigo (Ensley *et al.*, 1983; Woo *et al.*, 2000; Choi *et al.*, 2003; Doukyu *et al.*, 2003; van Hellemond *et al.*, 2007), which is synthesized via the oxidation of indole (Fig. 7A). *E. coli* DH5α cells harbouring pBBR:*ipoABC* were grown in M9 medium (colourless) amended with 0.5 mM indole. After 24 h of incubation at 37 °C, the culture turned blue, whereas the culture of the untransformed strain remained colourless. Furthermore, a Psv NCPPB 3335 Δ*ipoABC* mutant and its complemented strain harbouring the plasmid pBBR:*ipoABC* (strain Δ*ipoABC*-pBBR:*ipoABC*) were constructed and incubated in M9 minimal medium amended with 0.5 mM indole. While cultures of this medium inoculated with the wild type strain Psv NCPPB 3335 or its Δ*ipoABC* mutant remained colourless, the culture of the complemented strain turned blue and accumulated insoluble blue precipitates (Fig. 7B). HPLC analysis of these blue precipitates showed a single peak at Rt= 1.7 min (Fig. 7C) with an UV spectrum identical to that previously reported for indigo (Olvera Vargas

et al., 2010). These results confirm the involvement of the *ipoABC* operon in the transformation of indole into indigo, suggesting the codification of an oxygenase able to use aromatic compounds as substrates.
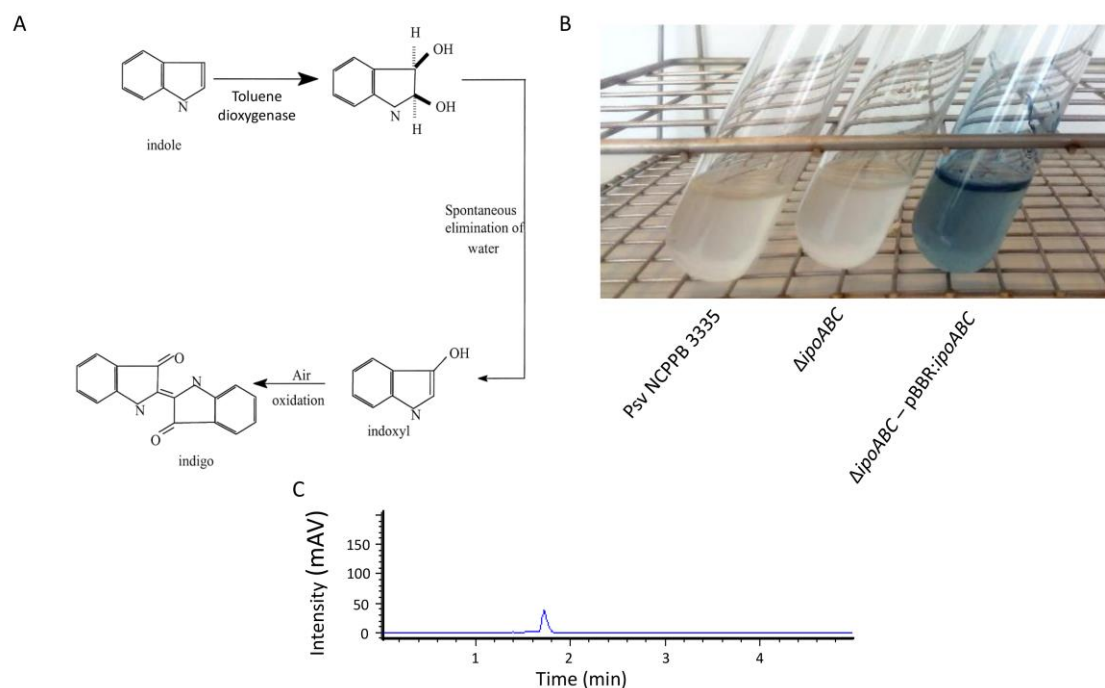
Figure 7. Functional analysis of the *ipoABC* operon. (A) Proposed pathway for the biosynthesis of indigo by toluene dioxygenase (Ensley *et al.*, 1983). Picture adapted from Woo *et al.* (2000) (B) Appearance of M9 minimal media supplemented with 0.5 mM indole after growth of Psv NCPPB 3335, its Δ*ipoABC* mutant and the complemented Δ*ipoABC* strain expressing the whole *ipoABC* operon on a plasmid (Δ*ipoABC*-pBBR:*ipoABC*). (C) HPLC chromatogram of the blue compound partially purified from the supernatant of the Δ*ipoABC*-pBBR:*ipoABC* culture.

Role of the WHOP region in virulence and *in planta* competitive fitness of Psv NCPPB 3335

Due to the exclusivity of the WHOP region to strains of the *P. syringae* complex infecting the woody organs of woody hosts (Table 4), it resulted particularly interesting to analyse its role in the interaction between Psv NCPPB 3335 and olive plants. For this purpose we used two different models, micropropagated olive explants (non-woody plants) (Fig. 8A) and one year-old woody olive plants (Fig. 8B). Plants were inoculated with the wild type Psv NCPPB 3335 or each of the derivative mutants affected in the WHOP region. After 30 days, no visual differences were observed in the knot sizes developed on micropropagated plants among the strains tested (Fig. 8A). In fact, quantification of the volume of the knots generated using a 3D scanner confirmed no significant differences among the samples (Fig. 8C). However, clear differences could be

observed in the knot size generated on woody plants by the strains 90 days post-inoculation (Fig. 8B). The largest reduction in knot volume was observed for the Δ*antA* mutant which induced knots 3.1 fold smaller than those formed with the wild type strain. In addition, plants inoculated with the Δ*catB* and Δ*ipoABC* mutants induced knot volumes with 2.37 and 1.57 fold reductions, respectively (Fig. 8D). Moreover, while the Δ*catB*-pBBR:*catBCA* and Δ*ipoABC*-pBBR:*ipoABC* developed knots similar to those observed in plants infected with the wild type strain, knots induced by the Δ*antA*-pBBR:*antABC* strain were 1.09 times bigger. No differences in the knot sizes developed on woody olive plants were observed for the Δ*06* and Δ*dhoAB* mutants and their respective complemented strains compared with the tumours developed by Psv NCPPB 3335. Independently of the observed differences in the virulence of the strains, all of them reached equal final populations within the developed knots, both on micropropagated (≈ 10^7 cfu per knot) and woody olive plants (≈ 10^6 cfu per knot) (not shown). Remarkably, the *antABC*, *catBCA* and *ipoABC* operons play a role in virulence of Psv NCPPB 3335 in woody olive plants, but not in micropropagated (non-woody) olive plants.
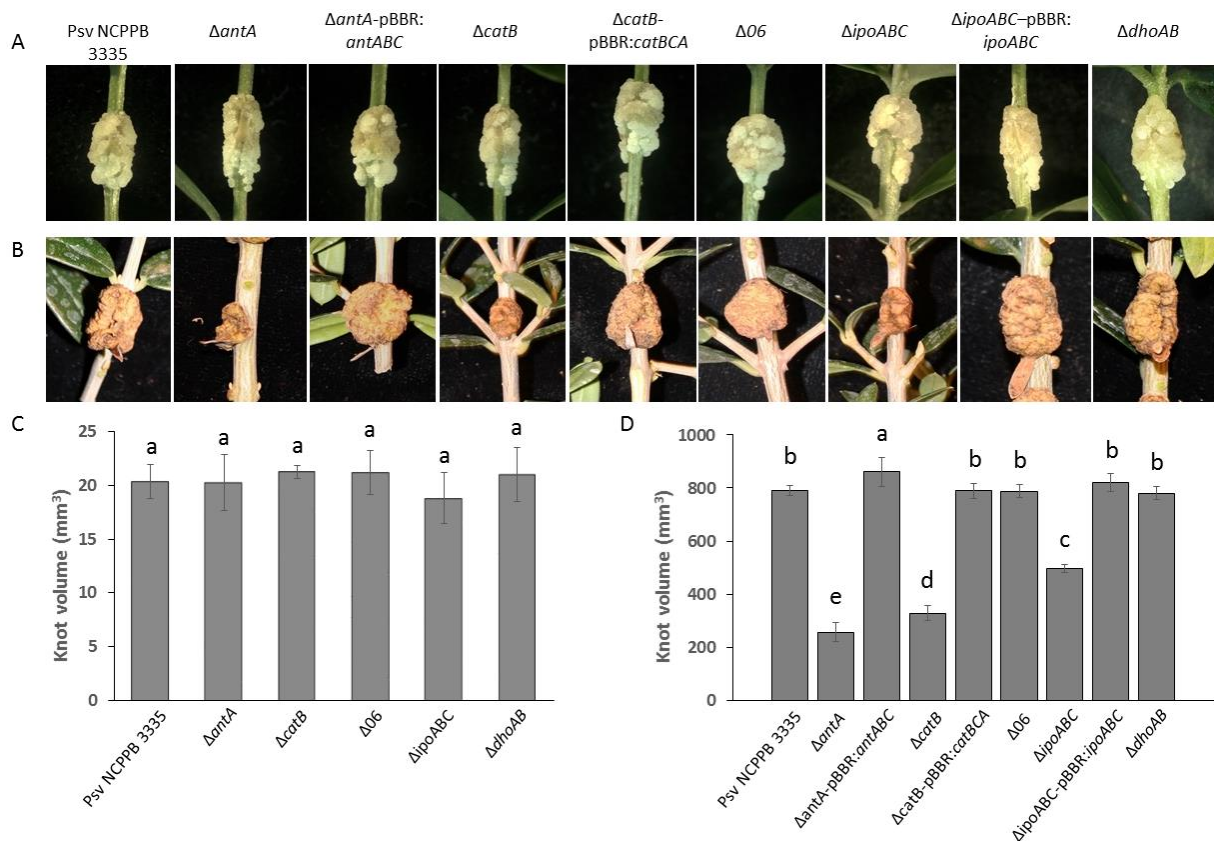
Figure 8. Role of the genetic clusters located within the WHOP region in the virulence of Psv NCPPB 3335 in olive plants. Knots developed by the indicated strains on (A) non-woody plants and (B) woody olive plants at 30 and 90 days post-inoculation, respectively. Quantification of the knot volume generated by the indicated strains on (C) non-woody plants (D) and woody olive plants. Error bars represent the

standard deviation from the average volume of a minimum of three knots. The same letters indicate differences that were not significant (α = 0.05) using the ANOVA statistical test.

Mixed suspensions of the wild type strain Psv NCPPB 3335 and each of the mutants affected in the WHOP region were prepared to perform competitive assays on both *in vitro* micropropagated (non-woody) and woody olive plants (Fig. 9). On non-woody olive plants, the resulting competitive index (CI) values were not statistically different to one, except for that of the Δ*ipoABC* mutant (CI= 0.39±0.16) (Fig. 9A). However, when mixed inoculations were carried out on woody olive trees, the obtained CI values were statistically lower than unity, except for the Δ*antA* mutant (Fig. 9B). The lowest value was observed for the Δ*catB* mutant (CI= 0.11±0.04). Similarly to the results described above in relation to the virulence of the mutant strains, the Δ*catB*, Δ*06* and Δ*dhoAB* mutants were impaired in their competitive growth exclusively in woody olive plants, whereas their fitness and survival in non-woody olive plants was similar to that of the wild type strain.
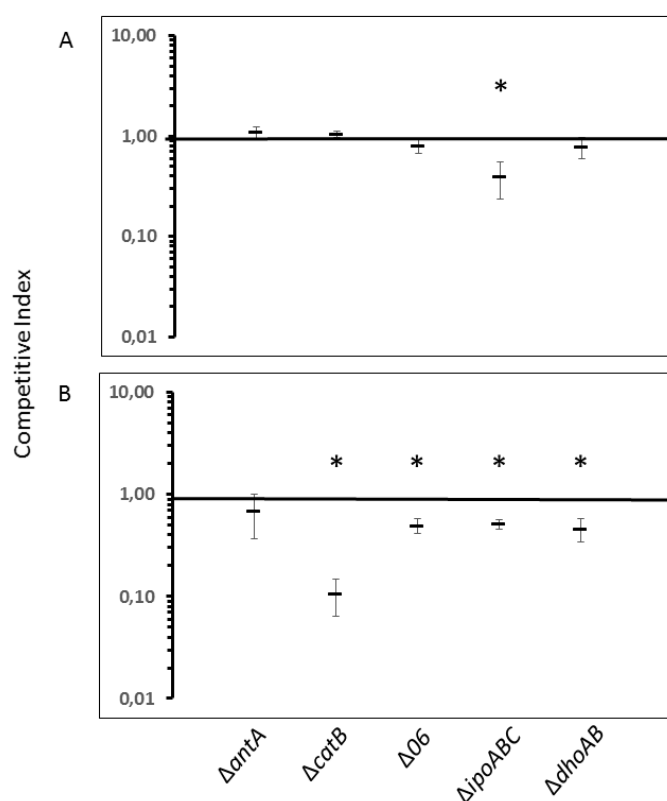
Figure 9. Fitness of *P. savastanoi* NCPPB 3335 mutants affected in the WHOP region *in planta*. Competitive index (CI) assays between Psv NCPPB 3335 and each of the indicated mutants on (A) non-woody olive plants at 30 days post inoculation (dpi) and (B) woody olive plants at 90 dpi. Error bars represent the

standard deviation from the mean of three independent replicates. Asterisks represent CI values significantly distinct from one using the T-Student test ($P<0.05$).

DISCUSSION

The WHOP region of the *P. syringae* complex, first described in Psv NCPPB 3335 (Rodriguez-Palenzuela *et al.*, 2010) and *P. syringae* pv. aesculi (Green *et al.*, 2010), is currently viewed as a relevant genomic feature for the evolution of *P. syringae* PG1 and PG3 strains associated with woody hosts (Bartoli *et al.*, 2015a; Nowell *et al.*, 2016). In this study, we extended the analysis of the WHOP region distribution to 40 additional members of the *P. syringae* species complex: 32 strains of *P. syringae* pathovars included in PG1 to PG7, *P. savastanoi* pv. retarcapa, *P. amygdali*, *Pseudomonas cannabina*, *Pseudomonas caricapapayae*, *Pseudomonas congelans*, *Pseudomonas fiscuserectae*, *P. meliae* and *Pseudomonas viridiflava*. Besides other PG3 strains also infecting woody organs of woody hosts (*P. savastanoi* pv. retacarpa, *P. syringae* pv. cunninghamiae and pv. photiniae, *P. meliae* and *P. amygdali*) a complete WHOP region was also found in *P. syringae* pv. actinidifoliorum (PG1) and *P. syringae* pv. ciccaronei (PG3), both inducing leaf spots in woody hosts (Table 4). It could be possible that these two pathovars represent a transition point from woody to herbaceous organs that maintain the WHOP region. In fact, strains of *P. syringae* pv. actinidifoliorum, which has been proposed to be a new and less virulent pathovar emerging from *P. syringae* pv. actinidiae, are unable to cause symptoms on woody organs of *Actinidia deliciosa* and *Actinidia chinensis* (Cunty *et al.*, 2015). *P. syringae* pv. avellanae and *P. syringae* pv. avii, both included in PG1 and pathogenic to woody hosts, have been shown not to encode the WHOP region (Nowell *et al*., 2016). Here we show that this cluster is neither found in *Pseudomonas tremae* (PG3), causing galls on trunks and twigs of urajiroenoki (*Trema orientalis*). The genetic traits governing adaptation of these strains to woody niches remain unknown.

Interestingly, we also found that some *P. syringae* pathovars of PG2 conserve a partial sequence of the WHOP region, the *catBCA* operon (Table 4). Similarly to the phylogeny of the genes flanking the WHOP region (Nowell *et al*., 2016), the evolutionary history of the *catBCA* operon shown in Figure 2 reveals phylogenetic discordance with that of the *P. syringae* complex based on housekeeping genes (Berge *et al*., 2014), suggesting the existence of horizontal transfer. Nowell *et al*. (2016) explained the presence of the WHOP region in both PG1 and PG3 by a recombination event between an ancestral PG1 lineage and an ancestral PG3 lineage, resulting in the horizontal transfer of the WHOP genes across these phylogroups. This hypothesis is further supported by the topology of the *catBCA* operon (Fig. 2). In relation to the exclusion of PG2 in the *catBCA* phylogeny, distinct recombination events between ancestral lineages of both PG2 and other *Pseudomonas*, might explain the acquisition of the *catBCA/catR* cluster in *P. syringae* pv. coryli, *P. syringae* pv. spinaceae and *P. syringae* pv. japonica. The *catBCA* operon,

which is widely distributed within the genus *Pseudomonas*, has been proposed to play an important role in the degradation of catechol and catechol-derived compounds in the plant-associated bacterium *P. putida* KT2440 (Jimenez *et al.*, 2002). Adaptation of *P. syringae* pathovars coryli, spinaceae and japonica to their respective hosts may have required the incorporation of the *catBCA* operon into their genomes, whereas the other WHOP-encoded pathways (except for the *antABC* operon in *P. syringae* pv. japonica) are dispensable in these niches. In agreement with this hypothesis, a transposase was found immediately downstream of the *catA* gene in *P. syringae* pv. japonica (Fig. 1C), suggesting that the *antABC* and *catBCA* operons, which are encoded in close proximity, may have been subjected to genetic instability in this pathovar. Interestingly, *P. resinovorans* NBRC 106553, isolated from activated sludge, carries the *antABC* operon in the plasmid pCAR1, a 200-kb plasmid of the incompatibility group (Inc) P-7 essential for the degradation of carbazole (Urata *et al.*, 2004), further supporting the hypothesis that these operons are subjected to horizontal transfer within the *Pseudomonas* genus.

Although Psv NCPPB 3335 is unable to utilize 6-chloro anthranilate, transcription of the *antABC* operon in this strain was demonstrated in this study to be induced by both anthranilate and 6-chloro anthranilate (Fig. 4C). These results are in agreement with previous observations in *P. fluorescens* (Retallack *et al.*, 2006). Despite transcription of the *catBCA* operon is activated by CatR in *P. putida* (Rothmel *et al.*, 1990), Psv NCPPB 3335 does not encode a *catR* homolog in its genome. Therefore, transcriptional regulation of *catBCA* in this strain is intriguing. Although expression of the *catB* gene in this strain was higher when anthranilate, the substrate of the upper *antABC* operon (Fig. 4A), was present in the media, this increase was not observed in a mutant unable to convert anthranilate into catechol (Fig. 4D). Thus, anthranilate or catechol-related compounds might also act as inductors of the *catBCA* operon. In relation to this, induction of the *catBCA* operon in *P. putida* by *cis,cis*-muconate, the product generated by oxidation of catechol via CatA*,* has been shown to be mediated by CatR (McFall *et al.*, 1998). Although both CatR and AntR belong to the LysR/XylS family of transcriptional regulators, their divergent sequences do not suggest that AntR might also be in charge of the regulation of *catBCA*. Codification of an orphan *benR* gene in Psv NCPPB 3335 (Fig. 1, Table 5) prompted us to analyse the possibility that BenR could be involved in the activation of *catBCA*. However, BenR boxes (Silva-Rocha & de Lorenzo, 2012) were not found upstream of this operon in Psv NCPPB 3335. Thus, the transcriptional activator of *catBCA* in Psv NCPPB 3335 and other *P. syringae* strains encoding the WHOP region remains unknown.

We confirmed the involvement of *antABC* and *catBCA* in the transformation of anthranilate and catechol, respectively, and determined an oxygenase activity for the *ipoABC* operon. The exposure of the Psv NCPPB 3335 Δ*catB* mutant to a medium with catechol resulted in the accumulation of several unidentified compounds that were not detected in the supernatants of the Δ*catB* complemented strain. Since catechol is highly toxic for *P. savastanoi* (Capasso *et al.*, 1995), this result suggest that Psv is able to detoxify catechol in the absence of the *catBCA* operon using alternative pathways. Catechol 2,3-dioxygenase, an enzyme that modifies catechol by opening the aromatic ring in position *meta* (Parales *et al.*, 1997), is widespread among plant associated bacteria (Olapade & Ronk, 2015), including an endophytic *Pseudomonas* strain (Pawlik & Piotrowska-Seget, 2015). However, the genome of Psv NCPPB 3335 does not encode this enzyme.

The contribution to the virulence and fitness of Psv NCPPB 3335 *in planta* was analysed for each of the individual clusters encoded within the WHOP region, with the exception of the orphan *benR* gene. Regarding the virulence of the bacteria, it was observed that the Δ*antA*, Δ*catB* and Δ*ipoABC* mutants generated olive knots significantly smaller than those induced by the wild type strain on woody plants, but not on non-woody plants. In relation to the Δ*antA* and Δ*catB* strains, several pathways for bacterial mineralisation of the auxin indole 3-acetic acid (IAA) involving anthranilate and catechol have been proposed (Leveau & Gerards, 2008). Also, IAA levels have been demonstrated to positively regulate knot size induced by Psv NCPPB 3335 on olive plants (Aragon *et al.*, 2014). Although *P. savastanoi* synthesizes IAA from tryptophan by the action of the *iaaMH* operon, which follows the indol-3-acetamide pathway (Kosuge *et al.*, 1966; Comai & Kosuge, 1982), a secondary pathway for the biosynthesis of this phytohormone remains to be elucidated (Aragon *et al.*, 2014). On the other hand, anthranilate is an intermediate metabolite in the biosynthesis of tryptophan in bacteria (Radwanski & Last, 1995). Taking into account that the Psv NCPPB 3335 Δ*antA* mutant is affected in its capacity to eliminate anthranilate (Fig. 5C), a disequilibrium of the tryptophan pool and, therefore, of the biosynthesis of IAA, could take place in this strain. Furthermore, several of the *iac* locus genes, which are involved in the catabolism of IAA in *P. putida* 1290 (Leveau & Gerards, 2008), showed relative similarity (around 30% amino acid identity) to genes located within the WHOP region; i.e. *antA* (*iacC*), *antB* (*iacD*), PSA3335_3210 (*iacE*), *antC* (*iacF*) and PSA3335_3208 (*iacG*).

Despite the virulence reduction observed in woody olive plants for the Δ*antA* mutant, its competitiveness in this tissue was similar to that of the wild type strain (Fig. 8). These results suggest that degradation of anthranilate-related compounds is not required for growth and survival of Psv in woody olive tissues. A recently published study showed that *P. syringae* strains

lacking the "catechol operon" were unable to grow endophytically in kiwifruit trees, whereas other strains that carry this region could do so (Bartoli *et al.*, 2015a). Similarly, the Psv NCPPB 3335 Δ*catBCA*, Δ*dhoAB* and *Δ06* mutants were less competent than the wild type strain on woody olive plants, but not on microprogated plants (Fig. 9), a finding that reinforces the hypothesis that the WHOP region contributes to the adaptation of bacteria from the *P. syringae* complex to woody niches. Although the chemical structure of wood cannot be defined precisely for a given tree specie; wood is composed mainly of the polysaccharides cellulose and hemicellulose (65-75%,) and lignin (18-35%) (Pettersen, 1984). Lignin is a complex organic network synthesized from three hydroxycinnamyl alcohols (*p*-coumaryl, coniferyl and sinapyl alcohols) (Boerjan *et al.*, 2003; Ralph *et al.*, 2004). It is well-known that lignin-related monomers are funnelled into protocatechuate and catechol prior to degradation through the β-ketoadipate pathway, which is widely distributed in soil bacteria and fungi (Harwood & Parales, 1996). While the catechol degradation machinery is restricted to several pathovars within the *P. syringae* complex (Table 4), the degradation of protocatechuate into Krebs cycle intermediaries is a feature widely distributed among *P. syringae* pathovars. Thus, the WHOP-encoded activities might complement the protocatechuate catabolic pathway to allow degradation of additional lignin-related compounds in bacteria that colonise woody organs. For example, cinnamate, an unsubstituted lignin-related compound, is metabolized via catechol (Andreoni *et al.*, 1991). Thus, the WHOP region could help bacteria to utilise lignin precursor compounds as carbon/nitrogen sources. Another putative advantage conferred to bacteria by the WHOP-encoded activities could be the modification of these compounds to decrease their toxicity. In fact, catechol and guaiacol, the latter a type of lignin subunit derived from coniferyl alcohol, are highly toxic for *P. savastanoi* (Capasso *et al.*, 1995). Some other published works support the linkage between lignin and catechol-degrading activities. For example, the amendment of a soil with wood sawdust favoured the development of bacteria carrying the *catA* gene (catechol 1,2-dioxygenase), in comparison with a non-amended soil (Cebron *et al.*, 2015). In addition, strains possessing high lignocellulose degrading activity were able to mineralise catechol partially (Vetrovsky *et al.*, 2014). Unlike the Δ*catBCA*, Δ*dhoAB* and *Δ06* mutants, which are impaired in their fitness exclusively on woody plants; the Psv NCPPB 3335 Δ*ipoABC* operon mutant displayed a slower growth rate in both woody and non-woody plants in comparison to the wild type strain. This finding suggests that this impairment is not directly related to compounds that may act as wood precursors. Phenolic compounds are secondary metabolites produced by plants upon pathogen attack (Poiatti *et al.*, 2009). Perhaps, the *ipoABC* operon is involved in the degradation of such defence compounds, which are produced by both non-woody and woody plants, to decrease their toxicity. However, further work is needed to confirm this hypothesis.

In summary, we show that besides PG1 and PG3 strains infecting woody organs of woody hosts, a complete WHOP region is also encoded in *P. syringae* pv. ciccaronei and *P. syringae* pv. actinidifoliorum, which cause leaf spots in woody hosts. Partial conservation of the WHOP occurs in only a few PG2 strains. Furthermore, several clusters located within the WHOP region play a role in the adaptation of Psv NCPPB 3335 to woody hosts, but not to non-woody plants, supporting the role of the WHOP region in the adaptation of other *P. syringae* pathovars to fruit trees and other woody hosts. We confirmed the function of the *antABC* and the *catBCA* operons and identified an oxygenase activity for the *ipoABC* operon. However, further work is necessary to determine the environmental or plant-derived substrate(s) used by the enzymes encoded in the WHOP region, as well as to elucidate the activity of the *dhoAB* operon and the PSA3335_3206 gene.

This work has been accepted for publication the 22nd of December 2016 in Molecular Plant-Microbe Interactions, a journal of the American Phytopathological Society (APS) (Caballo-Ponce *et al.*, 2016).

Chapter II

Comparative analysis of the quorum sensing system in *Pseudomonas savastanoi* pv. savastanoi NCPPB 3335 and other *Pseudomonas syringae* strains.

INTRODUCTION

Many bacteria assess their local population via the secretion of small signalling molecules in a process named quorum sensing. The signal molecules, commonly acylated homoserine lactones in Gram (-) bacteria (AHLs) are synthesized by a LuxI-family protein and diffuse through the bacterial membrane. The increase of a bacterial population brings to accumulation of AHLs in the environment and, upon reaching a threshold concentration (the quorum), are recognized inside the bacterial cells by a LuxR-family transcriptional regulator that controls the transcription of target genes (Bassler, 1999; Fuqua *et al.*, 2001; Miller & Bassler, 2001; Whitehead *et al.*, 2001). A canonical quorum sensing system is here defined as that composed of an adjacent *luxI/luxR* pair. However, the number of LuxI- and LuxR-type proteins is not always equal for a given bacterial species. In addition to the paired *luxI/luxR* genes, the analysis of a set of 265 protobacterial genomes showed that a number of genomes also contain a *luxR* gene, generally named *luxR* solos (Subramoni & Venturi, 2009), which are not encoded in the vicinity of *luxI* (Case *et al.*, 2008). LuxR solos are able to respond to endogenously produced AHLs (Chugani *et al.*, 2001) or to the AHLs produced by neighbouring bacteria (Ahmer *et al.*, 1998). Interestingly, a sub-family of LuxR solos unique to plant-associated bacteria, which respond to plant signals and are encoded in the proximity of the *pip* gene (encoding for a proline iminopeptidase) has been described (Patel *et al.*, 2013).

The quorum sensing system of *Pseudomonas aeruginosa* is the best characterized among Pseudomonads and consist of two interconnected *luxI/luxR* pairs (Chugani *et al.*, 2001; Heurlier *et al.*, 2006; Willcox *et al.*, 2008; Lee & Zhang, 2015). In *P. aeruginosa* PAO1 these two LuxI homologs govern the transcription of over 300 genes (Schuster *et al.*, 2003; Wagner *et al.*, 2003). Plant-associated Pseudomonads also interact via the quorum sensing system (Loh *et al.*, 2002; Von Bodman *et al.*, 2003), although some strains, including several *Pseudomonas syringae*, do not produce detectable amounts of AHLs (Dumenyo *et al.*, 1998). For instance, the genome of *P. syringae* pv. actinidiae does not encode for a *luxI* homolog, but carry several *luxR* homologs that allow for "eavesdropping" of the signals produced by other bacteria (Patel *et al.*, 2014). Many efforts have been dedicated to understand the quorum sensing system in the *P. syringae* complex, mainly using *P. syringae* pathovars syringae and tabaci as models. In *P. syringae* pv. syringae (hereafter Psy) B728a this system has been shown to regulate alginate production and motility, as well as bacterial virulence measured as the incidence of lesions caused on leaves. Moreover, AHL-deficient mutants did not provoke tissue maceration of bean pods, typical symptoms of wild type infections (Quinones *et al.*, 2005). Two different transcriptomic analyses identified quorum sensing-controlled genes in *P. syringae* strains. AhlR, a LuxR homolog in *P. syringae* B728a, activates a small number of genes that, in addition, are located on the vicinity

99

of the *luxI/luxR* pair (Yu *et al.*, 2014). In contrast, a *luxI* mutant of *P. syringae* pv. tabaci (hereafter Pst) 6605 showed a larger number of genes with an altered transcription level in comparison to the wild type strain (Taguchi *et al.*, 2015).

Despite the attention paid to the quorum sensing system of *P. syringae* strains pathogenic on non-woody host, very little research focused on the quorum sensing systems of woody-host pathogens of the *P. syringae* complex. In fact, up to our best knowledge, only two published works examined this regulation circuit in this type of bacteria. One of these studies focused on the intriguing regulation of the non AHL-producing kiwifruit pathogen *P. syringae* pv. actinidiae (Patel *et al.*, 2013), whereas the other explored the quorum sensing of the olive tree pathogen *Pseudomonas savastanoi* pv. savastanoi (Psv) (Hosni *et al.*, 2011). Bacteria-bacteria communication via quorum sensing critically affects the virulence and exopolysaccharides (EPS) production of Psv DAPP-PG 722. Moreover, this strain shares the same signal molecules with *Erwinia toletana* DAPP-PG 735, a bacterium commonly associated to Psv within olive knots (Rojas *et al.*, 2004; Hosni *et al.*, 2011; Passos da Silva *et al.*, 2014). The genome of Psv NCPPB 3335, reference Psv strain in our laboratory, harbours a canonical *luxI/luxR* pair (Rodriguez-Palenzuela *et al.*, 2010), which is identical to that of Psv DAPP-PG 722, although its quorum sensing system has not been investigated up to date.

In this chapter we examined the quorum sensing system of Psv NCPPB 3335. The first aim of this study was to determine differences in the presence of the *luxI/luxR* homologs among a collection of 27 strains of the *P. syringae* complex belonging to phylogroups (PGs) 1 to 4. Secondly, to identify genes controlled by the amount of AHL in Psv NCPPB 3335, as well as to analyse the similarities and differences among the quorum sensing regulons of NCPPB 3335 and those of other *P. syringae* strains.

MATERIAL AND METHODS

Bacterial strains, media and growth conditions

Bacterial strains used in this study are listed in Table 1. *P. savastanoi* pv. savastanoi and *Escherichia coli* were grown at 28 °C or 37 °C, respectively, in Luria-Bertani (LB) medium (Miller, 1972) and Super Optimal Broth (SOB) (Hanahan, 1983). Solid and liquid media were amended when required with the appropriate antibiotic. Antibiotic concentration used were: kanamycin (Km) 10 µg ml^{-1} for *P. savastanoi* and 50 µg ml^{-1} for *E. coli*, gentamycin (Gm) 10 µg ml^{-1}, ampicillin (Ap) 400 µg ml^{-1} for *P. savastanoi* and 100 µg ml^{-1} for *E. coli*; and tetracycline 10 µg ml^{-1}.

Table 1. Strains used in this study

Strain	Relevant characteristics[a]	Source
***Pseudomonas savastanoi* pv. savastanoi**		
NCPPB 3335	Wild type strain	(Perez-Martinez *et al.*, 2007)
Δ*pssI*	Deletion *pssI* (PSA3335_1621) mutant (Km^R)	This work
Δ*pssR*	Deletion *pssR* (PSA3335_1622) mutant (Km^R)	This work
***Pseudomonas syringae* pv. syringae**		
B728a	Wild type strain	(Loper & Lindow, 1987)
Escherichia coli		
DH5α	*F-, φ80dlacZ M15, (lacZYA-argF) U169, deoR, recA1, endA, hsdR17 (rk – mk-), phoA, supE44, thi-1, gyrA96, relA1*	(Hanahan, 1983)
GM2929	*F-, ara-14, leuB6, thi-1, tonA31, lacY1, tsx-78, galK2, galT22, glnV44, hisG4, rpsL136, xyl-5, mtl-1, dam13::Tn9, dcm-6, mcrB1, hsdR2, mcrA, recF143* (Sp^R Cm^R)	(Palmer & Marinus, 1994)
JB52	Harbours pJBA130 and is used as a sensor for acyl-homoserine lactone production	(Andersen *et al.*, 2001)

[a]Km, kanamycin

Construction of bacterial strains and plasmids

Plasmids and oligonucleotides used in this study are listed in Tables 2 and 3 approximately. For the generation of *P. savastanoi* pv. savastanoi NCPPB3335 mutants, DNA fragments of approximately 1 kb corresponding to the upstream and downstream flanking regions of the gene to be deleted were amplified in three rounds of polymerase chain reaction (PCR) using genomic DNA from NCPPB 3335 as a template and Expand High Fidelity polymerase (Roche Applied Science, Mannheim, Germany). Restriction sites for *Hind*III were included in the primers as previously described (Matas *et al.*, 2014). The resulting products, consisting on upstream and downstream flanking regions separated by the *Hind*III restriction site, were cloned into pGEM-T *easy* to yield pECP10 and pECP11 (Table 2), and sequenced to discard mutations. Later, the kanamycin resistance gene *nptII* was extracted by enzyme restriction from pGEM-T-KmFRT-

*Hind*III (Aragon *et al.*, 2014) and cloned into the plasmids mentioned above to generate pECP10-Km and pECP11-Km (Table 2). All plasmids generated for the construction of Psv NCPPB 3335 mutants were suicide vectors in *P. savastanoi*. Plasmids were transferred to NCPPB 3335 by electroporation (Perez-Martinez *et al.*, 2007) and transformants were selected in LB-Km plates. Plasmids pECP10-Km and pECP11-Km were used for the construction of Δ*pssI* and Δ*pssR* mutants respectively. To select the allelic interchange (double recombination event) and discard plasmid integration (single recombination event), individual colonies were replicated into LB-Ap plates and Ap[R] colonies were discarded. Finally, Southern blot analyses were carried out to confirm single integration in the correct position in Psv genome.

Plasmids for the complementation of the mutant strains were generated as follows. The complete open reading frames of *pssI* and *pssR* genes and their corresponding promoter and transcriptional terminator regions were amplified by PCR using NCPPB 3335 genomic DNA as a template and Expand High Fidelity polymerase (Roche Applied Science, Mannheim, Germany) and cloned into pGEM-T *easy* (Promega, Madison, WI, USA). After sequencing to discard mutations, the fragments were directionally subcloned into pBBR:MCS5. Plasmids pBBR:*pssI* and pBBR:*pssR* were used for the complementation of Δ*pssI* and Δ*pssR* respectively.

Table 2. Plasmids used in this study

Name	Description[a]	Source
pGEM-T *easy*	Cloning vector containing ori f1 and *lacZ* (Ap[R])	(Promega, Madison, WI, USA)
pBBR1:MCS5	Broad host-range cloning vector (Gm[R])	(Kovach *et al.*, 1995)
pJBA130	pME6031-*luxR*-P$_{luxI}$-RBSII-*gfp*mut3*-T$_0$-T$_1$ (Tc[r])	(Andersen *et al.*, 2001)
pGEM-T-KmFRT-*Hind*III	Contains Km[R] from pKD4 and *Hind*III sites (Ap[R] Km[R])	(Aragon *et al.*, 2014)
pECP10	pGEMT-derivative containing 1kb on each side of the *pssI* (PSA3335_1621) gene from NCPPB 3335 (Ap[R])	This work
pECP10-Km	pGEMT-derivative containing 1kb on each side of the *pssI* (PSA3335_1621) gene from NCPPB 3335 interrupted by the kanamycin resistance gene *nptII* (Ap[R], Km[R])	This work
pECP11	pGEMT-derivative containing 1kb on each side of the *pssR* (PSA3335_1622) gene from NCPPB 3335 (Ap[R])	This work
pECP11-Km	pGEMT-derivative containing 1kb on each side of the *pssR* (PSA3335_1622) gene from NCPPB 3335 interrupted by the kanamycin resistance gene *nptII* (Ap[R], Km[R])	This work
pBBR:*pssI*	pBBR1:MCS5-derivative containing the Psv NCPPB 3335 *pssI* and its promoter region (352 bp) flanked by *EcoR*I and *Xba*I restriction sites (Gm[R])	This work
pBBR:*pssR*	pBBR1:MCS5-derivative containing the Psv NCPPB 3335 *pssR* and its promoter region (435 bp) flanked by *EcoR*I and *Xba*I restriction sites (Gm[R])	This work
pMP220	Broad-host-range, low-copy-number promoter probe vector, IncP replicon, *lacZ* (Tc[R])	(Spaink *et al.*, 1987)

Plasmids used in this study (continuation)

Name	Description[a]	Source
pMP220-P$_{pssR}$	Contains a fragment of 338 bp corresponding with the *pssR* promoter from Psv NCPPB 3335 cloned with *Kpn*I and *Bgl*II restriction sites (Tc^R).	This work
pMP220-P$_{pssI}$	Contains a fragment of 352 bp corresponding with the *pssI* promoter from Psv NCPPB 3335 cloned with *Kpn*I and *Bgl*II restriction sites (Tc^R).	This work
pMP220-P$_{ahlI}$	Harbours a fragment of 344 bp corresponding with the *ahlI* promoter from *P. syringae* pv. syringae B728a cloned with *Kpn*I and *Bgl*II restriction sites (Tc^R).	This work

[a]Ap, ampicillin; Gm, gentamycin; Km, kanamycin; Tc, tetracycline; Gm, gentamycin.

Promoter activity assays

For the generation of promoter fusions to β-galactosidase, fragments of 338, 352 and 344 bp upstream the open reading frame of Psv NCPPB 3335 *pssI* and *pssR* genes and Psy B728a *ahlI* gene, respectively, were amplified by PCR using genomic DNA as a template. *Kpn*I and *Bgl*II restrictions sites were included in the primers. The amplicons were independently cloned into pGEM-T *easy*, sequenced to discard mutations and subcloned into pMP220. Finally, plasmids were introduced in bacteria by electroporation. For the measurement of *pssR* promoter activity, the Psv NCPPB 3335 and its derivative *pssI* mutant strains were grown in LB broth at an initial OD$_{600nm}$ of 0.2 and the β-galactosidase activity was monitored along the growth curve. For *pssI* promoter activity, Psv NCPPB 3335 and its derivative *pssI* and *pssR* mutant were grown in King's B (KB) (King *et al.*, 1954) and LB media at an initial OD$_{600nm}$ of 0.3 and samples for β-galactosidase activity were taken after 4, 6, 8 and 10 hours. An identical procedure was followed for the *pssI* promoter activity in *P. syringae* B728a, with the exception of an initial OD$_{600nm}$ of 0.1. β-galactosidase activity was quantified as previously described (Miller, 1972).

Production and identification of acyl-homoserine lactones

The production of AHLs in Psv NCPP 3335, Δ*pssI* and Δ*pssR* mutants was analysed as previously described (Andersen *et al.*, 2001). The indicated strains were incubated for 24 hours at 28ºC on a LB plate together with *E. coli* JB52- pJBA130 (sensor strain) and were visualized in a Leica MZ FLIII stereoscopic fluorescence microscope equipped with a 100 W mercury lamp and a GFP2 filter (excitation 480/40 nm; emission 510LP nm). For the identification of the AHLs produced, 100 ml of an overnight culture in LB broth of Psv NCPPB 3335, the *pssI* mutant and its complemented strain carrying pBBR:*pssI* (Table 2) were centrifuged to remove bacteria. The supernatant of each culture was filtered (pore diameter 0.45 μm) and mixed with the same

volume of 0.1% acetic acid (v/v) in ethyl acetate and shaken for 30 minutes (extraction step). The organic phase was recovered prior and the extraction step was repeated. The organic phases were put alltogether and dried. The AHLs produced by each strain were identified by high performance liquid chromatography coupled to mass spectrometry (HPLC-MS) as described previously (Coutinho *et al.*, 2013).

RNAseq experiment

Three independent cultures of Psv NCPPB 3335 and Δ*pssI* were incubated at 28ºC in LB to early stationary phase (OD$_{600nm}$= 2) and RNA was then extracted with the RiboPure™ RNA Purification Kit (Ambion, Thermo Scientific, MA, USA). Total RNA was treated with a TURBO DNA-free™-Kit (Applied Biosystems; CA, USA) as detailed by the manufacturer's instructions. DNA-free RNA samples were subjected to depletion of the ribosomal RNA using the Ribo-Zero Magnetic Kit specific for gram-negative bacteria (Epicentre, Madison, WI, USA). rRNA-depleted RNA were processed and sequenced as detailed previously (Coutinho *et al.*, 2015). RNA sequencing was performed by IGA Technology Services Srl (Udine, Italy). Bowtie2 software was used to map the raw reads to the Psv NCPPB 3335 genome (Langmead & Salzberg, 2012) and the reads in genes were counted with Granges (Lawrence *et al.*, 2013). Finally, analysis of differentially expressed genes was carried out with DESeq2 (Love *et al.*, 2014). Genes with a log$_2$(fold change) over 0.9 or under -0.9 were selected for validation by reverse transcription quantitative PCR (RT-qPCR) as detailed later.

Biofilm, EPS, motility and virulence assays

Biofilm formation by Psv NCPPB 3335, Δ*pssI* and Δ*pssR* was analysed on glass surfaces using a static microcosm assay, as detailed previously (Pliego *et al.*, 2008). Crystal violet (CV) was used to quantify biofilm formation (O'Toole & Kolter, 1998). For exopolysaccharide detection, a drop containing 10^6 cfu was placed on LB, KB, MM (Hosni *et al.*, 2011) and MGY+Sorbitol 0.6 M (Quinones *et al.*, 2005) agar plates containing 50 μg ml^{-1} of Congo Red and incubated at 25ºC for two days. The results were captured with a high-resolution camera Canon D6200 (Canon Corporation, Tokyo, Japan). Swimming motility assays were performed in AB minimal medium supplemented with 10mM citrate and containing 0.3% agar (Huber *et al.*, 2001). The centre of a Petri dish was inoculated with 2 μl of a bacterial suspension containing 10^8 cfu/ml and incubated at 25 °C for 96 hours. Swarming motility was examined as described before (Huber *et al.*, 2001; Quinones *et al.*, 2005). A drop 2 μl of bacterial suspension containing 10^7 cfu/ml was inoculated on the surface of a Petri dish containing KB or AB media and 0.4% agar and incubated at 25 °C for 96 hours. Olive plants were micropropagated and inoculated as detailed previously

(Rodriguez-Moreno *et al.*, 2008). The morphology of the knots developed was observed with a stereoscopic microscope 30 days post-inoculation (dpi) (Leica MZ FLIII; Leica Microsystems, Wetzlar, Germany). Bacteria were recovered from the knots using a mortar and pestle containing sterile $MgCl_2$ 10 mM. Serial dilutions were plated on LB plates supplemented with the corresponding antibiotic when required. Population sizes were determined from three different knots. A minimum of three representative knots were 3D scanned and the knot size determined using the Neftabb Basic 5.2 software. The virulence of Psv and its derived mutants and complemented strains was also analysed on 1-year old olive plants as detailed before (Penyalver *et al.*, 2006; Perez-Martinez *et al.*, 2007; Matas *et al.*, 2012). Morphological changes scored at 90 dpi were captured with a high-resolution camera Canon D6200 (Canon Corporation, Tokyo, Japan). The knot volume was calculated from a minimum of three representative knots as described previously (Moretti *et al.*, 2008; Hosni *et al.*, 2011).

RNA extraction and RT-qPCR

Total RNA was extracted from frozen pellets using TriPure Isolation Reagent (Roche Applied Science, Mannheim, Germany) according to the manufacturer's instructions, except that the TriPure was preheated at 65 °C, the lysis step was performed at 65 °C, and 1-Bromo-3-chloropropane (Molecular Research Center, Cincinnati, OH, U.S.A.) was used instead of chloroform as previously described (Matas *et al.*, 2014). The RNA concentration was determined spectrophotometrically and its integrity was assessed by agarose gel electrophoresis. Total RNA was treated with a TURBO DNA-free™-Kit (Applied Biosystems; CA, USA) as detailed by the manufacturer's instructions. Later the samples were tested for genomic contamination by PCR. DNA-free RNA was reverse transcribed using random hexamers included in the iScript™ cDNA synthesis kit (BioRad; CA, USA). To validate RNAseq data, Psv NCPPB 3335 and Δ*pssI* were incubated in LB at 28ºC to OD_{600nm}= 2, bacteria were collected by centrifugation and stored at -80 °C for RNA extraction. Genes with a $\log_2$(fold change) over 0.9 or under -0.9 in the RNAseq experiment were selected for validation. For the analysis of the genes controlled by AhlR in *P. syringae* pv.syringae B728a and since Psv NCPPB 3335 is not able to grow in HMM minimal media, NCPPB 3335 and its derivative *pssR* mutant were grown in LB broth amended with 10 μM C6-3-oxo homoserine lactone to OD_{600nm}= 2. Bacteria were collected by centrifugation and stored at -80 °C to purify RNA. Samples to analyse the expression in Psv NCPPB 3335 and Δ*pssI* of the genes regulated by quorum sensing in *P. syringae* pv. tabaci 6605 were collected as described previously (Taguchi *et al.*, 2015). Briefly, bacteria were grown in LB with 10 mM $MgCl_2$ at 27ºC to $OD_{600\ nm}$=0.3, centrifuged and incubated for additional 1h in MMMF medium. Then, bacteria were centrifuged and stored at -80 °C for further RNA extraction. Primers for RT-qPCR

were designed according to recommended instructions (Thornton & Basu, 2011). The primer efficiency tests, RT-qPCRs and confirmation of the specificity of the amplification reactions were performed as described previously (Vargas *et al.*, 2011) and the relative transcript abundance was calculated using the ΔΔ cycle-threshold (Ct) method (Livak & Schmittgen, 2001). Transcriptional data were normalized to the housekeeping gene *gyrA*. The relative expression ratio was calculated as the difference in qPCR threshold cycles (ΔCt = Ctgene of interest – Ct*gyrA*). One PCR cycle represents a twofold difference in template abundance; therefore, fold-change values were calculated as $2^{-\Delta\Delta Ct}$ as previously described (Pfaffl, 2001). RT-qPCR were performed in triplicate. Primers used for RT-qPCR are listed in Table 3.

Table 3. Oligonucleotides used in this study

Name	Sequence (5'→ 3')
Construction of the mutants strains	
PssR_F-1008	CATTCCAGTGCTCCTTGAGC
TAPssR_R3	AAGCTTGACTCACTATAGGGGCTTTCACGGTACGAACCTC
TDPssR_R739	CCCTATAGTGAGTCAAGCTTCCATCAACATGGGCATGG
TAPssl_R4	CCCTATAGTGAGTCAAGCTTCATGCATAGCGCTGCCTG
PssR_F-280	TGCGCTGTTCATCACTACTCC
Complementation of the mutant strains	
pssl_F-331	TCTAGATCGCTCTGATCCTGATGAGTG
pssl_R924	GAATTCCTCATCCGCTTCCATGACC
pssR-F-417	TCTAGAAGACGCTCGACGATGTCG
pssR_R993	GAATTCTTGCAATCGATCATCACGG
RT-qPCR	
PSA3335_0003-F	GGCTGGCTGTCAATTCGTC
PSA3335_0003-R	TCGAAGAAGAACGGGAGGTG
PSA3335_0454_F	TTCGCCAGGCAAGCTATCAA
PSA3335_0454_R	TCCTCGAAGCCCTGATCCA
PSA3335_1615-F	ACGCCGATCCATTACCTGTC
PSA3335_1615-R	CTACCTCAGTCGCCGAACC
PSA3335_1616-F	CAATCTGGCATTCGACCTGG
PSA3335_1616-R	CAGGCTCGTTCAAGGTTGG
PSA3335_1617-F	ATGTTCACCTCGCCGTTTAC
PSA3335_1617-R	GTCTTCTCGTTGCCTGACAG
PSA3335_1618-F	GACGGACACACTGCTCAAAG
PSA3335_1618-R	GGCTGTCTGACTTGGCTTTC
PSA3335_1619-F	GAAACGCCACGACGAAATCT
PSA3335_1619-R	TCGATGAGGTGAACAGGCTT
PSA3335_1620-F	CACTGACCGAAATGCTGCTGT
PSA3335_1620-R	TTGCTGACCACCGTGATGAT
PSA3335_1621-F	ACTGCCCACCGTTGAAGATAA
PSA3335_1621-R	CATAAGATTTCAGCCAGGAGTCG
PSA3335_1622-F	TCAAGGAGCACTGGAATGTCG
PSA3335_1622-R	TCTTCAAGGGATGGAAACGATT
PSA3335_1623-F	TGGTTCAGATTCGTCAGGGC
PSA3335_1624-R	GGGTCAGGTTGTAGCGTTCG
PSA3335_1624-F	CGATACCGTGCTGTGTGTCT

Table 3. Oligonucleotides used in this study

Name	Sequence (5'→ 3')
PSA3335_1624-R	GATCAGGGTGCGGGTAGTTC
PSA3335_2048_F	AATACCACCGCATCGACGAA
PSA3335_2048_R	TCACGCCGTTGACCAGAAA
PSA3335_2054_F	TGAGCATCTACAGGCTTCGGA
PSA3335_2054_R	CATGTTGATAAGGAATGAGGTTCG
AER-0003118-F	ATCAGGTCAATGTCCAGGCA
AER-0003118-R	CCGTGATGAAGCCGTTGTAG
PSA3335_2264-F	CCTGTATGCCCGTCTGAAAC
PSA3335_2264-R	TGTCCATCACCAGCACAAAC
PSA3335_2315_F	TGCCGTTCTTCCTGGCTTA
PSA3335_2315_R	ACCCGTCATTCATCCACCG
PSA3335_3135-F	TCTTCACTGCCTGTCCTGTC
PSA3335_3135-R	GCGTGTCCTTGGGCTTATTG
PSA3335_3741-F	GGATGCGGCGAAGGTTATTT
PSA3335_3741-R	CGCCACCGGAAAGAACATAG
PSA3335_3741-R	CGCCACCGGAAAGAACATAG
PSA3335_4121_F	CCAAGGTGCAGGACTGTTCA
PSA3335_4121_R	GATACGGGCGAAGGTGTTGT
PSA3335_4623_F	GACTCAAGCGATCAAGAACGATG
PSA3335_4623_R	CTGCTCGGGTGACAGACTG
PSA3335_4742_F	AGCGGGCATTCCTACCTTC
PSA3335_4742_R	AGAACAACGGGCGGATGTA
PSA3335_4922-F	CTGGCACTGTTCGTCTTCAC
PSA3335_4922-R	ATGGTCTGGATCTTCTCGCC

Promoter cloning

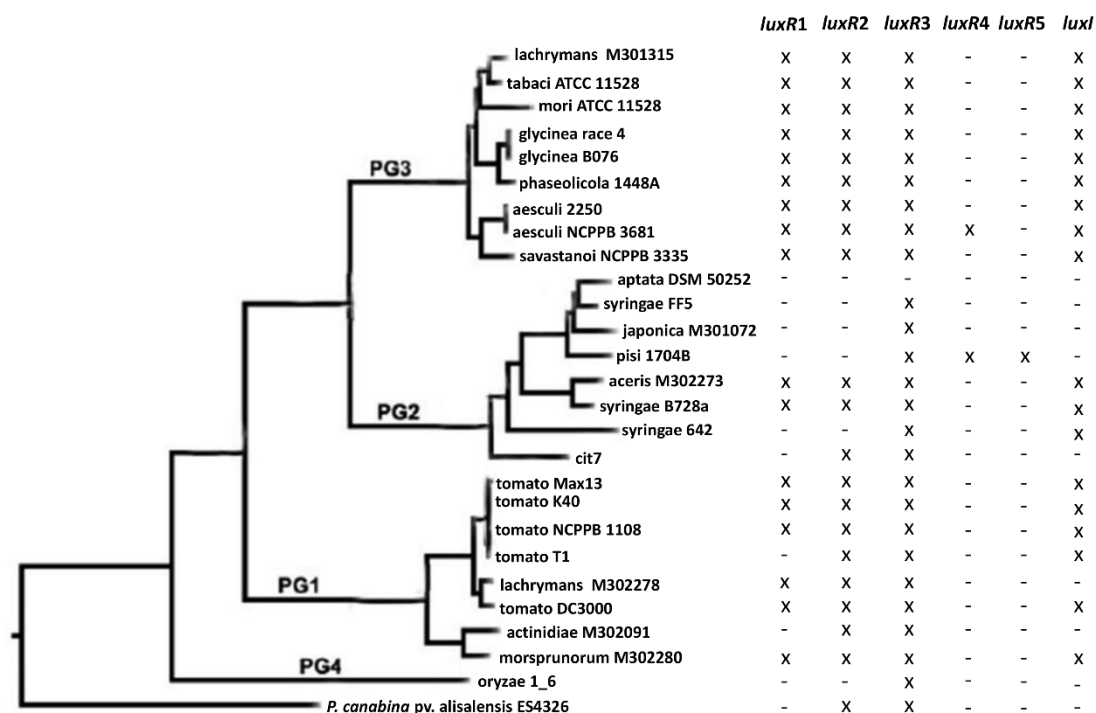|	
pssI_F-279	ACTCATGGAGATCTGGCAGAGATTTCGTGTTGGG
pssI_R35	ACTCATGGGGTACCGTAACGGGCATCGTCGTG
PluxB728a_F	AGATCTCTGATCCTGGTGCGTGTGG
PluxIB728a_R	GGTACCAAACCCACCCGGCGTCAC
pssR_F-264	AGATCTCCTTGCTGTCGGACAAGC
pssR_R36	GGTACCCCGTTTATCTTCAACGGTGG

RESULTS

Variable distribution of *luxI* and *luxR* homologs among *Pseudomonas syringae* pathovars

LuxI and LuxR homologous have been previously found in different *P. syringae* strains (Case *et al.*, 2008). However, a recent study described that *P. syringae* pv. actinidiae strains do not encode for a LuxI homolog, but possesses three LuxR solos (Patel *et al.*, 2014). This circumstance prompted us to analyse the presence/absence of *luxI* homologs and the number and type of *luxR* homologs among different strains of the *P. syringae* complex. 27 *P. syringae* strains belonging to PG1, PG2, PG3 and PG4 were chosen for these analyses. The genomes of all these strains, which are available at the ASAP database (https://asap.genetics.wisc.edu/asap/logon.php), have been used to construct a core genome phylogeny for *P. syringae*, derived from 2140 concatenated protein alignments (Nowell *et al.*, 2014). While all strains from PG3 contain a *luxI* homolog in their genomes, the presence of this gene was variable among strains of PG1 and PG2. Strains not encoding a *luxI* homolog among the 27 analysed include PG1 strains *P. syringae* pv. actinidiae and *P. syringae* pv. lachrymans M302278; several PG2 strains, i.e. *P. syringae* pv. aptata DSM 50252, Psy FF5, *P. syringae* pv. japonica M301072, *P. syringae* pv. pisi 1704B and *P. syringae* cit7; and *P. syringae* pv. oryzae 1_6 (PG4). Interestingly, different PG2 isolates belonging to *P. syringae* pv. syringae showed differences in their *luxI* content (Fig. 1).

A variable number of *luxR* homologs were also found among the strains analysed. The following nomenclature was used to differentiate among diverse *luxR* homologs: *luxR*1 is used for homologs encoded adjacent to a *luxI* gene; *luxR*2 refers to LuxR solos specific for plant-associated bacteria; and *luxR*3 and successive numbers correspond to LuxR solos homologs to those responding to AHLs. Most PG1 and PG3 strains contain a similar number and type of *luxR* homologs (*luxR1, luxR2* and *luxR3*), with the exception of *P. syringae* pv. aesculi NCPPB 3681 (PG3, also encoding a *luxR*4), and *P. syringae* pv. tomato T1 and *P. syringae* pv. actinidiae M302091 (PG1, both lacking *luxR1*). Strains of PG2 are more diverse; while Psy B728a and *P. syringae* pv. aceris M302273 encode a *luxR* content identical to most strains of PG3 analysed (*luxR1, luxR2* and *luxR3*), *P. syringae* pv. pisi 1704B also encodes three LuxR solos (*luxR3, luxR4* and *luxR5*), but none of them is the one typical of plant-associated bacteria (*luxR2*). In addition, *P. syringae* pv. aptata DSM 50252 does not contain either *luxR* nor *luxI* homologs and, *P. syringae* pv. japonica M301072 and Psy FF5, which are both *luxI⁻*, as well as Psy 642 (*luxI⁺*), only harbours a *luxR3* gene. Thus, Psy 642 contains an unpaired *luxI* gene. Interestingly, we found that different isolates of Psy display a different content of *luxR* homologs, similarly to their *luxI* content described above. Finally, *P. syringae* pv. oryzae 1_6 (PG4) only carry a *luxR3*. In summary, a high

variability in the content of the quorum sensing elements is observed among different strains and phylogroups of the *P. syringae* complex.

|	*luxR*1	*luxR*2	*luxR*3	*luxR*4	*luxR*5	*luxI*
lachrymans M301315	X	X	X	-	-	X
tabaci ATCC 11528	X	X	X	-	-	X
mori ATCC 11528	X	X	X	-	-	X
glycinea race 4	X	X	X	-	-	X
glycinea B076	X	X	X	-	-	X
phaseolicola 1448A	X	X	X	-	-	X
aesculi 2250	X	X	X	-	-	X
aesculi NCPPB 3681	X	X	X	X	-	X
savastanoi NCPPB 3335	X	X	X	-	-	X
aptata DSM 50252	-	-	-	-	-	-
syringae FF5	-	X	X	-	-	-
japonica M301072	-	-	X	-	-	-
pisi 1704B	-	-	X	X	X	-
aceris M302273	X	X	X	-	-	X
syringae B728a	X	X	X	-	-	X
syringae 642	-	-	X	-	-	X
cit7	-	X	X	-	-	-
tomato Max13	X	X	X	-	-	X
tomato K40	X	X	X	-	-	X
tomato NCPPB 1108	X	X	X	-	-	X
tomato T1	-	X	X	-	-	X
lachrymans M302278	X	X	X	-	-	-
tomato DC3000	X	X	X	-	-	X
actinidiae M302091	-	X	X	-	-	-
morsprunorum M302280	X	X	X	-	-	X
oryzae 1_6	-	-	X	-	-	-
P. canabina pv. alisalensis ES4326	-	X	X	-	-	-

Figure 1. Distribution of *luxR* and *luxI* homologs in the *P. syringae* complex. The phylogenetic tree was adapted from a previous study (Nowell *et al.*, 2014). *luxR*1 is defined as the *luxR* homolog encoded adjacent to *luxI*; *luxR*2 refers to *luxR* solos unique to plant-associated bacteria; *luxR*3 and successive numbers correspond to *luxR* solos that respond to AHLs. +/–, presence/absence of the corresponding homolog in a given strain. *Pseudomonas cannabina* pv. alisalensis ES4326 (PG5) was included as an outsider in the phylogenetic tree. PG, phylogroup.

The quorum sensing system of *Pseudomonas savastanoi* pv. savastanoi NCPPB 3335

Psv NCPPB 3335, reference strain in our laboratory (Perez-Martinez *et al.*, 2007), was the first sequenced *P. savastanoi* isolate (Rodriguez-Palenzuela *et al.*, 2010). The genome of this strain harbours a canonical *luxI/luxR* pair (hereafter named *pssI/pssR*) and two LuxR solos (Fig. 1), which according to their sequences are predicted to respond to plant signals (*luxR*2) or AHLs (*luxR*3). We also found that this content of quorum sensing elements is conserved in other strains belonging to different *P. savastanoi* pathovars whose genomes have been recently published (Moretti *et al.*, 2014; Bartoli *et al.*, 2015b; Thakur *et al.*, 2016).

To further analyse the quorum sensing system of Psv NCPPB 3335 we constructed deletion mutants of the *pssI* and *pssR* (*luxR*1) genes. Firstly, a bacterial biosensor strain was used to analyse the production of AHLs by the mutants in comparison with the wild type strain. This biosensor, which is based on the *Vibrio fischeri* quorum sensing system, is composed of a

plasmid-encoded *luxR* gene and a transcriptional fusion of the *luxI* promoter to the green fluorescent protein (GFP). Therefore, the sensor *E. coli* strain carrying this plasmid emits fluorescence in the presence of AHLs produced by a testing strain (Andersen *et al.*, 2001). Psv strains were T-streaked individually in combination with the sensor strain as depicted in Fig. 2A. While both the wild type Psv NCPPB 3335 strain (Fig. 2B) and its Δ*pssR* mutant (Fig. 2C) induced the emission of green fluorescence in the sensor strain, the Δ*pssI* mutant was not able to induce this phenotype (Fig. 2D). These results suggest that, as expected, AHL production was only impaired in the Δ*pssI* mutant.
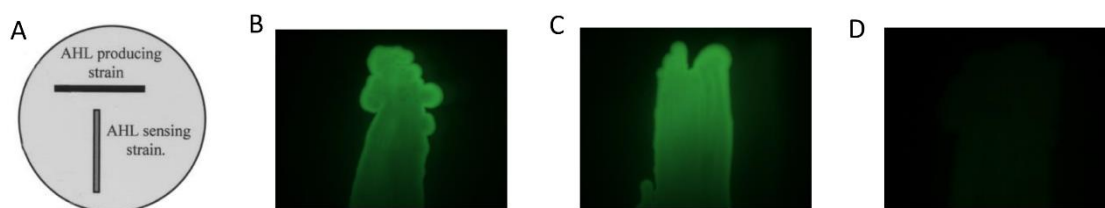
Figure 2. Production of AHLs by Psv NCPPB 3335 and its Δ*pssI* and Δ*pssR* mutants. (A) Diagram of the T-streak inoculation method used to detect production of AHLs (Andersen *et al.*, 2001). GFP fluorescence emission of the AHL sensor strain *E*. coli JB52 (pJBA130) growing in the vicinity of (B) wild type Psv NCPPB 3335, (C) NCPPB 3335 Δ*pssR* or (D) NCPPB 3335 Δ*pssI*. Images were taken 24 hours after incubation at 28 °C.

The structure of AHLs consist of a conserved homoserine lactone (HSL) ring, an acyl side chain with variable length (4 to 14 atoms of carbon) and a substitution group at position C3 (O-, H- or OH-) (Fuqua *et al.*, 2001). To identify the AHLs produced by Psv NCPPB 3335, the supernatant of an overnight culture of this strain was analysed by mass spectrometry. Only C6-HSL, an AHL containing an acyl chain of 6 atoms of carbon and a H- group at position 3, was detected. In contrast, no AHLs were detected in the supernatant of the Δ*pssI* mutant, confirming the inability of the strain to produce this kind of signal molecules. Interestingly, several types of AHLs were identified in the supernatant of the Δ*pssI* mutant complemented with the *pssI* gene expressed from its own promoter in a multicopy plasmid (Δ*pssI*-pBBR:*pssI*). Besides the C6-HSL produced by the wild type strain, C8-, 3-oxo-C6-, 3-oxo-C8- and 3-OH-C8-HSLs were also detected. Remarkably, production of 3-oxo-C6- and 3-oxo-C8-HSL has been reported in Psv DAPP-PG 722 (Hosni *et al.*, 2011). However, these two AHLs were only detected in the culture supernatant of the Δ*pssI*-pBBR:*pssI* strain but not in that of the wild type NCPPB 3335. Taking into account that the amino acid sequences of the PssI proteins encoded by Psv NCPPB 3335 and Psv DAPP-PG 722 are 100% identical, these results suggest that regulation of AHL production in these two strains is not identical.

Identification of the Psv NCPPB 3335 quorum sensing regulon

A whole-genome transcriptional comparative analysis of wild type Psv NCPPB 3335 and its derivative Δ*pssI* mutant was performed, a strategy previously used by several authors to establish the quorum sensing regulon in different plant-associated bacteria (Kim *et al.*, 2013; Kim *et al.*, 2014; Coutinho *et al.*, 2015; Taguchi *et al.*, 2015). The strains were grown in LB broth to late-log phase (OD$_{600nm}$= 2), RNA was then extracted and sequenced as described in material and methods. Three independent RNA samples where sequenced for each strain. The results of the comparative transcriptomic analysis yielded a small number of genes differentially expressed between the strains. Table 4 shows the genes with a log$_2$(fold change) over 0.9 or under -0.9; meaning a 1.87-fold upregulation/downregulation, respectively, in the Δ*pssI* mutant compared to the wild type strain. Only 10 genes fitted this criterion: five were upregulated and five were downregulated in the Δ*pssI* background compared to the wild type NCPPB 3335 (Table 4). These results contrast with the high number of genes showing expression dependency on *luxI* in other bacteria grown under the same conditions (Kim *et al.*, 2013; Kim *et al.*, 2014). In addition, a recent report described 236 genes with a log$_2$(fold change) over 0.9 or under -0.9 in a comparative transcriptome analysis between Pst 6605 and its derivative Δ*luxI* mutant. However, in this case bacterial cells where transferred to MMMF medium after growth in LB before RNA extraction (Taguchi *et al.*, 2015).

To validate the results obtained from these RNAseq experiments, the expression of all genes showing a 1.87-fold up- or down-regulation in the Δ*pssI* mutant (Table 4) was analysed by RT-qPCR. Significant upregulation in the Δ*pssI* mutant was found only for three genes (PSA3335_1621, PSA3335_1623 and PSA3335_1624) (Table 4). These genes encoded for the quorum sensing transcriptional regulator *pssR* (PSA3335_1621), a pyruvate dehydrogenase E1 component beta subunit (PSA3335_1622, *pdhT*) and a pyruvate dehydrogenase E1 component (PSA3335_1624, *pdhQ*) (Table 5). On the other hand, none of the five genes identified as downregulated by RNAseq analysis were validated by RT-qPCR (Table 4). As a control, the expression of *pssI* was analysed by RT-qPCR in Psv NCPPB 3335 and the Δ*pssI* mutant. As expected, expression of this gene was higher in the wild type strain. Thus, after validation of the RNAseq data by RT-qPCR, the *pssI* regulon of Psv NCPPB 3335 was restricted to three genes (*pssR*, *pdhT* and *pdhQ*) under the conditions tested, two of which (*pdhT* and *pdhQ*) are controlled by the *pssR* homolog in Psy B728a (Yu *et al.*, 2014). Similarly, expression of *pssR* in Pst 6605 has been demonstrated to be dependent on *pssI* (Taguchi *et al.*, 2015).

Table 4. Genes regulated by *pssI* in Psv NCPPB 3335

Locus tag[a]	Gene[b]	Gene product	RNAseq[c]	RT-qPCR[c]
Upregulated				
<u>PSA3335_1622</u>	*pdhT*	Pyruvate dehydrogenase E1 component, beta subunit	3.27	3.6
<u>PSA3335_1624</u>	*pdhQ*	Pyruvate dehydrogenase E1 component	2.97	2.32
<u>PSA3335_1621</u>	*pssR*	LuxR transcriptional regulator	1.44	3.95
PSA3335_2315	UN	Putative hydrocarbon oxygenase	1.33	-0.13
PSA3335_4742	UN	Urocanate hydratase	1.01	-1.56
Downregulated				
<u>PSA3335_1620</u>	*pssI*	Homoserine lactone synthase	-3.41	-8.01
PSA3335_4623	UN	Copper chaperone	-1.07	-0.82
PSA3335_2048	UN	Hypothetical protein	-0.99	-0.42
PSA3335_0454	*mcdE*	Malonate decarboxylase delta subunit	-0.94	-0.13
PSA3335_2054	UN	Hypothetical protein	-0.93	0.67
PSA3335_4121	UN	Pectin lyase precursor	-0.92	0.52

[a]Upregulated or downregulated genes in the Δ*pssI* mutant according to RNAseq data.
[b]UN, unnamed
[c]The log_2 (fold change) obtained in the RNAseq and RT-qPCR experiments are represented. The fold change refers to the ratio of the average expression obtained in the Δ*pssI* mutant versus its wild type strain of three biological replicates. In the RNAseq analysis, genes with a log_2 (fold change) over 0.9 or under -0.9 are shown. Genes validated by RT-qPCR are underlined (T-Student; $p < 0.05$).

Quorum sensing regulation in Psv NCPPB 3335 differs from that of other *P. syringae* strains

Up to date, only two published works delved into the quorum sensing regulons of *P. syringae* strains (Psy B728a and Pst 6605). In Psy B728a, a mutant of the *ahlR* gene (encoding a PssR homolog) was analysed in comparison to the wild type strain under several environmental conditions, i.e. synthetic media, epiphytically and endophytically grown cells. Interestingly, under all these conditions AhlR was shown to control a small number of genes, which are all located in a cluster surrounding the *ahlI*/*ahlR* pair (hereafter named the SyrQS cluster) (Fig. 3A) (Yu *et al.*, 2014). Among other conditions, in this work Psy B728a cells were grown in synthetic medium amended with the AHL produced by this strain (C6-3-oxo HSL), in order to enhance differential expression of genes between Psy B728a and its Δ*ahlR* mutant. As mentioned before, genes controlled by PssI in Psv NCPPB 3335 (*pdhT* and *pdhQ*) are regulated by AhlR (the PssR homolog) in Psy B728a. For comparison with the results obtained in Psy B728a, Psv NCPPB 3335 and its Δ*pssR* mutant were cultured in LB medium amended with C6-3-oxo HSL, and the involvement of *pssR* in the regulation of the SyrQS cluster was analysed by RT-qPCR. Enhanced expression of *paoA*, *paoB*, *paoC*, *paoD* and *pssI* was observed in the mutant compared to the wild type. On the contrary, all these genes were downregulated in the Δ*ahlR* of Psy B72a (Fig. 3B) (Yu *et al.*, 2014). Moreover, in Psv NCPPB 3335, PssR is not involved in the control of *paoE*, *pdhT*, *qrpR* and *pdhQ* under the conditions tested. As expected, the expression of *pssR* also differed in the Δ*pssR* mutant compared to Psv NCPPB 3335 (not shown).

A comparative transcriptome analysis between the tobacco pathogen Pst 6605 and its derivative *pssI* mutant showed that 236 genes were upregulated/downregulated in the *pssI* mutant (Taguchi *et al.*, 2015). In order to compare this pattern of expression with that of Psv NCPPB 3335, six of the genes showing high downregulation/upregulation in Pst 6605, as well as the *pssR* gene, were investigated in the Psv NCPPB 3335 Δ*pssI* mutant in comparison with the wild type strain. A completely different regulation pattern was observed between Psv NCPPB 3335 and Pst 6605. Transcription of most of the genes analysed resulted to be independent on *pssI* in Psv NCPPB 3335. On the other hand, and in agreement with the RNAseq results obtained in this study, but opposite to Pst 6605, transcription of *pssR* was upregulated in the Δ*pssI* mutant of Psv NCPPB 3335 (Table 4). All the findings described above support the existence of a distinct regulation mediated by quorum sensing between Psv NCPPB 3335 and other strains of the *P. syringae* complex.

Table 5. Genes controlled by quorum sensing in *P. syringae* strains analysed in this study

Locus tag[a]	Gene[b]	Predicted function	Strain reported[c]
PSA3335_1615	*paoE*	Rieske iron-sulfur domain-containing protein	Psy, Pst
PSA3335_1616	*paoD*	Hypothetical protein	Psy, Pst
PSA3335_1617	*paoC*	Dihydrodipicolinate synthase	Psy, Pst
PSA3335_1618	*paoB*	Hypothetical protein	Psy, Pst
PSA3335_1619	*paoA*	Aspartate/tyrosine/aromatic aminotransferase	Psy, Pst
PSA3335_1620	*pssI*	Homoserine lactone synthase	Psy, Pst
PSA3335_1621	*pssR*	LuxR transcriptional regulator PsyR	Psy, Pst
PSA3335_1622	*pdhT*	Pyruvate dehydrogenase E1 component beta subunit	Psy
PSA3335_1623	*qrpR*	Transcriptional regulator, MarR family	Psy, Pst
PSA3335_1624	*pdhQ*	Pyruvate dehydrogenase E1 component	Pst
PSA3335_0003	UN	hypothetical protein	Pst
AER-0003118	*mexF*	C-terminal fragment of a multidrug efflux transporter	Pst
PSA3335_2264	*mexE*	Membrane fusion protein of RND family multidrug efflux pump	Pst
PSA3335_3741	*trmD*	tRNA (Guanine37-N1) -methyltransferase	Pst
PSA3335_3135	*romA*	Outer membrane protein romA	Pst
PSA3335_4922	UN	sodium/alanine transporter	Pst

[a]Locus tags correspond to the Psv NCPPB 3335 genome, except for the *mexF* gene, which locus tag is not available. AER-0003118 indicate the AER code of the gene in the ASAP database (https://asap.genetics.wisc.edu/asap/logon.php).
[b]UN, unnamed.
[c]Psy, genes controlled by AhlR in *P. syringae* pv. syringae B728a; Pst genes controlled by PsyI in *Pseudomonas syringae* pv. tabaci 6605.
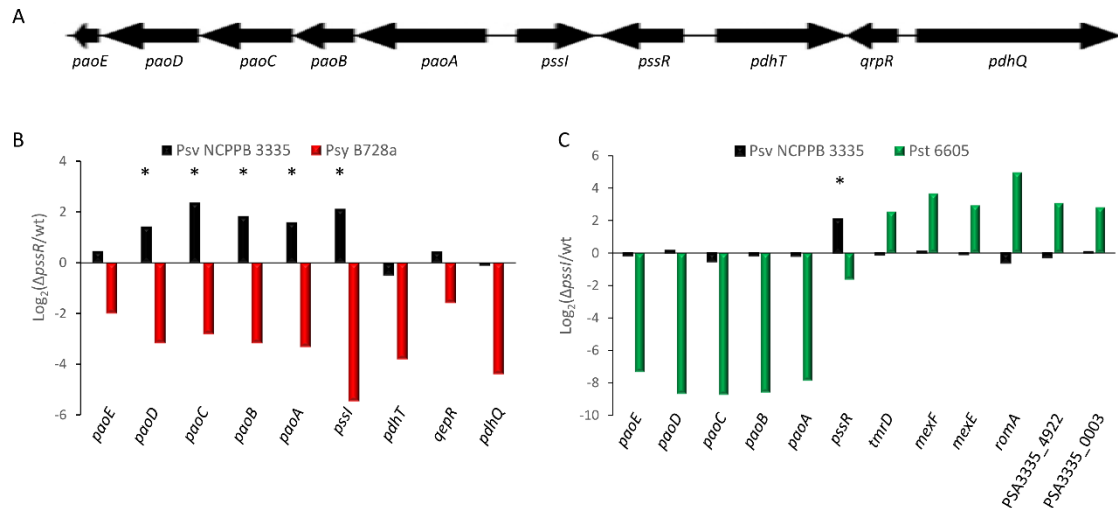
Figure 3. Comparative analysis of quorum sensing regulated genes in *P. syringae* strains. (A) Scheme of the gene cluster (SyrQS cluster) controlled by the LuxR homolog AhlR in Psy B728a (Yu *et al.*, 2014). Gene names are shown under the arrows. (B) RT-qPCR analysis of the SyrQS cluster in Psv NCPPB 3335 and its Δ*pssR* grown in LB medium. Results are compared with those obtained for Psy B728a cells grown in HMM medium (Yu *et al.*, 2014). (C) RT-qPCR analysis of selected genes in Psv NCPPB 3335 and its Δ*pssI* mutant incubated in MMMF medium. Genes were selected according to their altered expression pattern in a Pst 6605 *pssI* mutant grown under the same conditions (Taguchi *et al.*, 2015). For Psv NCPPB 3335, bars represent the log$_2$ of the average expression (three biological replicates) obtained for its (B) Δ*pssR* or (C) Δ*pssI* mutants relative to the wild type strain. Genes showing significant differences (T-Student, *P*<0.05) in their expression levels between Psv NCPPB 3335 and its respective mutants strains are indicated with an asterisk. Data corresponding to gene expression in (B) Psy B728a and (C) Pst 6605 were extracted from Yu *et al.* (2014) and Taguchi *et al.* (2015), respectively.

**Expression analysis of *pssI* and *pssR* in *P. savastanoi* NCPPB 3335**

While in *V. fischeri* LuxR controls its own transcription in an AHL-dependent manner (Dunlap & Ray, 1989; Shadel & Baldwin, 1991), transcription of *ahlR* in Psy B728a was shown to be independent on the cell concentration (Quinones *et al.*, 2004). Taking into account this dissimilar expression of *luxR* homologs and that *pssR* expression was shown to be *pssI*-dependent in Psv NCPPB 3335 according to our RNAseq experiments, we investigated the transcription of *pssR* in both Psv NCPPB 3335 and Psy B728a cells grown in LB. For this purpose, the promoter region of the Psv NCPPB 3335 *pssR* gene was fused to the *lacZ* gene (Table 2) and β-galactosidase activity was examined. As shown in Figure 4A, from 6 hours to the end of the experiment, expression of this gene was higher in the Δ*pssI* strain than in Psv NCPPB 3335. In addition, we observed that expression of the promoter was higher during late exponential phase and decreased as the bacteria reached the stationary phase. These results demonstrate that

transcription of *pssR* is not constant throughout the growth curve in either Psv NCPPB 3335 or its *pssI* mutant, and suggest that a mechanism independent of the presence of AHLs controls the expression of *pssR*.

A paradigm of the quorum sensing regulation is that, upon reaching a threshold concentration of AHLs, LuxR binds to its cognate AHL and promotes transcription of *luxI* leading to a positive feedback of the system (Whitehead *et al.*, 2001; Von Bodman *et al.*, 2003). Since all the results mentioned above suggest that Psv NCPPB 3335 possesses a particular quorum sensing regulation, the promoter region of *pssI* was fused to *lacZ* and β-galactosidase activity was monitored at different points during growth of Psv NCPPB 3335 and its *ΔpssI* and *ΔpssR* mutants in KB medium. In the wild type strain, expression of *pssI* was similar at 4 and 6 hours, but it doubled at 8 hours and remained at this level 10 hours after incubation (Fig. 4B). Furthermore, expression of the *pssI* promoter displayed an identical behaviour in the *ΔpssI* and *ΔpssR* mutant backgrounds. Similar results were obtained in LB medium (not shown). These results demonstrate that transcription of *pssI* is activated in stationary phase and is independent on PssI and PssR. In fact, *pssI* transcription was suggested to be independent on PssR in Psv DAPP-PG 722 (Hosni *et al.*, 2011).

Transcription of the Psv NCPPB 3335 *pssI* promoter was also analysed in Psy B728a (Fig. 4C). As observed for Psv strains, an increase in the transcription of the *pssI* promoter was observed at 8 hours and remained at the same level after 10 hours (Fig. 4C). However, a stronger transcription of the *pssI* promoter was detected in Psy B728a compared to Psv NCPPB 3335 (Fig. 4B, 4C). For example, at 6 hours the β-galactosidase activity measured in Psv NCPPB 3335 was 57 Miller Units, whereas in Psy B728a it was 2421 Miller Units. Similar results were obtained when the expression of the *ahlI* promoter was analysed in both bacteria (data not shown). In summary, although Psy B728a and Psv NCPPB 3335 shared the same activation behaviour of the *pssI* promoter, its overall expression was remarkably higher in Psy than in Psv, suggesting that regulation of the expression of *luxI* homologs is not identical in both bacteria.
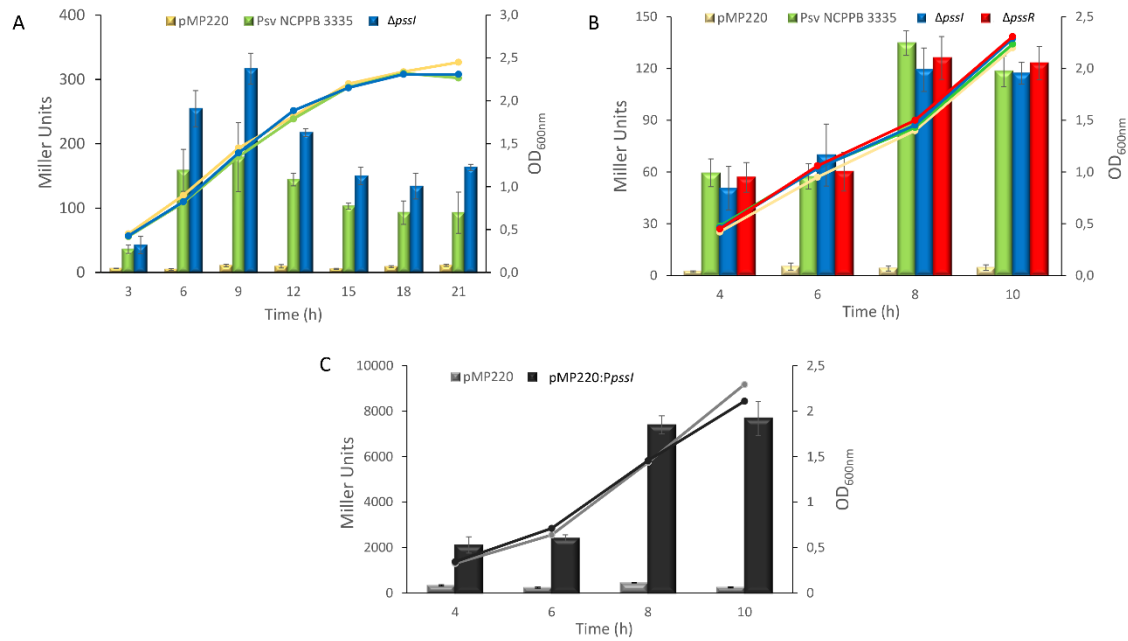
Figure 4. Expression of the *pssR* and *pssI* promoters from Psv NCPPB 3335. The ß-galactosidase activity from (A), the *pssR* (P*pssR*::'*lacZ*) and (B, C), the *pssI* (P*pssI*::'*lacZ*) promoters was determined in (A) Psv NCPPB 3335 and its *ΔpssI* mutant, (B) Psv NCPPB 3335 and its *ΔpssI* and *ΔpssR* mutants and, (C) Psy B728a. Lines and bars correspond, respectively, to the average OD_{600nm} and the mean β-galactosidase activity obtained from three different cultures; error bars correspond to the standard deviation from the average. pMPP220, promoterless empty vector used as control.

Phenotypes associated to quorum sensing in other *P. syringae* strains are not dependent on AHL production in Psv NCPPB 3335

EPS production, virulence, motility and biofilm formation, phenotypes all controlled by quorum sensing in other plant-pathogenic bacteria (Von Bodman *et al.*, 2003), were analysed in Psv NCPPB 3335. EPS production was tested in different media: LB, KB, minimal mannitol (MM) medium and MGY+Sorbitol. As shown in Figure 5, NCPPB 3335 and its derivative quorum sensing mutants (Δ*pssI* and Δ*pssR*) showed an identical appearance in all media tested, suggesting that quorum sensing does not control EPS production in this strain. Furthermore, complementation of the Δ*pssI* and Δ*pssR* mutants with *pssI* and *pssR*, respectively, cloned in a multicopy plasmid, also yielded identical phenotypes. EPS production deficiency of Psv DAPP-PG 722 *pssI* and *pssR* mutants have been reported both in KB and MM media (Hosni *et al.*, 2011), although we could not reproduce these observations under our laboratory conditions. Also related with EPS production, a double mutant of the paired *luxI*/*luxR* homologs in Psy B728a showed a reduced mucoid phenotype in comparison to the wild type strain growing in MGY+Sorbitol (Quinones *et al.*, 2005), a medium promoting alginate biosynthesis in Psy FF5 (Penaloza-Vazquez *et al.*, 1997).

However, this phenotype was neither observed for the Psv NCPPB 3335 Δ*pssI* and Δ*pssR* mutants.
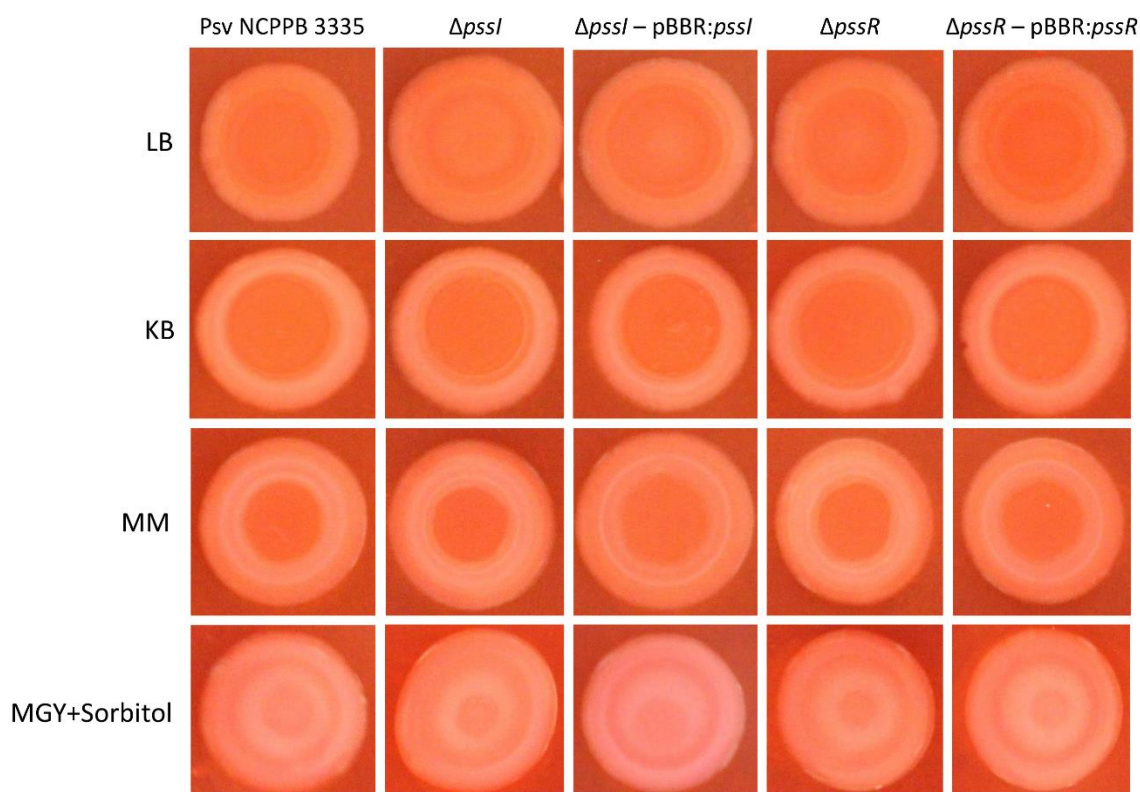
Figure 5. EPS production of Psv NCPPB 3335 quorum sensing mutants. Bacteria were inoculated in the indicated media, all amended with 50 µg ml^{-1} of Congo Red, and incubated for 24 hours at 28 °C. Psv, *Pseudomonas savastanoi* pv. savastanoi NCPPB 3335; Δ*pssI*, knockout mutant of the NCPPB 3335 *luxI* homolog; Δ*pssI*-pBBR:*pssI*, NCPPB 3335 Δ*pssI* expressing its *pssI* gene from a multicopy plasmid; Δ*pssR*, knockout mutant of the NCPPB 3335 *luxR*1 homolog; Δ*pssR*-pBBR:*pssR*, NCPPB 3335 Δ*pssR* expressing its *pssR* gene from a multicopy plasmid.

Swimming and swarming motilities were also analysed. A drop of a bacterial suspension was inoculated in the centre of a Petri dish containing 0.3% agar AB minimal medium (Huber *et al.*, 2001) and the diameter of the swimming halos were recorded after 96 hours. No differences in the swimming ability of Psv NCPPB 3335 and its derivative Δ*pssI* and Δ*pssR* mutants were found (Fig. 6A). Swarming motility was evaluated on 0.4% agar AB and KB media. For this purpose, a drop of a bacterial suspension was placed on top of the agar and swarming motility was analysed daily during 4 days. Although NCPPB 3335 and its quorum sensing mutants did not swarm on AB minimal medium, the three strains swarmed equally in KB (not shown). These results are in agreement with those previously reported in Psv DAPP-PG 722 (Hosni *et al.*, 2011). It should be noticed that the ability of NCPPB 3335 to swarm has not been reported before.

We also analysed the biofilm formation ability of Psv NCPPB 3335 and its *ΔpssI* and *ΔpssR* mutants on a glass surface. Figure 6B shows the quantification of biofilm formation measured after staining with crystal violet. No differences among the strains analysed were found. In summary, phenotypes typically regulated by quorum sensing in plant-pathogenic bacteria such as EPS production, motility and biofilm formation are not controlled by this system in Psv NCPPB 3335 under the conditions tested.
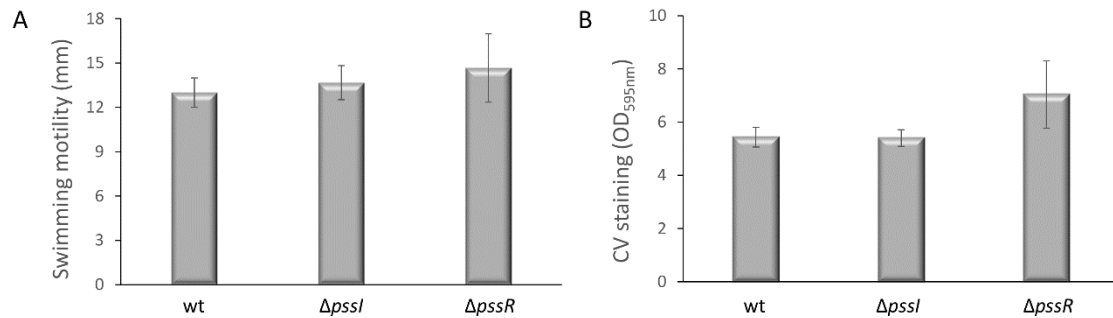
Figure 6. Swimming motility and biofilm formation of Psv NCPPB 3335 quorum sensing mutants. (A) Swimming motility of the indicated strains in AB minimal media amended with 10 mM citrate. The average diameter of the swimming halo is represented. Error bars represent the standard deviation from the average. (B) Quantification of biofilm formation by the indicated strains over glass slides using crystal violet (CV). Bars represent the average OD_{595nm} of three independent replicates and the error bars represent the standard deviation from the average.

Hosni and collaborators (2011) found that virulence of Psv DAPP-PG 722 in olive plants was severely reduced in their *pssI* and *pssR* mutants compared to the wild type strain. The *ΔpssI* and *ΔpssR* mutants of Psv NCPPB 3335 and their respective complemented strains were inoculated in micropropagated and woody olive plants. However, significant differences in knot development among the strains tested were not found either in non-woody (micropropagated) or woody olive plants (Fig. 7). It is important to mention that virulence attenuation of the Psv DAPP-PG722 *ΔpssI* and *ΔpssR* mutants was neither observed under the conditions tested in this study.
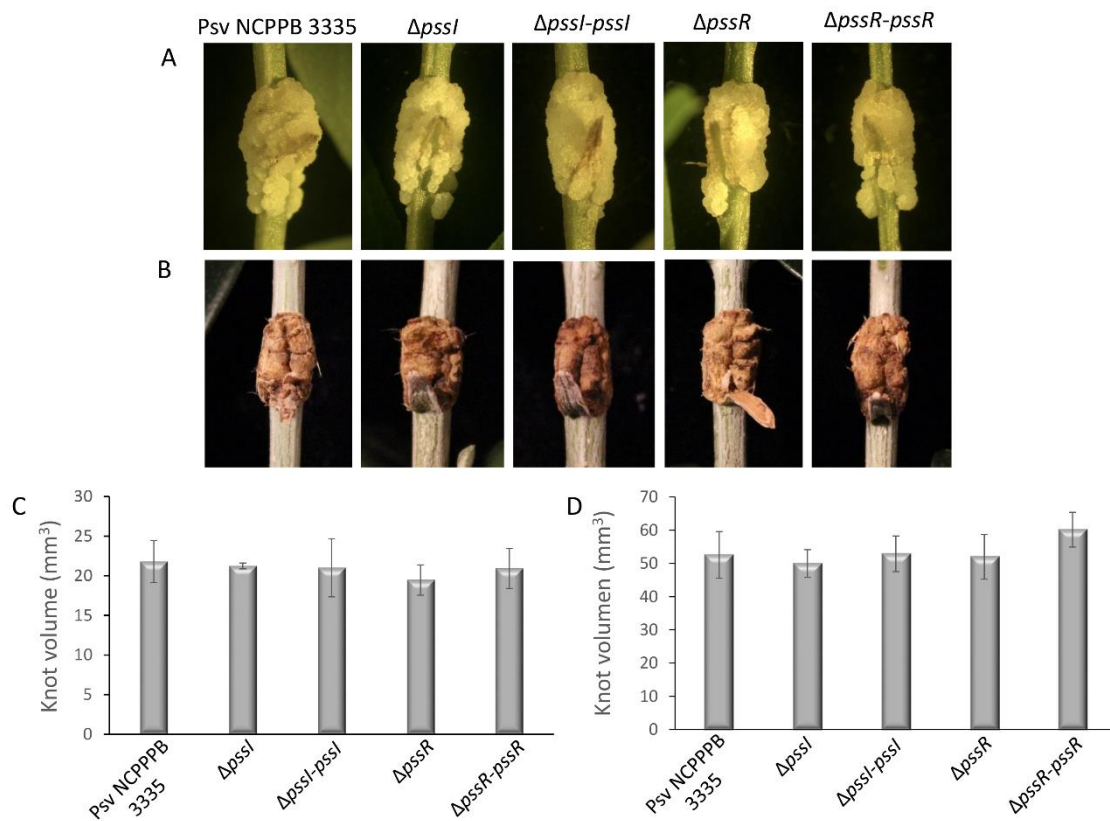
Figure 7. Virulence assay of the Psv NCPPB 3335 quorum sensing mutant on olive plants. Knots induced by the indicated strains on (A) non-woody and (B) woody olive plants at 30 dpi and 90 dpi, respectively. Knot volume (mm^3) induced by the indicated strains in (C) non-woody and (D) woody olive plants. Bars represent the mean of a minimum of three knots and error bars represent the standard deviation from the average.

DISCUSSION

Research on the quorum sensing system within the *Pseudomonas* genus has mainly focused in the widespread bacterium *P. aeruginosa*. Although this regulatory network has also been characterized in several *P. syringae*, most efforts have been devoted to *P. syringae* strains infecting non-woody plants. Up to our knowledge, only two works took a close look to the quorum sensing system of these kind of strains and, in addition, analysed two different regulatory networks: the AHL producing system of Psv (Hosni *et al.*, 2011) and the non-AHL producing system of *P. syringae* pv. actinidiae (Patel *et al.*, 2014). The intriguing quorum sensing circuit of the later, which lacks a *luxI* homolog, motivated our analysis of the presence of *luxI* and *luxR* homologs within a collection of 27 *P. syringae* strains of PG1 to PG4. Substantial differences were observed among the bacteria analysed: all type of LuxI LuxR genotypes were found, including several LuxI$^+$ LuxR$^-$ and LuxI$^-$ LuxR$^+$ strains, as well a LuxI$^-$ LuxR$^-$ strain (*P. syringae* pv. aptata DSM 50252). Furthermore, the number and type of *luxR* homologs greatly vary among different strains, although all of them, with the exception of the *P. syringae* pv. aptata DSM 50252, carry at least one LuxR solo predictably responding to AHLs. Conversely to other plant-associated Pseudomonads encoding two different *luxI* homologs (Zhang & Pierson, 2001; Mattiuzzo *et al.*, 2011), only one *luxI* gene was found in all LuxI$^+$ *P. syringae* strains analysed (Fig. 1). Similar *luxI luxR* content was observed in all PG3 strains examined, although this finding does not imply an identical quorum sensing regulation. For instance, several strains of *P. syringae* pv. phaseolicola and *P. syringae* pv. glycinea contain a *luxI* homolog, but do not produce detectable amounts of AHLs (Dumenyo *et al.*, 1998). Another example is the type of signal molecule(s) synthesized by different strains of PG3 sharing the same genomic content: whereas Psy B728a produce 3-oxo-C6-HSL (Cha *et al.*, 1998; Quinones *et al.*, 2004), Pst strains synthesize mainly C6-HSL and, in lower amounts, 3-oxo-C6-HSL (Taguchi *et al.*, 2006). Similarly, we found that wild type Psv NCPPB 3335 produces exclusively C6-HSL, whereas Psv DAPP-PG 722 synthesizes 3-oxo-C6- and 3-oxo-C8-HSLs (Hosni *et al.*, 2011). This particularly interesting result suggests that, in the *P. syringae* complex, the quorum sensing system may differ not only at the pathovar level but also among strains belonging to the same pathovar. Taking into account that the *luxI* homologs encoded by both Psv isolates are 100% identical, some other factor(s) might be responsible for the generation of different signal molecules. Nevertheless, overexpression of *pssI* in the Δ*pssI* mutant of Psv NCPPB 3335 also yielded 3-oxo-C6- and 3-oxo-C8-HSLs, suggesting that a different expression level of this gene between these two strains might explain differences in AHLs production. AHLs are synthesized by LuxI using *S*-adenosylmethionine and an acyl group, provided by an acyl-carrier protein (ACP), as substrates (Whitehead *et al.*, 2001). During AHLs synthesis, every LuxI protein shows higher affinity for a particular type of acyl-ACP (Schaefer *et*

al., 1996; Parsek *et al.*, 1999). Thus, it is possible that the respective LuxI proteins of Psv NCPPB 3335 and DAPP-PG 722 are provided with different acyl groups linked to ACPs and/or that their ACP content is different. In fact, we have identified an ACP-coding gene in the genome of Psv DAPP-PG 722 (locus tag GS14_RS0122650) not encoded in Psv NCBBP 3335, which consequently may lead to a dissimilar AHLs synthesis between these two strains.

Under the conditions tested in our study, the *pssI* regulon of Psv NCPPB is restricted to three genes (*pssR*, *pdhT* and *pdhQ*), encoded in the surrounding of the *luxI/luxR* genes, which expression have also been shown to be modulated by quorum sensing in other *P. syringae* strains. Although data related with the expression of the *pdhT* and *pdhQ* homologs in Pst 6605 are not available, the *pssR* and *qrpR* genes and the *paoABCD* operon homologs of this strain, all encoded in the SyrQS cluster, were shown to be downregulated in its *pssI* mutant (Taguchi *et al.*, 2015). On the contrary, we have shown that expression of *pssR* in Psv NCPPB 3335 is upregulated in its Δ*pssI* mutant (Table 4). In spite of the different growth conditions used for the RNAseq analysis of the quorum sensing regulons of these two strains, expression of the *pssR* gene in Psv NCPPB 3335 and its Δ*pssI* mutant was here performed under identical conditions to those used for Pst 6605 (Fig. 3C) (Taguchi *et al.*, 2015). In addition, in this study we also analysed other genes controlled by AHLs in Pst 6605, showing that this is not the case in Psv NCPPB 3335 (Fig. 3C). These findings suggest that, although Psv NCPPB 3335 and Pst share the same signal molecule and content of quorum sensing genes, they exhibit disparate quorum sensing regulation under the same laboratory conditions. It is important to highlight that these two strains do not inhabit similar ecological niches, which possibly affects their respective regulatory networks. In fact, the quorum sensing system regulons of *P. aeruginosa* strains isolated from diverse environments are variable (Chugani *et al.*, 2012). In this sense, many Gram (-) bacteria, including *P. syringae* (Quinones *et al.*, 2004) and *P. aeruginosa* (Reimmann *et al.*, 1997), integrate AHL signalling with the two component general regulatory system GacA/GacS, suggesting that environmental conditions likely plays an important role in quorum sensing regulation.

Additional differences between the quorum sensing systems of Psv NCPPB 3335 and *P. syringae* strains were evidenced after the examination of the promoter activity of the *pssI* gene in NCPPB 3335 and Psy B728a. Although an increase in the activity of the promoter was found in both strains after 6 to 8 hours of growth in KB broth, its overall expression was remarkably higher in B728a compared to NCPPB 3335 (Fig. 4B, 4C). In addition, the observed enhanced activity of this NCPPB 3335 promoter was not dependent on either PssI nor PssR (Fig. 4B), whereas AhlR promotes the expression of its *pssI* homolog in Psy B728a (Quinones *et al.*, 2004).

PssR-independent increase of the expression of *pssI* in NCPPB 3335 has also been suggested in Psv DAPP-PG 722 (Hosni *et al.*, 2011). Besides the GacA/GacS system, other proteins are able to promote transcription of the AHL synthase gene in other *P. syringae* strains. For instance, AefR (AHL epiphytic fitness regulator) stimulates transcription of the *pssI* homolog in Psy B728a (Quinones *et al.*, 2004) and *P. syringae* pv. phaseolicola NPS3121 (Deng *et al.*, 2009), but the epiphytic traits governed by AefR differs between these two strains. Although the genomes of both Psv NCPPB 3335 and Psv DAPP-PG 722 encode a AefR homolog which share 89% identity with that of Psy B728a, their involvement in the promotion of the transcription of *pssI* and in the regulation of epiphytic traits have not been addressed up to date. Further work is necessary to confirm the PssR-independent transcription of *pssI* in Psv strains NCPPB 3335 and DAPP-PG 722.

Several phenotypes regulated by quorum sensing in Psv DAPP-PG 722 (Hosni *et al.*, 2011) were not altered in the Δ*pssI* and Δ*pssR* mutants of Psv NCPPB 3335. On the one hand and related to EPS production, it should be mentioned that the colonies developed by DAPP-PG 722 in KB medium are more mucous than those of NCPPB 3335, suggesting that the type and/or amount of EPS produced by these strains might be different. Alginate, an EPS which production is impaired in Psy B728a mutants affected in the *ahlI*/*ahlR* pair or the *aefR* gene (Quinones *et al.*, 2005), has been reported as a factor involved in epiphytic fitness and virulence in *P. syringae* (Penaloza-Vazquez *et al.*, 1997). Although we did not find a link between PssI/PssR and production of alginate in NCPPB 3335 (Fig. 5), the genomes of both Psv NCPPB 3335 and DAPP-PG 722 encode the machinery necessary for the biosynthesis of alginate (Rodriguez-Palenzuela *et al.*, 2010; Moretti *et al.*, 2014). Further work is necessary to clarify the connection between PssR/PssI and alginate production in Psv. On the other hand, we could not reproduce the differences observed in the virulence between the Psv DAPP-PG 722 and its derivative Δ*pssI* and Δ*pssR* mutant strains. It is important to mention that the olive tree cultivar (cv.) used in this study (cv. Arbequina) is different to the one employed for testing the quorum sensing mutants of Psv DAPP-PG 722 (cv. Frantoio) (Hosni *et al.*, 2011). Since virulence of Psv isolates depends on the olive tree cultivar (Penyalver *et al.*, 2006), inoculation of Psv NCPPB 3335 and its Δ*pssI* and Δ*pssR* mutant strains on olive plants cv. Frantonio should be carried out to discard a putative effect of the cultivar in the virulence of the pathogen.

In this chapter we focused on the cell density-dependent regulation via quorum sensing in Psv NCPPB 3335. The type of signal molecule was determined as well as the genes which expression depends on *pssI*. We established remarkable differences between the quorum sensing system of this strain and its homolog systems in other phylogenetically related bacteria, including a different isolate belonging to the same *P. savastanoi* pathovar.

Chapter III

Pseudomonas savastanoi as an emerging pathogen: the case of dipladenia.

INTRODUCTION

Dipladenia (*Mandevilla* spp.), encompasses 176 different accepted species according to the World Checklist of Selected Plant Families (http://apps.kew.org/wcsp/home.do). Dipladenia are evergreen creeper bushes native to South America jungles, where sometimes reach up to ten metres height. This genus is highly appreciated for their smooth and intense green leaves, and for their trumpet-shaped flowers in red, pink, white or yellow, held by long stalks. Additionally, the flowering period begins during the spring season and commonly extends until autumn, which converts dipladenia in a profitable product for the ornamental market of plants. In fact, the worldwide market of dipladenia is estimated around 300-400 millions of euro per year (New Plants Motril SA, personal communication).

Few studies have focussed so far on dipladenia diseases, although viruses, fungi and bacteria have been reported as dipladenia pathogens. Symptoms caused by viruses consist on foliar lesions, described as leaf deformation, the appearance of yellow rings in older leaves and premature leaf senescence (Kelley & Weathers, 1985; Davino *et al.*, 2005; Mollov *et al.*, 2015). Furthermore, fungal diseases are characterized by spot lesions on leaves (Watanabe *et al.*, 2016) or more severe symptoms, as defoliation (Sella *et al.*, 2010), wilting or rotting (Pennisi *et al.*, 2002). *Ralstonia solanacearum* causes leaf dieback, wilting and reduced top growth of dipladenia plants (Ruhl *et al.*, 2011; Bocsanczy *et al.*, 2014); however, *Pseudomonas savastanoi* is considered the most prevalent bacterial pathogen of this host (Putnam *et al.*, 2010; Eltlbany *et al.*, 2012; Pirc *et al.*, 2014; Caballo-Ponce & Ramos, 2016). Symptoms caused by *P. savastanoi* on dipladenia comprise necrotic spots surrounded by a chlorotic halo on leaves and stems, as well as knot formation on stems. Knots on dipladenia stems caused by *P. savastanoi* were first described in *Mandevilla splendens* plants grown in the USA (Putnam *et al.*, 2010). A couple of years later, the isolation of a group of *P. savastanoi* strains from infected *Mandevilla sanderi* plants in Germany and France was reported (Eltlbany *et al.*, 2012). More recently, the same pathogen was reported as the causal agent of necrotic spots on dipladenia leaves in Slovenia (Pirc *et al.*, 2014). In the later studies 16s rDNA sequencing was used to identify *P. savastanoi* as the causal agent. However, the inability of the Slovenian isolates to trigger a hypersensitive reaction (HR) on tobacco leaves, a typical response induced by most *P. savastanoi* and *Pseudomonas syringae* strains (Schaad *et al.*, 2001), has been reported (Pirc *et al.*, 2014).

Over the last few years, dipladenia leaf and stem spot caused by *P. savastanoi* has been responsible for relevant economic losses. For instance, during spring 2010, up to 70% of the dipladenia plants maintained in Slovenian greenhouses were classified as unmarketable due to *P. savastanoi* infections (Pirc *et al.*, 2014). On the other hand, the occurrence of this emergent

disease is becoming a serious concern for Spain since it is one of the main producers of dipladenia in Europe. Taking into account that the European market (Italy and Spain) produces approximately 60 millions plants/year (New Plants Motril SA, personal communication), significant economic losses could result because of the high popularity of this plant, its high market value, and because the mere presence of the pathogen is a total plant loss, as it occurs with all ornamentals. Thus, a deep characterization of *P. savastanoi* strains isolated from dipladenia is required to design control strategies and prevent its economic losses. For instance, the hybridization patterns obtained with diverse type III effector (T3E) gene probes and the presence of a distinctive plasmid set in these *P. savastanoi* isolates (Eltlbany *et al.*, 2012), suggest that they might belong to a new pathovar, although to answer this hypothesis it would be necessary to carry out the corresponding pathogenicity tests.

In this chapter, *P. savastanoi* was identified as the causal agent of dipladenia leaf and stem spot in Spain. Phylogenetic analysis of a collection of *P. savastanoi* strains isolated from dipladenia (Psd) in different countries showed a closer relationship to oleander isolates of *P. savastanoi* (*P. savastanoi* pv. nerii, Psn). Moreover, cross-pathogenicity tests revealed that besides Psd, some Psn strains are also pathogenic on dipladenia, conversely to *P. savastanoi* strains isolated from olive (*P. savastanoi* pv. savastanoi, Psv), ash (*P. savastanoi* pv. fraxini, Psf) and Spanish broom (*P. savastanoi* pv. retacarpa, Psr). All together, and according to previous observations (Eltlbany *et al.*, 2012), these results suggest that Psd strains might have originated from infested oleander plantations in the vicinity of the dipladenia greenhouses. Finally, systemic infection of dipladenia plants by Psd was here demonstrated using a GFP derivative.

MATERIALS AND METHODS

Bacterial strains, media and growth conditions

Bacterial strains and plasmids used in this study are listed in Tables 1 and 2 respectively. *P. savastanoi* and *Escherichia coli* were grown at 28 °C and 37 °C respectively in Luria-Bertani (LB) medium (Miller, 1972) and Super Optimal Broth (SOB) (Hanahan, 1983). When required, media were supplemented with the appropriate antibiotic at the following concentration: kanamycin (Km) 10 μg ml^{-1} for *P. savastanoi* and 50 μg ml^{-1} for *E. coli*; gentamycin (Gm) 10 μg ml^{-1}; nitrofurantoin 20 μg ml^{-1}; and cycloheximide 100 μg ml^{-1}.

Table 1. *Pseudomonas* strains used in this study

Strain	Origin	Host of isolation	Source
Pseudomonas savastanoi			
Ph3	France	*Mandevilla sanderi*	(Eltlbany *et al.*, 2012)
MSI13L	Spain	*Mandevilla* spp.	(Caballo-Ponce & Ramos, 2016)
MSI14S	Spain	*Mandevilla* spp.	(Caballo-Ponce & Ramos, 2016)
MSI14L	Spain	*Mandevilla* spp.	(Caballo-Ponce & Ramos, 2016)
Ph5	Germany	*Mandevilla sanderi*	(Eltlbany *et al.*, 2012)
1397	EEUU	*Mandevilla splendens*	(Putnam *et al.*, 2010)
NIBZ1413	Slovenia	*Mandevilla sanderi*	(Pirc *et al.*, 2014)
CRpiaaM[a]			This study
pv. savastanoi NCPPB 3335	France	*Olea europaea*	(Perez-Martinez *et al.*, 2007)
pv. savastanoi CFBP 1670	Italy	*Olea europaea*	(Perez-Martinez *et al.*, 2007)
pv. savastanoi PseNe107	Nepal	*Olea europaea*	(Balestra *et al.*, 2009)
pv. nerii ITM 519	Italy	*Nerium oleander*	(Surico *et al.*, 1985)
pv. nerii ESC23	Italy	*Nerium oleander*	(Tegli *et al.*, 2011)
pv. nerii CFBP 5067	Spain	*Nerium oleander*	(Janse, 1991)
pv. fraxini NCPPB 1464	UK	*Fraxinus excelsior*	(Janse, 1991)
pv. fraxini NCPPB 1006	UK	*Fraxinus excelsior*	(Janse, 1991)
pv. fraxini CFBP 5062	Netherlands	*Fraxinus excelsior*	(Janse, 1991)
pv. retacarpa ICMP 16945	Spain	*Retama sphaerocarpa*	CECT[b]
Pseudomonas aeruginosa			
PAO1	Australia	Wound	(Holloway, 1955)
Pseudomonas syringae			
pv. tomato DC300	NA[c]	*Solanum lycopersicum*	(Cuppels, 1986)

[a]Plasmid-cured derivative of *P. savastanoi* Ph3 lacking the *iaaM* gene (see Appendix 1)
[b]CECT, Colección Española de Cultivos Tipo (Spanish Collection of Type Cultures).
[c]Not available

Table 2. Plasmid used in this study

Name	Description[a]	Source
pLRM1-GFP	pBBR1-MCS5::P$_{A1/O4/O3}$-RBSII-GFP*mut3**-T0-T1(Gm^R)	(Rodriguez-Moreno *et al.*, 2009)
pEXP-*hopA1*	pCPP5040 expressing PSA3335_5065-HA tag (Gm^R)	(Matas *et al.*, 2014)
pEXP-*hopBK1*	pCPP5040 expressing PSA3335_2068-HA tag (Gm^R)	(Matas *et al.*, 2014)
pEXP-*hopAO1*	pCPP5040 expressing PSA3335_0875-HA tag (Gm^R)	(Castaneda-Ojeda, 2014)
pAME8	pBBR1-MCS4 expressing *avrRpt2* from *nptII* and *lacZ* promoters (Km^R)	(Macho *et al.*, 2009)

[a]Km, kanamycin; Gm, gentamycin

LOPAT test

Levan production, oxidase, pectolysis, arginine dihydrolase and HR in tobacco leaves (LOPAT test) were evaluated for primary characterization of Psd (Lelliott *et al.*, 1966). For levan production, single colonies were streaked into solid PVF-I media (Surico & Lavernicocca, 1989) and incubated for 48h at 28 °C. Cytochrome oxidase activity was analysed by adding one drop of BactiDrop OXIDASE (Thermo Scientific, Rockford, IL, U.S.A.) on bacteria placed on a sterile filter paper. For potato pectolysis activity, potato slices (7-8 mm thick) were washed with distilled H$_2$O and alcohol-flamed prior to placing into Petri dishes containing a moistened and sterile filter paper. Bacterial suspensions were placed into a depression cut in the slices and incubated at 25 °C for 24 hours. Arginine dihydrolase activity was analysed on a semisolid media described by Thornley (Thornley, 1960). Tubes containing 5 ml of media were spike-inoculated, covered with a 1 centimetre thick paraffin oil layer and incubated at 28 °C for 5 days. For HR in tobacco leaves bacterial suspensions containing approximately 10^8 cfu/ml were infiltrated in the abaxial side using a needle-less syringe. *Nicotiana tabacum* cvs. Newdel and Xanthi were used and symptoms were recorded 48 hours post-infiltration with a high-resolution camera Canon D6200 (Canon Corporation, Tokyo, Japan). Different strains were used as controls: for levan production, *P. syringae* pv. tomato DC3000 (positive control) and *E. coli* DH5α (negative control); *P. aeruginosa* PAO1 for positive cytochrome oxidase and arginine dihydrolase activities; *Erwinia carotovora* pv. atroseptica SCRI1043 for positive potato pectolytic activity; and Psv NCPPB 3335 for positive HR in tobacco leaves.

For the heterologous expression of the T3E *avrRpt2*, *hopA1*, *hopBK1* and *hopAO1 P. savastanoi* Ph3 cells were transformed by electroporation (Perez-Martinez *et al.*, 2007) with plasmids pAME8, pEXP-*hopA1*, pEXP-*hopBK1* or pEXP-*hopAO1*, respectively (Table 2), transformants were selected in LB agar plates containing the appropriate antibiotic and single colonies were verified by polymerase chain reaction (PCR).

DNA techniques

For strains which genome sequences are not available g*yrB*, *rpoD*, *gapA* and *rpoA* housekeeping genes partial sequences were amplified by PCR using GoTaq Flexi DNA polymerase (Promega, Madison, WI, USA) and primers listed in Table 3. PCR fragments generated were sequenced (StabVida, Caparica, Portugal) and the sequences generated were submitted to GenBank (see accession numbers in Table 4). The three was constructed using MEGA5 (Tamura *et al.*, 2011) with the maximum likelihood, minimum evolution and neighbour-joining methods. 16s rDNA partial sequences of MSI13L, MSI14S and MSI14L were amplified by PCR using GoTaq Flexi DNA polymerase (Promega, Madison, WI, USA) and primers 16s_F and 16s_R (Table 3). PCR fragments generated were sequenced (StabVida, Caparica, Portugal) and the sequences were submitted to GenBank (accession numbers KP761689, KP743983 and KP743984). Polymerase chain reaction-restriction fragment length polymorphism (PCR-RFLP) analysis of the *iaaL* gene was carried out as described previously (Matas *et al.*, 2009). An internal 454 bp fragment of *iaaL* was amplified by PCR and digested with the restriction enzyme *Hae*III (Takara Biotech Cor.; Kaohsiung, Taiwan). DNA fragments were separated by 3% agarose gel electrophoresis pre-stained with ethidium bromide. Plasmid minipreparations of Psd were made following a quick protocol (Zhou *et al.*, 1990) with some modifications to minimize the isolation of chromosomal DNA (Murillo & Keen, 1994). Plasmids were separated by 0.8% agarose gel electrophoresis, transferred to a nylon membrane (GE Healthcare, Little Chalfont, UK) and hybridized with a dioxygenin-labelled *iaaM* probe. The *iaaM* probe was synthesized by PCR using iaaM_F615 and iaaM_R1090 primers (Table 3) and PCR DIG labelling mix (Roche, Applied Science, Mannheim, Germany) following the manufacturer's indications.

Table 3. Primers used in this study

Name	Sequence (5'→3')
Partial sequencing of housekeeping genes	
gyrB_F351	GTGGTCGCGACCTTGTGC
gyrB_R920	AAGTATCCGGCGGCTTG
rpoD_F383	CGCCAAACGTATCGAAGAAG
rpoD_R1055	GCTATTTTCAGGCCGGTTTC
gapA_F220	GACCGTCAATGGTGACCG
gapA_R931	GCCCATTCGTTGTCGTACC
rpoA_F22	ATGCAGATTTCGGTAAATGAGT
rpoA_R350	GGGTTAACGATCTCGACATC
16s_F	GCTCAGATTGAACGCTGGCG
16s_R	GCTACCTTGTTACGACTTCACCCC

Table 3. Primers used in this study (continuation)

Name	Sequence (5'→3')
PCR-based method for the detection of dipladenia isolates	
repA-F1	AGCTTCAAGAYCAGGGMAA
repA-R2	ARRTCCATCARYCGGTCRAA
Identification of type III secretion system effectors	
hopA1_F91	TAAATCCGAGGGTCAGTTGG
hopA1_R228	TTGAGCACTTGGGCTATCTG
hopBL1_ F1332	TCCAGCTTCGACCTTCAAC
hopBL1_ R1514	AACGGCAGATTGTCCACAT
hopBL2_ F1134	ACAGGGACGAAGGCTTGGA
hopBL2_ R1241	CGGAGACATGGTGGATGGA
hopAA1_F18	CACCATGCACATCAACCGATCC
hopAA1_R552	TCATGGATGCCTGTCCGG
hopBK1_F66	CGAGCACAGCAACTCCTTG
hopBK1_R195	TGGTGTACCGTCCAGGTAG
hopAF1-F	GCGGATGCATTGAAACAGCT
hopAF1-R	AATAACAGCGCCCAGCAGAGT
hopAF1-2F	CACTGCGGAGGCATTGAAAA
hopAF1-2R	AGAATAACGGCGCCAAGCA
hopAO1_F	TGGTTGTGAACGCATTTCCTC
hopAO1_R	GCATGAGATTCTTCGCGCA
hopAO2_F	TGCGTTTGATGGTGACCGA
hopAO2_R	ACCGCAATGGATATGTACCCG
PCR-RFLP of the *iaaL* gene	
iaaL-F-221	GGCACCAGCGGCAACATCAA
iaaL-R-696	CGCCCTCGGAACTGCCATAC
Synthesis of the *iaaM* probe	
iaaM_F615	GCATGGCAGGGATGGC
iaaM_R1090	CGCGGACAGCACGAGC

Quantification of indole 3-acetic acid production

The production of indole 3-acetic acid (IAA) was detected using Salkowski reagent (1.8% 0.5M FeCl$_3$ in 37% sulphuric acid). Culture supernatant were mixed with Salkowski reagent (1:2 v/v) and incubated at room temperature under dark conditions. After 20 minutes, IAA-producing bacteria developed a pink colour. For the quantification of IAA, bacterial cultures were incubated at 28 °C in King's B (KB) broth (King *et al.*, 1954) or KB amended with 2.5 mM tryptophan at an initial OD$_{600nm}$ of 0.1. After 24 hours, 5 ml of culture were centrifuged, the supernatant was collected and acidified to pH 2.5-3 with 1M HCl. Then, it was extracted with ethyl acetate (1:1 v/v) and, after incubation at room temperature in a shaker for 30 minutes (extraction step), the organic phase was recovered. The extraction step was repeated two more times, the organic phases of the three subsequent extractions were put together and evaporated at room

temperature. The pellet was dissolved in 1 ml methanol-water (10:90 v/v) and analysed by High Performance Liquid Chromatography coupled to Mass Spectrometry (HPLC-MS) as detailed recently (Aragon *et al.*, 2014). IAA amounts were normalized to the dry weight (DW) of 5 ml pellet, which was obtained by complete drying at 80 °C for, at least, two hours. Extractions of IAA were performed in triplicate.

Plant infections

Plants were pre-treated with 300 g/hl of Bordeaux mixture (stock containing 20% $CuSO_4$). After 3 weeks, plants were washed with 70% ethanol and air dried prior to inoculation. *Olea europaea* (olive), *Nerium oleander* (oleander), *Fraxinus excelsior* (ash) and *Mandevilla* spp. (dipladenia) were wounded along the stem with a scalpel and approximately 10^6 cfu were placed per wound. For *Retama sphaerocarpa* (Spanish broom) around 10^6 bacteria were inoculated with a needle coupled to a syringe. Each inoculation point was wrapped with parafilm (Bemis, Neenah, WI, USA) for 7 days. Plants were kept in a greenhouse for 3 months under natural photoperiod (15 hours light/9 hours dark) at room temperature (≈26 °C day/18 °C night). Symptoms developed were captured with a high-resolution camera Canon D6200 (Canon Corporation, Tokyo, Japan). For the isolation of *P. savastanoi* from dipladenia, knots were macerated in 10 mM $MgCl_2$ with a mortar and a pestle, serial diluted and plated into LB containing nitrofurantoin 20 µg ml^{-1} and cycloheximide 100 µg ml^{-1}. To fulfil Koch's postulates, identification of dipladenia isolates was carried out using the *repA* PCR-based method (Eltlbany *et al.*, 2012). To visualize bacterial infections in dipladenia, *P. savastanoi* Ph3 and CRpiaaM were tagged with pLRM1-GFP plasmid and plants were examined with a epifluorescence microscopy as previously described (Rodriguez-Moreno *et al.*, 2009). Psd Ph3 on dipladenia bacteria were transformed by electroporation (Perez-Martinez *et al.*, 2007) with plasmid pLRM1-GFP (Table 2) and transformants were selected as green colonies under UV light. To visualize bacterial infection on dipladenia in real-time, plants were inoculated as described above and symptomatic areas were examined at 23 days post-inoculation directly with a stereoscopic fluorescence microscope (Leica MZ FLIII) equipped with a 100 W mercury lamp and a GFP2 filter (excitation 480/40 nm; emission 510LP nm). Images were captured with a high-resolution digital camera (Nikon DXM 1200).

Table 4. Locus tag/accession numbers for the gene sequences used to construct the phylogenetic tree shown in Figure 1

Strains	*gyrB*	*rpoD*	*gapA*	*rpoA*
Pseudomonas savastanoi isolated from dipladenia				
Ph3	KX296761[a]	KP730688[a]	KX353842[a]	KX379606[a]
13L	KX296762[a]	KP730689[a]	KX353843[a]	KX379607[a]
Ph5	KX296763[a]	KX369597[a]	KX353844[a]	KX379608[a]
1397	KX296764[a]	KX369598[a]	KX353845[a]	KX379609[a]
NIBZ1413	KX296765[a]	KX369599[a]	KX353846[a]	KX379610[a]
P.savastanoi pv. savastanoi				
NCPPB 3335	PSA3335_0009	PSA3335_0701	PSA3335_1269	PSA3335_4553
CFBP 1670	ALO58_04531	ALO58_02277	ALO58_00431	ALO58_04894
DAPP-PG 722	GS14_RS0118475	GS14_RS0120510	GS14_RS0113260	GS14_RS0115670
PseNe107	PSAVPseNe107_RS21055	PSAVPseNe107_RS21455	PSAVPseNe107_RS06270	PSAVPseNe107_RS20530
P. savastanoi pv. nerii				
ESC23	KX296766[a]	KX369600[a]	KX353847[a]	KX379611[a]
CFBP 5067	ALO61_04256	ALO61_03410	ALO61_04841	ALO61_03136
P. savastanoi pv. fraxini				
NCPPB 1006	KX296767[a]	KX369601[a]	KX353848[a]	KX379612[a]
CFBP 5062	ALP79_200380	ALP79_04657	ALP79_02304	ALP79_00291
P. savastanoi pv. retacarpa ICMP 16945	ALO49_04129[b]	ALO49_200246	ALO49_03177	ALO49_00201
P. syringae				
pv. actinidae M302091	PSYAC_05930	PSYAC_04173	PSYAC_00605	PSYAC_19988
pv. aesculi NCPPB 3681	PsyrpaN_010100024288	PsyrpaN_010100021637	PsyrpaN_010100017259	PsyrpaN_010100001555
pv. glycinea race 4	Pgy4_23473	Pgy4_22411	Pgy4_05892	Pgy4_14629
pv. japonica M301072	PSYJA_14042	PSYJA_15502	PSYJA_03099	PSYJA_19971
pv. lachrymans M302278	PLA106_16879	PLA106_16494	PLA106_04632	PLA106_19276
pv. mori 301020	PSYMO_16078	PSYMO_21228	PSYMO_17513	PSYMO_25203
pv. morsprunorum M302280	PSYMP_13789	PSYMP_21479	PSYMP_02311	PSYMP_24736

Table 4. Locus tag/accession numbers for the gene sequences used to construct the phylogenetic tree shown in Figure 1 (continuation).

Strains	*gyrB*	*rpoD*	*gapA*	*rpoA*
pv. oryzae 1_6	Psyrpo1_010100022716	Psyrpo1_010100026871	Psyrpo1_010100037909	Psyrpo1_010100001310
pv. phaseolicola 1448A	PSPPH_0004	PSPPH_0619	PSPPH_1176	PSPPH_4567
pv. syringae B728a	Psyr_0004	Psyr_4641	Psyr_1108	Psyr_4524
pv. tabaci ATCC11528	PSYTB_19816	PSYTB_18734	PSYTB_04965	PSYTB_22761
pv. tomato DC3000	PSPTO_0004	PSPTO_0537	PSPTO_1287	PSPTO_0651
Pseudomonas aeruginosa PAO1	PA0004	PA0576	PA3195	PA4238

[a]Accession numbers at GenBank for the sequences generated in this study
[b]Sequence cured manually

RESULTS

### First Report of Dipladenia (*Mandevilla* spp.) Leaf and Stem Spot Caused by *Pseudomonas savastanoi* in Spain

The evergreen climber dipladenia (*Mandevilla* spp.), native to South and Central America, has lately become widespread as an ornamental plant around the world. In May 2013 and in November 2014, dipladenia plants showing necrotic lesions surrounded by a chlorotic halo on leaves and stems were detected in the south of Spain (Fig. 1A-B). To isolate the causal agent, symptomatic leaves and stems were homogenized by mechanical disruption into 10 mM MgCl$_2$, and serial dilutions were plated. Circular, smooth, flat, cream-colored colonies were isolated on LB containing 20 µg/ml nitrofurantoin and 100 µg/ml cycloheximide. Three single isolates, two from leaves (MSI13L, 2013 and MSI14L, 2014) and one from a stem (MSI14S, 2014), were obtained and identified as *Pseudomonas savastanoi* on the basis of phenotypic and molecular tests. In agreement with Pirc *et al*. (2014), the three isolates were weakly fluorescent on KB under UV light and showed a negative reaction in all phenotypes included in the LOPAT test (levan, oxidase, arginine dihydrolase, pectinolytic activity and tobacco hypersensitivity). Genomic DNA was extracted from the isolates, and DNA fragments corresponding to the *rpoD* and the 16s ribosomal RNA genes were amplified (Parkinson et al. 2011) and sequenced. The obtained sequences were submitted to GenBank (accession numbers KP730689, KP739953 and KP739954 for the *rpoD* gene; KP761689, KP743983 and KP743984 for the 16s ribosomal RNA gene). All sequences showed 100% identity and coverage with those corresponding to *P. savastanoi* Ph3 (JX678983 and KP730688), a strain isolated from *Mandevilla sanderi* (Eltlbany et al. 2012). Additionally, PCR amplicons of the expected size were obtained from all isolates using a *repA*-based method (1,100 bp) directed specifically to *P. savastanoi* isolates from *Mandevilla* (Eltlbany et al. 2012). Pathogenicity was examined on both leaves and stems of dipladenia. Bacterial suspensions (≈1x10^8 cfu/ml in 10 mM MgCl$_2$) were prepared and ≈200 µl were infiltrated into the abaxial side of the leaves using a needless syringe. Stems were wounded with a sterile scalpel and inoculated with bacteria (≈2x10^5 cfu per wound). Negative control plants were inoculated with 10 mM MgCl$_2$. Three to five plants (4 months old), inoculated in three leaves or three stem points, were used for each strain and treatment. Plants were grown with a 16/8 h light/dark photoperiod at 24/18 °C day/night. Necrotic symptoms were observed on inoculated leaves and stems at seven (Fig. 1C) and 21 (Fig. 1D) days post-inoculation (dpi), respectively. Infected stems also showed a slight swelling, which increased over time and developed into a necrotic overgrowth at 60 dpi (Fig. 1E). Control plants did not develop any symptoms. Bacterial cells were re-isolated from symptomatic leaves and stems and identified as

P. savastanoi by the *repA*-based detection method described above (Fig. 2). Thus, Koch's postulates were fulfilled for the three Spanish isolates used in this study. After identification of dipladenia leaf and stem spot caused by *P. savastanoi* in France (Eltlbany et al. 2012), Germany (Eltlbany et al. 2012), USA (Putnam et al. 2010) and Slovenia (Pirc et al. 2014), this study shows the spread of this emergent disease into Spain.

This work has been recently published in Plant Disease, a journal of the American Phytopathological Society (APS) (Caballo-Ponce & Ramos, 2016). Strain MSI13L was included in a collection of Psd strains used for the characterization tests described below. Apart from the Spanish Psd isolate, other Psd strains from France (Ph3), Germany (Ph5), the USA (1397) and Slovenia (NIBZ1413) were included in this collection (Table 1).
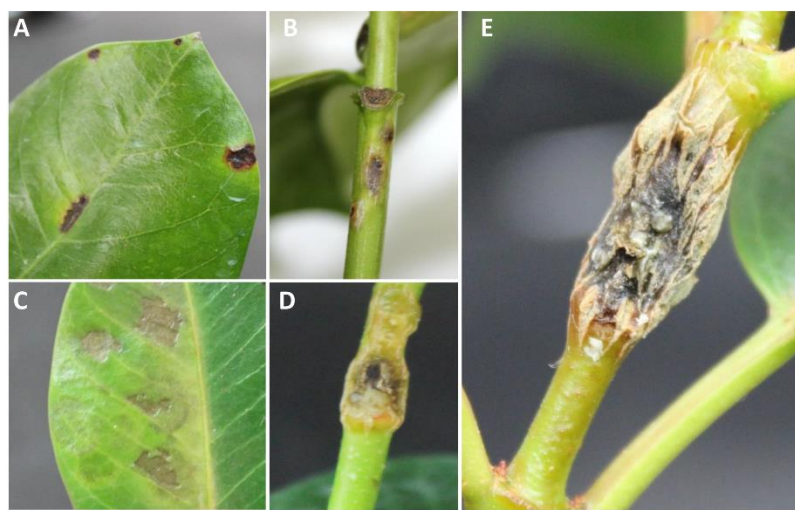
Figure 1. Symptomatology incited by *P. savastanoi* in dipladenia. Symptoms caused by *P. savastanoi* on naturally infected dipladenia (A) leaves and (B) stems from which strains MSI13L and MSI14S were respectively isolated. Symptoms induced on the (C) leaves and (D, E) stems of dipladenia plants (C) 7, (D) 21 and (E) 60 days after artificial inoculation with strain MSI13L.
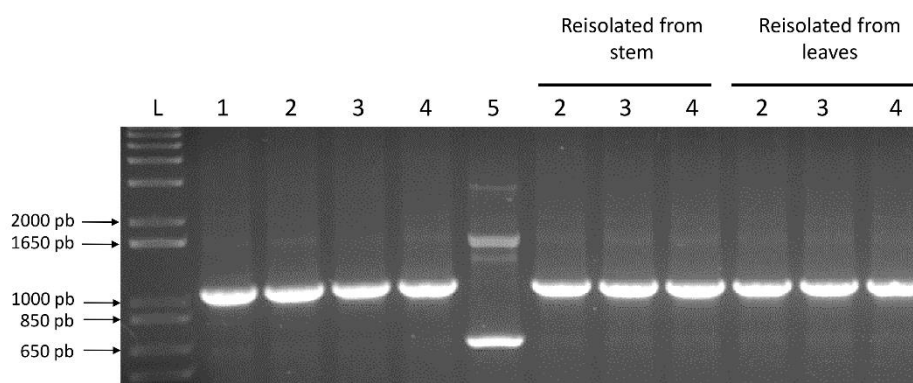
Figure 2. Identification of *P. savastanoi* strains isolated from dipladenia plants using a PCR method based on the *repA* gene (Eltlbany *et al.*, 2012). (L) Molecular weight DNA marker (1 kb plus DNA ladder,

Invitrogen); *P. savastanoi* strains (1) Ph3; (2) MSI13L; (3) MSI14S; (4) MSI14L and (5) *P. savastanoi* pv. savastanoi NCPPB 3335.

P. savastanoi strains isolated from dipladenia encode a functional T3SS but are unable to elicit the HR in tobacco leaves

Biochemical features included in the LOPAT test (<u>L</u>evan, <u>O</u>xidase, <u>P</u>ectolysis, <u>A</u>rginine dihydrolase and hypersensitive response in <u>T</u>obacco leaves) have been traditionally used for the identification of bacteria from the *P. syringae* complex, which also include *P. savastanoi*. Most *P. syringae* strains are L+O-P-A-T+. However, over 80% of *P. savastanoi* strains are negative for levan, oxidase, and arginine dihydrolase (L-O-A-), are able to trigger an HR on tobacco leaves (T+) but show a variable pectolysis phenotype on potato (P+/-) (Schaad *et al.*, 2001). Interestingly, the LOPAT profile of Psd strains isolated in Spain and Slovenia has been shown to be negative for every LOPAT feature (L-O-P-A-T-) (Pirc *et al.*, 2014; Caballo-Ponce & Ramos, 2016). To further analyse this observation, five Psd strains (Ph3, MSI13L, Ph5, 1397 and NIBZ1413; Table 1) isolated in different countries were selected and their LOPAT profiles were established. As shown for the Slovenian and Spanish isolates, all five strains resulted to be L-O-P-A-T-. Figure 3A shows the results obtained for the HR test in tobacco leaves in comparison to Psv NCPPB 3335. Taking into account that the HR response is a reaction triggered by the plant immune system after recognition of type III secretion system (T3SS) effectors (T3E) secreted by the pathogen into the plant cell, we analysed the functionality of the T3SS in the model Psd strain Ph3, isolated from *M. sanderi* in France (Eltlbany *et al.*, 2012). Psd Ph3 was transformed with plasmid pAME8 (Table 2) expressing the T3E *avrRpt2* from *P. syringae* pv. tomato 1065 (Macho *et al.*, 2009), an effector known to elicit a visible HR in *N. tabacum* cv. Xanthi (Mudgett & Staskawicz, 1999). As shown in Figure 3B, tobacco leaves infected with the transformed strain Ph3 (pAME8) developed an eye visible cell death typical of the HR 48h after inoculation, demonstrating the functionality of the T3SS in this strain.

Translocation of nine T3E through the Psv NCPPB 3335 T3SS has recently been reported (Matas *et al.*, 2014; Castañeda-Ojeda *et al.*, 2016). Codification of these nine T3E in the genome of Psd Ph3 was analysed by PCR using primers designed according to the sequences of their respective genes in the genome of Psv NCPPB 3335. Whereas no amplicons were obtained for *hopAO1*, *hopA1* and *hopBK1*, fragments of the expected sizes were visualized for *hopAA1*, *hopBL1*, *hopBL2*, *hopAF1*, *hopAF1-2* and *hopAO2* (data not shown). *P. savastanoi* Ph3 was transformed with plasmids expressing the Psv NCPPB 3335 T3E *hopAO1*, *hopA1* or *hopBK1* (Table

2). The resulting strains were infiltrated into *N. tabacum* cv. Xanthi leaves; however, none of them elicited an eye visible HR (Fig. 3B), suggesting that lack of these T3E does not explain the inability of Psd Ph3 to induce the HR in tobacco plants.
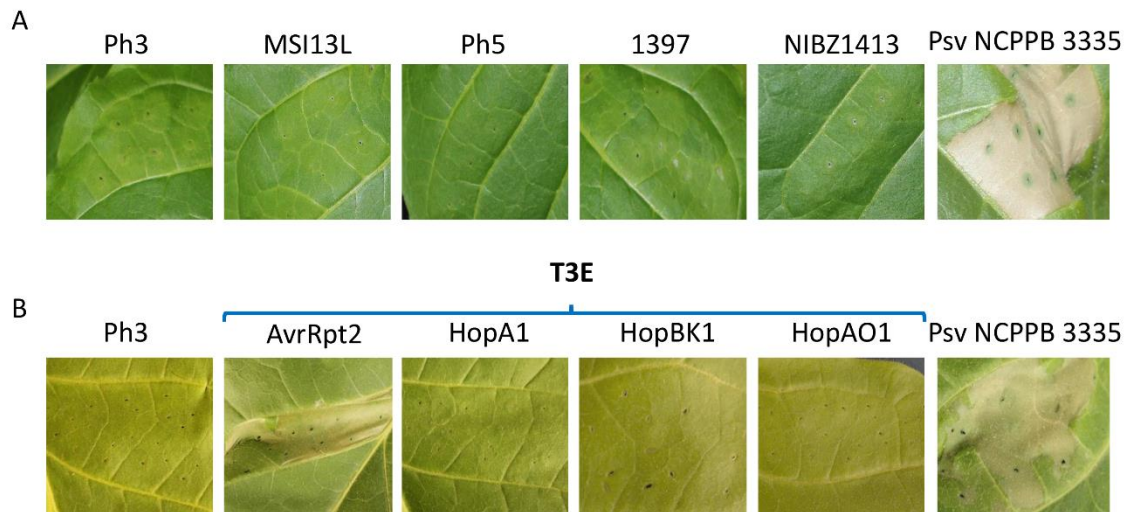
Figure 3. Hypersensitive response on tobacco leaves. (A) Appearance of *N. tabacum* cv. Xanthi leaves inoculated with the indicated *P. savastanoi* strains after 48 hours. (B) Appearance of *N. tabacum* cv. Xanthi leaves inoculated with *P. savastanoi* Ph3 expressing the indicated effector of the Type III Secretion System (T3E). Images were taken at 48 hours post-inoculation. *P. savastanoi* pv. savastanoi (Psv) NCPPB 3335 was used as a positive control for the induction of the hypersensitive response (HR). Bacteria were infiltrated at a concentration of 10^8 cfu/ml.

The analysis of two epidemiological markers reveals high similarity among Psd isolates

Previous work in our laboratory established a PCR-RFLP method for strain typing of Psv isolates. This method is based on the PCR amplification of a 454 base pairs internal fragment of the *iaaL* gene, followed by digestion with the restriction enzyme *Hae*III (Matas *et al.*, 2009). Three different *iaaL* alleles (*iaaL*$_{Psv}$, *iaaL*$_{Psn}$ and *iaaL*$_{Pto}$) were differentiated according to the fragments generated using this method (Fig. 4A). As shown in Figure 4B, identical PCR-RFLP fragments were obtained for the five different Psd strains. These fragments, which are similar to those obtained for Psv NCPPB 3335, correspond to the 279 bp and 46/40 bp fragments typical of the *iaaL*$_{Psn}$ and *iaaL*$_{Psv}$ alleles, respectively. Additionally, the intermediate fragment (175 bp) is common to *iaaL*$_{Psv}$, *iaaL*$_{Psn}$ and *iaaL*$_{Pto}$, whereas the other fragment (≈193 bp) corresponds to the *iaaL*$_{Psv}$ or the *iaaL*$_{Pto}$ alleles. Thus, all Psd strains analysed encode two distinct *iaaL* alleles: *iaaL*$_{Psv}$ and *iaaL*$_{Psn}$. The obtained PCR-RFLP results suggest high genomic similarity among Psd

strains, in contrast with the high variability of the $iaaL_{Psv}$ allele reported for diverse Psv strains (Matas *et al.*, 2009).

Genomic similarity among French and German Psd isolates has been reported before (Eltlbany *et al.*, 2012). In fact, BOX-PCR fingerprints generated from these Psd strains were almost identical, but also highly similar to those obtained from other *P. savastanoi* strains isolated from oleander, olive, jasmine and privet. Furthermore, this work also showed that Psd strains also yield identical hybridization patterns of digested plasmid DNA with a *repA* probe, suggesting that their plasmid content was similar. To determine if these similarities are shared with other Psd strains isolated in different countries, the plasmids content of the selected Psd strains was also analysed. As shown in Figure 4C, all five Psd strains displayed a plasmid pattern that consists in a minimum of three plasmids: two plasmids of 10-42 kb and a third plasmid of 44-63 kb. The main differences found among Psd strains were (i) the lack of a 63-73 kb plasmid in *P. savastanoi* 1397, and (ii) the presence of two plasmids of around 44 kb and 73-88 kb exclusives to *P. savastanoi* Ph5. In summary, the plasmid pattern of the French, Slovenian and Spanish Psd isolates are identical, but show slight variations in comparison to the German and American isolates.
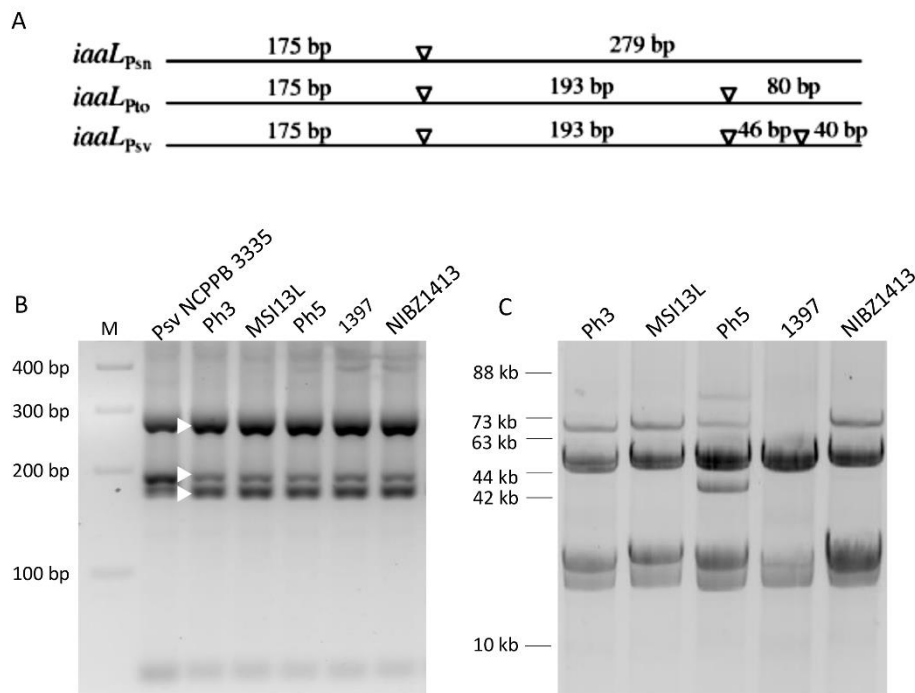
Figure 4. Analysis of a collection of *P. savastanoi* strains isolated from dipladenia (Psd) using two epidemiological markers. (A) Alleles of the *iaaL* gene distinguishable by PCR-RFLP (Matas *et al.*, 2009). (B) Gel electrophoresis of PCR-RFLP fragments generated from the *iaaL* alleles of the indicated strainsWhite arrowheads indicate DNA fragments of 279, 193 and 173 bp generated from Psd strain Ph3. M, Molecular weight DNA marker (1 kb plus DNA ladder, Invitrogen). (C) Gel electrophoresis of native plasmids isolated

from the indicated Psd strains. Psn, *P. savastanoi* pv. nerii; Pto, *P. syringae* pv. tomato; Psv, *P. savastanoi* pv. savastanoi.

Psd and Psn strains are phylogenetically related

French and German Psd isolates were initially identified as Psn or *P. syringae* pv. glycinea based on a metabolic profiling assay (Biolog). However, a phylogenetic analysis using the 16s rDNA partial sequence grouped Psd isolate Ph3 together with Psv NCPPB 3335 and Psn ITM 313, whereas *P. syringae* pv. glycinea B076 was placed in a different branch of the tree (Eltlbany *et al.*, 2012). On the other hand, Slovenian isolates (including NIBZ1413) have been genetically associated to Psn strains, as partial sequences of their *rpoD* gene were identical to that of Psn NCPPB 3334 (Pirc *et al.*, 2014). Therefore, the association of Psd with Psn or *P. syringae* pv. glycinea needs a deeper molecular study. A phylogenetic tree based on concatenated partial DNA sequences of the *gyrA*, *rpoD*, *gapA* and *rpoA* genes (total length 2439 bp) was constructed. The tree was built using MEGA5 (Tamura *et al.*, 2011) with the neighbour-joining method (Saitou & Nei, 1987) and included five Psd strains and several *P. syringae* and *P. savastanoi* strains which genome sequences are available. PCR amplicons corresponding to these four genes were obtained for all five Psd strains and sequenced, as well as for Psf NCPPB 1006 and Psn ESC23. The obtained sequences were submitted to GenBank (Table 4). The phylogenetic tree obtained is shown in Figure 5. The tree generated was consistent with a phylogeny of the core genome of *P. syringae* (Nowell *et al.*, 2014), and its topology was identical when the maximum likelihood or the minimum evolution methods were used for its construction. All dipladenia isolates and *P. savastanoi* strains clustered within the same branch (boxed in red) and separated from other *P. syringae* strains. Remarkably, Psd strains clustered in a well-separated sub-branch together with both Psn strains included in this study. However, Psn CFBP 5067 separated from Psn ESC23 and all Psd isolates. Going into sequence alignment detail, a major change is observed among the *P. savastanoi* sequences included in the analysis: the partial region of their *rpoD* gene used for the construction of the tree contains a six-nucleotide (ACGAAG) insertion at position 269, which is present exclusively in all dipladenia isolates and both Psn strains. In addition, the sequence of the *rpoA* gene obtained from the Psd and Psn strains differed in two nucleotides (positions 210 and 265) from those of the other *P. savastanoi* strains examined. These two changes lead to the association of Psd and Psn in a sub-branch within the main *P. savastanoi* branch. In addition, two minor changes are observed among Psd and Psn strains: the *rpoD* partial sequence of Psn CFBP 5067 differs in two nucleotides (positions 514 and 546) to that of Psn ESC23 and the five Psd strains, being the change at position 546 responsible of an amino acid substitution (proline

in Psd and Psn ESC23 strains to leucine in Psn CFBP 5067). In summary, these results provide further evidences for the phylogenetic relationship of Psn and Psd strains.
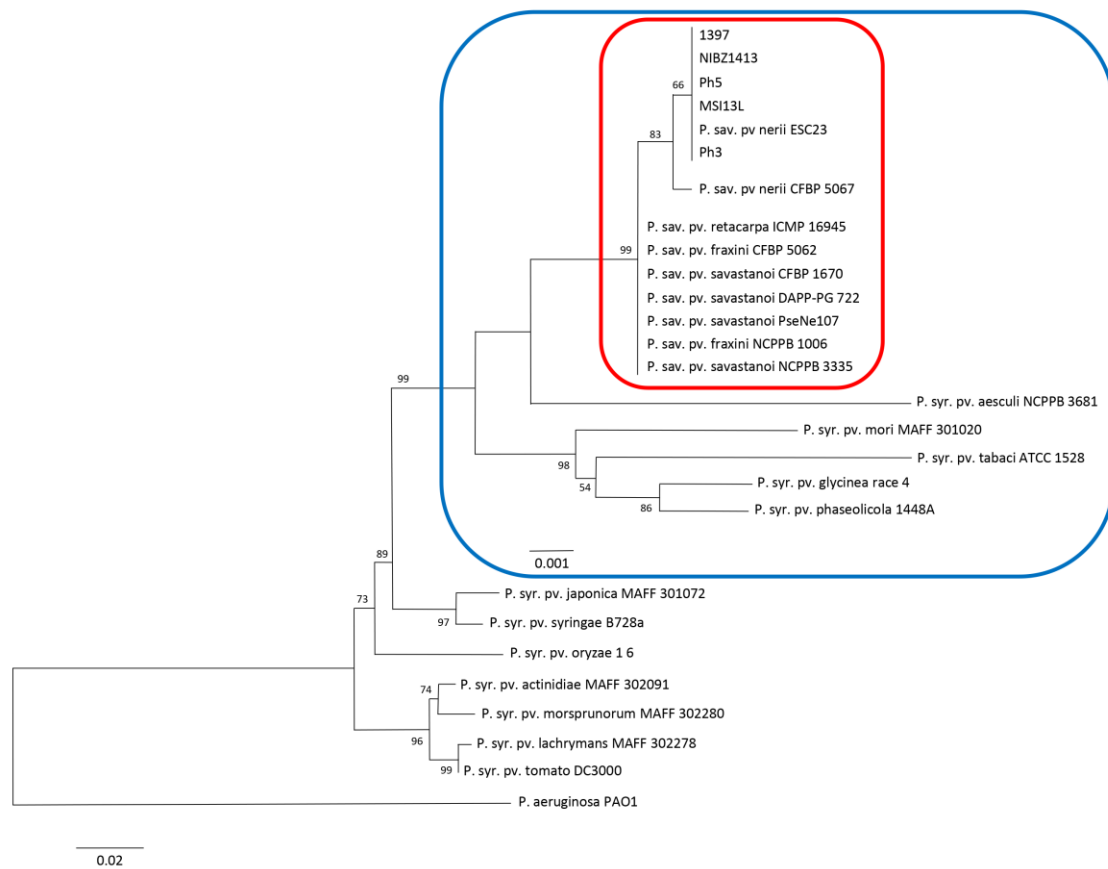
Figure 5. Phylogenetic analysis of five *P. savastanoi* strains isolated from dipladenia (Psd). The tree was constructed using concatenated partial DNA sequences of four housekeeping genes (*gyrB*, *rpoD*, *gapA* and *rpoA*) with a total length of 2439 bp. The analysis was performed using MEGA5 (Tamura *et al.*, 2011) with the Neighbour-Joining method (Saitou & Nei, 1987). The percentages of replicate trees in which the associated strains clustered together in the bootstrap test (10.000 replicates) are shown in the branches. The locus tags/accession numbers used for the construction on the tree are shown in Table 4. P. syr., *Pseudomonas syringae*; P. sav., *Pseudomonas savastanoi*. *Pseudomonas aeruginosa* PAO1 is included as an outsider. The blue box indicates a subtree overlapped with the main tree. A branch corresponding to *P. savastanoi strains* is boxed in red.

The host range of Psd isolates differs from those of the established *P. savastanoi* pathovars

Although cross-pathogenicity tests have helped to establish the host range of *P. savastanoi* pathovars savastanoi, nerii, fraxini and retacarpa (Janse, 1982; Alvarez *et al.*, 1998; Iacobellis *et al.*, 1998; Ramos *et al.*, 2012), very little is known about the pathogenicity of Psd on the typical woody hosts infected by this group of bacteria. Eltbany *et al*., (2012) mentioned that Psd strains

isolated in France and Germany induce similar infection patterns on oleander and dipladenia leaves and stems, no symptoms on olive plants and leaf lesions in privet. However, these results have not been published. To investigate the pathogenicity of Psd strains isolated from diverse countries (Table 1) artificial infections on olive, oleander, ash and Spanish broom were carried out. Figure 6 shows the scale of symptoms used to describe the results shown in Table 5. None of the Psd strains examined induced symptoms on oleander and Spanish broom whereas the positive controls, Psn ESC23 and Psr ICMP 16495, caused the development of knots on their respective hosts (Table 5). Pathogenicity of all five Psd strains on olive plants was similar to that of the control strain Psv NCPPB 3335 (induction of knots on olive stems). These results contrast with the previously reported observations mentioned above (Eltlbany *et al.*, 2012). All Psd strains were also pathogenic on ash, although the observed symptoms were different from those induced by Psf NCPPB 1006 and the virulence varied among them. Psd Ph5 was the most virulent strain, inducing nine knots out of ten inoculation points on ash, whereas Psd 1397 only generated one knot in this specie. On dipladena stems, as expected, all Psd strains induced knot formation and reached similar populations inside the plant tissues (10^8 cfu per knot).

Table 5. Pathogenicity test of *P. savastanoi* strains isolated from dipladenia

Strain[a]	Olive[b]	Oleander[b]	Ash[b]	Spanish broom[b]	Dipladenia[b]
Psd strains					
Ph3	10K	-	10S	-	10K
MSI13L	10K	-	5S 5K	-	10K
Ph5	10K	-	1S 9K	-	10K
1397	10K	-	9S 1K	-	10K
NIBZ1413	10K	-	8S 2K	-	10K
Psv NCPPB 3335	10K	-	10S	-	-
Psn ESC23	1S 9K	8K 2E	10S	-	-
Psf NCPPB 1006	-	-	10E	-	-
Psr ICMP 16495	-	-	10S	10K	-

[a]Psv, *P. savastanoi* pv. savastanoi; Psn, *P. savastanoi* pv.; Psf, *P. savastanoi* pv. fraxini; Psr, *P. savastanoi* pv. retacarpa.
[b]K, Knot; S, swelling; E, excrescence; -, similar to the negative control. For each host and strain, numbers indicate the amount of a particular symptom generated out of 10 points of inoculation. Olive, *Olea europaea*; oleander, *Nerium oleander*; ash, *Fraxinus excelsior*; Spanish broom, *Retama sphaerocarpa*; dipladenia, *Mandevilla* spp.

| Knot (K) | Swelling (S) | Excrescence (E) | Negative control (-) |

Figure 6. Diversity of symptoms induced by *P. savastanoi* strains isolated from different host**.** Symptoms correspond to those induced on ash by *P. savastanoi* Ph5 (knot, K), *P. savastanoi* 1397 (swelling, S) and *P. savastanoi* pv. fraxini NCPPB 1006 (excrescence, E). Plants inoculated with MgCl$_2$ developed no symptoms (negative control -). See also Table 5.

Pathogenicity of Psv, Psn, Psf and Psr strains on dipladenia was also examined. In a first experiment, dipladenia stems were infected with Psv NCPPB 3335, Psn ESC23, Psf NCPPB 1006 and Psr ICMP 16945. Whereas the positive control *P. savastanoi* Ph3 incited the generation of a knot, no symptoms were formed on plants inoculated with the *P. savastanoi* strains mentioned above. To confirm these previous observations, two additional isolates of Psv, Psn and Psf were inoculated on dipladenia. While Psv strains CFBP 1670 and PseNe107 and Psf isolates CFBP 5062 and NCPPB 1464 did not induce symptoms on dipladenia (Fig. 7), Psn strains promoted the generation of diverse symptoms: Psn ITM 519 and Psn CFBP 5067 induced excrescences and knot-like overgrowths, respectively, at the inoculation points (Fig. 7). In summary, our results demonstrate that the host range of all five Psd isolates is similar in all hosts tested and different from those of the four recognized *P. savastanoi* pathovars. Thus, Psd strains might constitute a novel *P. savastanoi* pathovar. Additionally, these results reveal that besides Psd strains, some Psn strains are able to induce symptoms on dipladenia stems, varying from excrescences to the development of knots. These results are in agreement with the phylogenetic proximity observed between Psn and Psd isolates mentioned above.

| Psd strain Ph3 | Psn CFBP 5067 | Psn ITM 519 | Psv strains | Psf strains |
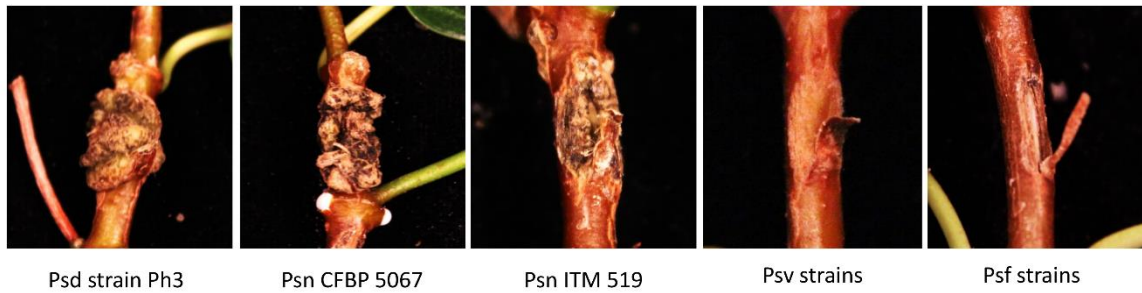
Figure 7. Symptoms generated by *P. savastanoi* strains isolated from diverse hosts on dipladenia at 90 dpi. Psf strains, symptoms induced by *P. savastanoi* pv. fraxini isolates NCPPB 1006, NCPPB 1464 and CFBP 5062; Psv strains, symptoms induced by *P. savastanoi* pv. savastanoi strains NCPPB 3335, PseNe107 and CFBP 1670; Psd Ph3; symptoms induced by the dipladenia isolate *P. savastanoi* strain Ph3. Symptoms generated by *P. savastanoi* pv. nerii (Psn) were strain-dependent.

A plasmid-cured derivative of *P. savastanoi* Ph3 lacking the *iaaM* gene is unable to induce tumour formation in dipladenia

P. savastanoi synthesizes the auxin IAA through the indole 3-acetamide pathway, where tryptophan is firstly transformed by the IaaM protein to indole 3-acetamide, that is further converted into IAA by IaaH. Psd Ph3 and Psd Ph5 contain a plasmid-encoded copy of the *iaaM* gene (EltIbany *et al.*, 2012), although its role in the production of IAA and the virulence of Psd has not been reported. Using a method developed for curing *P. savastanoi* plasmids encoding a copy of the *iaaM* gene (Comai & Kosuge, 1980), a *P. savastanoi* Ph3 plasmid-cured derivative lacking the *iaaM* gene (CRpiaaM) was isolated (see Appendix 1). To analyse whether production of IAA was impaired in CRpiaaM in comparison to the wild type strain, the supernatant of bacterial cultures amended or not with 2.5 mM tryptophan were analysed by HPLC-MS as described in the materials and methods section. In addition, all five selected Psd strains were included in these assays. As shown in Figure 8A, all five wild type Psd strains analysed produced IAA in KB broth, and the production was enhanced when tryptophan was supplied exogenously. However, production of IAA by Psd CRpiaaM was reduced more than 10 times in comparison with Psd Ph3. These results are in agreement with the loss of the *iaaM* gene in the CRpiaaM strain (see Appendix 1). Taking into account that CRpiaaM still produces a small amount of IAA, which is also increased in the presence of tryptophan (Fig. 8A), it could be possible that a second copy of the *iaaMH* operon is encoded in the chromosome of this strain.

Psd CRpiaaM was inoculated on dipladenia stems to analyse its ability to cause an infection. After two weeks, plants inoculated with the wild type strain Psd Ph3 developed symptoms,

consisting on a light green halo around the inoculation point, but these symptoms were not observed in the plants infected with CRpiaaM. Whereas no symptoms were generated on the plants inoculated with CRpiaaM at 60 days post-inoculation, Psd Ph3 induced the development of necrotic overgrowths (Fig. 8B). Additionally, approximately 10^8 cfu of *P. savastanoi* Ph3 were isolated per knot, but less than 10^2 cfu were recovered from the inoculation points of plants infected with CRpiaaM. All these results suggest that IAA production might be crucial for bacterial survival and for the induction of symptoms by Psd on dipladenia plants. These results are in agreement with the attenuation of the virulence observed for Psv and Psn mutants impaired in the production of this phytohormone (Smidt & Kosuge, 1978; Surico *et al.*, 1985; Iacobellis *et al.*, 1994; Aragon *et al.*, 2014).
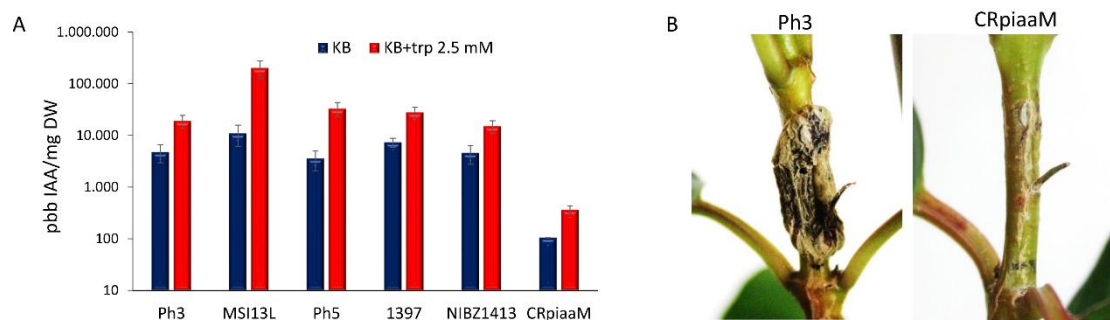

Figure 8. IAA production and virulence of *P. savastanoi* strain Ph3 and its mutant derivative cured of the plasmid-encoded *iaaM* gene. (A) Quantification of IAA produced by the indicated *P. savastanoi* strains isolated from dipladenia. Bacteria were grown in KB (blue bars) or KB amended with 2.5 mM tryptophan (red bars) for 24 hours at 28 °C. Data are represented as part per billion (ppb) of IAA per milligram of dry weight of biomass (DW). Bars represent the mean of three biological replicates, error bars correspond to the standard deviation. (B) Symptoms induced by *P. savastanoi* Ph3 and its plasmid-cured derivative lacking the *iaaM* gene (CRpiaaM) on dipladenia stems at 60 days post-inoculation.

P. savastanoi Ph3 can produce a systemic infection that leads to plant death

Secondary symptoms, which consist on the generation of overgrowths on the stems in sites distant to the points of inoculation and the appearance of chlorotic and necrotic areas on non-inoculated leaves, were occasionally observed in dipladenia plants inoculated with Psd Ph3, suggesting that the pathogen might spread systemically through the plant. To address the possible migration, Psd Ph3 was transformed with pLRM1-GFP, a plasmid expressing the green fluorescent protein (GFP) from a constitutive promoter (Rodriguez-Moreno *et al.*, 2009), and inoculated on dipladenia stems. After 23 days, secondary symptoms were clearly visualized (Fig. 9A) and GFP fluorescence was then examined using an epifluorescence microscope. GFP fluorescence was clearly visible under UV light in symptomatic non-inoculated leaves (Fig. 9B)

and petioles (Fig. 9C), whereas no fluorescence was detected in the leaves (Fig. 9D) and petioles (Fig. 9E) of a non-inoculated plant, showing the migration of *P. savastanoi* Ph3 through the plant. Secondary symptoms were more evident with time and led to the dieback of the plant after 90 days (Fig. 9F).
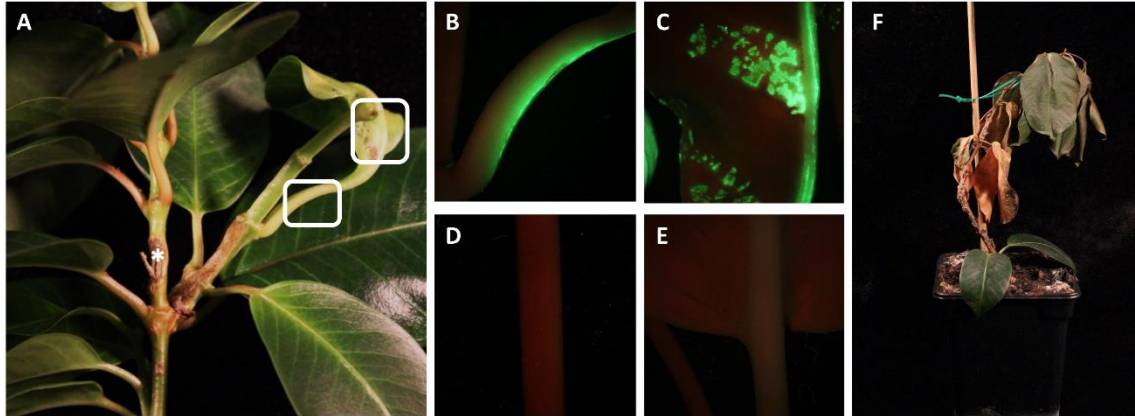
Figure 9. Systemic infection caused by *P. savastanoi* Ph3 on dipladenia plants. (A) Development of secondary symptoms induced at 23 days post-inoculation by a GFP-tagged derivative of *P. savastanoi* Ph3. The asterisk indicate the inoculation point. White boxes correspond to the leaf and petiole areas which epifluorescence images are shown in (B) and (C), respectively. (D) and (E) epifluorescence images of a leaf and petiole from a non-inoculated dipladenia plant (negative control). The red background is due to chlorophyll fluorescence. (F) Bacterial wilt occasionally observed in dipladenia plants infected with *P. savastanoi* Ph3 at 90 days post-inoculation.

DISCUSSION

P. savastanoi is a prevalent pathogen of dipladenia, although only one study delved into the genotypic characterization of Psd strains isolated in Germany and France (Eltlbany *et al.*, 2012). Dipladenia plants showing leaf and stem spots were detected during this PhD Thesis in Spain and the causative agent was identified as *P. savastanoi* (Caballo-Ponce & Ramos, 2016). In agreement with results reported for Slovenian isolates (Pirc *et al.*, 2014), here we show that *P. savastanoi* strains isolated from dipladenia in Spain are unable to trigger an HR on tobacco leaves. Results exposed in this Chapter broaden this observation to all Psd strains examined here and discarded the possibility that Psd strain Ph3 encoded a non-functional T3SS. Therefore, it is possible that (i) Psd strains lack a T3E recognized by the plant immune system leading to HR elicitation in the tobacco cultivar used in this study, or (ii) Psd strains encode a T3E that supress plant immune responses and prevent induction of the HR on *N. tabacum* leaves. Additional work is necessary to determine the T3E repertoire in Psd and to identify the T3SS effector(s) responsible for this phenotype.

An epidemiological marker established before by our laboratory (Matas *et al.*, 2009) was used to examine five Psd strains isolated in different countries. No variability was found among these Psd strains, which is in agreement with previous data that revealed similarities between BOX-PCR fingerprints of French and German isolates (Eltlbany *et al.*, 2012). In addition, Psd strains isolated in France and Germany showed identical plasmid restriction hybridization patterns using a *repA* probe (Eltlbany *et al.*, 2012), which might indicate that these strains harbour the same plasmid content. However, results in this Chapter showed that Psd Ph3 and Psd Ph5 differ in their native plasmid content, although the analysed French, Slovenian and Spanish isolates shared the same plasmid profile. Therefore, plasmid purification and separation in agarose gel seems to be more resolutive than digestion followed by hybridization with a *repA* probe to identify differences in the plasmid content of the strains. Gathering all this information and considering that the first report of dipladenia spots caused by *P. savastanoi* date back to the late 2000s (Putnam *et al.*, 2010), it is possible that this disease has emerged recently, not allowing the generation of substantial genetic diversity among different Psd isolates.

The phylogenetic analysis shown in this Chapter, constructed with the partial sequence of four housekeeping genes, revealed that all Psd are phylogenetically related to Psn strains. These results are in agreement with those obtained by analysis of the 16s rDNA (Eltlbany *et al.*, 2012) and *rpoD* partial sequences (Pirc *et al.*, 2014). Another finding supporting the proximity of Psn and Psd strains emerged from the cross-pathogenicity tests: two out of three Psn strains were able to induce knots/excrescences on dipladenia. Curiously, the most virulent Psn isolate on

dipladenia was CFBP 5067, which did not show a 100% phylogenetic association with the other Psd strains analysed. In contrast, Psn ESC23 was not pathogenic on this host. It is well described that the T3E repertoire highly vary in the *P. syringae* complex from one strain to another and this diversity might explain differences in host range (Baltrus *et al.*, 2011). Thus, the T3E pool of Psn CFBP 5067 might be different to that of Psn ESC23 and permit the pathogenicity on dipladenia. In relation to this, it is important to mention that oleander and dipladenia belong to the *Apocynaceae* family, what might have facilitated adaptation of the pathogen from one host to the other. Thus, placing dipladenia nurseries close to oleander plantations should be avoided to prevent the generation new outbreaks of the disease.

Cross-pathogenicity test showed a unique host range for Psd strains compared to those of the well established *P. savastanoi* pathovars. Moreover, the host range of all Psd strains here analysed is common, which contrast with the strain-dependent pathogenicity observed for *P. savastanoi* strains isolated from myrtle (Cinelli *et al.*, 2014) and with the results here obtained for Psn strains in dipladenia. Symptoms generated by Psd on oleander and olive (Table 5) also differ from the observations mentioned by Eltlbany *et al.* (2012), but not published. Among other factors, it is well known that the age of the plant and the cultivar contribute to the generation of symptoms after artificial *P. savastanoi* inoculations (Penyalver *et al.*, 2006). Therefore, the observed differences could be attributed to the selection of distinct plant cultivars and/or to the age of the plants.

A Psd Ph3 plasmid-cured derivative lacking the *iaaM* gene (CRpiaaM, see Appendix 1) did not develop a knot on dipladenia (Figure 8B), which is consistent with the role of this gene in the virulence of *P. savastanoi* (Smidt & Kosuge, 1978; Surico *et al.*, 1985; Iacobellis *et al.*, 1994; Aragon *et al.*, 2014). Approximately 10^8 cfu were isolated from the knots generated by wild type Psd Ph3, whereas very little or no cfu were recovered from the sites inoculated with CRpiaaM, indicating that this strain is impaired on its survival in dipladenia. Consistent with this observation is that a Psv NCPPB 3335 mutant strain in the *iaaMH*-1 operon is outcompeted by the wild type strain on olive plants (Aragon *et al.*, 2014). Curiously, CRpiaaM still produces a small amount of IAA, perhaps due to the presence of a chromosome-encoded copy of the *iaaMH* operon. In this regard, codification of a second *iaaMH* operon (*iaaMH*-2) has been reported in Psv NCPPB 3335; however, this operon is not functional and does not contribute to the synthesis of IAA nor to the virulence of the strain on olive (Aragon *et al.*, 2014). As also suggested for Psv NCPPB 3335, a different pathway for the biosynthesis of IAA might be encoded in the genome of Psd Ph3. As IAA production by CRpiaaM is also enhanced by tryptophan, an IAA pathway different from that dependent on the *iaaMH* operon might be active in this strain. Three

additional tryptophan-dependent pathways (indole 3-acetonitrile, indole 3-pyruvate and tryptamine) have been proposed for bacterial production of IAA (Spaepen *et al.*, 2007). However, all sequenced *P. savastanoi* strains lack genes required to complete each of these three pathways. Considering the later information, two situations are possible: (i) that none of these biosynthetic pathways is active in *P. savastanoi*, or (ii) that other *P. savastanoi* enzymes complement the function of the missing proteins.

Results in this Chapter demonstrate that Psd Ph3 is able to migrate in dipladenia and induce the development of necrotic lesions several centimetres away from the point of inoculation, a phenotype previously observed for Psv and Psn strains (Wilson, 1935; Wilson & Magie, 1964; Penyalver *et al.*, 2006). Previously, it was reported the association of Psv cells with xylem vessels (Marchi *et al.*, 2009; Rodriguez-Moreno *et al.*, 2009; Maldonado-González *et al.*, 2013) and of Psn with laticifers (Wilson & Magie, 1964). Since dipladenia and oleander belong to the *Apocynaceae* family and share latex production, Psn and Psd might use a common mechanism(s) for their dissemination through the plant. When occurring, the systemic spreading of *P. savastanoi* in dipladenia brings the wilting of the plant, a phenomenon not reported before in dipladenia plants infected with *P. savastanoi*. The systemic infection caused by Psd on dipladenia must be considered by nurseries to control the disease and prevent its dissemination. Implementation of control methods including plant removal and incineration of infected plants might help preventing dissemination of the pathogen.

In summary, results shown in this Chapter suggest that the *P. savastanoi* strains pathogenic to dipladenia might have emerged recently. Evidences for the proximity of Psn and Psd strains from a phylogenetic and pathogenicity perspectives are provided. However, the unique host range of Psd isolates compared with those of the four well-established *P. savastanoi* pathovars suggest that these strains might constitute a novel pathovar of this specie. Wilting of dipladenia due to systemic infection of Psd was observed, which should be considered in dipladenia management to prevent pathogen dissemination.

Concluding remarks

The study of *Pseudomonas savastanoi* interactions with its hosts has been addressed from diverse perspectives in this PhD Thesis. *P. savastanoi* pv. savastanoi (Psv) has been established as a model for the study of bacterial molecular interactions with a woody host (Ramos *et al.*, 2012); in this regard considerable advances have been achieved over the last years in unveiling the factors contributing to the virulence and adaptation of Psv to olive (Perez-Martinez *et al.*, 2010; Bardaji *et al.*, 2011; Hosni *et al.*, 2011; Matas *et al.*, 2012; Aragon *et al.*, 2014; Matas *et al.*, 2014; Aragon *et al.*, 2015a; Aragon *et al.*, 2015b). A genomic region probably involved in the metabolism of phenolic compounds has been shown to be unique to strains from the *P. syringae* complex isolated from woody hosts (Rodriguez-Palenzuela *et al.*, 2010; Ramos *et al.*, 2012; Nowell *et al.*, 2016). Chapter I of this PhD Thesis broaden the distribution of this region to many other *P. syringae* strains which genomes have been recently sequenced (Moretti *et al.*, 2014; Bartoli *et al.*, 2015b; Thakur *et al.*, 2016) and provides the first evidence of the WHOP region (from <u>w</u>oody <u>ho</u>st and *Pseudomonas*) contribution to virulence and fitness of Psv NCPPB 3335 into woody olive plants (Figure 1). The identification and functional characterization of virulence factors capture the scientific interest. However, compared to herbaceous plant pathogens, little attention is currently paid to bacterial virulence factors of woody host pathogens. In this sense, Chapter I confirmed the aromatic compounds catabolism as a novel virulence factor of Psv NCPPB 3335 that play a role in bacteria-woody host interactions and particularly enhance the knowledge of bacterial interactions with a woody host. In addition, Chapter II focused on the quorum sensing system of Psv NCPPB 3335, a well-defined virulence factor for Psv DAPP-PG 722 (Hosni *et al.*, 2011), and show differences with the quorum sensing systems of two *P. syringae* strains.

Comparative genomic analyses of strains from the *P. syringae* complex will allow future identification of novel pathovar-specific elements that might define the host range of particular strains. In this sense, the identification of *P. savastanoi* strains causing stem knots and leaf spots on dipladenia was reported during progression of this PhD Thesis (EltIbany *et al.*, 2012; Pirc *et al.*, 2014). Evidences of the relationship between *P. savastanoi* strains isolated from dipladenia (Psd) and oleander (*P. savastanoi* pv. nerii, Psn) are provided in Chapter III, although their host range is different. Sequencing of the genome of a Psd strain and comparative analysis with the pathotype Psn strain ICMP 16943, which genome sequence has been recently published (Thakur *et al.*, 2016), could explain the differences found in the host range of these bacteria. Furthermore, the type III secretion system (T3SS) effectors (T3E) repertoire has been proposed to play a key role in determining the host range (Baltrus *et al.*, 2011). Variability in the T3E repertoire of *P. savastanoi* Ph3 and Psv NCPPB 3335 might be responsible for the different plant

responses observed after infiltration of these strains in tobacco leaves. A RNAseq-based strategy similar to that used in Chapter II could be used to find genes regulated by HrpL, a transcription factor that promotes the transcription of the T3SS and its T3E (Lindeberg *et al.*, 2005). Unlike the LB medium used for the RNAseq in Chapter II, a minimal medium that mimics the plant apoplast and promote T3E expression, as the hrp medium (Huynh *et al.*, 1989), should be used for the identification of the HrpL regulon. Since Psv NCPPB 3335 is unable to grow in hrp medium and, hence, do not reach the quorum, it could not be used in this PhD Thesis for the identification of genes controlled by PssI. It is important to remark here that many Psv virulence genes are not expressed in LB and its *pssI*-dependency could not be examined. Nonetheless, RNA sequencing data shown in Chapter II might also serve to map the transcription start points and to identify the active promoters of Psv NCPPB 3335 under the conditions tested.

P. savastanoi strains pathogenic on dipladenia (Psd) in Spain were isolated during progression of this PhD Thesis (Chapter III) (Caballo-Ponce & Ramos, 2016), which constitute a severe problem given that Spain is one of the main European producers of dipladenia. Sequencing of a Psd strain genome would also help to identify putative targets to design control strategies against the pathogen. Dissemination of Psd strain Ph3 through dipladenia has been observed (Chapter III, Figure 9), which occasionally led to the bacterial wilting of the plant and contrast with the consequences of systemic Psv strains infections in one-year old woody olive plants (Penyalver *et al.*, 2006). Bacterial wilting of dipladenia was observed in four-month old non-woody plants, which is the plant format chosen for its commercialisation. Data not shown in this PhD Thesis revealed high sensitivity of Psd strains to cupric compounds; therefore, chemical treatments to prevent the disease should be carried out, as well as incinerating the infected plants to prevent the dissemination of the pathogen. Additionally, identification of dipladenia cultivars more resistant to *P. savastanoi* infections is a future challenge for breeders. All these practices should be integrated for an efficient control of *P. savastanoi* infections in dipladenia.

Sequencing of the Psv NCPPB 3335 genome (Rodriguez-Palenzuela *et al.*, 2010) opened a vast repertoire of putative virulence factors in this bacterial pathogen, several of which were later confirmed using a functional genomic strategy (Matas *et al.*, 2012). Although the role in virulence of the indole 3-acetic acid (Smidt & Kosuge, 1978; Surico *et al.*, 1985; Iacobellis *et al.*, 1994) and cytokinins (Iacobellis *et al.*, 1994) was reported more than 30 years ago, during the last few years several studies offered new insights into the mode of action of these phytohormones in Psv (Bardaji *et al.*, 2011; Aragon *et al.*, 2014). In addition, several other mechanisms have been recently studied in detail, i.e. the T3SS and the T3E repertoire of Psv

NCPPB 3335 (Castaneda-Ojeda, 2014; Matas *et al.*, 2014; Castaneda-Ojeda *et al.*, 2016), the quorum sensing system of Psv DAPP-PG 722 (Hosni *et al.*, 2011) and the metabolism of the second messenger cyclic diguanylate (Aragon *et al.*, 2015a; Aragon *et al.*, 2015b) (Figure 1). A novel factor, the catabolism of aromatic compounds (the WHOP region), has been added in this PhD Thesis (Chapter I) to the list of Psv NCPPB 3335 virulence determinants. On the other hand, results in this PhD Thesis show that quorum-sensing regulation varies among different strains of Psv, as this system does not contribute to the virulence of Psv NCPPB 3335 (Chapter II), contrasting with the results reported for Psv DAPP-PG 722 (Hosni *et al.*, 2011). Knowledge of the factors influencing virulence in Psv facilitated in this PhD Thesis the analysis of the virulence and adaptation of *P. savastanoi* strains to dipladenia plants. The relationship between the production of indole 3-acetic acid and the virulence of this pathogen was confirmed in Chapter III. In addition, the role of the T3SS in determining the host range is also suggested in this Chapter. Future work should focus on genomic comparative analyses among *P. savastanoi* strains isolated from different hosts, which will help to identify novel factors contributing to the virulence and adaptation of this group of bacteria.
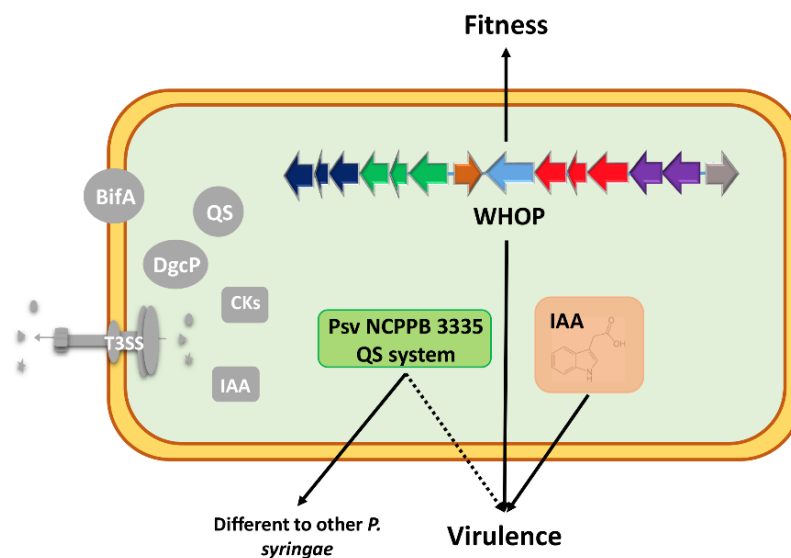
Figure 1. Schematic representation of *Pseudomonas savastanoi* virulence and adaptation factors. Virulence factors previously studied in *P. savastanoi* are represented in grey: production of cytokinins (CKs) and indole 3-acetic acid (IAA); the quorum sensing system (QS); metabolism of cyclic di-guanylate (BifA, DgcP); and the type III secretion system (T3SS). The WHOP region clusters are represented with different coloured arrows: *catBCA*, dark blue; *antABC*, green; *antR*, brown; a putative aerotaxis receptor, light blue; *ipoABC*, red; purple, *dhoAB*; grey, *benR*. Solid lines indicate a role of the WHOP region in the virulence and fitness of Psv NCPPB 3335 . A black dotted line indicates the absence of a role of the Psv NCPPB 3335 quorum sensing system in the virulence.

Conclusions

1. Bacteria from the *Pseudomonas syringae* complex belonging to phylogroups 1 and 3 isolated from woody organs of woody hosts, share a genomic region here named WHOP (from <u>w</u>oody <u>ho</u>st and *Pseudomonas*) not present in strains isolated from herbaceous organs, except for *P. syringae* pv. actinidifoliorum and *P. syringae* pv. ciccaronei.

2. The *Pseudomonas savastanoi* pv. savastanoi (Psv) NCPPB 3335 WHOP region is organized in four operons (*catBCA*, *antABC*, *ipoABC* and *dhoAB*) and three independently transcribed genes (*antR*, a gene encoding a putative aerotaxis receptor and *benR*).

3. The Psv NCPPB 3335 *antABC* and *catBCA* operons are involved in the catabolism of anthranilate and catechol, respectively; the *ipoABC* operon confers oxygenase activity on aromatic compounds.

4. The *antABC*, *catBCA* and *ipoABC* operons are required for full virulence of Psv NCPPB 3335 in woody olive plants; the *catBCA* and *dhoAB* operons and the gene encoding the putative aerotaxis receptor contribute to the fitness of this bacterium in woody olive tissues.

5. Bacteria from the *P. syringae* complex encode a highly variable content of *luxI/luxR* homologs potentially involved in quorum sensing regulation.

6. A Psv NCPPB 3335 *pssI* mutant grown in LB medium shows overexpression of three genes encoded in close proximity to the *pssI/pssR* gene pair.

7. The transcription of twelve genes regulated by quorum sensing in *P. syringae* pv. tabaci is PssI independent in Psv NCPPB 3335.

8. Exopolysaccharide production, biofilm formation, motility and virulence are not altered in quorum sensing mutants of Psv NCPPB 3335.

9. *P. savastanoi* is the causative agent of dipladenia leaf and stem spot in Spain.

10. *P. savastanoi* strains isolated from dipladenia are phylogenetically related to *P. savastanoi* pv. nerii and show a different host range than the four well established *P. savastanoi* pathovars.

11. *P. savastanoi* Ph3 is able to migrate through dipladenia causing a systemic infection and, occasionally, total wilt of the plant.

Appendix

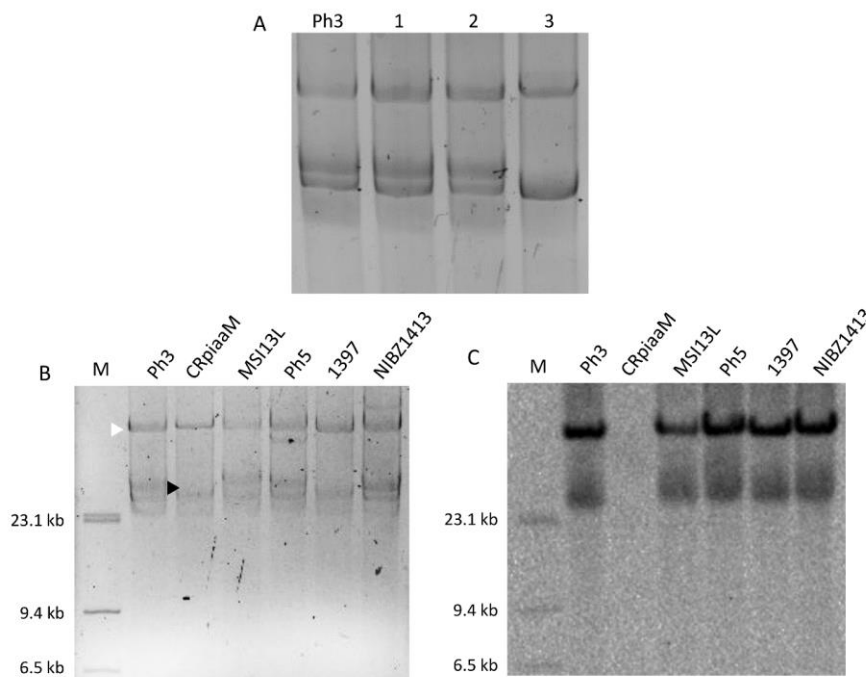**Construction of a *P. savastanoi* Ph3-derived strain lacking the plasmid-encoded copy of the *iaaM* gene**

Plasmid-cured derivatives of *P. savastanoi* strains have been obtained by counterselection of a *sacB*-encoding Tn5 transposon (Tn5-GDYN1) (Brom *et al.*, 1992) in sucrose-amended medium (Bardaji *et al.*, 2011). After several failed attempts to cure the plasmids of several Psd strains using Tn5-GDYN1, and taking into account that *P. savastanoi* Ph3 carry a plasmid-encoded copy of the *iaaM* gene (Eltlbany *et al.*, 2012), hereafter named plasmid pIAAM, we decided to try an alternative method based on this gene. The strategy followed is the treatment of *P. savastanoi* cells with a curing agent, acridine orange in this case, followed by the selection of strains sensitive to 5-methyl tryptophan (5-MT). In this protocol, log phase cells (approximately 10^3-10^4) are inoculated in KB broth (King *et al.*, 1954) containing 75 µg/ml of acridine orange; and after 48 hours incubation at 28 °C, bacteria are diluted 30 fold, incubated at 28 °C for additional 24 hours, and plated into solid KB medium. Later, single colonies are replicated in M9 minimal media (Sambrook, 2001) containing 1.5% glucose as carbon source and supplemented or not with 200 µg/ml 5-MT. Since the *iaaM* gene (tryptophan monooxygenase) confers resistance to 5-MT, *P. savastanoi* strains cured of plasmids encoding the *iaaM* gene are identified by their sensitiveness to this compound (Comai & Kosuge, 1980). Only three out of one thousand Ph3 colonies sensitive to 5-MT were isolated after treatment with acridine orange. Production of IAA by these three isolates was tested using previously reported protocols (Mitchell & Brunstetter, 1939) and none of them developed the pink colour typical of IAA-producing bacteria. Native plasmids of these three strains were extracted and visualized in agarose gels; however, only one of them (Ph3-derivative number 3) seemed to have lost a plasmid when compared to the plasmid profile of Ph3 (Fig. 1A). Thus, this strain (CRpiaaM) was selected for further analyses. Loss of an *iaaM*-encoding plasmid in CRpiaaM was assessed by Southern blot hybridization using an *iaaM* probe that was synthesized by PCR using iaaM_F615 and iaaM_R1090 primers (Table 3 in Chapter III) and the PCR DIG labelling mix (Roche, Mannheim, Germany) following the manufacturer's indications. *P. savastanoi* Ph3 and another four *P. savastanoi* strains isolated from dipladenia (MSI13L, Ph5, 1397 and NIBZ1413; see Table 1 in Chapter III) were used as positive control. Native plasmids of Psd were separated by agarose gel electrophoresis (Fig. 1B) and hybridized with the *iaaM* probe. As shown in Figure 1C, while *P. savastanoi* Ph3 and the other four isolates harbour a plasmid of similar size hybridizing with the *iaaM* probe, hybridization was not observed for CRpiaaM. However and surprisingly, CRpiaaM carries a plasmid of similar size than pIAAM, which is present in Ph3 and the other four Psd strains, but has lost a plasmid of a smaller size (plasmid pPh3A) (Fig. 1B).

Sequencing of the three native plasmids of the olive pathogen Psv NCPPB 3335 (pPsv48A, pPsv48B and pPsv48C) revealed the presence of several genetic elements probably essential for the maintenance of the plasmids (Bardaji *et al.*, 2011). In particular, plasmids pPsv48A and pPsv48B carry several toxin-antitoxin systems, and, in addition, pPsv48B contains a bacteriocin immunity protein. In this sense, the generation of a strain lacking only pPsv48B could not be accomplished; however, this plasmid was cured in a strain lacking pPsv48A (Bardaji *et al.*, 2011). Considering all this information, it could be speculated that the pIAAM plasmid of *P. savastanoi* Ph3 might carry maintenance elements that prevent its complete loss. Our results suggest that a pIAAM derivative lacking the *iaaM* gene has been generated in CRpiaaM. Additionally, since CRpiaaM has lost plasmid pPh3A, it is likely that a plasmid rearrangement have occurred between pIAAM and pPh3A, leading to a pPh3A derivative encoding the *iaaM* gene that has been subsequently lost, leading to a 5-MT sensitive phenotype.

Figure 1. Isolation of a *P. savastanoi* Ph3 derivative strain lacking the pIAAM-encoded *iaaM* gene**. (A) Gel electrophoresis of plasmids preparations from *P. savastanoi* Ph3 and three derivative strains (1, 2, 3) sensitive to 5-methyl tryptophan. (B) Gel electrophoresis of plasmid preparations from the indicated *P. savastanoi* strains isolated from dipladenia. White arrowhead indicates plasmid pIAAM; black arrowhead indicates the absence of plasmid pPh3A in CRpiaaM. (C) Southern blot hybridization of the plasmids shown in (B) using an *iaaM* probe. M, DNA Molecular Weight Marker II DIG-labelled (Roche, Mannheim, Germany).

References

Ahmer, B. M., van Reeuwijk, J., Timmers, C. D., Valentine, P. J. and Heffron, F. (1998) *Salmonella typhimurium* encodes an SdiA homolog, a putative quorum sensor of the LuxR family, that regulates genes on the virulence plasmid. Journal of Bacteriology, 180, 1185-1193.

Alvarez, F., García de los Ríos, J. E., Jimenez, P., Rojas, A., Reche, P. and Troya, M. T. (1998) Phenotypic variability in different strains of *Pseudomonas syringae* subsp. savastanoi isolated from different hosts. European Journal of Plant Pathology, 104, 603-609.

Andersen, J. B., Heydorn, A., Hentzer, M., Eberl, L., Geisenberger, O., Christensen, B. B., Molin, S. and Givskov, M. (2001) *gfp*-based N-acyl homoserine-lactone sensor systems for detection of bacterial communication. Applied and Environental Microbiology, 67, 575-585.

Andreoni, V., Bernasconi, S., Bestetti, P. and Villa, M. (1991) Metabolism of lignin-related compounds by *Rhodococcus rhodochrous*: bioconversion of anisoin. Applied microbiology and biotechnology, 36, 410-415.

Aragon, I. M., Perez-Martinez, I., Moreno-Perez, A., Cerezo, M. and Ramos, C. (2014) New insights into the role of indole-3-acetic acid in the virulence of *Pseudomonas savastanoi* pv. savastanoi. FEMS microbiology letters, 356, 184-192.

Aragon, I. M., Perez-Mendoza, D., Gallegos, M. T. and Ramos, C. (2015a) The c-di-GMP phosphodiesterase BifA is involved in the virulence of bacteria from the *Pseudomonas syringae* complex. Molecular plant pathology, 16, 604-615.

Aragon, I. M., Perez-Mendoza, D., Moscoso, J. A., Faure, E., Guery, B., Gallegos, M. T., Filloux, A. and Ramos, C. (2015b) Diguanylate cyclase DgcP is involved in plant and human *Pseudomonas* spp. infections. Environmental microbiology, 17, 4332-4351.

Balestra, G. M., Lamichhane, J. R., Kshetri, M. B., Mazzaglia, A. and Varvaro, L. (2009) First report of olive knot caused by *Pseudomonas savastanoi* pv. savastanoi in Nepal. Plant Pathology, 58, 393-393.

Baltrus, D. A., Nishimura, M. T., Romanchuk, A., Chang, J. H., Mukhtar, M. S., Cherkis, K., Roach, J., Grant, S. R., Jones, C. D. and Dangl, J. L. (2011) Dynamic evolution of pathogenicity revealed by sequencing and comparative genomics of 19 *Pseudomonas syringae* isolates. PLoS pathogens, 7, e1002132.

Bardaji, L., Perez-Martinez, I., Rodriguez-Moreno, L., Rodriguez-Palenzuela, P., Sundin, G. W., Ramos, C. and Murillo, J. (2011) Sequence and role in virulence of the three plasmid complement of the model tumor-inducing bacterium *Pseudomonas savastanoi* pv. savastanoi NCPPB 3335. PLoS One, 6, e25705.

Bartoli, C., Lamichhane, J. R., Berge, O., Guilbaud, C., Varvaro, L., Balestra, G. M., Vinatzer, B. A. and Morris, C. E. (2015a) A framework to gauge the epidemic potential of plant pathogens in environmental reservoirs: the example of kiwifruit canker. Molecular plant pathology, 16, 137-149.

Bartoli, C., Carrere, S., Lamichhane, J. R., Varvaro, L. and Morris, C. E. (2015b) Whole-Genome Sequencing of 10 *Pseudomonas syringae* strains representing different host range spectra. Genome announcements, 3.

Bassler, B. L. (1999) How bacteria talk to each other: regulation of gene expression by quorum sensing. Current opinion in microbiology, 2, 582-587.

Berge, O., Monteil, C. L., Bartoli, C., Chandeysson, C., Guilbaud, C., Sands, D. C. and Morris, C. E. (2014) A user's guide to a data base of the diversity of *Pseudomonas syringae* and its application to classifying strains in this phylogenetic complex. PLoS One, 9, e105547.

Bocsanczy, A. M., Yuen, J. M. F., Palmateer, A. J. and Norman, D. J. (2014) Comparative genomics of *Ralstonia solanacearum* strain P781 that infects *Mandevilla* and Dipladenia plants. Phytopathology, 104, 16-16.

Boerjan, W., Ralph, J. and Baucher, M. (2003) Lignin biosynthesis. Annual review of plant biology, 54, 519-546.

Bozkurt, I. A., Soylu, S., Mirik, M., Ulubas Serce, C. and Baysal, O. (2014) Characterization of bacterial knot disease caused by *Pseudomonas savastanoi* pv. savastanoi on

pomegranate (*Punica granatum* L.) trees: a new host of the pathogen. Letters in applied microbiology*, 59***,** 520-527.

Bradbury, J. F. (1986) Guide to plant pathogenic bacteria. CAB International, Wallingford, U.K.

Brom, S., Garcia de los Santos, A., Stepkowsky, T., Flores, M., Davila, G., Romero, D. and Palacios, R. (1992) Different plasmids of *Rhizobium leguminosarum* bv. phaseoli are required for optimal symbiotic performance. Journal of Bacteriology*, 174***,** 5183-5189.

Buell, C. R., Joardar, V., Lindeberg, M., Selengut, J., Paulsen, I. T., Gwinn, M. L., Dodson, R. J., Deboy, R. T., Durkin, A. S., Kolonay, J. F., Madupu, R., Daugherty, S., Brinkac, L., Beanan, M. J., Haft, D. H., Nelson, W. C., Davidsen, T., Zafar, N., Zhou, L., Liu, J., Yuan, Q., Khouri, H., Fedorova, N., Tran, B., Russell, D., Berry, K., Utterback, T., Van Aken, S. E., Feldblyum, T. V., D'Ascenzo, M., Deng, W. L., Ramos, A. R., Alfano, J. R., Cartinhour, S., Chatterjee, A. K., Delaney, T. P., Lazarowitz, S. G., Martin, G. B., Schneider, D. J., Tang, X., Bender, C. L., White, O., Fraser, C. M. and Collmer, A. (2003) The complete genome sequence of the *Arabidopsis* and tomato pathogen *Pseudomonas syringae* pv. tomato DC3000. Proceedings of the National Academy of Sciences 100*,* 10181-10186.

Bullock, W. O., Femandez, J. M. and Short, J. M. (1987) XLl-Blue: a high efficiency plasmid transforming *recA Escherichia coli* strain with β-galactosidase selection. BioTechniques*, 5***,** 376-378.

Buonaurio, R., Moretti, C., da Silva, D. P., Cortese, C., Ramos, C. and Venturi, V. (2015) The olive knot disease as a model to study the role of interspecies bacterial communities in plant disease. Frontiers in plant science*, 6***,** 434.

Büttner, D. and He, S. Y. (2009) Type III Protein Secretion in Plant Pathogenic Bacteria. Plant Physiology*, 150***,** 1656-1664.

Caballo-Ponce, E. and Ramos, C. (2016) First Report of Dipladenia (*Mandevilla* spp.) Leaf and Stem Spot Caused by *Pseudomonas savastanoi* in Spain. Plant Disease**,** PDIS-03-16-0334-PDN.

Caballo-Ponce, E., van Dillewijn, P., Wittich, R.-M. and Ramos, C. (2016) WHOP, a genomic region associated with woody hosts in the *Pseudomonas syringae* complex contributes to the virulence and fitness of *Pseudomonas savastanoi* pv. savastanoi in olive plants. Molecular Plant-Microbe Interactions.

Capasso, R., Evidente, A., Schivo, L., Orru, G., Marcialis, M. A. and Cristinzio, G. (1995) Antibacterial polyphenols from olive oil mill waste waters. Journal of Applied Bacteriology*, 79***,** 393-398.

Caponero, A., Contesini, A. M. and Iacobellis, N. S. (1995) Population diversity of *Pseudomonas syringae* subsp. savastanoi on olive and oleander. Plant Pathology*, 44***,** 848-855.

Case, R. J., Labbate, M. and Kjelleberg, S. (2008) AHL-driven quorum-sensing circuits: their frequency and function among the Proteobacteria. The ISME journal*, 2***,** 345-349.

Castaneda-Ojeda, M. P. (2014) Functional Analysis of *Pseudomonas savastanoi* pv. savastanoi Type III Secretion System Effectors. PhD Thesis. University of Malaga.

Castaneda-Ojeda, M. P., Lopez-Solanilla, E. and Ramos, C. (2016) Differential modulation of plant immune responses by diverse members of the *Pseudomonas savastanoi* pv. savastanoi HopAF type III effector family. Molecular plant pathology.

Castañeda-Ojeda, M. P., López-Solanilla, E. and Ramos, C. (2016) Differential modulation of plant immune responses by diverse members of the Pseudomonas savastanoi pv. savastanoi HopAF type III effector family. Molecular plant pathology**,** n/a-n/a.

Castillo-Lizardo, M. G., Aragon, I. M., Carvajal, V., Matas, I. M., Perez-Bueno, M. L., Gallegos, M. T., Baron, M. and Ramos, C. (2015) Contribution of the non-effector members of the HrpL regulon, *iaaL* and *matE*, to the virulence of *Pseudomonas syringae* pv. tomato DC3000 in tomato plants. BMC microbiology*, 15***,** 165.

Cebron, A., Beguiristain, T., Bongoua-Devisme, J., Denonfoux, J., Faure, P., Lorgeoux, C., Ouvrard, S., Parisot, N., Peyret, P. and Leyval, C. (2015) Impact of clay mineral, wood sawdust or

root organic matter on the bacterial and fungal community structures in two aged PAH-contaminated soils. Environmental Science and Pollution Research, 22, 13724-13738.

Cerboneschi, M., Decorosi, F., Biancalani, C., Ortenzi, M. V., Macconi, S., Giovannetti, L., Viti, C., Campanella, B., Onor, M., Bramanti, E. and Tegli, S. (2016) Indole-3-acetic acid in plant–pathogen interactions: a key molecule for in planta bacterial virulence and fitness. Research in microbiology.

Cimmino, A., Andolfi, A., Marchi, G., Surico, G. and Evidente, A. (2006) Phytohormone Production by Strains of *Pantoea agglomerans* from Knots on Olive Plants Caused by *Pseudomonas savastanoi* pv. savastanoi. Phytopathologia Mediterranea, 45.

Cinelli, T., Marchi, G., Cimmino, A., Marongiu, R., Evidente, A. and Fiori, M. (2014) Heterogeneity of *Pseudomonas savastanoi* populations infecting *Myrtus communis* in Sardinia (Italy). Plant Pathology, 63, 277-289.

Comai, L. and Kosuge, T. (1980) Involvement of plasmid deoxyribonucleic acid in indoleacetic acid synthesis in *Pseudomonas savastanoi*. Journal of Bacteriology, 143, 950-957.

Comai, L. and Kosuge, T. (1982) Cloning characterization of *iaaM*, a virulence determinant of *Pseudomonas savastanoi*. Journal of Bacteriology, 149, 40-46.

Coutinho, B. G., Mitter, B., Talbi, C., Sessitsch, A., Bedmar, E. J., Halliday, N., James, E. K., Camara, M. and Venturi, V. (2013) Regulon studies and *in planta* role of the BraI/R quorum-sensing system in the plant-beneficial *Burkholderia* cluster. Applied and Environmental Microbiology, 79, 4421-4432.

Coutinho, B. G., Licastro, D., Mendonca-Previato, L., Camara, M. and Venturi, V. (2015) Plant-Influenced Gene Expression in the Rice Endophyte *Burkholderia kururiensis* M130. Molecular Plant Microbe Interactions, 28, 10-21.

Cunty, A., Poliakoff, F., Rivoal, C., Cesbron, S., Fischer-Le Saux, M., Lemaire, C., Jacques, M. A., Manceau, C. and Vanneste, J. L. (2015) Characterization of *Pseudomonas syringae* pv. actinidiae (Psa) isolated from France and assignment of Psa biovar 4 to a de novo pathovar: *Pseudomonas syringae* pv. actinidifoliorum pv. nov. Plant Pathology, 64, 582-596.

Cuppels, D. A. (1986) Generation and Characterization of Tn5 Insertion Mutations in Pseudomonas syringae pv. tomato. Applied and Environmental Microbiololgy, 51, 323-327.

Cha, C., Gao, P., Chen, Y. C., Shaw, P. D. and Farrand, S. K. (1998) Production of acyl-homoserine lactone quorum-sensing signals by gram-negative plant-associated bacteria. Molecular Plant Microbe Interactions, 11, 1119-1129.

Chapman, J. R., Taylor, R. K., Weir, B. S., Romberg, M. K., Vanneste, J. L., Luck, J. and Alexander, B. J. R. (2012) Phylogenetic relationships among global populations of *Pseudomonas syringae* pv. actinidiae. Phytopathology, 102, 1034-1044.

Choi, H. S., Kim, J. K., Cho, E. H., Kim, Y. C., Kim, J. I. and Kim, S. W. (2003) A novel flavin-containing monooxygenase from *Methylophaga* sp strain SK1 and its indigo synthesis in *Escherichia coli*. Biochemical and biophysical research communications, 306, 930-936.

Christen, B., Christen, M., Paul, R., Schmid, F., Folcher, M., Jenoe, P., Meuwly, M. and Jenal, U. (2006) Allosteric Control of Cyclic di-GMP Signaling. Journal of Biological Chemistry, 281, 32015-32024.

Christen, M., Christen, B., Folcher, M., Schauerte, A. and Jenal, U. (2005) Identification and characterization of a cyclic di-GMP-specific phosphodiesterase and its allosteric control by GTP. The Journal of biological chemistry, 280, 30829-30837.

Chugani, S., Kim, B. S., Phattarasukol, S., Brittnacher, M. J., Choi, S. H., Harwood, C. S. and Greenberg, E. P. (2012) Strain-dependent diversity in the *Pseudomonas aeruginosa* quorum-sensing regulon. Proceedings of the National Academy of Sciences U S A, 109, E2823-2831.

Chugani, S. A., Whiteley, M., Lee, K. M., D'Argenio, D., Manoil, C. and Greenberg, E. P. (2001) QscR, a modulator of quorum-sensing signal synthesis and virulence in Pseudomonas aeruginosa. Proceedings of the National Academy of Sciences 98**,** 2752-2757.

Davino, M., Bellardi, M. G., Di Bella, M., Davino, S. and Bertaccini, A. (2005) Characterization of a Cucumber mosaic virus Isolate infecting *Mandevilla sanderi* (Hemsl.) Woodson. Phytopathologia Mediterranea 44**,** 220-225.

Deng, X., Xiao, Y., Lan, L., Zhou, J. M. and Tang, X. (2009) *Pseudomonas syringae* pv. phaseolicola Mutants Compromised for type III secretion system gene induction. Molecular Plant Microbe Interactions 22**,** 964-976.

Doukyu, N., Toyoda, K. and Aono, R. (2003) Indigo production by *Escherichia coli* carrying the phenol hydroxylase gene from *Acinetobacter* sp strain ST-550 in a water-organic solvent two-phase system. Applied microbiology and biotechnology*,* 60**,** 720-725.

Dumenyo, C. K., Mukherjee, A., Chun, W. and Chatterjee, A. K. (1998) Genetic and physiological evidence for the production of *N*-acyl homoserine lactones by *Pseudomonas syringae* pv. syringae and other fluorescent plant pathogenic *Pseudomonas* species. European Journal of Plant Pathology*,* 104**,** 569-582.

Dunlap, P. V. and Ray, J. M. (1989) Requirement for autoinducer in transcriptional negative autoregulation of the *Vibrio fischeri* luxR gene in *Escherichia coli*. Journal of Bacteriology*,* 171**,** 3549-3552.

Eltlbany, N., Prokscha, Z. Z., Castaneda-Ojeda, M. P., Krogerrecklenfort, E., Heuer, H., Wohanka, W., Ramos, C. and Smalla, K. (2012) A new bacterial disease on *Mandevilla sanderi*, caused by *Pseudomonas savastanoi*: lessons learned for bacterial diversity studies. Applied and Environmental Microbiology*,* 78**,** 8492-8497.

Ensley, B., Ratzkin, B., Osslund, T., Simon, M., Wackett, L. and Gibson, D. (1983) Expression of naphthalene oxidation genes in *Escherichia coli* results in the biosynthesis of indigo. Science*,* 222**,** 167-169.

Ercolani, G. L. and Caldarola, M. (1972) *Pseudomonas ciccaronei* sp. N., agente di una maculatura fogliare del Carrubo in Puglia. Phytopatol Mediterr*,* 11**,** 71-73.

Ercolani, G. L. (1978) *Pseudomonas savastano*i and Other Bacteria Colonizing the Surface of Olive Leaves in the Field. Microbiology*,* 109**,** 245-257.

Fatmi, M. B., Collmer, A., Iacobellis, N. S., Mansfield, J. W., Murillo, J., Schaad, N. W. and Ullrich, M. (2008) *Pseudomonas syringae* Pathovars and Related Pathogens. Identification, Epidemiology and Genomics. Springer.

Fuqua, C., Parsek, M. R. and Greenberg, E. P. (2001) Regulation of gene expression by cell-to-cell communication: acyl-homoserine lactone quorum sensing. Annual review of genetics*,* 35**,** 439-468.

Gao, X., Huang, Q., Zhao, Z., Han, Q., Ke, X., Qin, H. and Huang, L. (2016) Studies on the Infection, Colonization, and Movement of *Pseudomonas syringae* pv. actinidiae in Kiwifruit Tissues Using a GFPuv-Labeled Strain. PLoS One*,* 11**,** e0151169.

Gardan, L., Bollet, C., Abu Ghorrah, M., Grimont, F. and Grimont, P. A. D. (1992a) DNA relatedness among the pathovar strains of *Pseudomonas syringae* subsp. savastanoi Janse (1982) and proposal of *Pseudomonas savastanoi* sp. nov. International Journal of Systematic Bacteriology*,* 42**,** 606-612.

Gardan, L., David, C., Morel, M., Glickmann, E., Abu-Ghorrah, M., Petit, A. and Dessaux, Y. (1992b) Evidence for a correlation between auxin production and host plant species among strains of *Pseudomonas syringae* subsp. savastanoi. Applied and Environmental Microbiology*,* 58**,** 1780-1783.

Gardan, L., Shafik, H., Belouin, S., Broch, R., Grimont, F. and Grimont, P. A. (1999) DNA relatedness among the pathovars of *Pseudomonas syringae* and description of *Pseudomonas tremae* sp. nov. and P*seudomonas cannabina* sp. nov. (ex Sutic and Dowson 1959). International Journal of Systematic Microbiology*,* 49 Pt 2**,** 469-478.

Glass, N. L. and Kosuge, T. (1988) Role of indoleacetic acid-lysine synthetase in regulation of indoleacetic acid pool size and virulence of *Pseudomonas syringae* subsp. savastanoi. Journal of Bacteriology*, 170***,** 2367-2373.

Gohre, V. and Robatzek, S. (2008) Breaking the barriers: microbial effector molecules subvert plant immunity. Annual review of phytopathology*, 46***,** 189-215.

Goumas, D. E., Malathrakis, N. E. and Chatzaki, A. K. (2000) First report of *Pseudomonas savastanoi* pv. savastanoi on *Myrtus communis* sp. Phytopathologia Mediterranea*, 39***,** 313–338.

Green, S., Studholme, D. J., Laue, B. E., Dorati, F., Lovell, H., Arnold, D., Cottrell, J. E., Bridgett, S., Blaxter, M., Huitema, E., Thwaites, R., Sharp, P. M., Jackson, R. W. and Kamoun, S. (2010) Comparative genome analysis provides insights into the evolution and adaptation of *Pseudomonas syringae* pv. aesculi on *Aesculus hippocastanum*. PLoS One*, 5***,** e10224.

Hanahan, D. (1983) Studies on transformation of *Escherichia coli* with plasmids. Journal of molecular biology*, 166***,** 557-580.

Harwood, C. S. and Parales, R. E. (1996) The beta-ketoadipate pathway and the biology of self-identity. Annual review of microbiology*, 50***,** 553-590.

Heurlier, K., Denervaud, V. and Haas, D. (2006) Impact of quorum sensing on fitness of *Pseudomonas aeruginosa*. International Journal of Medical Microbiology*, 296***,** 93-102.

Holloway, B. W. (1955) Genetic recombination in Pseudomonas aeruginosa. Journal of general microbiology*, 13***,** 572-581.

Hosni, T., Moretti, C., Devescovi, G., Suarez-Moreno, Z. R., Fatmi, M. B., Guarnaccia, C., Pongor, S., Onofri, A., Buonaurio, R. and Venturi, V. (2011) Sharing of quorum-sensing signals and role of interspecies communities in a bacterial plant disease. The ISME journal*, 5***,** 1857-1870.

Houghton, J. E., Brown, T. M., Appel, A. J., Hughes, E. J. and Ornston, L. N. (1995) Discontinuities in the evolution of *Pseudomonas putida cat* genes. Journal of Bacteriology*, 177***,** 401-412.

Huber, B., Riedel, K., Hentzer, M., Heydorn, A., Gotschlich, A., Givskov, M., Molin, S. and Eberl, L. (2001) The *cep* quorum-sensing system of *Burkholderia cepacia* H111 controls biofilm formation and swarming motility. Microbiology*, 147***,** 2517-2528.

Hutcheson, S. W., Bretz, J., Sussan, T., Jin, S. and Pak, K. (2001) Enhancer-binding proteins HrpR and HrpS interact to regulate hrp-encoded type III protein secretion in *Pseudomonas syringae* strains. Journal of Bacteriology*, 183***,** 5589-5598.

Hutzinger, O. and Kosuge, T. (1968) Microbial synthesis and degradation of indole-3-acetic acid. 3. The isolation and characterization of indole-3-acetyl-epsilon-L-lysine. Biochemistry*, 7***,** 601-605.

Huynh, T. V., Dahlbeck, D. and Staskawicz, B. J. (1989) Bacterial blight of soybean: regulation of a pathogen gene determining host cultivar specificity. Science*, 245***,** 1374-1377.

Iacobellis, N. S., Sisto, A., Surico, G., Evidente, A. and DiMaio, E. (1994) Pathogenicity of *Pseudomonas syringae* subsp. savastanoi Mutants Defective in Phytohormone Production. Journal of Phytopathology*, 140***,** 238-248.

Iacobellis, N. S., Caponero, A. and Evidente, A. (1998) Characterization of *Pseudomonas syringae* ssp. savastanoi strains isolated from ash. Plant Pathology*, 47***,** 73-83.

Janse, J. D. (1982) *Pseudomonas syringae* subsp. savastanoi (ex Smith) subsp. nov., nom. rev., the Bacterium Causing Excrescences on *Oleaceae* and *Neriurn oleander* L. International journal of systematic and evolutionary microbiology*, 32***,** 166-169.

Janse, J. D. (1991) Pathovar Discrimination within *Pseudomonas syringae* subsp. savastanoi Using Whole Cell Fatty Acids and Pathogenicity as Criteria. Systematic and Applied Microbiology*, 14***,** 79-84.

Jeffrey, W. H., Cuskey, S. M., Chapman, P. J., Resnick, S. and Olsen, R. H. (1992) Characterization of Pseudomonas putida mutants unable to catabolize benzoate: cloning and characterization of Pseudomonas genes involved in benzoate catabolism and isolation

of a chromosomal DNA fragment able to substitute for xylS in activation of the TOL lower-pathway promoter. Journal of Bacteriology, 174, 4986-4996.

Jimenez, J. I., Minambres, B., Garcia, J. L. and Diaz, E. (2002) Genomic analysis of the aromatic catabolic pathways from *Pseudomonas putida* KT2440. Environmental microbiology, 4, 824-841.

Kelley, R. D. and Weathers, L. W. (1985) A possible new viral disease of *Mandevilla* sp. Phytopathology, 75, 1359-1360.

Kim, S., Park, J., Kim, J. H., Lee, J., Bang, B., Hwang, I. and Seo, Y. S. (2013) RNAseq-based Transcriptome Analysis of *Burkholderia glumae* Quorum Sensing. The plant pathology journal, 29, 249-259.

Kim, S., Park, J., Choi, O., Kim, J. and Seo, Y. S. (2014) Investigation of quorum sensing-dependent gene expression in *Burkholderia gladioli* BSR3 through RNA-seq analyses. Journal of microbiology and biotechnology, 24, 1609-1621.

Kim, S. K., Im, S. J., Yeom, D. H. and Lee, J. H. (2012) AntR-mediated bidirectional activation of *antA* and *antR*, anthranilate degradative genes in *Pseudomonas aeruginosa*. Gene, 505, 146-152.

King, E. O., Ward, M. K. and Raney, D. E. (1954) Two simple media for the demonstration of pyocyanin and fluorescin. Journal of Laboratory and Clinical Medicine, 44, 301-307.

Kosuge, T., Heskett, M. G. and Wilson, E. E. (1966) Microbial synthesis and degradation of indole-3-acetic acid. I. The conversion of L-tryptophan to indole-3-acetamide by an enzyme system from *Pseudomonas savastanoi*. The Journal of biological chemistry, 241, 3738-3744.

Kovach, M. E., Elzer, P. H., Hill, D. S., Robertson, G. T., Farris, M. A., Roop, R. M. and Peterson, K. M. (1995) Four new derivatives of the broad-host-range cloning vector pBBR1MCS, carrying different antibiotic-resistance cassettes. Gene, 166, 175-176.

Krid, S., Triki, M. A., Gargouri, A. and Rhouma, A. (2012) Biocontrol of olive knot disease by *Bacillus subtilis* isolated from olive leaves. Annals of Microbiology, 62, 149-154.

Lamichhane, J. R., Varvaro, L., Parisi, L., Audergon, J.-M. and Morris, C. E. (2014) Chapter Four - Disease and Frost Damage of Woody Plants Caused by *Pseudomonas syringae*: Seeing the Forest for the Trees. In: *Advances in Agronomy.* (Donald, L. S., ed.). Academic Press, pp. 235-295.

Langmead, B. and Salzberg, S. L. (2012) Fast gapped-read alignment with Bowtie 2. Nature methods, 9, 357-359.

Lavermicocca, P., Lonigro, S. L., Valerio, F., Evidente, A. and Visconti, A. (2002) Reduction of Olive Knot Disease by a Bacteriocin from *Pseudomonas syringae* pv. ciccaronei. Applied and Environmental Microbiology, 68, 1403-1407.

Lawrence, M., Huber, W., Pages, H., Aboyoun, P., Carlson, M., Gentleman, R., Morgan, M. T. and Carey, V. J. (2013) Software for computing and annotating genomic ranges. PLoS computational biology, 9, e1003118.

Lee, J. and Zhang, L. (2015) The hierarchy quorum sensing network in *Pseudomonas aeruginosa*. Protein & cell, 6, 26-41.

Lelliott, R. A., Billing, E. and Hayward, A. C. (1966) A determinative scheme for the fluorescent plant pathogenic pseudomonads. The Journal of applied bacteriology, 29, 470-489.

Leveau, J. H. and Gerards, S. (2008) Discovery of a bacterial gene cluster for catabolism of the plant hormone indole 3-acetic acid. FEMS microbiology ecology, 65, 238-250.

Li, D., Yan, Y., Ping, S., Chen, M., Zhang, W., Li, L., Lin, W., Geng, L., Liu, W., Lu, W. and Lin, M. (2010) Genome-wide investigation and functional characterization of the beta-ketoadipate pathway in the nitrogen-fixing and root-associated bacterium *Pseudomonas stutzeri* A1501. BMC microbiology, 10, 36.

Lindeberg, M., Stavrinides, J., Chang, J. H., Alfano, J. R., Collmer, A., Dangl, J. L., Greenberg, J. T., Mansfield, J. W. and Guttman, D. S. (2005) Proposed guidelines for a unified

nomenclature and phylogenetic analysis of type III Hop effector proteins in the plant pathogen *Pseudomonas syringae*. Molecular Plant-Microbe Interactions*, 18,* 275-282.

Livak, K. J. and Schmittgen, T. D. (2001) Analysis of Relative Gene Expression Data Using Real-Time Quantitative PCR and the 2−ΔΔCT Method. Methods*, 25,* 402-408.

Loh, J., Pierson, E. A., Pierson, L. S., 3rd, Stacey, G. and Chatterjee, A. (2002) Quorum sensing in plant-associated bacteria. Current opinion in plant biology*, 5,* 285-290.

Loper, J. E. and Lindow, S. E. (1987) Lack of evidence for in situ fluorescent pigment production by *Pseudomonas syringae* pv. syringae on bean leaf surfaces. Phytopathology 77*,* 1449-1454.

Love, M. I., Huber, W. and Anders, S. (2014) Moderated estimation of fold change and dispersion for RNA-seq data with DESeq2. Genome biology*, 15,* 550.

Macho, A. P., Ruiz-Albert, J., Tornero, P. and Beuzon, C. R. (2009) Identification of new type III effectors and analysis of the plant response by competitive index. Molecular plant pathology*, 10,* 69-80.

Maeda, K., Nojiri, H., Shintani, M., Yoshida, T., Habe, H. and Omori, T. (2003) Complete nucleotide sequence of carbazole/dioxin-degrading plasmid pCAR1 in *Pseudomonas resinovorans* strain CA10 indicates its mosaicity and the presence of large catabolic transposon Tn4676. Journal of molecular biology*, 326,* 21-33.

Magie, A. R. and Wilson, E. E. (1962) Expression of virulence among isolates of *Pseudomonas savastanoi* from olive and oleander. Phytopathology*, 52,* 741.

Magie, A. R., Wilson, E. E. and Kosuge, T. (1963) Indoleacetamide as an Intermediate in the Synthesis of Indoleacetic Acid in *Pseudomonas Savastanoi*. Science*, 141,* 1281-1282.

Maldonado-González, M. M., Prieto, P., Ramos, C. and Mercado-Blanco, J. (2013) From the root to the stem: interaction between the biocontrol root endophyte *Pseudomonas fluorescens* PICF7 and the pathogen *Pseudomonas savastanoi* NCPPB 3335 in olive knots. Microbial biotechnology*, 6,* 275-287.

Mansfield, J., Genin, S., Magori, S., Citovsky, V., Sriariyanum, M., Ronald, P., Dow, M. A. X., Verdier, V., Beer, S. V., Machado, M. A., Toth, I. A. N., Salmond, G. and Foster, G. D. (2012) Top 10 plant pathogenic bacteria in molecular plant pathology. Molecular plant pathology*, 13,* 614-629.

Marchi, G., Sisto, A., Cimmino, A., Andolfi, A., Cipriani, M. G., Evidente, A. and Surico, G. (2006) Interaction between *Pseudomonas savastanoi* pv. savastanoi and *Pantoea agglomerans* in olive knots. Plant Pathology*, 55,* 614-624.

Marchi, G., Mori, B., Pollacci, P., Mencuccini, M. and Surico, G. (2009) Systemic spread of *Pseudomonas savastanoi* pv. savastanoi in olive explants. Plant Pathology*, 58,* 152-158.

Matas, I. M., Perez-Martinez, I., Quesada, J. M., Rodriguez-Herva, J. J., Penyalver, R. and Ramos, C. (2009) *Pseudomonas savastanoi* pv. savastanoi contains two *iaaL* paralogs, one of which exhibits a variable number of a trinucleotide (TAC) tandem repeat. Applied and Environmental Microbiology*, 75,* 1030-1035.

Matas, I. M., Lambertsen, L., Rodriguez-Moreno, L. and Ramos, C. (2012) Identification of novel virulence genes and metabolic pathways required for full fitness of *Pseudomonas savastanoi* pv. savastanoi in olive (*Olea europaea*) knots. New Phytologist*, 196,* 1182-1196.

Matas, I. M., Castaneda-Ojeda, M. P., Aragon, I. M., Antunez-Lamas, M., Murillo, J., Rodriguez-Palenzuela, P., Lopez-Solanilla, E. and Ramos, C. (2014) Translocation and functional analysis of *Pseudomonas savastanoi* pv. savastanoi NCPPB 3335 type III secretion system effectors reveals two novel effector families of the *Pseudomonas syringae* complex. Molecular Plant Microbe Interactions*, 27,* 424-436.

Mattiuzzo, M., Bertani, I., Ferluga, S., Cabrio, L., Bigirimana, J., Guarnaccia, C., Pongor, S., Maraite, H. and Venturi, V. (2011) The plant pathogen *Pseudomonas fuscovaginae* contains two conserved quorum sensing systems involved in virulence and negatively

regulated by RsaL and the novel regulator RsaM. Environental Microbiology 13**,** 145-162.

McCann, H. C., Rikkerink, E. H., Bertels, F., Fiers, M., Lu, A., Rees-George, J., Andersen, M. T., Gleave, A. P., Haubold, B., Wohlers, M. W., Guttman, D. S., Wang, P. W., Straub, C., Vanneste, J. L., Rainey, P. B. and Templeton, M. D. (2013) Genomic analysis of the Kiwifruit pathogen *Pseudomonas syringae* pv. actinidiae provides insight into the origins of an emergent plant disease. PLoS pathogens*,* 9**,** e1003503.

McFall, S. M., Chugani, S. A. and Chakrabarty, A. M. (1998) Transcriptional activation of the catechol and chlorocatechol operons: variations on a theme. Gene*,* 223**,** 257-267.

Miller, J. H. (1972) Experiments in Molecular Genetics. Cold Spring Harbor Laboratory, Cold Spring Harbor, NY.

Miller, M. B. and Bassler, B. L. (2001) Quorum sensing in bacteria. Annual review of microbiology*,* 55**,** 165-199.

Mirik, M., Aysan, Y. and Sahin, F. (2011) Characterization of *Pseudomonas savastano*i pv. savastanoi strains isolated from several host plants in Turkey and report of fontanesia as a new host. Journal of Plant Pathology*,* 93**,** 263-270.

Mitchell , J. W. and Brunstetter, B. C. (1939) Colorimetric methods for the quantitative estimation of indole(3)acetic acid. Botanical Gazette*,* 100**,** 802-816.

Mollov, D., Guaragna, M. A., Lockhart, B., Rezende, J. A. M. and Jordan, R. (2015) First Report of Catharanthus mosaic virus in *Mandevilla* in the United States. Plant Disease*,* 99**,** 165-165.

Moretti, C., Ferrante, P., Hosni, T., Valentini, F., D'Onghia, A., Fatmi, M. B. and Buonaurio, R. (2008) Characterization of *Pseudomonas savastanoi* pv. Savastanoi Strains Collected from Olive Trees in Different Countries. In: *Pseudomonas syringae Pathovars and Related Pathogens – Identification, Epidemiology and Genomics.* (Fatmi, M. B., Collmer, A., Iacobellis, N., Mansfield, J., Murillo, J., Schaad, N.*, et al.*, eds.). Springer Netherlands, pp. 321-329.

Moretti, C., Hosni, T., Vandemeulebroecke, K., Brady, C., De Vos, P., Buonaurio, R. and Cleenwerck, I. (2011) *Erwinia oleae* sp. nov., isolated from olive knots caused by *Pseudomonas savastanoi* pv. savastanoi. International journal of systematic and evolutionary microbiology*,* 61**,** 2745-2752.

Moretti, C., Cortese, C., Passos da Silva, D., Venturi, V., Ramos, C., Firrao, G. and Buonaurio, R. (2014) Draft Genome Sequence of *Pseudomonas savastanoi* pv. savastanoi Strain DAPP-PG 722, Isolated in Italy from an Olive Plant Affected by Knot Disease. Genome announcements*,* 2.

Moretti, C., Vinatzer, B. A., Onofri, A., Valentini, F. and Buonaurio, R. (2016) Genetic and phenotypic diversity of Mediterranean populations of the olive knot pathogen, Pseudomonas savastanoi pv. savastanoi. Plant Pathology**,** n/a-n/a.

Morris, C. E., Kinkel, L. L., Xiao, K., Prior, P. and Sands, D. C. (2007) Surprising niche for the plant pathogen *Pseudomonas syringae*. Infection, Genetics and Evolution*,* 7**,** 84-92.

Morris, C. E., Sands, D. C., Vanneste, J. L., Montarry, J., Oakley, B., Guilbaud, C. and Glaux, C. (2010) Inferring the evolutionary history of the plant pathogen *Pseudomonas syringae* from its biogeography in headwaters of rivers in North America, Europe, and New Zealand. mBio, 1.

Morris, R. O. (1986) Genes Specifying Auxin and Cytokinin Biosynthesis in Phytopathogens. Annual Review of Plant Physiology*,* 37**,** 509-538.

Mudgett, M. B. and Staskawicz, B. J. (1999) Characterization of the *Pseudomonas syringae* pv. tomato AvrRpt2 protein: demonstration of secretion and processing during bacterial pathogenesis. Molecular microbiology*,* 32**,** 927-941.

Murillo, J. and Keen, N. T. (1994) Two native plasmids of *Pseudomonas syringae* pathovar tomato strain PT23 share a large amount of repeated DNA, including replication sequences. Molecular microbiology*,* 12**,** 941-950.

Nojiri, H., Maeda, K., Sekiguchi, H., Urata, M., Shintani, M., Yoshida, T., Habe, H. and Omori, T. (2002) Organization and transcriptional characterization of catechol degradation genes involved in carbazole degradation by *Pseudomonas resinovorans* strain CA10. Bioscience, biotechnology, and biochemistry, 66, 897-901.

Nowell, R. W., Green, S., Laue, B. E. and Sharp, P. M. (2014) The extent of genome flux and its role in the differentiation of bacterial lineages. Genome biology and evolution, 6, 1514-1529.

Nowell, R. W., Laue, B. E., Sharp, P. M. and Green, S. (2016) Comparative genomics reveals genes significantly associated with woody hosts in the plant pathogen *Pseudomonas syringae*. Molecular plant pathology.

O'Brien, H. E., Thakur, S. and Guttman, D. S. (2011) Evolution of plant pathogenesis in *Pseudomonas syringae*: a genomics perspective. Annual review of phytopathology, 49, 269-289.

O'Toole, G. A. and Kolter, R. (1998) Flagellar and twitching motility are necessary for Pseudomonas aeruginosa biofilm development. Molecular microbiology, 30, 295-304.

Olapade, O. A. and Ronk, A. J. (2015) Isolation, characterization and community diversity of indigenous putative toluene-degrading bacterial populations with catechol-2,3-dioxygenase genes in contaminated soils. Microbial ecology, 69, 59-65.

Ornston, L. N. (1966) The Conversion of Catechol and Protocatechuate to β-Ketoadipate by *Pseudomonas putida* : III. ENZYMES OF THE CATECHOL PATHWAY. Journal of Biological Chemistry, 241, 3795-3799.

Ortiz-Martin, I., Thwaites, R., Macho, A. P., Mansfield, J. W. and Beuzon, C. R. (2010) Positive regulation of the Hrp type III secretion system in *Pseudomonas syringae* pv. phaseolicola. Molecular Plant-Microbe Interactions, 23, 665-681.

Palmer, B. R. and Marinus, M. G. (1994) The dam and dcm strains of *Escherichia coli*--a review. Gene, 143, 1-12.

Parales, R. E., Ontl, T. A. and Gibson, D. T. (1997) Cloning and sequence analysis of a catechol 2,3-dioxygenase gene from the nitrobenzene-degrading strain *Comamonas* sp JS765. Journal of Industrial Microbiology and Biotechnology, 19, 385-391.

Parkinson, N., Bryant, R., Bew, J. and Elphinstone, J. (2011) Rapid phylogenetic identification of members of the *Pseudomonas syringae* species complex using the *rpoD* locus. Plant Pathology, 60, 338-344.

Parsek, M. R., Val, D. L., Hanzelka, B. L., Cronan, J. E., Jr. and Greenberg, E. P. (1999) Acyl homoserine-lactone quorum-sensing signal generation. Proceedings of the National Academy of Sciences U S A, 96, 4360-4365.

Passos da Silva, D., Castaneda-Ojeda, M. P., Moretti, C., Buonaurio, R., Ramos, C. and Venturi, V. (2014) Bacterial multispecies studies and microbiome analysis of a plant disease. Microbiology, 160, 556-566.

Patel, H., Ferrante, P., Covaceuszach, S., Lamba, D., Scortichini, M. and Venturi, V. (2014) The Kiwifruit Emerging Pathogen *Pseudomonas syringae* pv. actinidiae Does Not Produce AHLs but Possesses Three LuxR Solos. PLoS ONE, 9, e87862.

Patel, H. K., Suarez-Moreno, Z. R., Degrassi, G., Subramoni, S., Gonzalez, J. F. and Venturi, V. (2013) Bacterial LuxR solos have evolved to respond to different molecules including signals from plants. Frontiers in plant science, 4, 447.

Paul, R., Weiser, S., Amiot, N. C., Chan, C., Schirmer, T., Giese, B. and Jenal, U. (2004) Cell cycle-dependent dynamic localization of a bacterial response regulator with a novel di-guanylate cyclase output domain. Genes & development, 18, 715-727.

Pawlik, M. and Piotrowska-Seget, Z. (2015) Endophytic Bacteria Associated with *Hieracium piloselloides*: Their Potential for Hydrocarbon-Utilizing and Plant Growth-Promotion. Journal of Toxicology and Environmental Health, 78, 860-870.

Penaloza-Vazquez, A., Kidambi, S. P., Chakrabarty, A. M. and Bender, C. L. (1997) Characterization of the alginate biosynthetic gene cluster in *Pseudomonas syringae* pv. syringae. Journal of Bacteriology*,* 179**,** 4464-4472.

Pennisi, A. M., Cacciola, S. O., Raudino, F. and Pane, A. (2002) First Report of *Botrytis* Blight on *Medinilla magnifica* and Various Species of *Mandevilla* and *Allamanda* in Italy. Plant Disease*,* 86.

Penyalver, R., Garcia, A., Ferrer, A., Bertolini, E., Quesada, J. M., Salcedo, C. I., Piquer, J., Perez-Panades, J., Carbonell, E. A., Del Rio, C., Caballero, J. M. and Lopez, M. M. (2006) Factors Affecting *Pseudomonas savastanoi* pv. savastanoi Plant Inoculations and Their Use for Evaluation of Olive Cultivar Susceptibility. Phytopathology*,* 96**,** 313-319.

Perez-Martinez, I., Rodriguez-Moreno, L., Matas, I. M. and Ramos, C. (2007) Strain selection and improvement of gene transfer for genetic manipulation of *Pseudomonas savastanoi* isolated from olive knots. Research in microbiology*,* 158**,** 60-69.

Perez-Martinez, I., Zhao, Y., Murillo, J., Sundin, G. W. and Ramos, C. (2008) Global genomic analysis of *Pseudomonas savastanoi* pv. savastanoi plasmids. Journal of Bacteriology*,* 190**,** 625-635.

Perez-Martinez, I., Rodriguez-Moreno, L., Lambertsen, L., Matas, I. M., Murillo, J., Tegli, S., Jimenez, A. J. and Ramos, C. (2010) Fate of a *Pseudomonas savastano*i pv. savastanoi type III secretion system mutant in olive plants (*Olea europaea* L.). Applied and Environmental Microbiology*,* 76**,** 3611-3619.

Pérez-Mendoza, D., Coulthurst, S. J., Sanjuán, J. and Salmond, G. P. C. (2011) N-Acetylglucosamine-dependent biofilm formation in *Pectobacterium atrosepticum* is cryptic and activated by elevated c-di-GMP levels. Microbiology*,* 157**,** 3340-3348.

Petriccione, M., Salzano, A. M., Di Cecco, I., Scaloni, A. and Scortichini, M. (2014) Proteomic analysis of the *Actinidia deliciosa* leaf apoplast during biotrophic colonization by *Pseudomonas syringae* pv. actinidiae. Journal of proteomics*,* 101**,** 43-62.

Pettersen, R. C. (1984) The Chemical Composition of Wood. In: *The Chemistry of Solid Wood.* American Chemical Society, pp. 57-126.

Pfaffl, M. W. (2001) A new mathematical model for relative quantification in real-time RT–PCR. Nucleic acids research*,* 29**,** e45.

Pirc, M., Ravnikar, M. and Dreo, T. (2014) First Report of *Pseudomonas savastanoi* Causing Bacterial Leaf Spot of *Mandevilla sanderi* in Slovenia. Plant Disease*,* 99**,** 415-415.

Pliego, C., de Weert, S., Lamers, G., de Vicente, A., Bloemberg, G., Cazorla, F. M. and Ramos, C. (2008) Two similar enhanced root-colonizing *Pseudomonas* strains differ largely in their colonization strategies of avocado roots and *Rosellinia necatrix* hyphae. Environental Microbiology*,* 10**,** 3295-3304.

Poiatti, V. A., Dalmas, F. R. and Astarita, L. V. (2009) Defense mechanisms of *Solanum tuberosum* L. in response to attack by plant-pathogenic bacteria. Biological research*,* 42**,** 205-215.

Powell, G. K. and Morris, R. O. (1986) Nucleotide sequence and expression of a *Pseudomonas savastanoi* cytokinin biosynthetic gene: homotogy with *Agrobacterium tumefaciens tmr* and *tzs* loci. Nucleic acids research*,* 14**,** 2555-2565.

Putnam, M. L., Curtis, M., Serdani, M. and Palmateer, A. J. (2010) *Pseudomonas savastanoi* found in association with stem galls on *Mandevilla*. Phytopathology*,* 100**,** S104-S104.

Quesada, J. M., García, A., Bertolini, E., López, M. M. and Penyalver, R. (2007) Recovery of *Pseudomonas savastanoi* pv. savastanoi from symptomless shoots of naturally infected olive trees. International Microbiology 10, 77-84.

Quesada, J. M., Penyalver, R., Pérez-Panadés, J., Salcedo, C. I., Carbonell, E. A. and López, M. M. (2009) Dissemination of *Pseudomonas savastanoi* pv. savastanoi populations and subsequent appearance of olive knot disease. Plant Pathology*,* 59**,** 262-269.

Quesada, J. M., Penyalver, R., Pérez-Panadés, J., Salcedo, C. I., Carbonell, E. A. and López, M. M. (2010) Comparison of chemical treatments for reducing epiphytic *Pseudomonas*

savastanoi pv. savastanoi populations and for improving subsequent control of olive knot disease. Crop Protection*, 29***,** 1413-1420.

Quinones, B., Pujol, C. J. and Lindow, S. E. (2004) Regulation of AHL production and its contribution to epiphytic fitness in *Pseudomonas syringae*. Molecular Plant Microbe Interactions*, 17***,** 521-531.

Quinones, B., Dulla, G. and Lindow, S. E. (2005) Quorum sensing regulates exopolysaccharide production, motility, and virulence in *Pseudomonas syringae*. Molecular Plant Microbe Interactions*, 18***,** 682-693.

Radwanski, E. R. and Last, R. L. (1995) Tryptophan biosynthesis and metabolism: biochemical and molecular genetics. The Plant cell*, 7***,** 921-934.

Ralph, J., Lundquist, K., Brunow, G., Lu, F., Kim, H., Schatz, P. F., Marita, J. M., Hatfield, R. D., Ralph, S. A., Christensen, J. H. and Boerjan, W. (2004) Lignins: Natural polymers from oxidative coupling of 4-hydroxyphenyl- propanoids. Phytochemistry Reviews*, 3***,** 29-60.

Ramos, C., Matas, I. M., Bardaji, L., Aragon, I. M. and Murillo, J. (2012) *Pseudomonas savastanoi* pv. savastanoi: some like it knot. Molecular plant pathology*, 13***,** 998-1009.

Recouvreux, D. O. S., Carminatti, C. A., Pitlovanciv, A. K., Rambo, C. R., Porto, L. M. and Antônio, R. V. (2008) Cellulose Biosynthesis by the Beta-Proteobacterium, *Chromobacterium violaceum*. Current Microbiology*, 57***,** 469-476.

Reimmann, C., Beyeler, M., Latifi, A., Winteler, H., Foglino, M., Lazdunski, A. and Haas, D. (1997) The global activator GacA of *Pseudomonas aeruginosa* PAO positively controls the production of the autoinducer *N*-butyryl-homoserine lactone and the formation of the virulence factors pyocyanin, cyanide, and lipase. Molecular microbiology*, 24***,** 309-319.

Retallack, D. M., Thomas, T. C., Shao, Y., Haney, K. L., Resnick, S. M., Lee, V. D. and Squires, C. H. (2006) Identification of anthranilate and benzoate metabolic operons of *Pseudomonas fluorescens* and functional characterization of their promoter regions. Microbial Cell Factories*, 5***,** 1-13.

Rodriguez-Moreno, L., Barcelo-Munoz, A. and Ramos, C. (2008) In vitro analysis of the interaction of *Pseudomonas savastanoi* pvs. savastanoi and nerii with micropropagated olive plants. Phytopathology*, 98***,** 815-822.

Rodriguez-Moreno, L., Jimenez, A. J. and Ramos, C. (2009) Endopathogenic lifestyle of *Pseudomonas savastanoi* pv. savastanoi in olive knots. Microbial biotechnology*, 2***,** 476-488.

Rodriguez-Palenzuela, P., Matas, I. M., Murillo, J., Lopez-Solanilla, E., Bardaji, L., Perez-Martinez, I., Rodriguez-Moskera, M. E., Penyalver, R., Lopez, M. M., Quesada, J. M., Biehl, B. S., Perna, N. T., Glasner, J. D., Cabot, E. L., Neeno-Eckwall, E. and Ramos, C. (2010) Annotation and overview of the *Pseudomonas savastanoi* pv. savastanoi NCPPB 3335 draft genome reveals the virulence gene complement of a tumour-inducing pathogen of woody hosts. Environmental microbiology*, 12***,** 1604-1620.

Rojas, A. M., de Los Rios, J. E., Fischer-Le Saux, M., Jimenez, P., Reche, P., Bonneau, S., Sutra, L., Mathieu-Daude, F. and McClelland, M. (2004) *Erwinia toletana* sp. nov., associated with *Pseudomonas savastanoi*-induced tree knots. International journal of systematic and evolutionary microbiology*, 54***,** 2217-2222.

Rotenberg, D., Thompson, T. S., German, T. L. and Willis, D. K. (2006) Methods for effective real-time RT-PCR analysis of virus-induced gene silencing. Journal of Virological Methods*, 138***,** 49-59.

Rothmel, R. K., Aldrich, T. L., Houghton, J. E., Coco, W. M., Ornston, L. N. and Chakrabarty, A. M. (1990) Nucleotide sequencing and characterization of *Pseudomonas putida catR*: a positive regulator of the *catBC* operon is a member of the LysR family. Journal of Bacteriology*, 172***,** 922-931.

Ruhl, G., Twieg, E., DeVries, R., Levy, L., Byrne, J., Mollov, D. and Taylor, N. (2011) First Report of Bacterial Wilt in *Mandevilla* (= Dipladenia) *splendens* 'Red Riding Hood' in the United States Caused by *Ralstonia solanacearum* Biovar 3. Plant Disease*, 95***,** 614-615.

Ryan, R. P., Fouhy, Y., Lucey, J. F., Jiang, B. L., He, Y. Q., Feng, J. X., Tang, J. L. and Dow, J. M. (2007) Cyclic di-GMP signalling in the virulence and environmental adaptation of *Xanthomonas campestris*. Molecular microbiology*,* 63**,** 429-442.

Saitou, N. and Nei, M. (1987) The neighbor-joining method: a new method for reconstructing phylogenetic trees. Molecular biology and evolution*,* 4**,** 406-425.

Sambrook, J., and Russell, D. (2001) Molecular Cloning: A Laboratory Manual. Cold Spring Harbor, NY, USA: Cold Spring Harbor Laboratory.

Sarkar, S. F. and Guttman, D. S. (2004) Evolution of the core genome of *Pseudomonas syringae*, a highly clonal, endemic plant pathogen. Applied and Environmental Microbiology*,* 70**,** 1999-2012.

Savastano, L. (1886) Le maladies de l'olivier et la tuberculose en particuler. Comptes-rendu de l'Académie d'Agriculture de France**,** 103-114.

Scortichini, M., Rossi, M. P. and Salerno, M. (2004) Relationship of genetic structure of *Pseudomonas savastanoi* pv. savastanoi populations from Italian olive trees and patterns of host genetic diversity. Plant Pathology*,* 53**,** 491-497.

Schaad, N. W., Jones, J. B., Chun, W. and Committee, A. P. S. B. (2001) Laboratory Guide for Identification of Plant Pathogenic Bacteria. St Paul, USA: American Phytopathological Society.

Schaefer, A. L., Val, D. L., Hanzelka, B. L., Cronan, J. E., Jr. and Greenberg, E. P. (1996) Generation of cell-to-cell signals in quorum sensing: acyl homoserine lactone synthase activity of a purified *Vibrio fischeri* LuxI protein. Proceedings of the National Academy of Sciences U S A*,* 93**,** 9505-9509.

Schlomann, M., Schmidt, E. and Knackmuss, H. J. (1990) Different types of dienelactone hydrolase in 4-fluorobenzoate-utilizing bacteria. Journal of Bacteriology*,* 172**,** 5112-5118.

Schroth, M. N., Osgood, J. W. and Miller, T. D. (1973) Quantitative assessment of the effect of the olive knot disease on olive yield and quality. Phytopathology 63**,** 1064-1065.

Schuster, M., Lostroh, C. P., Ogi, T. and Greenberg, E. P. (2003) Identification, timing, and signal specificity of *Pseudomonas aeruginosa* quorum-controlled genes: a transcriptome analysis. Journal of Bacteriology*,* 185**,** 2066-2079.

Sella, L., Cosmi, T., Giacomello, F., Saccardi, A. and Favaron, F. (2010) First report of *Fusarium oxysporum* on Dipladenia sp. in Italy. Journal of Plant Pathology*,* 92**,** 543.

Shadel, G. S. and Baldwin, T. O. (1991) The *Vibrio fischeri* LuxR protein is capable of bidirectional stimulation of transcription and both positive and negative regulation of the luxR gene. Journal of Bacteriology*,* 173**,** 568-574.

Silva-Rocha, R. and de Lorenzo, V. (2012) Broadening the signal specificity of prokaryotic promoters by modifying cis-regulatory elements associated with a single transcription factor. Molecular bioSystems*,* 8**,** 1950-1957.

Sisto, A., Cipriani, M. G. and Morea, M. (2004) Knot Formation Caused by *Pseudomonas syringae* subsp. savastanoi on Olive Plants Is *hrp*-Dependent. Phytopathology*,* 94**,** 484-489.

Smidt, M. and Kosuge, T. (1978) The role of indole-3-acetic acid accumulation by alpha methyl tryptophan-resistant mutants of *Pseudomonas savastanoi* in gall formation on oleanders. Physiological Plant Pathology*,* 13**,** 203-213.

Solano, C., García, B., Valle, J., Berasain, C., Ghigo, J.-M., Gamazo, C. and Lasa, I. (2002) Genetic analysis of *Salmonella enteritidis* biofilm formation: critical role of cellulose. Molecular microbiology*,* 43**,** 793-808.

Spaepen, S., Vanderleyden, J. and Remans, R. (2007) Indole-3-acetic acid in microbial and microorganism-plant signaling. FEMS microbiology reviews*,* 31**,** 425-448.

Spaink, H. P., Okker, R. J., Wijffelman, C. A., Pees, E. and Lugtenberg, B. J. (1987) Promoters in the nodulation region of the *Rhizobium leguminosarum* Sym plasmid pRL1JI. Plant molecular biology*,* 9**,** 27-39.

Subramoni, S. and Venturi, V. (2009) LuxR-family 'solos': bachelor sensors/regulators of signalling molecules. Microbiology, 155, 1377-1385.

Surico, G. (1977) Histological observations on tumours of olive knot. Phytopathologia Mediterranea, 16, 106-125.

Surico, G., Iacobellis, N. S. and Sisto, A. (1985) Studies on the role of indole-3-acetic acid and cytokinins in the formation of knots on olive and oleander plants by *Pseudomonas syringae* pv. savastanoi. Physiological Plant Pathology, 26, 309-320.

Surico, G. and Lavernicocca, P. (1989) A semiselective medium for the isolation of *Pseudomonas syringae* pv. savastanoi. Phytopathology, 79, 185-190.

Taghavi, M. and Hasan, S. (2012) Occurrence of *Pseudomonas savastanoi* the Causal Agent of Winter Jasmine Gall in Iran Iran Agricultural Research, 31, 39-47.

Taguchi, F., Ogawa, Y., Takeuchi, K., Suzuki, T., Toyoda, K., Shiraishi, T. and Ichinose, Y. (2006) A homologue of the 3-oxoacyl-(acyl carrier protein) synthase III gene located in the glycosylation island of *Pseudomonas syringae* pv. tabaci regulates virulence factors via *N*-acyl homoserine lactone and fatty acid synthesis. Journal of Bacteriology, 188, 8376-8384.

Taguchi, F., Inoue, Y., Suzuki, T., Inagaki, Y., Yamamoto, M., Toyoda, K., Noutoshi, Y., Shiraishi, T. and Ichinose, Y. (2015) Characterization of quorum sensing-controlled transcriptional regulator MarR and Rieske (2Fe-2S) cluster-containing protein (Orf5), which are involved in resistance to environmental stresses in *Pseudomonas syringae* pv. tabaci 6605. Molecular plant pathology, 16, 376-387.

Tamura, K., Peterson, D., Peterson, N., Stecher, G., Nei, M. and Kumar, S. (2011) MEGA5: molecular evolutionary genetics analysis using maximum likelihood, evolutionary distance, and maximum parsimony methods. Molecular biology and evolution, 28, 2731-2739.

Taniuchi, H., Hatanaka, M., Kuno, S., Hayaishi, O., Nakajima, M. and Kurihara, N. (1964) Enzymatic Formation of Catechol from Anthranilic Acid. Journal of Biological Chemistry, 239, 2204-2211.

Tegli, S., Gori, A., Cerboneschi, M., Cipriani, M. G. and Sisto, A. (2011) Type Three Secretion System in *Pseudomonas savastanoi* Pathovars: Does Timing Matter? Genes, 2, 957-979.

Temsah, M., Hanna, L. and Saad, A. T. (2007a) Anatomical observations of *Pseudomonas savastanoi* on *Rhamnus alaternus*. Forest Pathology, 37, 64-72.

Temsah, M., Hanna, L. and Saad, A. T. (2007b) Histology of pathogenesis of *Pseudomonas savastanoi* on *Myrtus communis*. Journal of Plant Pathology, 89, 241-249.

Teviotdale, B. L. and Krueger, W. H. (2004) Effects of Timing of Copper Sprays, Defoliation, Rainfall, and Inoculum Concentration on Incidence of Olive Knot Disease. Plant Disease, 88, 131-135.

Thakur, S., Weir, B. S. and Guttman, D. S. (2016) Phytopathogen Genome Announcement: Draft Genome Sequences of 62 *Pseudomonas* syringae Type and Pathotype Strains. Molecular Plant-Microbe Interactions Journal, 4, 243-246.

Thornley, M. J. (1960) The differentiation of *Pseudomonas* from other Gram-negative bacteria on the basis of arginine metabolism Journal of Applied Bacteriology, 23, 37-52.

Thornton, B. and Basu, C. (2011) Real-time PCR (qPCR) primer design using free online software. Biochemistry and Molecular Biology Education, 39, 145-154.

Tischler, A. D. and Camilli, A. (2005) Cyclic diguanylate regulates *Vibrio cholerae* virulence gene expression. Infection and immunity, 73, 5873-5882.

Trapero, A. and Blanco, M. A. (1998) Enfermedades. In: *El cultivo del olivo.* (D. Barranco, D. F.-E. y. L. R., ed.). Junta de Andalucía, Mundi-Prensa, Madrid, España., pp. 461-507.

Urata, M., Miyakoshi, M., Kai, S., Maeda, K., Habe, H., Omori, T., Yamane, H. and Nojiri, H. (2004) Transcriptional regulation of the *ant* operon, encoding two-component anthranilate 1,2-dioxygenase, on the carbazole-degradative plasmid pCAR1 of *Pseudomonas resinovorans* strain CA10. Journal of Bacteriology, 186, 6815-6823.

van Hellemond, E. W., Janssen, D. B. and Fraaije, M. W. (2007) Discovery of a novel styrene monooxygenase originating from the metagenome. Applied and Environmental Microbiology, 73, 5832-5839.

Vargas, P., Felipe, A., Michan, C. and Gallegos, M. T. (2011) Induction of *Pseudomonas syringae* pv. tomato DC3000 MexAB-OprM multidrug efflux pump by flavonoids is mediated by the repressor PmeR. Molecular Plant-Microbe Interactions Journal, 24, 1207-1219.

Varvaro, L. and Surico, G. (1978) Comportamento di diverse cultivars di Olivo (*Olea europaea* L.) alla inoculazione artificiale con *Pseudomonas savastanoi* (E. F. Smith) Stevens. Phytopathologia Mediterranea, 17, 174-177.

Vetrovsky, T., Steffen, K. T. and Baldrian, P. (2014) Potential of cometabolic transformation of polysaccharides and lignin in lignocellulose by soil *Actinobacteria*. PLoS One, 9, e89108.

Von Bodman, S. B., Bauer, W. D. and Coplin, D. L. (2003) Quorum sensing in plant-pathogenic bacteria. Annual review of phytopathology, 41, 455-482.

Wagner, V. E., Bushnell, D., Passador, L., Brooks, A. I. and Iglewski, B. H. (2003) Microarray analysis of *Pseudomonas aeruginosa* quorum-sensing regulons: effects of growth phase and environment. Journal of Bacteriology, 185, 2080-2095.

Watanabe, K., Ikeda, H., Sakashita, T. and Sato, T. (2016) Anthracnose of genus *Mandevilla* caused by *Colletotrichum truncatum* and *C. siamense* in Japan. Journal of General Plant Pathology, 82, 33-37.

Whitehead, N. A., Barnard, A. M., Slater, H., Simpson, N. J. and Salmond, G. P. (2001) Quorum-sensing in Gram-negative bacteria. FEMS microbiology reviews, 25, 365-404.

Wilson, E. (1935) The olive knot disease: its inception, development, and control. Hilgardia 9, 231-264.

Wilson, E. and Magie, A. (1964) Systemic invasion of the host plant by the tumor-inducing bacterium, *Pseudomonas savastanoi*. Phytopathology, 54, 577–579.

Willcox, M. D., Zhu, H., Conibear, T. C., Hume, E. B., Givskov, M., Kjelleberg, S. and Rice, S. A. (2008) Role of quorum sensing by *Pseudomonas aeruginosa* in microbial keratitis and cystic fibrosis. Microbiology, 154, 2184-2194.

Woo, H., Sanseverino, J., Cox, C. D., Robinson, K. G. and Sayler, G. S. (2000) The measurement of toluene dioxygenase activity in biofilm culture of *Pseudomonas putida* F1. Journal of microbiological methods, 40, 181-191.

Young, J. M. (2004) Olive knot and its pathogens. Australasian Plant Pathology, 33, 33-39.

Young, J. M. (2010) Taxonomy of *Pseudomonas syringae*. Journal of Plant Pathology, 92, S5-S14.

Yu, X., Lund, S. P., Greenwald, J. W., Records, A. H., Scott, R. A., Nettleton, D., Lindow, S. E., Gross, D. C. and Beattie, G. A. (2014) Transcriptional analysis of the global regulatory networks active in *Pseudomonas syringae* during leaf colonization. mBio, 5, e01683-01614.

Zhang, Z. and Pierson, L. S. (2001) A Second Quorum-Sensing System Regulates Cell Surface Properties but Not Phenazine Antibiotic Production in *Pseudomonas aureofaciens*. Applied and Environmental Microbiology, 67, 4305-4315.

Zhou, C., Yang, Y. and Jong, A. Y. (1990) Mini-prep in ten minutes. BioTechniques, 8, 172-173.

Zogaj, X., Nimtz, M., Rohde, M., Bokranz, W. and Römling, U. (2001) The multicellular morphotypes of *Salmonella typhimurium* and Escherichia coli produce cellulose as the second component of the extracellular matrix. Molecular microbiology, 39, 1452-1463.

Zumaquero, A., Macho, A. P., Rufian, J. S. and Beuzon, C. R. (2010) Analysis of the role of the type III effector inventory of *Pseudomonas syringae* pv. phaseolicola 1448a in interaction with the plant. Journal of Bacteriology, 192, 4474-4488.